Two loop integrals and QCD scattering

A thesis presented for the degree of

Doctor of Philosophy

by

Charalampos Anastasiou

Physics Department

University of Durham

April 2001

Abstract

We present the techniques for the calculation of one- and two-loop integrals contributing to the virtual corrections to 2→2 scattering of massless particles. First, tensor integrals are related to scalar integrals with extra powers of propagators and higher dimension using the Schwinger representation. Integration By Parts and Lorentz Invariance recurrence relations reduce the number of independent scalar integrals to a set of master integrals for which their expansion in $\epsilon = 2 - D/2$ is calculated using a combination of Feynman parameters, the Negative Dimension Integration Method, the Differential Equations Method, and Mellin-Barnes integral representations. The two-loop matrix-elements for light-quark scattering are calculated in Conventional Dimensional Regularisation by direct evaluation of the Feynman diagrams. The ultraviolet divergences are removed by renormalising with the $\overline{\rm MS}$ scheme. Finally, the infrared singular behavior is shown to be in agreement with the one anticipated by the application of Catani's formalism for the infrared divergences of generic QCD two-loop amplitudes.

Acknowledgements

I would like to thank my supervisor Nigel Glover for his continuous support and excellent guidance. His inspiration, enthusiasm and confidence has been motivating at all stages, and his unique pedagogic approach has made my studies in Durham a valuable learning experience. I am indebted to him for his efforts to establish a solid base for my future research.

The collaboration with several people has helped me complete this study. Thanks go to Maria Elena Tejeda-Yeomans whose friendship, kindness and willingness to discuss all sorts of problems that arose during the course of this project have proven indispensable and are much appreciated; Carlo Oleari for our lively yet constructive and very "Mediterranean" sessions; and Bas Tausk for the insight he has patiently given me into the secrets of Mellin-Barnes integrations.

Special mention should be made to my friend and colleague Thanos Koukoutsakis, for his long-time friendship since our first year in Athens University and his "destructively" distractive challenges which he set me on.

I would also like to express my gratitude to Steve Burby and Jeppe Andersen for sharing their computer expertise, for numerous conversations on Physics and "Physics rumors" at almost any hour of the day, and their ability to detach working routine from monotony.

The exchange of ideas with the Maple wizards and multiloop fans, Lee Garland and Marco Zimmer, has always been helpful in putting into perspective technical and other difficulties arising in the implementation of two-loop computations.

I would not have been able to start my postgraduate studies had it not been for the inspiration and guidance of Athanasios Lahanas, Jose M. Vilchez, Thanasis Karampelas and Vangelis Aggelou who helped me to make important choices in my life.

I acknowledge the financial support of the Greek State's Scholarship Foundation.

Last but certainly not least, I am thankful to Mum, Gregory and Vicky, for their love and support. Their strength and determination through hard times has motivated me the most.

I dedicate this PhD thesis to my father's memory.

Declaration

I declare that I have previously submitted no material in this thesis for a degree at this or any other university.

The research presented in this thesis has been carried out in collaboration with E. W. N. Glover, Carlo Oleari, M. E. Tejeda-Yeomans and J. B. Tausk. Aspects of Chapters 3-6 are based on the following publications:

- C. Anastasiou, E. W. N. Glover and C. Oleari, *Scalar one-loop integrals using the negative-dimension approach,* Nucl. Phys. **B572**, 307 (2000), [hep-ph/9907494].

- C. Anastasiou, E. W. N. Glover and C. Oleari, *Application of the negative-dimension approach to massless scalar box integrals,* Nucl. Phys. **B565**, 445 (2000), [hep-ph/9907523].

- C. Anastasiou, E. W. N. Glover and C. Oleari, *The two-loop scalar and tensor pentabox graph with light-like legs,* Nucl. Phys. **B585**, 763 (2000), [hep-ph/9912251].

- C. Anastasiou, T. Gehrmann, C. Oleari, E. Remiddi and J. B. Tausk, *The tensor reduction and master integrals of the two-loop massless crossed box with light-like legs,* Nucl. Phys. **B580**, 577 (2000), [hep-ph/0003261].

- C. Anastasiou, J. B. Tausk and M. E. Tejeda-Yeomans, *The on-shell massless planar double box diagram with an irreducible numerator,* Nucl. Phys. Proc. Suppl. **89**, 262 (2000), [hep-ph/0005328].

- C. Anastasiou, E. W. N. Glover, C. Oleari and M. E. Tejeda-Yeomans, *Two-loop QCD corrections to the scattering of massless distinct quarks,* hep-ph/0010212.

- C. Anastasiou, E. W. N. Glover, C. Oleari and M. E. Tejeda-Yeomans, *Two-loop QCD corrections to massless identical quark scattering,* hep-ph/0011094.

- C. Anastasiou, E. W. N. Glover, C. Oleari and M. E. Tejeda-Yeomans, *One-loop QCD corrections to quark scattering at NNLO*, hep-ph/0012007.

Contents

1 Basic aspects of QCD **1**

1.1 The quark model 1

1.2 The QCD Lagrangian 2

1.3 Feynman rules 4

1.4 Dimensional Regularisation 8

1.5 Renormalisation 11

1.6 Running a_s and perturbative expansions in QCD 13

1.7 Higher order corrections in QCD 15

2 Infrared Divergences **19**

2.1 Virtual infrared divergences 21

2.2 Real infrared divergences 23

2.3 Cancellation of infrared divergences 25

2.4 Matrix elements in color space 26

2.5 Singular behavior of one-loop amplitudes 28

2.5.1 Application: $Z \to q\bar{q}$ one-loop singularities 29

2.6 Singular behavior of two-loop amplitudes 29

2.7 Color charge operator **I** for unlike-quark scattering 30

3 Representations of Feynman Integrals **33**

3.1 Generic tensor integrals using Schwinger parameters 37

3.2 Feynman Parameters 42

3.2.1 The one-loop triangle 43

3.2.2 The Bow-tie topology 46

3.2.3 The TrianA topology 47

3.2.4 The TrianB topology . . . 48
3.3 Mellin-Barnes representations . . . 49
3.3.1 Representation of one-loop integrals . . . 50
3.3.2 The adjacent-mass box . . . 53
3.3.3 The box with one leg off-shell and the on-shell box . . . 56
3.3.4 The one-loop triangle with MB . . . 57
3.3.5 The Penta-box topology . . . 59
3.3.6 The TrianC topology . . . 61
3.3.7 The Cross-triangle topology . . . 63
3.4 Laurent expansion in ϵ of MB representations . . . 65
3.4.1 Isolation of the poles . . . 67
3.4.2 Evaluating the finite integrals . . . 70
3.5 Summary . . . 72

4 Negative Dimensions Integration Method **73**
4.1 The general massless one-loop box integral . . . 75
4.1.1 The negative-dimension approach . . . 76
4.1.2 Classification of the groups of solutions from their region of convergence . . . 81
4.1.3 Analytic Continuations-Limiting cases . . . 83
4.2 Application to two-loop box graphs: The Abox topology . . . 85
4.3 Discussion . . . 89

5 Integration by Parts **92**
5.1 Integration by Parts and Lorentz Invariance identities . . . 94
5.2 Dimensional shift . . . 96
5.3 The one-loop box topology . . . 98
5.4 IBP algorithm for the bubble-box (**Abox**) topology . . . 102
5.5 The diagonal-box (**Cbox**) topology . . . 104
5.6 IBP algorithm for topologies with a triangle subgraph . . . 108
5.7 Reduction algorithm for the Cross-Triangle topology . . . 110
5.8 The Cross-Box topology . . . 112
5.8.1 IBP and LI identities . . . 113

5.8.2 Differential equations for the master integrals of the cross-box topology . . . 121
5.8.3 Analytic expansion of the second master integral . . . 123
5.9 The planar double-box topology . . . 127
5.9.1 IBP algorithm for the planar double-box . . . 127
5.9.2 Calculation by Mellin-Barnes contour integrals of a master integral . . . 130
5.9.3 Differential equations for double-box master integrals . . . 134
5.9.4 Master integrals in D=6 dimensions . . . 136
5.10 Synopsis: The Master Integrals . . . 136

6 NNLO virtual corrections for quark scattering 138
6.1 Notation . . . 140
6.2 Method . . . 144
6.3 One-loop contributions for unlike-quark scattering . . . 147
6.4 One-loop contributions for like-quark scattering . . . 149
6.5 Unlike-quark scattering two-loop contributions . . . 151
6.5.1 Infrared pole structure . . . 152
6.5.2 Finite contributions . . . 153
6.6 Like-quark scattering two-loop contributions . . . 167
6.6.1 Infrared Pole Structure . . . 167
6.6.2 Finite contributions . . . 170
6.7 Summary . . . 178

7 Conclusions 180

A Hypergeometric definitions and identities 185
A.1 Series representations . . . 185
A.2 Integral representations . . . 187
A.3 Example of explicit evaluation of an integral representation . . . 187
A.4 Identities amongst the hypergeometric functions . . . 190
A.5 Analytic continuation formulae . . . 190

B Polylogarithms **192**

B.1 Definition . . . 192

B.2 Analytic continuation formulae . . . 194

B.3 Useful identities . . . 195

Bibliography **196**

Preface

Since the beginning of history, mankind has been involved in a continuous exploration of everything that can be observed or apprehended. The pursuit for finding the "real" nature of the world is not only a means to satisfy instinctive curiosity but also a principal tool for the advancement and progress of civilization.

The initial approach was rather spiritual and Gods were called upon to explain the diversity of nature. As time passed our perception of the world has matured into theories which aim to interpret observations in a more fundamental way by unifying the underlying mechanisms governing the complex variety of phenomena. The concurrent development of Mathematics has crystallized the content of physical laws and disclosed their simplicity.

Theories not only serve as an explanation of existing observations but also have predictive powers for new phenomena which may be probed by experiment. The interplay between theory and experiment is the cornerstone for the development of Physics, filtering the ideas and consolidating our knowledge.

Nowadays, we have reached a very compact conception of nature. The world consists of elementary particles communicating with each other via the electromagnetic force, the weak and the strong nuclear forces and gravity. With the Standard Model we have a very good description of the unified electroweak and strong forces. Gravity is still a puzzle at small scales, but since it is much weaker than the other forces, it plays a minor role at the energies we are probing with Particle Physics experiments and is usually ignored.

The electroweak sector of the Standard model is a field theory based on the invariance under the local transformations of the $U(1) \otimes SU(2)$ group. This symmetry is not observed at low energies, since it gets broken with the Higgs mechanism, providing masses to the particles and leaving a residual $U(1)$ symmetry characteristic of the electromagnetic interactions.

In this thesis we deal with the part of the Standard Model known as Quantum Chromodynamics (QCD) describing the strong interaction that glues together the constituents of the nuclei. It is a field theory invariant under local transformations of the $SU(3)$ group. We shall give an overview of the basic aspects of QCD in Chapter 1.

The theory at high energies is characterized by a small coupling making possible the calculation of physical observables by means of a perturbative expansion. Feynman diagrams provide the natural framework for such expansion in Quantum Field Theories with small coupling. The calculations are getting more and more cumbersome as we proceed with higher order terms. One is faced with multiple integrations in momentum space that exhibit ultraviolet (UV) and infrared divergences (IR) in the high and the low energy limits respectively.

We can quantify the divergences with the adoption of a suitable regularisation scheme. The UV divergences are then removed with a procedure called renormalisation where one has to redefine the fields of the QCD Lagrangian. The renormalisation procedure will be explained in Chapter 1.

The IR divergences are of different nature and can be treated separately. They are the result of situations were two massless particles cannot be distinguished from each other in phase space, either because one has very small energy relatively to the other (soft limit) or their relative angle is very small (collinear limit). The IR divergences cancel out for carefully defined observables as we will see in Chapter 2.

In Chapters 3, 4 and 5 we will study methods for the calculation of multi-loop integrals. We will use these techniques to compute one and two-loop integrals with up to four light-like external legs which are relevant for the scattering of two initial state massless particles to two final state massless particles. In particular, they can be used for the calculation of the hadron-hadron$\rightarrow$2 jets cross-sections at Next-to-Next-to-Leading-Order (NNLO) accuracy in perturbation series.

Knowledge of the cross-section at NNLO accuracy is important for many reasons. First, one would improve the state-of-the-art theoretical prediction truncated at next-to-leading order (NLO) which, although it gives a good description of experimental data, suffers from a big dependence on unphysical scales. Such scales are present whenever we terminate the perturbation series in a truncation point. In an all-orders calculation the dependence on unphysical scales of the higher order terms counteracts the dependence of the lower-order terms. Therefore it is important to calculate as many higher order terms as possible in order to allow this cancellation to happen. A calculation of the NNLO term is thus important since we expect the sensitivity of physical observables on the variation of such scales to be reduced resulting in a more accurate theoretical prediction. In addition, one can start discussing the validity of the perturbative expansions, since a comparison of the relative size of the NNLO result to the NLO result will be possible. Finally, the forthcoming experiments at Tevatron and LHC are expected to yield experimental data of very high quality at a very broad range of energies superseding the accuracy of the current NLO theoretical prediction.

In Chapter 6 we compute the matrix elements at NNLO for the quark scattering processes $q\bar{q}\rightarrow q\bar{q}$, and $q\bar{q}\rightarrow Q\bar{Q}$, using Conventional Dimensional Regularisation and renormalising with the $\overline{\mathrm{MS}}$ scheme. This consists the main result of the thesis. Similar results have been recently produced for the whole set of virtual corrections for the processes contributing to hadron-hadron→2 jets (see [1, 2, 3, 4, 5]).

Chapter 1

Basic aspects of QCD

In this Chapter we give a brief introduction to QCD emphasizing only the aspects needed for the rest of this thesis. For a detailed introduction to Particle Theory, Quantum Field Theory and QCD the references [6, 7, 8, 9, 10, 11, 12] may be consulted.

1.1 The quark model

Hadrons are the particles which undergo strong interactions. They are observed either in fermionic (baryons) or bosonic (mesons) states. The big number of observed hadrons was an indication that they were not elementary entities but composite objects of other elementary constituents. According to the quark model, the baryons are bound states of three quarks (qqq) while the mesons are bound states of a quark and an anti-quark ($q\bar{q}$). There have been observed six species (flavors) of quarks: up(u), down(d), strange(s), charm(c), bottom(b) and top(t), all carrying spin 1/2. The electric charge of u, c, and t is $+2/3$ while the charge of d, s and b is $-1/3$.

Problems with the spin statistics of baryon bound states, suggested that quarks must be allowed an additional degree of freedom to the electric charge and the flavor, which is named color charge. To distinguish between three otherwise identical quarks making for example the uuu baryon state, one has to introduce at least three different color indices (e.g red, blue, green). Another experimental fact is that all observed hadrons are confined to colorless states (red+blue+green, red+anti-red, etc). No single quark or bound colorful states of two quarks qq, etc have ever been observed.

Confinement, is an additional theoretical hypothesis but it is believed that it may be a consequence of the dynamical properties of the quarks.

The dynamics of the elementary particles in hadrons is described by Quantum Chromodynamics (QCD). Quarks are considered to be point-like entities, as demonstrated from the scaling behavior observed in deep inelastic experiments, carrying color charge. In analogy with QED where charged particles interact via the mediation of the photon, in QCD the carriers of the strong interaction are bosons called gluons.

The theory postulates invariance under local transformations of the $SU(3)$ group. The quarks transform according to the fundamental representation and the anti-quarks according to the complex conjugate representation. The gluons transform in the adjoint representation. As a consequence, the basic color singlet states $q_i\bar{q}^i$ and the totally antisymmetric $\epsilon^{ijk}q_iq_jq_k$ correspond to the observed meson and baryon states.

1.2 The QCD Lagrangian

The full QCD Lagrangian density consists of

$$\mathcal{L}_{QCD} = \mathcal{L}_{classical} + L_{gauge-fixing} + \mathcal{L}_{ghost} \tag{1.1}$$

$\mathcal{L}_{classical}$ describes the dynamics of the quarks as relativistic spin-1/2 particles, carrying color charge. Invariance under local $SU(N)$ transformations, with $N = 3$ color degrees of freedom, demands the existence of $N^2 - 1$ vector boson gluons mediating the interactions between quarks. Specifically, we write

$$\mathcal{L}_{classical} = \sum_f \bar{\psi}_{f,i}\left(i\not{D}_{ij} - m_f\delta_{ij}\right)\psi_{f,j} - \frac{1}{4}F^{\alpha}_{\mu\nu}F^{\mu\nu,\alpha} \tag{1.2}$$

where the quark fields $\psi_{f,i}$ carry a flavor index f and a color index i. We adopt the notation $\not{A} = \gamma_\mu A^\mu$ where the Dirac gamma matrices satisfy the Clifford algebra

$$\{\gamma^\mu, \gamma^\nu\} \equiv \gamma^\mu\gamma^\nu + \gamma^\nu\gamma^\mu = 2g^{\mu\nu}. \tag{1.3}$$

The covariant derivative is

$$D^\mu_{ij} = \partial^\mu\delta_{ij} - igA^\mu_\alpha t^\alpha_{ji} \tag{1.4}$$

where the gluon fields A^{μ}_{α} carry color indices α running from $1, \ldots, N^2 - 1$. The matrices t^{α}_{ij} are the generators of the fundamental representation of $SU(N)$, and their commutator defines the group structure constants

$$\left[t^a, t^b\right] = i f_{abc} t^c. \tag{1.5}$$

The coupling strength of the quarks to the gluons is g. The kinetic energy term of the gluon fields is built in terms of the field strength tensor constructed by the commutator of two covariant derivatives

$$[D_\mu, D_\nu] = i g t^a F^a_{\mu\nu}, \tag{1.6}$$

where

$$F^a_{\mu\nu} = \partial_\mu A^a_\nu - \partial_\nu A^a_\mu + g f_{abc} A^b_\mu A^c_\nu. \tag{1.7}$$

In QCD, gluons carry color charge themselves and due to the last term of Eq. 1.7 we can have gluon self-interactions. In QED this non-abelian term is missing and we do not observe interactions between the neutral photons.

The classical part of the Lagrangian respects the basic principle of gauge invariance, where the fields transform as:

$$\psi'_f = U\psi_f, \tag{1.8}$$

$$t^a {A'_\mu}^a = U\left(t^a {A_\mu}^a - \frac{i}{g} U^{-1} \partial_\mu U\right) U^{-1} \tag{1.9}$$

with U a local transformation of the fundamental representation of $SU(N)$

$$U = \exp\left(-i t^a \theta^a(x)\right) \tag{1.10}$$

where $\theta^a(x)$ is an arbitrary function.

One gets quickly into problems trying to quantize $\mathcal{L}_{classical}$. The first difficulty arises from the freedom of the gluon fields (the same problem is apparent in QED for photons) to change by a total derivative and leave the Lagrangian invariant (gauge transformation). In the canonical quantization method this problem appears as a vanishing conjugate momentum for the time-like components of the gluon field, thereby invalidating the canonical commutation relations. In the path integral formalism, the contribution of each gluon field to the path integral over the exponential of the action is overestimated by an infinite amount since one can perform an infinite number of gauge transformations to the field without changing the action. It is necessary to impose a constraint on the gluon fields by forcing them to choose only one of the possible gauges. This is the role of the gauge-fixing term in the total QCD Lagrangian

$$\mathcal{L}_{gauge-fixing} = -\frac{1}{2\xi}\left(\partial_\mu A_a^\mu\right)^2 \tag{1.11}$$

which specifies the gauge in a covariant manner. The parameter ξ is arbitrary. The total Lagrangian is no longer gauge invariant, but the physical predictions stemming from it should be gauge invariant and independent of the parameter ξ. In the rest of this thesis we shall choose the value $\xi = 1$ corresponding to the so called Feynman gauge.

Even with the addition of the gauge-fixing term we still have not restricted the gluon fields to only two physical polarisations [1]. To account for this we need to introduce a new fictitious field which is called the Fadeev-Popov ghost. Although it is a scalar field with a boson-like propagator it exhibits fermionic behavior since it satisfies anticommutation relations. The ghost term in the Lagrangian has the form

$$\mathcal{L}_{ghost} = \left(\partial_\mu \chi_a^*\right)\left(\partial^\mu \delta_{ab} - g f_{abc} A_c^\mu\right)\chi_b \tag{1.12}$$

In QED ($f_{abc} = 0$) there is no need to introduce a ghost, since it does not interact with any other physical field, and can be integrated out from the path integral of the exponential of the action.

1.3 Feynman rules

The QCD Lagrangian is the basis for theoretical calculations of physical observables which can ultimately be compared with experiment. Experimental information usually consists of measurements of cross-sections for the scattering of particles, or their decay rates. In general, we start from a very well prepared initial state with a given particle content and after interactions take place we measure the production rates of particles in the final state.

From the theoretical point of view, the initial and final states are related to each other through the $S-$matrix, which describes the evolution of the system during

[1] Alternatively, we could have chosen the so called axial gauges restricting the gluons to two physical polarisations right from the beginning.

the interactions. Unfortunately, it is very hard to attempt a complete evaluation of the $S-$matrix, and we usually restrict ourselves to finding approximate solutions using perturbation theory. The success of the approximation relies on the size of the perturbation parameter, which in QCD is the coupling constant a and is related to the strength which the fields interact (couple) with each other g via

$$a = \frac{g^2}{4\pi}. \tag{1.13}$$

As we will see later, a becomes small at high energies and the perturbative expansion is valid.

There is a pictorial method to find the terms of the perturbative expansion with the use of Feynman diagrams. One has to draw all the possible configurations of propagating particles and interactions connecting the initial and final states which are allowed from the Lagrangian. Each diagram, belongs to a specific order in the perturbation series and we consider only those which contribute to the order of the approximation. From the Lagrangian we can read off the Feynman rules that assign a meaningful mathematical expression to the various parts of the diagrams. Finally, we have to compute each of the diagrams and take their sum.

Here, we present the Feynman rules for QCD. Gluons are denoted with curly-lines, quarks with solid-lines and ghosts with dashed-lines. The color indices of gluons and ghosts are denoted with $\alpha, \beta, \gamma, \delta$ and for the quarks with i, j. The Lorentz indices are denoted with $\mu, \nu, \ldots$ while spinor and flavor indices for quarks are implicit.

The gluon quark and ghost propagators are respectively,

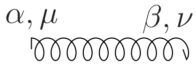

$$\delta_{\alpha\beta}\left[-g_{\mu\nu} + (1-\xi)\frac{p_\mu p_\nu}{p^2+i0}\right]\frac{i}{p^2+i0}$$

$$\delta_{ij}\frac{i}{\not{p}-m+i0}$$

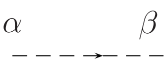

$$\delta_{ab}\frac{i}{p^2+i0}$$

At the denominator of each propagator we assign a small positive imaginary part (Feynman prescription) originating from causality arguments and its role is to ensure that the propagation of particles is from earlier to later moments in time.

The interaction vertices are:

- The triple-gluon vertex

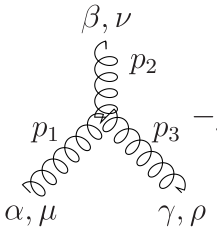

$$-g\, f_{\alpha\beta\gamma}\; [(p_1 - p_2)^\rho g^{\mu\nu} + (p_2 - p_3)^\mu g^{\nu\rho} + (p_3 - p_1)^\nu g^{\rho\mu}]$$

All particles are incoming, $p_1^\mu + p_2^\mu + p_3^\mu = 0$.

- The four-gluon vertex

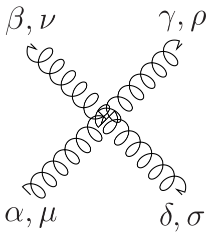

$$\begin{aligned}
&-g^2\, f_{\lambda\alpha\gamma}\, f_{\lambda\beta\delta}\; [g^{\mu\nu} g^{\rho\sigma} - g^{\mu\sigma} g^{\nu\rho}] \\
&-g^2\, f_{\lambda\alpha\delta}\, f_{\lambda\beta\gamma}\; [g^{\mu\nu} g^{\rho\sigma} - g^{\mu\rho} g^{\nu\sigma}] \\
&-g^2\, f_{\lambda\alpha\beta}\, f_{\lambda\gamma\delta}\; [g^{\mu\rho} g^{\nu\sigma} - g^{\mu\sigma} g^{\nu\rho}]
\end{aligned}$$

- The quark-gluon vertex

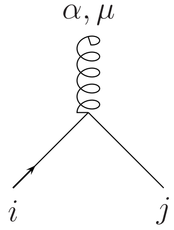

$$-i\, g\, t^{\alpha}_{ji}\, \gamma^\mu$$

- The ghost-gluon vertex

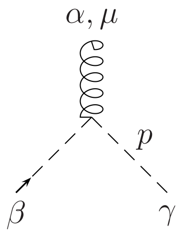

$g\, f_{\alpha\beta\gamma}\, p^{\mu}$

In addition,

- for each loop with momentum k we perform the integration with measure $\int d^D k/(2\pi)^D$, where D is the dimension,
- multiply with -1 for each quark or ghost loop,
- multiply with a symmetry factor, accounting for equivalent permutations of the fields of the diagram.

Given the Feynman rules we can write a mathematical expression for any physical amplitude at any order in perturbation theory. The difficulty lies in evaluating these expressions and especially in performing the integrations over the loop-momenta. Loop integrals in $D = 4$ dimensions often diverge. We separate the divergences in ultraviolet (UV) and infrared (IR).

- UV are the divergences due to the singular behavior of Feynman integrals at large loop momenta. They can be systematically removed order by order in QCD by a procedure called renormalisation, where the parameters of the Lagrangian are rendered finite by an infinite shift.
- IR divergences occur when one of the propagators in the loop becomes zero for a specific value of the loop momentum. For massive propagators this never happens, but in QCD the presence of gluons and light-quarks gives rise to IR divergences. As we shall see in Chapter 2, IR divergences cancel for carefully defined quantities, and can be largely predicted for one and two-loop amplitudes

In order to apply the renormalisation procedure or to make manifest the cancellation of the IR divergences, it is necessary to quantify the infinities and separate them from the finite part of the integrals. This procedure is called regularisation. There are quite a few regularisation schemes treating the problem of quantifying the infinities of the integral. The most commonly used is dimensional regularisation (Ref. [13, 14, 15]), where we treat the number of dimensions as a non-integer number. Dimensional regularisation respects all the symmetries of the original Lagrangian and the resulting Green's functions, and it will be used throughout this thesis.

1.4 Dimensional Regularisation

With dimensional regularisation we assume that the Feynman integrals are analytic functions of the number of dimensions D. UV or IR divergent integrals in D=4 dimensions are well behaved when D is not integer. We can calculate them in $D = 4-2\epsilon$ dimensions where ϵ is a parameter continuing the integral to non-integer values of the dimension. The divergences are then quantified in the form of poles $1/\epsilon^n,\ n = 1, 2, \ldots$.

As we shall see in Chapter 3 in order to integrate out the loop-momenta from a Feynman integral, it is sufficient to know the integral

$$I = \int \frac{d^D k}{i\pi^{D/2}} \frac{1}{(k^2 - A + i0)^n}, \tag{1.14}$$

where the integration is typically in $D = 4$ dimensions and n is a positive integer. The $i0$ term is the result of the Feynman prescription for the propagators and makes the integral convergent for all values of A. In the calculation of this integral we will assume that the values of the parameters of the integral are such that all convergence criteria are satisfied. This sets stringent criteria for the values of n and D. Nevertheless, at the end of our calculation we will be able to extend the applicability of our results, via an analytic continuation of the Gamma function to complex values, to a larger domain of the space of n and D.

We assume one time and $D-1$ space dimensions. The integral is in Minkowski space, and we perform a Wick rotation

$$k_0 = \to ik_0, \quad k_i = \to k_i, \quad i = 1, 2, 3 \tag{1.15}$$

to bring it in Euclidean space where it is written as

$$I = \int \frac{d^D k}{\pi^{D/2}} \frac{1}{(-k^2 - A)^n} = (-1)^n \int \frac{d\Omega_D}{\pi^{D/2}} \int_0^\infty dk \frac{k^{D-1}}{(k^2 + A)^n}, \tag{1.16}$$

We can perform the integration over the solid angle $d\Omega_D$ in D dimensions with the following trick

$$\begin{aligned}
\pi^{D/2} &= \left(\int_{-\infty}^{+\infty} dx e^{-x^2} \right)^D = \int_{-\infty}^{+\infty} d^D x \exp\left(-\sum_{i=1}^{D} x_i^2 \right) \\
&= \int d\Omega_D \int dx x^{D-1} e^{-x^2} = \left(\int d\Omega_D \right) \frac{1}{2} \int_0^\infty d\left(x^2\right) \left(x^2\right)^{\frac{D}{2}-1} e^{-\left(x^2\right)} \\
&= \left(\int d\Omega_D \right) \frac{1}{2} \Gamma\left(\frac{D}{2} \right),
\end{aligned}$$

yielding

$$\int d\Omega_D = \frac{2\pi^{\frac{D}{2}}}{\Gamma\left(\frac{D}{2}\right)}. \tag{1.17}$$

The second factor in Eq. 1.16, with the change of variables

$$x = \frac{A}{k^2 + A},$$

becomes

$$\begin{aligned}
&\int_0^\infty dk \frac{k^{D-1}}{(k^2 + A)^n} = \frac{1}{2} A^{D/2-n} \int_0^1 dx x^{n-D/2-1} (1-x)^{D/2-1} \\
&= \frac{1}{2} A^{D/2-n} \frac{\Gamma\left(n - \frac{D}{2}\right) \Gamma\left(\frac{D}{2}\right)}{\Gamma(n)},
\end{aligned} \tag{1.18}$$

where we used the definition of the Beta function

$$B(a,b) = \int_0^1 dx\, x^{a-1} (1-x)^{b-1} = \frac{\Gamma(a)\Gamma(b)}{\Gamma(a+b)}. \tag{1.19}$$

Finally, substituting Eq. 1.17 and Eq. 1.18 into Eq. 1.16 we obtain the basic formula for integration in Dimensional Regularisation (in Minkowski space)

$$\int \frac{d^D k}{i\pi^{\frac{D}{2}}} \frac{1}{(k^2 - A + i0)^n} = (-1)^n \frac{\Gamma\left(n - \frac{D}{2}\right)}{\Gamma(n)} A^{\frac{D}{2}-n}. \tag{1.20}$$

For the derivation of the above equation it was important to assume that the dimension was a positive integer, and in order to safeguard convergence in all steps, it was necessary to satisfy the constraint $n > \frac{D}{2}$. We can relax these conditions by considering a generalized definition of the Gamma function

$$\Gamma(z) = \int_0^\infty e^{-t} t^{z-1} \tag{1.21}$$

which is valid for complex numbers z with positive real parts. Using the property

$$\Gamma(x+1) = x\Gamma(x),$$

we can obtain an analytic continuation to all complex numbers except negative integers. This is very important, since it is now possible to calculate integrals, otherwise divergent, by shifting the parameters involved (dimension, powers of propagators) by a small amount away from their integer values.

In this point we should examine the behavior of the integral in terms of the variable A. When $A > 0$, the integral of Eq. 1.16 is well defined. For $A < 0$, the denominator might vanish, producing singularities. A is typically a linear combination of masses with positive coefficients and momentum invariants (Mandelstam variables) with negative coefficients. Inevitably singularities arise when the Mandelstam variables become time-like. These singularities, by their nature, cannot be regulated with dimensional regularisation. However, the small positive imaginary part assigned to the denominators of the propagators with the Feynman rules, provides appropriate analytic continuations of the integral to otherwise non-accessible kinematic regions. Whenever a crossing of a discontinuity occurs, then the integral gains an imaginary part. A thorough investigation of the analyticity properties of Feynman integrals can be found in Ref. [16].

Returning to dimensional regularisation, shifting the dimension has to be followed by some modifications in the Lagrangian of QCD in order to ensure dimensional consistency. Since the action

$$S = \int d^D x \mathcal{L} \tag{1.22}$$

is a dimensionless quantity, it is easy to deduce the mass dimensionalities of the quark and gluon fields

$$[\psi_{f,i}] = \frac{D-1}{2}, \quad [A^\alpha_\mu] = \frac{D}{2} - 1, \tag{1.23}$$

by inspection of their kinetic energy terms. From the interaction part of the Lagrangian it is then easy to deduce that the coupling constant has dimension

$$[g] = 2 - \frac{D}{2}. \tag{1.24}$$

In $D = 4$, the coupling constant has no dimension. Since we decided to use the number of dimensions as a regulator, our theory acquires one more scale. We choose to write explicitly this new scale dependence introducing an arbitrary mass μ and replacing the coupling strength with

$$g \to g\mu^{\epsilon}, \tag{1.25}$$

where $\epsilon = \frac{4-D}{2}$.

Having made the analytic continuation of loop momenta to $D = 4 - 2\epsilon$, and postulated dimensionless action in arbitrary D dimensions to fix the dimensionality of the fields, we are still left with some freedom for the number of polarisations of the internal and external quark and gluon fields. This freedom defines different dimensional regularisation schemes. Throughout this thesis we choose to work in Conventional Dimensional Regularisation (CDR), where no distinction is made between particles in loops or external states, and we consider two helicity states for massless quarks and $D-2$ helicity states for gluons.

1.5 Renormalisation

As we have already mentioned, QCD suffers from ultraviolet infinities in the Feynman integrals at each order of the perturbation series. Fortunately, it turns out that QCD is a renormalisable theory.

Starting from the Lagrangian given in Section 1.2, we can redefine all the fields and parameters by a multiplicative factor. For example we can set

$$A_{\mu}^{a} = Z_3^{1/2} A_{r,\mu}^{a}, \tag{1.26}$$

$$\psi_{f,i} = Z_2^{1/2} \psi_{fr,i}, \tag{1.27}$$

$$g = Z_g g_s, \tag{1.28}$$

$$\ldots$$

So far we have done nothing apart of a simple renaming of the terms of the Lagrangian, and we would therefore expect the path integral over the action (which generates the Green's functions of the theory and the S-matrix elements) to remain the same.

The Green's functions in terms of the original fields have divergences in the ultraviolet limit. With the above redefinition we can express the same divergent quantities in terms of the new renormalised fields $A_r, \psi_r, \ldots$ and the multiplicative factors $Z_3, Z_2, Z_g, \ldots$. In other words, one could write a Green's function of the original fields as the product of a Green's function of the renormalised fields times the multiplicative factors Z. We can successfully renormalise our theory if we can absorb all the UV divergences in the multiplicative factors, leaving the renormalised Green's functions UV-divergence free.[2] We can then re-interpret the Green's functions of the renormalised fields as the ones that have physical meaning [15].

Renormalisability is a desirable property for every serious candidate for a physical theory since predictions for observables, such as cross-sections, decay rates, etc, should be finite. QCD enjoys this property and one can prove by induction that the cancellation of the UV divergences works at all orders for all Green's functions by readjusting the multiplicative factors Z at each order. The proof is a difficult one but it is simplified by exploiting the symmetries of the Lagrangian (e.g. gauge invariance) which yield relations among the Z factors (Slavnov - Taylor identities).

The renormalisation procedure has a certain degree of arbitrariness. Practically, there are two choices that one has to make. In subtracting the divergences from the Green's functions, together with the singular parts, we have the freedom to absorb different amounts of finite parts into the infinite multiplicative factors Z. The prescription one uses to subtract the divergences defines the *renormalisation scheme*. We shall use the $\overline{\text{MS}}$ (modified minimal subtraction) scheme, where the prescription used is to remove only the UV poles in $\bar{\epsilon}$, where we have defined

$$\frac{1}{\bar{\epsilon}} = \frac{1}{\epsilon} e^{-\gamma\epsilon} (4\pi)^{\epsilon} . \tag{1.29}$$

and γ is the Euler-Marchesini constant.

The second choice concerns the mass scale μ (renormalisation scale) introduced with dimensional regularisation in order to preserve a dimensionless action. The renormalisation scale remains in the finite part of the Green's functions leaving an arbitrariness for the renormalised Green's functions after the subtraction of divergences.

According to the choices for the renormalisation scheme and scale we end up with different expressions for the same physical quantity. Self-consistency requires

[2] They can still have infrared (IR) divergences due to vanishing propagators, but these divergences will safely cancel out for physically meaningful quantities.

that those expressions are all equivalent with each other. This imposes very strict limits on the behavior of physical (renormalised) quantities when varying renormalisation scale or changing the renormalisation scheme and they need to satisfy appropriate differential equations known as *renormalisation group equations.* They can be derived by demanding that the original unrenormalised ("bare") parameters of the Lagrangian or measurable physical quantities are independent of μ.

1.6 Running a_s and perturbative expansions in QCD

In the basic relation between the bare and the renormalised coupling strength

$$g = Z_g \, g_s \mu^\epsilon$$

or, equivalently for the coupling constant,

$$\alpha = Z_g^2 \alpha_s \left(\mu^2\right)^\epsilon \tag{1.30}$$

the multiplicative factor Z_g can be calculated in a perturbative expansion, yielding (in $\overline{\mathrm{MS}}$),

$$\alpha \, S_\epsilon = \alpha_s \, (\mu^2)^\epsilon \left[1 - \frac{\beta_0}{\epsilon}\left(\frac{\alpha_s}{2\pi}\right) + \left(\frac{\beta_0^2}{\epsilon^2} - \frac{\beta_1}{2\epsilon}\right)\left(\frac{\alpha_s}{2\pi}\right)^2 + \mathcal{O}(\alpha_s^3)\right], \tag{1.31}$$

where

$$S_\epsilon = (4\pi)^\epsilon e^{-\epsilon\gamma}, \qquad \gamma = 0.5772\ldots = \text{Euler constant.} \tag{1.32}$$

The coefficients β_0 and β_1 for N_F (massless) quark flavours are

$$\beta_0 = \frac{11C_A - 4T_R \, N_F}{6} \quad , \qquad \beta_1 = \frac{17C_A^2 - 10C_A T_R \, N_F - 6C_F T_R \, N_F}{6} \quad . \tag{1.33}$$

where N is the number of colours, and

$$C_F = \frac{N^2 - 1}{2N}, \qquad C_A = N, \qquad T_R = \frac{1}{2}. \tag{1.34}$$

for $SU(N)$.

The bare coupling α does not depend on the renormalisation scale μ,

$$\mu^2 \frac{\partial \alpha}{\partial \mu^2} = 0 \tag{1.35}$$

which, by inserting Eq. 1.30 and defining the beta function

$$\beta\left(\alpha_s\right) \equiv \mu^2 \frac{\partial \alpha_s}{\partial \mu^2}, \tag{1.36}$$

yields the result,

$$\beta(\alpha_s) = \frac{-\epsilon \alpha_s}{1 + 2\frac{\alpha_s}{Z_g}\frac{\partial Z_g}{\partial \alpha_s}} \tag{1.37}$$

From Eq. (1.31) it is easy to infer Z_g order by order in a_s, and substituting into Eq. (1.37), after an expansion in a_s we obtain

$$\mu^2 \frac{\partial \alpha_s}{\partial \mu^2} = \beta(\alpha_s) = -\beta_0 \alpha_s^2 - \beta_1 \alpha_s^3 - \ldots \tag{1.38}$$

The solution of the above differential equation, which takes the integral form

$$\int_{\alpha_s(\mu_0^2)}^{\alpha_s(\mu^2)} \frac{d\alpha}{\beta(\alpha)} = \log\left(\frac{\mu^2}{\mu_0^2}\right), \tag{1.39}$$

determines the behavior of the strong coupling with the energy scale μ^2, given a known value of it at an energy scale μ_0^2.

When both $\alpha_s(\mu^2)$ and $\alpha_s(\mu_0^2)$ are small, one can attempt a perturbative solution. For example, keeping only the two first terms from the r.h.s of Eq. (1.38), we obtain the solution

$$\frac{1}{\alpha_s(\mu^2)} - \frac{1}{\alpha_s(\mu_0^2)} + \frac{\beta_1}{\beta_0}\log\left(\frac{\alpha_s(\mu^2)}{\alpha_s(\mu_0^2)}\right) - \beta_0 \log\left(\frac{\mu^2}{\mu_0^2}\right) = 0 \tag{1.40}$$

For up to sixteen active light quark flavors the coefficient β_0 is positive. This has very important consequences for the validity of perturbative expansions in QCD since with increasing energy scale μ^2, the strong coupling becomes smaller. Let us justify this statement further.

A dimensionless physical observable R should be independent of the renormalisation scale μ. If R depends on the squared energy scale s, it will be a function of the dimensionless ratio s/μ^2 and the strong coupling $\alpha_s(\mu^2)$. We can then write the renormalisation group equation

$$\frac{dR}{d\mu^2} = 0, \tag{1.41}$$

which takes the form

$$\left[\frac{\partial}{\partial \log(\mu^2)} + \beta\left(\alpha_s\right)\frac{\partial}{\partial \alpha_s}\right] R\left(\alpha_s(\mu^2), s/\mu^2\right) = 0 \tag{1.42}$$

or, by defining $t = \log(s/\mu^2)$,

$$\left[-\frac{\partial}{\partial t} + \beta(\alpha_s)\frac{\partial}{\partial \alpha_s}\right] R\left(\alpha_s(\mu^2), e^t\right) = 0 \tag{1.43}$$

It is easy to prove that $R(\alpha_s(s), 1)$ is a solution of the last equation. Indeed,

$$\begin{aligned}\frac{\partial R(\alpha_s(s),1)}{\partial t} &= \frac{\partial \alpha_s}{\partial t}\frac{\partial R(\alpha_s(s),1)}{\partial \alpha_s}\\ &= \beta(\alpha_s)\frac{\partial R(\alpha_s(s),1)}{\partial \alpha_s},\end{aligned}$$

which completes the proof.

So we can conclude that the dimensionless physical quantity R measured at the energy scale s, is a function of the strong coupling at the same energy $\alpha_s(s)$. From Eq. (1.40) we found that for big energy scales α_s becomes small. This is the very property of QCD (*"asymptotic freedom"*) which allows a perturbative expansion of R in terms of α_s for large energies.

$$R = R(\alpha_s(s), 1) = r_1\alpha_s(s) + r_2\alpha_s(s)^2 + r_3\alpha_s(s)^3 + \dots \tag{1.44}$$

1.7 Higher order corrections in QCD

There are a few challenges in the perturbative expansion of the last section. The first challenge comes from the fact that α_s is a free parameter of the QCD Lagrangian. Therefore we can only extract its value comparing with experimental data for the physical observable R. For a reliable comparison, we need to know as many of the r_i coefficients as possible. In practice we truncate the perturbation series just after a few first terms, inducing a systematic error in calculating the physical observable R due to the ignorance of the higher order corrections. This error is then reflected as an uncertainty in the determination of α_s.

Another problem due to the truncation of the series is that the theoretical predictions become sensitive to the variation of unphysical scales, such as the renormalisation scale. In Eq. 1.44 we choose to resum all the logarithms depending on μ^2 in terms of the "physical" scale s. An equivalent perturbative series would be

$$R = R(\alpha_s(s), \mu^2/s) = r_1(s/\mu^2)\alpha_s(\mu^2) + r_2(s/\mu^2)\alpha_s(\mu^2)^2 + r_3(s/\mu^2)\alpha_s(\mu^2)^3 + \dots, \tag{1.45}$$

where μ^2 can take an arbitrary value (as long as $\alpha_s(\mu^2)$ is small). Inserting the last expansion in Eq. (1.43), it is easy to see that the first term r_1 does not depend on μ^2,

$$\frac{\partial r_1}{\partial t} = 0.$$

As a consequence, the leading order of the series term depends on μ^2 only through $\alpha_s(\mu^2)$. From the expansion of the β function,

$$\mu^2 \frac{\partial \alpha_s}{\partial \mu^2} = -\beta_0 \alpha_s^2 - \beta_1 \alpha_s^3 - \ldots,$$

we see that the variation (derivative) of α_s with μ^2 is of higher order than $\mathcal{O}(\alpha_s)$, since the leading term of the r.h.s is of order $\mathcal{O}(\alpha_s^2)$. Therefore, the variation due to α_s of the LO term in Eq. 1.45 is compensated by the higher order terms in the series. Working upwards for the general $r_n \alpha_s^n$ term, we find that the variation of r_n serves to cancel the dependence on μ of lower order terms, while the variation of α_s^n gets canceled from higher orders. Inevitably, if we truncate the series we do not allow the cancellation of the scale dependence between different orders, and we are therefore left with a residual dependence on μ^2 of one order higher of the truncation point.

It is natural to expect that the sensitivity of the truncated series on μ^2 decreases as we increase the number of calculated terms. For example, figure 1.1 shows the predicted differential cross section for producing jets with transverse energy of 100 GeV in the CDF detector at the Tevatron. The renormalisation scale dependence is shown for the LO, NLO and NNLO order predictions (this is known from the renormalisation group equation up to a renormalisation scale independent constant). Note that the factorization scale is kept constant. We see that for renormalisation scales within a factor of two of the jet energy, the renormalisation scale uncertainty is reduced from 20% to 9% to 1%. Interestingly, the experimental statistical error from CDF with Run 1 data for this data point is currently about 2%, while the systematic error is about 10%.

The majority of theoretical predictions for physical observables in QCD include Next to Leading Order (NLO) terms in perturbation series and in general they show very good agreement with experimental data. Nevertheless, the dependence on unphysical scales is still significant. What is more, forthcoming experiments in the new generation accelerators (Tevatron, LHC) are expected to obtain high

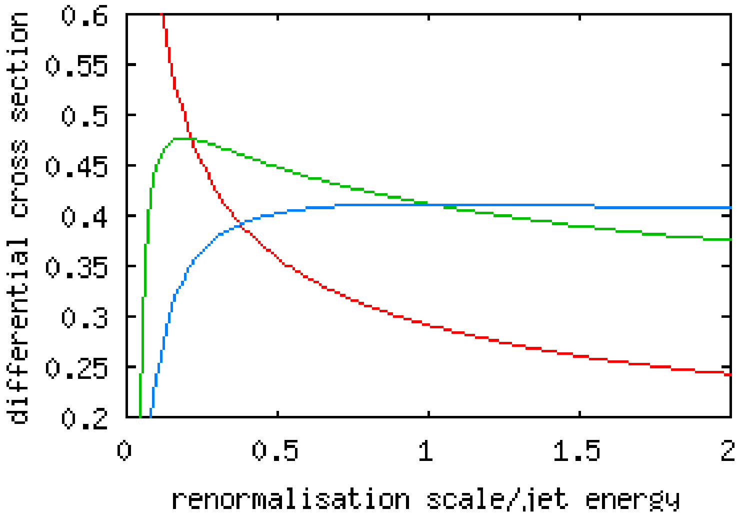

Figure 1.1: The scale dependence decreases at higher orders. The LO is in red, NLO in green and NNLO in blue.

quality data for a much larger range of energies. The experimental uncertainties are believed to drop far below the accuracy of the theoretical predictions. It is then important to improve the theoretical calculations to a comparable precision.

The calculation of the Next-to-Next-to-Leading-Order (NNLO) terms is a very challenging work at both mathematical and computational level. The first major task is the calculation of matrix-elements at two-loop level. The number of Feynman diagrams ranges up to thousands, and their calculation involves a very big number of tensor and scalar two-loop integrals. It is the aim of this thesis to present some of the methods used for multi-loop matrix-elements calculations.

We are primarily interested in the one- and two-loop integrals for the scattering of two initial-state to two final-state massless particles where the virtual particles produced during the interaction have massless propagators. The techniques tackling these integrals are presented in Chapters 3, 4 and 5. We will finally use the computed integrals in an explicit calculation of the matrix elements for the scattering of light-quarks (Chapter 6), which is part of the set of processes contributing to the two-jet production from hadron-hadron scattering. The calculation of matrix-elements of other contributing sub-processes can be performed with a similar approach. Before that, in Chapter 2 we shall look at general features of cross sections for hadron-

hadron interactions. The requirement that the total cross-section is free of infrared singularities provides the tools to largely predict the poles in ϵ of the NNLO matrix elements of Chapter 6, and serves as a very stringent check of our results. The formalism for the prediction of the poles at NNLO matrix elements is almost process independent and was developed by Catani (Ref.[17, 18])

Chapter 2

Infrared Divergences

In subsequent chapters we will study integrals for $2 \to 2$ scattering of massless particles, and we will use them to calculate matrix-elements at NNLO for physical processes such as the scattering of two initial-state to two final-state quarks. Using the same techniques we can calculate matrix elements for other QCD processes such as $q\bar{q} \to gg$ [1], $gg \to gg$ [5] or the processes $e^+e^- \to \mu^+\mu^-$ [19], $e^+e^- \to e^+e^-$ [19], $\gamma\gamma \to \gamma\gamma$, $q\bar{q} \to \gamma\gamma$, etc. where we can consider that external particles are light-like and the internal propagators are massless.

The processes involving quarks and gluons at initial states are very important for the study of the hadron-hadron scattering at the Tevatron and LHC. The computation of the hadronic cross-section at NNLO accuracy is anticipated to improve the state of the art NLO approximation and match better the experimental precision.

There is a direct connection of the cross-section with hadronic initial states to the cross-section of the quark and gluon constituents (partons). For inclusive quantities one can write the following *factorization* formula

$$\sigma(P_1, P_2) = \sum_{i,j} \int dx_1 dx_2 f_i(x_1, \mu_F^2) f_j(x_2, \mu_F^2) \sigma_{ij}(p_1, p_2, \alpha_s(\mu^2), s/\mu^2, s/\mu_F^2) \tag{2.1}$$

The initial hadrons have momenta P_1 and P_2 where the partons which participate in the hard scattering carry a fraction of the initial momenta $p_1 = x_1 P_1$ and $p_2 = x_2 P_2$. The scale $s = (P_1 + P_2)^2$ may serve as a reference ("physical") scale of the hard scattering.

The functions $f_{i,j}(x, \mu_F^2)$ are *parton distribution functions* (pdf) which describe the initial state of the hadrons in terms of their constituents. The effects binding together the partons in the hadrons are not calculable with perturbation theory. Nevertheless, they are independent of the particular process, and may be extracted from other scattering experiments such as Deep Inelastic Scattering (DIS).

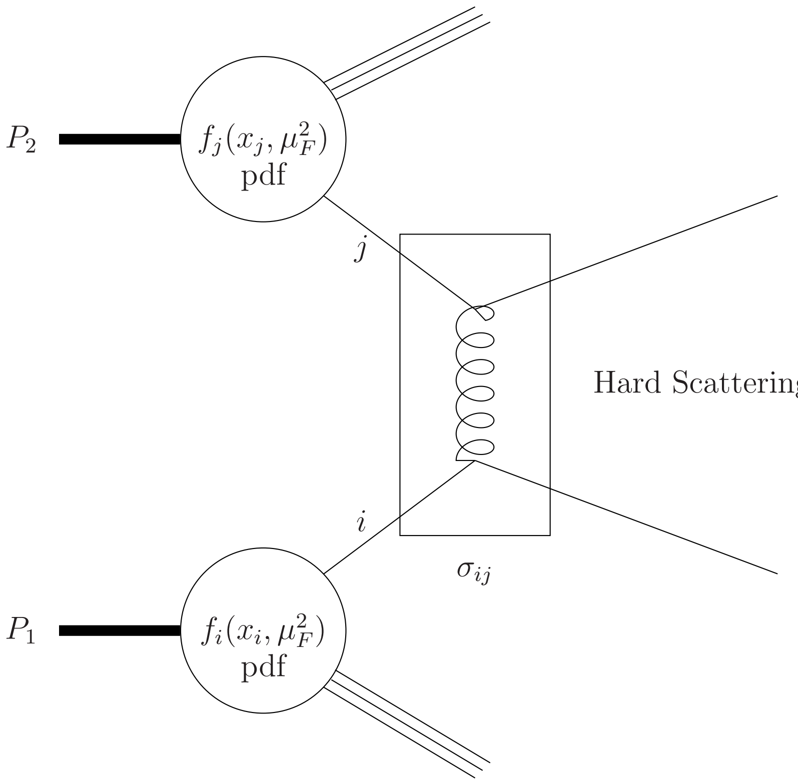

In order to distinguish between the non-perturbative effects in the hadrons from the perturbative interactions of the partons we have to introduce an unphysical scale μ_F^2. We can think of μ_F^2 as a cutoff discriminating between soft and hard radiation from the initial partonic states. For example, when a gluon with small transverse momentum is emitted from a parton in one of the hadrons it is not able to probe the other hadron, and its effect is only to alter the initial state of the partonic cross-sections. Therefore its contribution should be included in the evolution of the pdf's. On the contrary, emitted gluons with high transverse momentum resolve the second hadron and are included in the hard scattering matrix-elements of the partonic cross-sections.

The total hadronic cross-section is independent of μ_F^2, but the pdf's and the partonic cross-sections depend on it separately. Similar to the renormalisation scale

μ^2, fixed order perturbation theory introduces a sensitivity with the variation of μ_F^2. We expect that the more terms in perturbation series we calculate the less sensitive the cross-section will be.

From calculating the matrix-elements for the partonic cross-sections to the total hadronic cross-section there are many technical issues to be resolved, concerning the phase-space integrations and the determination of the pdf's and their evolution at NNLO accuracy. In this thesis we deal only with the matrix-elements. Nevertheless, the requirement of a finite cross-section puts very strict limitations on their singularity structure.

Catani and Seymour [18] found a general (process-independent) algorithm to predict the infrared singular behavior of one-loop amplitudes. Later, Catani [17] generalized the method at two-loops. Unlike the one-loop case where all poles are predicted, at two-loops we can predict precisely the $1/\epsilon^4$, $1/\epsilon^3$ and $1/\epsilon^2$ poles, and the part of the $1/\epsilon$ pole which depends on logarithms and generalized polylogarithms. There is a residual $1/\epsilon$ piece depending on constants (π^2, ζ_3, C_F, $C_A, \ldots$) which is particular for the process and depends on the renormalisation scheme.

After an explicit calculation of the two-loop matrix elements, it is very important to be able to check that their pole structure is correct so that we can guarantee the cancellation of the poles in the total cross-section. The fact that we agree with the predictions stemming from Catani's formalism, is a very strong check for the correctness of the calculation because typically all Feynman diagrams of the massless QCD amplitudes are infrared divergent. In the rest of this chapter we will explain the origin of the infrared singularities, and motivate Catani's formalism. We will finally apply it for the case of the unlike-quark scattering at two-loops.

2.1 Virtual infrared divergences

We consider the process of a Z boson splitting into a quark and anti-quark

$$Z(p) \rightarrow q(p_1) + \bar{q}(p_2), \tag{2.2}$$

where the momentum assignments are in parenthesis, and $p = p_1 + p_2$, with $p^2 = M_Z^2$ and $p_1^2 = p_2^2 = 0$.

We shall use this process in order to demonstrate the origin of the infrared divergences and define physical observables which are finite after renormalisation. We shall also explain how to apply Catani's formalism for general one and two-loop QCD amplitudes and give some motivation for it from the process of Eq. 2.2.

The differential decay rate for the Z-decay to a quark-antiquark pair takes the form

$$d\sigma^{q\bar{q}} = \frac{1}{2M_Z}\, d\Pi_2 \,\overline{|\mathcal{M}|}^2 \tag{2.3}$$

where the two particle phase-space is

$$d\Pi_2 = \frac{d^{D-1}p_1}{(2\pi)^{D-1}2E_1}\frac{d^{D-1}p_2}{(2\pi)^{D-1}2E_2}\,(2\pi)^D\,\delta^D(p-p_1-p_2) \tag{2.4}$$

and the matrix-element $\mathcal{M}$ can be expanded perturbatively as

$$\mathcal{M}^{q\bar{q}} = \mathcal{M}_0^{q\bar{q}} + \mathcal{M}_1^{q\bar{q}} + \mathcal{O}(\alpha_s^2) \tag{2.5}$$

with

$\mathcal{M}_0^{q\bar{q}} =$ 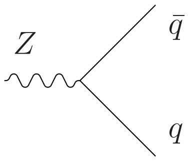

and

$\mathcal{M}_1^{q\bar{q}} =$ 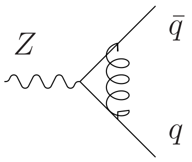

In Eq. 2.3 we sum over all helicities and colors.

At leading order (LO) it is straightforward to calculate $\overline{|\mathcal{M}_0|}^2$ and perform the phase-space integrations yielding the finite result in $D = 4$

$$\sigma_0^{q\bar{q}} = \int d\sigma_0^{q\bar{q}} = \frac{1}{2M_Z}\, d\Pi_2\,\overline{|\mathcal{M}_0|}^2 = \frac{1}{3}N\alpha Q_f^2 M_Z \tag{2.6}$$

where N is the number of colors, Q_f is the charge of the produced quark flavor, and α is the electromagnetic coupling constant.

We now want to include the next order in perturbation series. $\mathcal{M}_1$ is harder to evaluate, since we face a one-loop integral computation. Such computations can be performed by the tools developed in subsequent chapters, and we find that

$$\mathcal{M}_1 = \frac{\alpha_s}{2\pi}\mathcal{M}_0\Omega, \tag{2.7}$$

where

$$\Omega = C_F \left(-\frac{\mu^2}{M_Z^2}\right)^{\epsilon} \frac{e^{\gamma\epsilon}\Gamma\left(1+\epsilon\right)\Gamma\left(1-\epsilon\right)^2}{\Gamma\left(1-2\epsilon\right)} \left[-\frac{1}{\epsilon^2} - \frac{3}{2\epsilon} - 4 + \mathcal{O}(\epsilon)\right] \tag{2.8}$$

This result is very worrying since it diverges in $D = 4$ ($\epsilon = 0$), and the decay rate is unavoidably singular

$$\sigma_1^{q\bar{q}} = \int \frac{1}{2M_Z} d\Pi_2 \left(\overline{|\mathcal{M}_0|}^2 + 2\,\mathrm{Re}\,\overline{\mathcal{M}_0^\dagger \mathcal{M}_1}\right) = \sigma_0^{q\bar{q}} \left\{1 + \frac{\alpha_s}{2\pi} 2\,\mathrm{Re}\,\Omega\right\} \tag{2.9}$$

It is easy to trace the origin of the singularities in this calculation. From the renormalisation group equation we know that there are no ultraviolet singularities in this order, so this is not the place to look at. For the derivation of Ω we had to calculate integrals of the type

$$\int \frac{d^D k_1}{i\pi^{D/2}} \frac{f(k_1^\mu, p_1^\mu, p_2^\mu)}{k_1^2 (k_1 + p_1)^2 (k_1 + p_2)^2} \tag{2.10}$$

where f is a second degree polynomial. The above integral becomes divergent for the loop-momentum configurations where one of the terms in the denominator vanishes. The divergences of this kind are called infrared because they occur for small values of the loop-momentum. It should also be noted, that this is a consequence of the existence of massless particles (light-quarks, gluons) in the theory. If all propagators had a mass term the infrared singularities would have been regulated by the mass, producing a finite result.

2.2 Real infrared divergences

Before trying to make sense of Eq. (2.9) we turn our attention to the process of the quark-antiquark pair creation together with the emission of a gluon

$$Z(p) \rightarrow q(p_1)\bar{q}(p_2)g(k), \tag{2.11}$$

where the momenta of the particles are shown in parenthesis, and $p = p_1 + p_2 + k$.

At order $\mathcal{O}(\alpha_s)$ we have the contribution of the following two diagrams

$\mathcal{M}_1^{q\bar{q}} =$

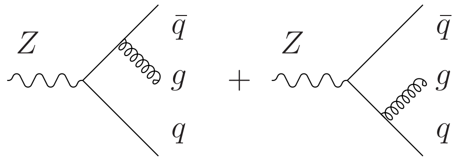

and the total decay rate is

$$\sigma_0^{q\bar{q}g} = \frac{1}{2M_Z}\int d\Pi_3 \overline{\left|\mathcal{M}_0^{q\bar{q}g}\right|^2} \tag{2.12}$$

Defining

$$x_q = \frac{2E_q}{M_Z}, \quad x_{\bar{q}} = \frac{2E_{\bar{q}}}{M_Z}, \quad x_g = \frac{2E_g}{M_Z}, \tag{2.13}$$

for the quark, antiquark and gluon energies respectively, we can write

$$\begin{aligned}\sigma_0^{q\bar{q}g} &= \sigma_0^{q\bar{q}}\left(\frac{\alpha_s}{2\pi}\right) C_F 2\frac{e^{\gamma\epsilon}}{\Gamma(1-\epsilon)}\left(\frac{\mu^2}{M_Z^2}\right)^{\epsilon}\int dx_q dx_{\bar{q}}\frac{(x_q + x_{\bar{q}} - 1)^{-\epsilon}}{(1-x_q)^{\epsilon+1}x_{\bar{q}}^{\epsilon+1}} \\ &\quad \times\left[(1-\epsilon)\frac{x_q^2 + x_{\bar{q}}^2}{2} + \epsilon\left(x_q + x_{\bar{q}} - 1\right)\right]\end{aligned} \tag{2.14}$$

where the integration region is $0 \leq x_q, x_{\bar{q}} \leq 1$, $x_q + x_{\bar{q}} \geq 1$. From momentum conservation we obtain the constraint $x_q + x_{\bar{q}} + x_g = 2$ and we can also show that

$$\begin{aligned}1 - x_q &= x_{\bar{q}}\frac{E_g}{M_Z}\left(1 - \cos\theta_{\bar{q}g}\right) \\ 1 - x_{\bar{q}} &= x_q\frac{E_g}{M_Z}\left(1 - \cos\theta_{qg}\right)\end{aligned} \tag{2.15}$$

where θ_{qg} ($\theta_{\bar{q}g}$) is the angle between the quark (antiquark) and the gluon.

In four dimensions ($\epsilon = 0$) the integral becomes divergent when $x_{q,\bar{q}}{\to}1$. From Eqs. 2.15 we see that the singularities originate from regions of phase-space where the gluon is either "soft" ($\frac{E_g}{M_Z}{\to}0$) or it is collinear to the quark ($\theta_{qg}{\to}0$) or the antiquark ($\theta_{\bar{q}g}{\to}0$). In $D = 4 - 2\epsilon$ these singularities are manifest as poles in $\epsilon = 0$ and after performing the integrations over the phase space we obtain the total decay rate

$$\sigma_0^{q\bar{q}g} = \sigma_0^{q\bar{q}}\left(\frac{\alpha_s}{2\pi}\right) C_F\left(\frac{\mu^2}{M_Z^2}\right)^{\epsilon}\frac{e^{\gamma\epsilon}\Gamma(1-\epsilon)^2}{\Gamma(1-3\epsilon)}2\left\{\frac{1}{\epsilon^2} + \frac{3}{2\epsilon} + \frac{19}{4} + \mathcal{O}(\epsilon)\right\} \tag{2.16}$$

2.3 Cancellation of infrared divergences

Comparing Eq. 2.9 with Eq. 2.16 we see that the poles in ϵ have opposite signs, i.e. the divergences due to the emission of a real soft or a collinear gluon cancel against the divergences due to the emission and re-absorption of a virtual gluon. In the final-state phase-space the configuration of a soft or collinear gluon emitted after the creation of the quark-antiquark pair is very similar to the configuration where only the pair is created. Actually, after the fragmentation of the final-state partons into hadrons producing jets the two configurations are indistinguishable.

In general, if one considers physical observables summing together all radiative processes (of the same order in α_s) which degenerate into the same final-state when some of the external particles become soft or collinear, then the result is finite. This is guaranteed by the Kinoshita-Lee-Nauenberg theorem which states that any transition probability in a theory involving massless particles is finite, provided summation over degenerate states is performed.

Returning to our example, we can write that the total rate for the Z decay into jets (partons) at order $\mathcal{O}(\alpha_s)$

$$\sigma = \sigma_1^{q\bar{q}} + \sigma_0^{q\bar{q}g} = \sigma_0^{q\bar{q}} \left(1 + \frac{3}{4} C_F \frac{\alpha_s}{\pi}\right) + \mathcal{O}(\alpha_s^2) \tag{2.17}$$

The result is finite since the sum of the two decay rates together satisfies the condition of the previous theorem in this order of the perturbation series. Obviously, if we consider only the decay rate for the production of three-jets this is not an "infrared safe" quantity. To obtain a meaningful result we need to impose an arbitrary cutoff in the integrations of Eq. 2.14 excluding the soft and collinear regions of the phase-space. The cutoff serves to distinguish between a three and a two jet configuration and the divergences in ϵ are replaced by the logarithms of the cutoff.

The situation is more complicated if we consider cross-sections where the initial state particles can radiate. This is for example the case of the partonic cross-sections contributing to the cross-section of the hadron-hadron scattering. The initial state radiation can lead again to degenerate states producing infrared singularities. The Kinoshita-Lee–Nauenberg theorem, modified to account for the sum of all degenerate external states, is still working guaranteeing the cancellation of the divergences. In this case, the sum over the initial degenerate states, involves all partonic processes contributing to the hadronic cross-section. The infrared divergences associated with the initial states are then factorized and absorbed in the parton distribution functions, yielding a finite result.

Based on the fact that the singular parts of the sum of all degenerate states cancel against each other order by order in perturbation theory, we can predict the infrared singularities of the one and two-loop amplitudes in QCD with light-quark flavors. The amplitudes are computed in conventional dimensional regularisation and all UV singularities have been removed with renormalisation in the $\overline{\mathrm{MS}}$ scheme. In addition, they depend on the color indices of the initial and final state particles so we can consider them to be vectors of a color space. In the following section we shall define more precisely the color space and examine the operations we can apply to it.

2.4 Matrix elements in color space

A general QCD amplitude with m external legs $\mathcal{M}_m$, depends on the colors c_i, helicities s_i and momenta p_i carried by the external particles,

$$\mathcal{M}_m = \mathcal{M}_m^{c_1,c_2,\ldots,c_m;s_1,s_2,\ldots,s_m}(p_1,p_2,\ldots,p_m). \tag{2.18}$$

If the particle i is a gluon (quark), it can take $c_i = 1,\ldots,N^2-1$ ($c_i = 1,\ldots,N$) color values and $s_i = 1,\ldots,D-2$ ($s_i = 1,2$) helicities. Therefore, we can consider the amplitude as existing in a color + helicity space such that

$$\mathcal{M}_m^{c_1,\ldots,c_m;s_1,\ldots,s_m}(p_1,\ldots,p_m) \equiv (< c_1,\ldots,c_m| \otimes < s_1,\ldots,s_m|)\,|1,2,\ldots,m>, \tag{2.19}$$

where $< c_1,\ldots,c_m|\otimes < s_1,\ldots,s_m|$ is a basis of the space. We then define the matrix-element square, summed over colors and spins, as

$$\overline{|\mathcal{M}_m|^2} =< 1,\ldots,m|1,\ldots,m > . \tag{2.20}$$

We now concentrate on the color components of the amplitude. We are interested in the case where an external parton of the amplitude radiates a gluon with color c. Then the color space increases by one particle, in order to accommodate the emitted gluon. In addition, the emitter of the gluon changes its color index according to the $SU(N)$ color algebra, while the rest of the particles retain their original color. Thus we can define a "color charge" operator $\mathbf{T_i^c}$ (acting on the color component of the amplitude only) which represents the emission of a gluon with color c from the parton i,

$$< c_1, \ldots, c_i, \ldots, c_m, c|\mathbf{T_i^a}|b_1, \ldots, b_i, \ldots, b_m >= \delta_{c_1 b_1} \ldots T^a_{c_i b_i} \ldots \delta_{c_m b_m}. \tag{2.21}$$

The matrix T^a_{cb} depends on the emitter and we have the following cases

- $T^a_{cb} = i f_{cab}$ for a gluon,
- $T^a_{cb} = t^a_{cb}$ for a final-state quark or an initial-state antiquark,
- $T^a_{cb} = -t^a_{bc}$ for a final-state antiquark or an initial-state quark.

It is useful to consider the amplitudes with $m+1$ external legs, produced from another amplitude with m partons by insertion in different places of a gluon radiation. Taking squares we produce terms of the form

$$\begin{aligned} \left|M_m^{i,k}\right|^2 &= < 1, \ldots, m|\mathbf{T_i} \cdot \mathbf{T_k}|1, \ldots, m > \\ &= \left[\mathcal{M}_m^{a_1 \ldots b_i \ldots b_k \ldots a_m}\right]^\dagger T^c_{a_i b_i} T^c_{b_k a_k} \mathcal{M}_m^{a_1 \ldots a_i \ldots a_k \ldots a_m} \end{aligned} \tag{2.22}$$

where

$$\mathbf{T_i} \cdot \mathbf{T_k} = \mathbf{T_k} \cdot \mathbf{T_i} \equiv T_i^c T_k^c.$$

for $i \neq k$. For $i = k$ we have

$$\begin{aligned} \left|M_m^{i,i}\right|^2 &= < 1, \ldots, m|\mathbf{T_i} \cdot \mathbf{T_i}|1, \ldots, m > \\ &= \left[\mathcal{M}_m^{a_1 \ldots b_i \ldots a_m}\right]^\dagger T^c_{a_i a_k} T^c_{a_k b_i} \mathcal{M}_m^{a_1 \ldots a_i \ldots a_m} \\ &= \left[\mathcal{M}_m^{a_1 \ldots b_i \ldots a_m}\right]^\dagger C_i \delta_{a_i b_i} \mathcal{M}_m^{a_1 \ldots a_i \ldots a_m} = C_i < 1, \ldots, m|1, \ldots, m > \end{aligned} \tag{2.23}$$

or, otherwise,

$$T_i^2 = C_i \, \mathbf{1},$$

with

$$C_i = C_F = \frac{N^2 - 1}{2N}, \quad \text{if } i \text{ is a quark} \tag{2.24}$$

$$C_i = C_A = N, \quad \text{if } i \text{ is a gluon} \tag{2.25}$$

The last two identities can be easily proved using the decomposition

$$f_{abc} = \frac{2}{i} \mathrm{tr}\left(\left[t^a, t^b\right] t^c\right) \tag{2.26}$$

and the Fierz identity

$$t^a_{ij} t^a_{lm} = \frac{1}{2}\left(\delta_{im}\delta_{jl} - \frac{1}{N}\delta_{ij}\delta_{lm}\right) \tag{2.27}$$

Finally, from color conservation, we have

$$\sum_{i=1}^{m} \mathbf{T_i}|1,\ldots,m>= 0. \tag{2.28}$$

2.5 Singular behavior of one-loop amplitudes

We consider the QCD amplitude $|\mathcal{M}\rangle$ (in color space) with m external legs. As usual we work in CDR and renormalise with the $\overline{\mathrm{MS}}$ scheme. Performing a perturbative expansion we can write

$$|\mathcal{M}\rangle = \left(\frac{\alpha_s}{2\pi}\right)^n \left[|\mathcal{M}^0\rangle + \frac{\alpha_s}{2\pi}|\mathcal{M}^1\rangle + \left(\frac{\alpha_s}{2\pi}\right)^2|\mathcal{M}^2\rangle + \mathcal{O}(\alpha_s^3)\right] \tag{2.29}$$

with n depending on the process.

We separate the singularities of the one-loop amplitude $|M^1\rangle$ from the finite part with the formula

$$|\mathcal{M}^1\rangle = \mathbf{I}(\epsilon)|\mathcal{M}^0\rangle + |\mathcal{M}^{1,fin}\rangle \tag{2.30}$$

where $|\mathcal{M}^{1,fin}\rangle$ is a finite function when $\epsilon\to 0$. All one-loop divergences are factorized with respect to the tree-level amplitude $|\mathcal{M}^0\rangle$. The operator $\mathbf{I}$ is meant to act on the color vector $|\mathcal{M}^0\rangle$ and encapsulates all the singular dependence. Specifically,

$$\mathbf{I}(\epsilon) = \frac{1}{2}\frac{e^{\gamma\epsilon}}{\Gamma\left(1-\epsilon\right)}\sum_i \frac{1}{\mathbf{T_i^2}}\mathcal{V}_i^{\mathrm{sing}}(\epsilon)\sum_{j\neq i}\mathbf{T_i}\cdot\mathbf{T_j}\left(\frac{\mu^2 e^{-i\lambda_{ij}\pi}}{2p_i\cdot p_j}\right)^{\epsilon} \tag{2.31}$$

where the indices i, j run over the external legs. The momenta of the external particles i, are denoted by p_i and $\lambda_{ij} = 1$ if both particles are incoming or outgoing, otherwise $\lambda_{ij} = 0$. The singularities appear in the form of $1/\epsilon^2$ and $1/\epsilon$ poles in the function

$$\mathcal{V}_i^{\mathrm{sing}}(\epsilon) = \mathbf{T_i}^2\frac{1}{\epsilon^2} + \gamma_i\frac{1}{\epsilon} \tag{2.32}$$

where

$$\gamma_q = \gamma_{\bar{q}} = \frac{3}{2}C_F, \quad \gamma_g = \frac{11}{6}C_A - \frac{2}{3}T_R N_F. \tag{2.33}$$

2.5.1 Application: $Z \rightarrow q\bar{q}$ one-loop singularities

Let us first check the above formalism against our earlier results for the Z-decay to a quark-antiquark pair. Defining the $\mathbf{T_i}, (i = q, \bar{q})$ operators in color space as in Section 2.4, from color conservation

$$\mathbf{T_q} + \mathbf{T_{\bar{q}}} = 0,$$

we obtain

$$\mathbf{T_q} \cdot \mathbf{T_{\bar{q}}} = \mathbf{T_{\bar{q}}} \cdot \mathbf{T_q} = -\mathbf{T_q^2} = -\mathbf{T_{\bar{q}}^2} = -C_F \mathbf{1}. \tag{2.34}$$

Therefore the color-charge operator takes the simple factorized form

$$\mathbf{I}(\epsilon) = \omega(\epsilon)\mathbf{1}, \tag{2.35}$$

with

$$\omega(\epsilon) = C_F \frac{e^{\gamma\epsilon}}{\Gamma(1-\epsilon)} \left[-\frac{1}{\epsilon^2} - \frac{3}{2\epsilon} \right] \left(-\frac{\mu^2}{M_Z^2} \right)^{\epsilon}. \tag{2.36}$$

Acting on the tree-level amplitude we obtain the singular part of the virtual one-loop amplitude which is

$$\mathcal{M}_1^{\text{sing}} = \frac{\alpha_s}{2\pi} \mathbf{I}(\epsilon) |\mathcal{M}_0\rangle = \frac{\alpha_s}{2\pi} \omega(\epsilon) \mathcal{M}_0. \tag{2.37}$$

It is easy to verify, after an ϵ-expansion of the r.h.s of Eq. 2.37 and Eq. 2.7, that their difference is indeed finite.

2.6 Singular behavior of two-loop amplitudes

The singular behavior of two-loop amplitudes is more complicated and the singularities appear as $1/\epsilon^4, 1/\epsilon^3, 1/\epsilon^2$ and $1/\epsilon$ poles. Catani gave the following factorization formula in terms of the one-loop and tree-level amplitudes

$$|\mathcal{M}^2\rangle = \mathbf{I}(\epsilon)|\mathcal{M}^1\rangle + \mathbf{I}^{(2)}(\epsilon)|\mathcal{M}^0\rangle + |\mathcal{M}^{2,fin}\rangle \tag{2.38}$$

Again, $|\mathcal{M}^{2,fin}\rangle$ is a finite function when $\epsilon \rightarrow 0$. The divergences of the amplitude receive contributions from two sources. First the double and single poles of our known operator $\mathbf{I}$ multiply the singularities $(1/\epsilon^2, 1/\epsilon)$ of the one-loop amplitude $|\mathcal{M}^1\rangle$. Second, a new divergent operator $\mathbf{I}^{(2)}$ acts on the tree-level amplitude $|\mathcal{M}^0\rangle$, producing poles as deep as $1/\epsilon^4$. In fact,

$$\begin{aligned}\mathbf{I}^{(2)}(\epsilon) &= -\frac{1}{2}\mathbf{I}(\epsilon)\left(\mathbf{I}(\epsilon)+4\pi\beta_0\frac{1}{\epsilon}\right)+\frac{e^{-\gamma\epsilon}\Gamma\left(1-2\epsilon\right)}{\Gamma\left(1-\epsilon\right)}\left(2\pi\beta_0\frac{1}{\epsilon}+K\right)\mathbf{I}(2\epsilon) \\ &\quad +\mathbf{H}^{(2)}(\epsilon),\end{aligned} \tag{2.39}$$

with

$$K=\left(\frac{67}{18}-\frac{\pi^2}{6}\right)C_A-\frac{10}{9}T_R N_F. \tag{2.40}$$

The function $\mathbf{H}^{(2)}$ is of order $1/\epsilon$, and it depends both on the specific process and the renormalisation scheme and consists of constants such as ζ_3, C_F, C_N, π^2. Therefore, with Eq. 2.38 we can completely predict the singular behavior of the two-loop amplitudes through to order $\mathcal{O}(1/\epsilon^2)$, together with a large part of the $1/\epsilon$ poles depending on logarithms and generalized polylogarithms. The remaining part due to $\mathbf{H}^{(2)}$ has to be found with the explicit calculation of the two-loop amplitude from the Feynman diagrams.

In Chapter 6 we perform an explicit computation of the two-loop amplitudes for quark scattering. Using the above formalism we verify that the pole structure is the one anticipated and we compute the $\mathbf{H}^{(2)}$ function for the relevant processes. In the next section, we construct the $\mathbf{I}$ operator for the scattering of unlike-quarks, in terms of which we develop our analysis of the infrared behavior in Chapter 6.

2.7 Color charge operator I for unlike-quark scattering

We now consider the amplitude for the process

$$q(p_1)+\bar{q}(p_2)\rightarrow\bar{Q}(p_3)+Q(p_4), \tag{2.41}$$

where a quark and an anti-quark in the initial state interact to produce an quark and anti-quark pair in the final-state with different flavor. The momenta assigned to the external particles are shown in parenthesis and the total momentum is conserved ($p_1^\mu+p_2^\mu+p_3^\mu+p_4^\mu=0$). The Mandelstam variables are

$$s=(p_1+p_2)^2,\ t=(p_2+p_3)^2,\ u=(p_1+p_3)^2=-s-t,$$

and all particles are light-like.

To obtain the singular parts of the renormalised one and two-loop amplitudes it is essential to construct the color-charge operator I of Eq. 2.31 in color space. The amplitude at tree-level consists of the diagram

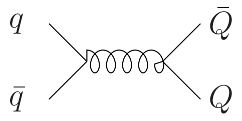

with color factor

$$t^a_{q\bar{q}} t^a_{\bar{Q}Q} = \frac{1}{2}\left(\delta_{qQ}\delta_{\bar{q}\bar{Q}} - \frac{1}{N}\delta_{q\bar{q}}\delta_{Q\bar{Q}}\right) = \frac{1}{2}\left(|h\rangle - \frac{1}{N}|v\rangle\right),$$

where we have defined the color-vectors

$$|h\rangle = \delta_{qQ}\delta_{\bar{q}\bar{Q}} = \tag{2.42}$$

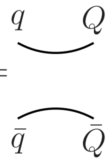

and

$$|v\rangle = \delta_{q\bar{q}}\delta_{Q\bar{Q}} = \tag{2.43}$$

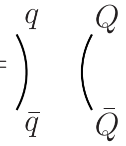

It turns out that the one and two-loop amplitudes for the unlike quark scattering can be written in color-space as linear combinations of the above two-vectors. Therefore, they are a color basis for this process. It is then enough to find the action of the color charge operator on the vectors of the basis only. From the definition it is easy to verify the normalization relations

$$\begin{aligned} \langle v|v\rangle &= \langle h|h\rangle = N^2 \\ \langle v|h\rangle &= \langle h|v\rangle = N. \end{aligned} \tag{2.44}$$

We now define the color charge operators $\mathbf{T_q}$, $\mathbf{T_{\bar{q}}}$, $\mathbf{T_Q}$, $\mathbf{T_{\bar{Q}}}$, corresponding to the color emission of a gluon from the external particles q, $\bar{q}$, Q and $\bar{Q}$ accordingly. For the construction of the $\mathbf{I}$ operator of Eq. 2.31, we need to find the vectors $\mathbf{T_i} \cdot \mathbf{T_j}|h\rangle$ and $\mathbf{T_i} \cdot \mathbf{T_j}|v\rangle$, with $i, j = q, \bar{q}, Q, \bar{Q}$. For example,

$$\mathbf{T_q} \cdot \mathbf{T_Q}|v\rangle =$$

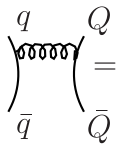

$$= -\left(\delta_{qi} t^{\alpha}_{ij} \delta_{jQ}\right) \times \left(\delta_{\bar{q}k} t^{\alpha}_{kl} \delta_{l\bar{Q}}\right) = -\frac{1}{2}\left(|h\rangle - \frac{1}{N}|v\rangle\right). \tag{2.45}$$

Writing the general element $|\mathcal{M}\rangle$ of the color space in the form

$$|\mathcal{M}\rangle = \mathcal{M}_h|h\rangle + \mathcal{M}_v|v\rangle = \begin{pmatrix} \mathcal{M}_h \\ \mathcal{M}_v \end{pmatrix} \tag{2.46}$$

the above products of operators can be written as matrices.

$$\mathbf{T_Q} \cdot \mathbf{T_{\bar{Q}}} = \mathbf{T_q} \cdot \mathbf{T_{\bar{q}}} = \begin{pmatrix} -C_F & 0 \\ -\frac{1}{2} & \frac{1}{2N} \end{pmatrix}, \tag{2.47}$$

$$\mathbf{T_q} \cdot \mathbf{T_Q} = \mathbf{T_{\bar{q}}} \cdot \mathbf{T_{\bar{Q}}} = \begin{pmatrix} \frac{1}{2N} & -\frac{1}{2} \\ 0 & -C_F \end{pmatrix} \tag{2.48}$$

and

$$\mathbf{T_q} \cdot \mathbf{T_{\bar{Q}}} = \mathbf{T_{\bar{q}}} \cdot \mathbf{T_Q} = \begin{pmatrix} -\frac{1}{2N} & \frac{1}{2} \\ \frac{1}{2} & -\frac{1}{2N} \end{pmatrix} \tag{2.49}$$

Substituting into Eq. 2.31, we obtain the color charge matrix

$$\mathbf{I}(\epsilon) = \frac{e^{\gamma\epsilon}}{\Gamma(1-\epsilon)} \left[-\frac{1}{\epsilon^2} - \frac{3}{2\epsilon} \right] \frac{1}{N} \begin{pmatrix} [N^2-1]\mathcal{S} + \mathcal{U} - \mathcal{T} & N[\mathcal{T} - \mathcal{U}] \\ N[\mathcal{S} - \mathcal{U}] & [N^2-1]\mathcal{T} + \mathcal{U} - \mathcal{S} \end{pmatrix} \tag{2.50}$$

with

$$\begin{aligned} \mathcal{S} &= \left(-\frac{\mu^2}{s}\right)^{\epsilon}, \\ \mathcal{T} &= \left(-\frac{\mu^2}{t}\right)^{\epsilon}, \\ \mathcal{U} &= \left(-\frac{\mu^2}{u}\right)^{\epsilon}. \end{aligned} \tag{2.51}$$

The operator matrix of Eq. 2.50 together with the normalization equations 2.44 for the contraction of the vectors of the color-space basis, make up the ingredients for the application of the formalism of Catani for the infrared divergences of the one and two-loop quark scattering amplitudes. The pole structure will be evaluated in Chapter 6 by a direct computation of the Feynman diagrams and agrees with the one anticipated. We now concentrate on the problem of calculating Feynman one and two-loop integrals.

Chapter 3

Representations of Feynman Integrals

One of the most formidable task for the evaluation of matrix elements at NNLO accuracy, is the calculation of the tensor and scalar one and two-loop integrals that naturally arise. Here we consider the problem in its most general form and we will try to establish general methods that simplify it.

We denote the generic m-loop integral in D dimensions with n propagators $1/A_i$ raised to arbitrary powers ν_i as

$$J^D\left(\{\nu_i\};\{Q_i^2\}\right)[1;\,k_1^\mu;\,k_2^\mu;\,k_1^\mu k_1^\nu;\,k_1^\mu k_2^\nu;\,\ldots] = \int \frac{d^Dk_1}{i\pi^{D/2}}\cdots\int\frac{d^Dk_m}{i\pi^{D/2}}\frac{[1;\,k_1^\mu;\,k_2^\mu;\,k_1^\mu k_1^\nu;\,k_1^\mu k_2^\nu;\,\ldots]}{A_1^{\nu_1}\cdots A_n^{\nu_n}}, \tag{3.1}$$

where the external momentum scales are indicated by $\{Q_i^2\}$. For scalar integrals the numerator in Eq. (3.1) is unity, $J^D(\{\nu_i\};\{Q_i^2\})[1] \equiv J^D(\{\nu_i\};\{Q_i^2\})$. The tensor integrals $J^D(\{\nu_i\};\{Q_i^2\})[k_1^\mu;\ldots]$, bear products of loop-momentum vectors k_i^μ in the numerator and they are harder to evaluate. The propagators for particles of mass M_i have typically the form

$$\frac{1}{A_i} = \frac{1}{(\sum_j \xi_{ij}k_j + q_i)^2 - M_i^2 + i0} \tag{3.2}$$

where $\xi_{ij} = 0, 1, -1$ for $j = 1\ldots m$, and q_i is linear combination of the external momenta. Feynman integrals have generally complex values, and branch-cuts in the space of the kinematic variables $\{Q_i^2\}$ define distinct regions in which they have to be computed. Expressions for the same integral in different kinematic regions are connected through analytic continuations. The $+i0$ Feynman prescription in the propagators defines the analyticity properties of the integral and serves to correctly find the analytic continuations between the various regions.

In this thesis, we are interested in QCD physical processes that involve light-quarks and we always assume $M_i^2 = 0$. We also restrict ourselves to the cases where the number of loops m is either one or two. What is more, we apply the techniques developed here for integrals with at most four external legs, the main physics goal in mind being the matrix elements evaluation of $2 \to 2$ scattering of light-like particles. Nevertheless, the same techniques can be in principle generalized to calculate integrals with massive propagators and/or more loops and external legs.

It is generally very hard to perform a brute force integration of the loop momenta k_m in Eq. 3.1. Instead we rewrite the product of the propagators as a multiple integral over new real parameters squeezing the k_m's in a single quadratic form, so that they can be integrated out trivially. What is left are the integrations over the new parameters which are often more convenient. The prescription used for the representation of the product of the propagators defines the representation of the Feynman integral. Integral representations in real parameters are more promising than the original integrals over the loop-momenta and they show explicitly the dependence on scales such as propagator masses, Mandelstam variables, etc. They also serve to find relations among the integrals of the same topology[1]. The most commonly used representations are the ones in Schwinger and Feynman parameters.

The Schwinger parametric form is based on writing each of the propagators as an exponential integral over a positive real variable ranging up to infinity. Traditionally this representation is not very popular for a direct evaluation. Instead, it is very convenient to find relations between tensor and scalar integrals. Theories with par-

[1]For the rest of this thesis we will say that two integrals belong in the same topology, if their sets of propagators are related to each other by a linear transformation of the loop-momenta and/or a rearrangement of the external momenta. The powers of the propagators or the dimension of the integrals can be still different, or they can possibly carry different scalar products or tensors in the numerator of the integrand. An integral belongs to a subtopology of another integral, if by shifting its loop momenta or interchanging the position of the external particles, we produce a subset of the propagators of the integral of the topology

ticles that carry spin, give rise to tensor integrals whose evaluation demands some extra effort. With the Schwinger representation we can easily displace the problem of evaluating tensor integrals to evaluating scalar integrals of the topology with extra powers of propagators and higher dimension. Making no distinction between scalar and tensor integrals is often very useful when a large number of tensors has to be calculated, allowing for a uniform approach that can be easily automated.

The Feynman representation is more popular. The integrations are often viable, especially because the parameters are not completely free and obey the constraint to sum up to unity. This has been proven very convenient in order to find nice transformations that simplify the original representation. Unfortunately, there does not exist a systematic method to directly evaluate the integrals over the Feynman parameters and success very much depends on specialized clever tricks that can be applied mainly within the integrals of the same topology. One can very quickly run out of such tricks as the complexity of the integral rises with the introduction of additional propagators or kinematic scales.

We bypass the difficulties of evaluating the Feynman representation with the introduction of Mellin-Barnes integrals. Their main advantage is that the new integration variables are complex and the integration is across straight lines parallel to the imaginary axis. The integrands typically vanish at infinity, so one can close the contour and attempt a brute force summation of all the residues enclosed leading to a hypergeometric series representations. Hypergeometric representations are naturally derived within the framework of the Negative Dimension Integration Method (NDIM) as well, and we discuss it in the next chapter.

Unfortunately, the hypergeometric structure of many Feynman integrals of interest is still very complicated and cumbersome for practical purposes. Feynman integrals, as explained earlier, are singular objects and we have chosen the dimension as a regulator of their singularities. Divergences arise either because of vanishing propagators (infrared) or due to exploding loop-momenta in the numerator at infinity (ultraviolet). It is a great challenge to isolate them since they sit in nested integrals or sums in the Feynman or hypergeometric series representations. A method to extract the singularities of the Feynman parametric form has been proposed by Binoth and Heinrich [20], but the aim of an analytic solution is sacrificed due to a rapid proliferation of the resulting divergence-free integrals which must be evaluated numerically.

Mellin-Barnes integral representations are very well equipped for an analytic isolation of the poles. The divergences are due to a small number of residues which cross the contours of integration when we continue the value of $\epsilon = 2 - \frac{D}{2}$ to zero. They can be easily spotted and isolated. The remaining series of residues are finite and with some effort they can be expressed in terms of generalized polylogarithms. Major breakthroughs occurred using this method during the last two years which opened wide the road for matrix elements calculation of 2→2 light-like particles. Smirnov [21] first calculated the double-box integral with unit powers of propagators followed by Tausk [22] on an analogous calculation for the cross box topology. Recently, Smirnov [23, 24] calculated the same integrals considering one of the external legs to be massive.

In this chapter, we explain how to derive the Schwinger and Feynman representations of Feynman integrals. Starting from the Schwinger parametric form we propose an algorithm to relate tensor integrals to scalar integrals of the same topology with extra powers of propagators and higher dimension. We also evaluate some one and two-loop integrals from their Feynman representation. Furthermore, we derive Mellin-Barnes representations of various one and two-loop integrals and show how we can use simple one-loop integrals as building block for the derivation of Mellin-Barnes representation of multi-loop diagrams. Finally, we explain how we can isolate the ϵ poles of an integral, choosing to work with the Mellin-Barnes representation of the cross-triangle diagram.

We should also mention that very recently methods have been proposed for calculating Feynman integrals without a direct evaluation of their integral or series representations. These methods are based on the construction and the solution of differential or difference equations. Gehrmann and Remiddi [25, 26, 27, 28, 29] derive differential equations with respect to the kinematic scales of the integrals by using recursive Integration By Parts (IBP) and Lorentz Invariance (LI) identities. Then they solve the differential equations order by order in an ϵ-expansion. Using again recursive identities from IBP, Tarasov [30, 31] and Laporta [32, 33] derive difference equations with respect to parameters such as the dimension and the powers of propagators which they can systematically solve. The above methods are very promising for an automatized calculation of integrals with many loops giving hope for very accurate theoretical predictions for physical observables.

In Chapter 5, we shall explain how IBP and LI work in order to reduce the number of basic integrals needed from a topology (master integrals), and we shall find differential equations satisfied by them. We shall use the differential equations to calculate some of the master integrals in terms of other master integrals which have previously calculated from their integral or series representations. Finally, we shall use the differential equations to verify our reduction algorithms to master integrals and the analytic expansions in ϵ of the master integrals. We now return to the study of the representations of tensor and scalar integrals.

3.1 Generic tensor integrals using Schwinger parameters

In this section, we deal with the generic tensor integral, $J^D\left(\{\nu_i\};\{Q_i^2\}\right)[k_1^\mu;\ldots]$, and develop an algorithm to reduce it to a set of scalar integrals.

A method to reduce tensor integrals constructing differential operators that change the powers of the propagators as well as the dimension of the integral was presented in Ref. [34]. However, it is in our view simpler to obtain the tensor integrals directly from the Schwinger parameterized form of the integral expressing the product of the propagators as

$$\frac{1}{A_1^{\nu_1}\ldots A_n^{\nu_n}} = \int \mathcal{D}x\ \exp\left(\sum_{i=1}^{n} x_i A_i\right), \tag{3.3}$$

where

$$\int \mathcal{D}x = \prod_{i=1}^{n} \frac{(-1)^{\nu_i}}{\Gamma(\nu_i)} \int_0^\infty dx_i\, x_i^{\nu_i-1}. \tag{3.4}$$

For a two-loop integral,

$$\sum_{i=1}^{n} x_i A_i = a\,k_1^2 + b\,k_2^2 + 2\,c\,k_1\cdot k_2 + 2\,d\cdot k_1 + 2\,e\cdot k_2 + f, \tag{3.5}$$

where a, b, c, d^μ, e^μ and f are linear in the x_i and characterize the topology of the integral. With the change of variables

$$k_1^\mu \;\to\; K_1^\mu - \frac{cK_2^\mu}{a} + \mathcal{X}^\mu, \tag{3.6}$$

$$k_2^\mu \;\to\; K_2^\mu + \mathcal{Y}^\mu, \tag{3.7}$$

where

$$\mathcal{X}^\mu = \frac{c e^\mu - b d^\mu}{\mathcal{P}}, \qquad \mathcal{Y}^\mu = \frac{c d^\mu - a e^\mu}{\mathcal{P}}, \tag{3.8}$$

and

$$\mathcal{P} = ab - c^2, \tag{3.9}$$

we can diagonalize Eq. 3.5, so that

$$\sum_{i=1}^{n} x_i A_i = a K_1^2 + \frac{\mathcal{P}}{a} K_2^2 + \frac{\mathcal{Q}}{\mathcal{P}}, \tag{3.10}$$

with

$$\mathcal{Q} = -a\, e^2 - b\, d^2 + 2\, c\, e \cdot d + f\, \mathcal{P}. \tag{3.11}$$

The scalar two-loop integral can be cast in the form

$$J^D\left(\{\nu_i\};\{Q_i^2\}\right)[1] = \int \mathcal{D}x \int \frac{d^D K_1}{i\pi^{D/2}} \int \frac{d^D K_2}{i\pi^{D/2}} \exp\left[a K_1^2 + \frac{\mathcal{P}}{a} K_2^2 + \frac{\mathcal{Q}}{\mathcal{P}}\right], \tag{3.12}$$

and the Gaussian integrals over the shifted loop momenta are evaluated (using similar tricks as for the proof of Eq. 1.20) to produce

$$J^D\left(\{\nu_i\};\{Q_i^2\}\right)[1] = \int \mathcal{D}x\, \mathcal{I}, \tag{3.13}$$

the integrand $\mathcal{I}$ being given by

$$\mathcal{I} = \frac{1}{\mathcal{P}^{D/2}} \exp\left(\frac{\mathcal{Q}}{\mathcal{P}}\right). \tag{3.14}$$

Similarly, the tensor integrals can be easily obtained by using identities such as

$$\int \frac{d^D K_1}{i\pi^{D/2}} K_1^\mu \exp\left(a K_1^2\right) = 0, \tag{3.15}$$

$$\int \frac{d^D K_1}{i\pi^{D/2}} K_1^\mu K_1^\nu \exp\left(a K_1^2\right) = -\frac{1}{2a}\, g^{\mu\nu}\, \frac{1}{a^{D/2}}, \tag{3.16}$$

$$\int \frac{d^D K_1}{i\pi^{D/2}} K_1^\mu K_1^\nu K_1^\rho K_1^\sigma \exp\left(a K_1^2\right) = \frac{1}{4a^2}\left\{g^{\mu\nu} g^{\rho\sigma} + g^{\mu\rho} g^{\nu\sigma} + g^{\mu\sigma} g^{\nu\rho}\right\} \frac{1}{a^{D/2}}. \tag{3.17}$$

To give a concrete example, we consider the tensor integral associated with k_1^μ

$$\begin{aligned} J^D\left(\{\nu_i\};\{Q_i^2\}\right)[k_1^\mu] &= \int \mathcal{D}x \\ &\times \int \frac{d^D K_1}{i\pi^{D/2}} \int \frac{d^D K_2}{i\pi^{D/2}} \left\{K_1^\mu - \frac{c K_2^\mu}{a} + \mathcal{X}^\mu\right\} \exp\left(a K_1^2 + \frac{\mathcal{P}}{a} K_2^2 + \frac{\mathcal{Q}}{\mathcal{P}}\right) \\ &= \int \mathcal{D}x\, \mathcal{X}^\mu \mathcal{I}. \end{aligned} \tag{3.18}$$

Recalling the definition (3.8), we see that $\mathcal{X}^\mu$ consists of the ratio of a set of bilinears in x_i divided by $\mathcal{P}$. We can therefore absorb the factors of x_i into $\mathcal{D}x$ (see Eq. 3.4) by increasing the power to which the i-th propagator is raised

$$\frac{(-1)^{\nu_i} x_i^{\nu_i - 1}}{\Gamma(\nu_i)}\, x_i \implies -\nu_i \frac{(-1)^{\nu_i+1} x_i^{\nu_i}}{\Gamma(\nu_i + 1)} \equiv -\nu_i \mathbf{i}^+, \tag{3.19}$$

while the factor $\mathcal{P}$ can be absorbed into $\mathcal{I}$ (see Eq. (3.14))

$$\frac{1}{\mathcal{P}^{D/2}}\, \frac{1}{\mathcal{P}} \implies \frac{1}{\mathcal{P}^{(D+2)/2}}, \tag{3.20}$$

increasing the dimension

$$\frac{1}{\mathcal{P}} \Longrightarrow \mathbf{d}^+ \tag{3.21}$$

In this way, each x_i in the numerator increases by one the power of the associated propagator, and each power of $\mathcal{P}$ in the denominator increases the space-time dimension D by two. Schematically we have

$$J^D\left(\{\nu_i\}; \{Q_i^2\}\right)[k_1^\mu] = \sum \nu_i \nu_j\; p_k^\mu\; J^{D+2}\left(\{\ldots, \nu_{i+1}, \ldots, \nu_{j+1}, \ldots\}; \left\{Q_i^2\right\}\right)[1]\,, \tag{3.22}$$

where the summation runs over the elements of $(ce^\mu - bd^\mu)$ which fix the values of i, j and p_k.

For generic four-point integrals, we need tensor integrals with up to four free indices, each associated with a Lorentz index of an external leg. Integrals with higher powers of the loop-momenta are of course possible, but must yield dot products with other momenta when the available free Lorentz indices are saturated. In many cases, these dot products can be immediately expressed in terms of the propagators and canceled through.

The procedure previously described can be iterated ad libitum and we can express every tensor integral in terms of scalar ones with increased powers of the propagators and dimension D. For example, we have

$$
\begin{aligned}
J^D[k_2^\mu] &= \int \mathcal{D}x\ \mathcal{Y}^\mu\ \mathcal{I},\\
J^D[k_1^\mu k_1^\nu] &= \int \mathcal{D}x\ \left(\mathcal{X}^\mu \mathcal{X}^\nu - \frac{b}{2P} g^{\mu\nu}\right)\ \mathcal{I},\\
J^D[k_1^\mu k_2^\nu] &= \int \mathcal{D}x\ \left(\mathcal{X}^\mu \mathcal{Y}^\nu + \frac{c}{2P} g^{\mu\nu}\right)\ \mathcal{I},\\
J^D[k_2^\mu k_2^\nu] &= \int \mathcal{D}x\ \left(\mathcal{Y}^\mu \mathcal{Y}^\nu - \frac{a}{2P} g^{\mu\nu}\right)\ \mathcal{I},\\
J^D[k_1^\mu k_1^\nu k_1^\rho] &= \int \mathcal{D}x\ \left(\mathcal{X}^\mu \mathcal{X}^\nu \mathcal{X}^\rho - \frac{b}{2\mathcal{P}}\,\{g^{\mu\nu}\mathcal{X}^\rho + g^{\mu\rho}\mathcal{X}^\nu + g^{\nu\rho}\mathcal{X}^\mu\}\right)\ \mathcal{I},\\
J^D[k_1^\mu k_1^\nu k_2^\rho] &= \int \mathcal{D}x\ \left(\mathcal{X}^\mu \mathcal{X}^\nu \mathcal{Y}^\rho - \frac{b}{2\mathcal{P}} g^{\mu\nu}\mathcal{Y}^\rho + \frac{c}{2\mathcal{P}}\{g^{\mu\rho}\mathcal{X}^\nu + g^{\nu\rho}\mathcal{X}^\mu\}\right)\ \mathcal{I},
\end{aligned}
$$

$$
\begin{aligned}
J^D[k_1^\mu k_2^\nu k_2^\rho] &= \int \mathcal{D}x\ \left(\mathcal{X}^\mu \mathcal{Y}^\nu \mathcal{Y}^\rho - \frac{a}{2\mathcal{P}} g^{\nu\rho}\mathcal{X}^\mu + \frac{c}{2\mathcal{P}}\{g^{\mu\nu}\mathcal{Y}^\rho + g^{\mu\rho}\mathcal{Y}^\nu\}\right)\ \mathcal{I},\\
J^D[k_2^\mu k_2^\nu k_2^\rho] &= \int \mathcal{D}x\ \left(\mathcal{Y}^\mu \mathcal{Y}^\nu \mathcal{Y}^\rho - \frac{a}{2\mathcal{P}}\{g^{\mu\nu}\mathcal{Y}^\rho + g^{\mu\rho}\mathcal{Y}^\nu + g^{\nu\rho}\mathcal{Y}^\mu\}\right)\ \mathcal{I},\\
J^D[k_1^\mu k_1^\nu k_1^\rho k_1^\sigma] &= \int \mathcal{D}x\ \Bigg(\mathcal{X}^\mu \mathcal{X}^\nu \mathcal{X}^\rho \mathcal{X}^\sigma + \frac{b^2}{4\mathcal{P}^2}\{g^{\mu\nu}g^{\rho\sigma} + g^{\mu\rho}g^{\nu\sigma} + g^{\mu\sigma}g^{\nu\rho}\}\\
&\quad - \frac{b}{2\mathcal{P}}\{g^{\mu\nu}\mathcal{X}^\rho\mathcal{X}^\sigma + g^{\mu\rho}\mathcal{X}^\nu\mathcal{X}^\sigma + g^{\mu\sigma}\mathcal{X}^\nu\mathcal{X}^\rho + g^{\nu\rho}\mathcal{X}^\mu\mathcal{X}^\sigma\\
&\quad + g^{\nu\sigma}\mathcal{X}^\mu\mathcal{X}^\rho + g^{\rho\sigma}\mathcal{X}^\mu\mathcal{X}^\nu\}\Bigg)\ \mathcal{I},\\
J^D[k_1^\mu k_1^\nu k_1^\rho k_2^\sigma] &= \int \mathcal{D}x\ \Bigg(\mathcal{X}^\mu \mathcal{X}^\nu \mathcal{X}^\rho \mathcal{Y}^\sigma - \frac{b}{2\mathcal{P}}\{g^{\mu\nu}\mathcal{X}^\rho + g^{\mu\rho}\mathcal{X}^\nu + g^{\nu\rho}\mathcal{X}^\mu\}\mathcal{Y}^\sigma\\
&\quad + \frac{c}{2\mathcal{P}}\{g^{\mu\sigma}\mathcal{X}^\nu\mathcal{X}^\rho + g^{\nu\sigma}\mathcal{X}^\mu\mathcal{X}^\rho + g^{\rho\sigma}\mathcal{X}^\mu\mathcal{X}^\nu\}\\
&\quad - \frac{bc}{4\mathcal{P}^2}\{g^{\mu\nu}g^{\rho\sigma} + g^{\mu\rho}g^{\nu\sigma} + g^{\mu\sigma}g^{\nu\rho}\}\Bigg)\ \mathcal{I},
\end{aligned}
$$

$$
\begin{aligned}
J^D[k_1^\mu k_1^\nu k_2^\rho k_2^\sigma] &= \int \mathcal{D}x \left(\mathcal{X}^\mu \mathcal{X}^\nu \mathcal{Y}^\rho \mathcal{Y}^\sigma - \frac{a}{2\mathcal{P}} g^{\rho\sigma} \mathcal{X}^\mu \mathcal{X}^\nu - \frac{b}{2\mathcal{P}} g^{\mu\nu} \mathcal{Y}^\rho \mathcal{Y}^\sigma \right. \\
&+ \frac{c}{2\mathcal{P}} \{ g^{\mu\rho} \mathcal{X}^\nu \mathcal{Y}^\sigma + g^{\nu\rho} \mathcal{X}^\mu \mathcal{Y}^\sigma + g^{\mu\sigma} \mathcal{X}^\nu \mathcal{Y}^\rho + g^{\nu\sigma} \mathcal{X}^\mu \mathcal{Y}^\rho \} \\
&\left. + \frac{ab}{4\mathcal{P}^2} g^{\mu\nu} g^{\rho\sigma} + \frac{c^2}{4\mathcal{P}^2} \{ g^{\mu\rho} g^{\nu\sigma} + g^{\mu\sigma} g^{\nu\rho} \} \right) \mathcal{I}, \\
J^D[k_1^\mu k_2^\nu k_2^\rho k_2^\sigma] &= \int \mathcal{D}x \left(\mathcal{X}^\mu \mathcal{Y}^\nu \mathcal{Y}^\rho \mathcal{Y}^\sigma - \frac{a}{2\mathcal{P}} \{ g^{\nu\rho} \mathcal{Y}^\sigma + g^{\nu\sigma} \mathcal{Y}^\rho + g^{\rho\sigma} \mathcal{Y}^\nu \} \mathcal{X}^\mu \right. \\
&+ \frac{c}{2\mathcal{P}} \{ g^{\mu\nu} \mathcal{Y}^\rho \mathcal{Y}^\sigma + g^{\mu\rho} \mathcal{Y}^\nu \mathcal{Y}^\sigma + g^{\mu\sigma} \mathcal{Y}^\nu \mathcal{Y}^\rho \} \\
&\left. - \frac{ac}{4\mathcal{P}^2} \{ g^{\mu\nu} g^{\rho\sigma} + g^{\mu\rho} g^{\nu\sigma} + g^{\mu\sigma} g^{\nu\rho} \} \right) \mathcal{I}, \\
J^D[k_2^\mu k_2^\nu k_2^\rho k_2^\sigma] &= \int \mathcal{D}x \left(\mathcal{Y}^\mu \mathcal{Y}^\nu \mathcal{Y}^\rho \mathcal{Y}^\sigma + \frac{a^2}{4\mathcal{P}^2} \{ g^{\mu\nu} g^{\rho\sigma} + g^{\mu\rho} g^{\nu\sigma} + g^{\mu\sigma} g^{\nu\rho} \} \right. \\
&- \frac{a}{2\mathcal{P}} \{ g^{\mu\nu} \mathcal{Y}^\rho \mathcal{Y}^\sigma + g^{\mu\rho} \mathcal{Y}^\nu \mathcal{Y}^\sigma + g^{\mu\sigma} \mathcal{Y}^\nu \mathcal{Y}^\rho + g^{\nu\rho} \mathcal{Y}^\mu \mathcal{Y}^\sigma \\
&\left. + g^{\nu\sigma} \mathcal{Y}^\mu \mathcal{Y}^\rho + g^{\rho\sigma} \mathcal{Y}^\mu \mathcal{Y}^\nu \} \right) \mathcal{I}.
\end{aligned}
$$

Note that these expressions are valid for arbitrary two-loop integrals and to use them we just need to identify a, b, c, d^μ, e^μ and f and construct $\mathcal{X}^\mu$ and $\mathcal{Y}^\mu$. The powers of x_i and $\mathcal{P}$ can then be exchanged for scalar integrals with higher ν_i and higher D. This procedure is straightforward to implement in an algebraic program.

It is very easy to obtain similar expressions for one-loop tensor integrals. We can view the generic one-loop diagram as a limiting case of the generic two-loop diagram where we first take the limit $c = 0$ (corresponding to the common propagators of the two loops) and then the limits $b = 0$, $e^\mu = 0$ eliminating the propagators of the second loop. Finally, we advance $a \rightarrow \mathcal{P}$ of the final one-loop diagram. Thus we have:

$$
\begin{aligned}
&\frac{c}{\mathcal{P}} \rightarrow 0, \\
&\frac{b}{\mathcal{P}} \longrightarrow \frac{1}{a} \longrightarrow \frac{1}{\mathcal{P}}, \\
&\mathcal{X}^\mu \longrightarrow -\frac{d^\mu}{\mathcal{P}}, \quad \mathcal{Y}^\mu \longrightarrow 0.
\end{aligned}
$$

and

$$
\frac{\mathcal{Q}}{\mathcal{P}} \longrightarrow \frac{-d^2 + f\mathcal{P}}{\mathcal{P}}
$$

Finally, for the one-loop tensors up to fourth-rank we obtain

$$\begin{aligned}
J^D[k_1^\mu] &= \int \mathcal{D}x\; \mathcal{X}^\mu\, \mathcal{I}, \\
J^D[k_1^\mu k_1^\nu] &= \int \mathcal{D}x\; \left(\mathcal{X}^\mu \mathcal{X}^\nu - \frac{1}{2P} g^{\mu\nu}\right) \mathcal{I}, \\
J^D[k_1^\mu k_1^\nu k_1^\rho] &= \int \mathcal{D}x\; \left(\mathcal{X}^\mu \mathcal{X}^\nu \mathcal{X}^\rho - \frac{1}{2\mathcal{P}}\left\{g^{\mu\nu}\mathcal{X}^\rho + g^{\mu\rho}\mathcal{X}^\nu + g^{\nu\rho}\mathcal{X}^\mu\right\}\right) \mathcal{I}, \\
J^D[k_1^\mu k_1^\nu k_1^\rho k_1^\sigma] &= \int \mathcal{D}x\; \Bigg(\mathcal{X}^\mu \mathcal{X}^\nu \mathcal{X}^\rho \mathcal{X}^\sigma + \frac{1}{4\mathcal{P}^2}\{g^{\mu\nu}g^{\rho\sigma} + g^{\mu\rho}g^{\nu\sigma} + g^{\mu\sigma}g^{\nu\rho}\} \\
&\quad - \frac{1}{2\mathcal{P}}\{g^{\mu\nu}\mathcal{X}^\rho\mathcal{X}^\sigma + g^{\mu\rho}\mathcal{X}^\nu\mathcal{X}^\sigma + g^{\mu\sigma}\mathcal{X}^\nu\mathcal{X}^\rho + g^{\nu\rho}\mathcal{X}^\mu\mathcal{X}^\sigma \\
&\quad + g^{\nu\sigma}\mathcal{X}^\mu\mathcal{X}^\rho + g^{\rho\sigma}\mathcal{X}^\mu\mathcal{X}^\nu\}\Bigg)\, \mathcal{I}.
\end{aligned}$$

linking them to integrals with extra powers of propagators and higher dimension.

There is no problem at all to repeat the same steps for a general n-rank tensor m-loop integral. With this tool at hand we can now concentrate on the evaluation of scalar integrals only.

3.2 Feynman Parameters

In this section we describe the representation of Feynman integrals in Feynman parameters. The goal is again to squeeze the denominators of the propagators into a single quadratic form in the loop-momenta so that, after completing perfect squares, we can integrate them out. The main advantage in using Feynman instead of Schwinger parameters is that due to an additional constraint, one has one less integration to perform. Feynman parameters yield expressions which either can be directly computed or they can be used as a benchmark to derive Mellin-Barnes representations, which are suitable for expansion in $\epsilon = 2 - D/2$.

We consider the generic scalar two-loop integral in D dimensions with n propagators $1/A_i$ raised to arbitrary powers ν_i

$$J^D\left(\{\nu_i\};\{Q_i^2\}\right)[1] = \int \frac{d^D k_1}{i\pi^{D/2}} \int \frac{d^D k_2}{i\pi^{D/2}} \frac{1}{A_1^{\nu_1}\cdots A_n^{\nu_n}}, \tag{3.23}$$

Feynman's trick is to write the product of propagators as

$$\frac{1}{A_1^{\nu_1}\cdots A_n^{\nu_n}} = \frac{\Gamma(\nu_1+\ldots+\nu_n)}{\Gamma(\nu_1)\cdots\Gamma(\nu_n)} \int_0^1 dx_1\cdots dx_n \delta(1-\Sigma x_i) \frac{x_1^{\nu_1-1}\cdots x_n^{\nu_n-1}}{[\sum x_i A_i]^{\Sigma\nu_i}}. \tag{3.24}$$

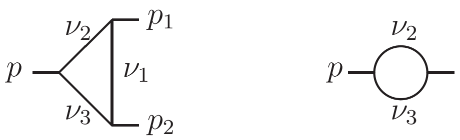

Figure 3.1: The one-loop triangle topology (left) and the one-loop bubble (right) topology with arbitrary powers of propagators

With the same change of variables (Eq. 3.6 and Eq 3.7) as in the Schwinger parametric form we can complete the squares. Integrating out the shifted loop-momenta is now easy, using the identity (Eq. 1.20)

$$\int \frac{d^D K}{i\pi^{\frac{D}{2}}} \frac{1}{(K^2+\Delta)^n} = (-1)^{\frac{D}{2}} \frac{\Gamma(n-\frac{D}{2})}{\Gamma(n)} \Delta^{\frac{D}{2}-n} \tag{3.25}$$

yielding

$$J^D\left(\{\nu_i\};\{Q_i^2\}\right)[1] = (-1)^D \frac{\Gamma(N-D)}{\prod \Gamma(\nu_i)} \int_0^1 \left(\prod_i dx_i x_i^{\nu_i-1}\right) \delta(1-\Sigma x_i) \mathcal{P}^{N-\frac{3D}{2}} \mathcal{Q}^{D-N} \tag{3.26}$$

where $\mathcal{P}$ and $\mathcal{Q}$ are given in Eqs. 3.9 and 3.11, respectively. Similarly, for a one-loop scalar integral we obtain

$$J^D\left(\{\nu_i\};\{Q_i^2\}\right)[1] = (-1)^{\frac{D}{2}} \frac{\Gamma(N-D/2)}{\prod \Gamma(\nu_i)} \int_0^1 \left(\prod_i dx_i x_i^{\nu_i-1}\right) \delta(1-\Sigma x_i) \mathcal{P}^{N-D} \mathcal{Q}^{\frac{D}{2}-N} \tag{3.27}$$

Note that since $\mathcal{P} = \sum_i x_i$, for one-loop integrals $\mathcal{P} = 1$.

These forms can be straightforwardly generalized to multi-loop integrals.

3.2.1 The one-loop triangle

With the Feynman representations in hand, we can now try to evaluate Feynman integrals, starting from the one-loop triangle with one massive external leg (Fig. 3.1).

$$I_3^D(\nu_1,\nu_2,\nu_3;M^2) = \int \frac{d^D k_1}{i\pi^{D/2}} \frac{1}{A_1^{\nu_1} A_2^{\nu_2} A_3^{\nu_3}} \tag{3.28}$$

with

$$\begin{aligned} A_1 &= k_1^2 + i0, \\ A_2 &= (k_1+p_1)^2 + i0, \\ A_3 &= (k_1-p_2)^2 + i0, \end{aligned}$$

and

$$p_1^2 = 0, \quad p_2^2 = 0, \quad \text{and} \quad p_3^2 = (p_1 + p_2)^2 = M^2. \tag{3.29}$$

We write down the Feynman representation of the integral

$$I_3^D = (-1)^{\frac{D}{2}} \frac{\Gamma(\nu_{123} - D/2)}{\Gamma(\nu_1)\Gamma(\nu_2)\Gamma(\nu_3)} \int_0^1 dx_1 dx_2 dx_3 x_1^{\nu_1 - 1} x_2^{\nu_2 - 1} x_3^{\nu_3 - 1} \delta(1 - x_{123}) \mathcal{P}^{\nu_{123} - D} \mathcal{Q}^{\frac{D}{2} - \nu_{123}} \tag{3.30}$$

where

$$\mathcal{P} = x_1 + x_2 + x_3 = 1 \tag{3.31}$$

and

$$\mathcal{Q} = x_2 x_3 M^2. \tag{3.32}$$

Throughout this thesis we shall make extensive use of the shorthand notation

$$\nu_{ij} = \nu_i + \nu_j, \quad \nu_{ijk} = \nu_i + \nu_j + \nu_k, \quad \nu_{ijj} = \nu_i + 2\nu_j, \quad \text{etc.}$$

Because of the presence of the δ function we can change variables:

$$\begin{aligned} x_1 &= \chi, \\ x_2 &= (1 - \chi)\rho \\ x_3 &= (1 - \chi)(1 - \rho) \end{aligned}$$

so that

$$\begin{aligned} I_3^D(\nu_1, \nu_2, \nu_3; M^2) &= (-1)^{\frac{D}{2}} \frac{\Gamma(\nu_{123} - D/2)}{\Gamma(\nu_1)\Gamma(\nu_2)\Gamma(\nu_3)} (M^2)^{\frac{D}{2} - \nu_{123}} \\ &\times \int_0^1 d\chi\, \chi^{\nu_1 - 1} (1 - \chi)^{D - \nu_{1123} - 1} \\ &\times \int_0^1 d\rho\, \rho^{\frac{D}{2} - \nu_{13} - 1} (1 - \rho)^{\frac{D}{2} - \nu_{12} - 1} \end{aligned} \tag{3.33}$$

Using the identity

$$\int_0^1 da\, a^{R-1} (1 - a)^{M-1} = \frac{\Gamma(R)\Gamma(M)}{\Gamma(R + M)} \tag{3.34}$$

we find

$$I_3^D(\nu_1, \nu_2, \nu_3; M^2) = (-1)^{\frac{D}{2}} \left(M^2\right)^{\frac{D}{2} - \nu_{123}} \frac{\Gamma(\nu_{123} - \frac{D}{2})\Gamma(\frac{D}{2} - \nu_{12})\Gamma(\frac{D}{2} - \nu_{13})}{\Gamma(\nu_2)\Gamma(\nu_3)\Gamma(D - \nu_{123})} \tag{3.35}$$

With the above analytic expression we can evaluate any graph of the triangle topology. We can also evaluate the graphs belonging to the bubble topology which is a subtopology. Indeed, if we pinch the first propagator by setting $\nu_1 = 0$ in Eq. 3.35, we get an expression for the bubble graph (Fig. 3.1)

$$I_2^D(\nu_2,\nu_3;M^2) = I_3^D(0,\nu_2,\nu_3;M^2) = \Pi^D(\nu_2,\nu_3)\left(M^2\right)^{\frac{D}{2}-\nu_{23}} \tag{3.36}$$

where for future reference we define

$$\Pi^D(\nu_2,\nu_3) = (-1)^{\frac{D}{2}} \frac{\Gamma(\nu_{23}-\frac{D}{2})\Gamma(\frac{D}{2}-\nu_2)\Gamma(\frac{D}{2}-\nu_3)}{\Gamma(\nu_2)\Gamma(\nu_3)\Gamma(D-\nu_{23})} \tag{3.37}$$

We will later see that it is convenient to write the integrals of a topology and its subtopologies as a linear combination of as few as possible integrals that we call masters. The practical benefit is not very important for topologies with "easy" analytic expressions such as the triangle topology, but it becomes considerable when analytic expressions, or more specifically, ϵ expansions for every integral of the topology are very hard to obtain individually. In such cases we try to find algorithms that produce the linear combinations of the master integrals equivalent to the different integrals of the topology and deal with the ϵ expansions of the master integrals only.

The triangle topology possesses one master integral; the one-loop Bubble integral with unit powers of propagators in $d = 4-2\epsilon$ dimensions (**BUB**).

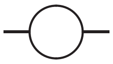

$$\boxed{(M^2) \; = I_2^{4-2\epsilon}(1,1;M^2)} \tag{3.38}$$

Indeed, starting from a general tensor one-loop triangle graph in $d = 4-2\epsilon$ dimensions, our tensor reduction algorithm produces scalar integrals with extra powers of propagators in $D = d+2n$ dimensions, where n is an integer. We can trivially relate all these scalar integrals to the Bubble master integral

$$I_3^{4-2\epsilon+2n}(\nu_1,\nu_2,\nu_3;M^2) = \frac{I_3^{4-2\epsilon+2n}(\nu_1,\nu_2,\nu_3;M^2)}{I_2^{4-2\epsilon}(1,1;M^2)}$$

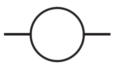

$$(M^2) \tag{3.39}$$

where, introducing the definition of the Pochhammer symbol,

$$(z,n) \equiv \frac{\Gamma(z+n)}{\Gamma(z)} = z(z+1)\cdots(z+n-1), \tag{3.40}$$

the ratios of Γ functions combine together yielding

$$I_3^{4-2\epsilon+2n}(\nu_1,\nu_2,\nu_3;M^2) = \left(M^2\right)^{2+n-\nu_{123}} c_{tr}(n,\nu_1,\nu_2,\nu_3)$$

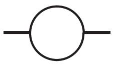

$$(M^2) \tag{3.41}$$

with

$$c_{tr}(n,\nu_1,\nu_2,\nu_3) = \frac{(1-\epsilon, 1+n-\nu_{12})\,(1-\epsilon, 1+n-\nu_{13})\,(\epsilon, \nu_{123}-2-n)}{(1,\nu_2-1)\,(1,\nu_3-1)\,(2-2\epsilon, 2+2n-2\nu_{123})} \tag{3.42}$$

In the limit $\nu_2 = 0$ or $\nu_3 = 0$, the function c_{tr} becomes zero, since the Pochhammer term $1/\left(1,\nu_2-1\right)$ (similarly for $1/\left(1,\nu_3-1\right)$) becomes

$$\frac{1}{(1,\nu_2-1)} = \frac{\Gamma(1)}{\Gamma(\nu_2)} \overset{\nu_2=0}{\Longrightarrow} \frac{1}{\Gamma(0)} = \frac{1}{\infty} = 0. \tag{3.43}$$

We now turn to the calculation of two-loop diagrams. It is possible to start from Eq. 3.26 and attempt to evaluate the integrals over the Feynman parameters. Nevertheless, it is often easier to adopt a different approach and view the two-loop graph as the composition of two one-loop diagrams. In this way we can perform the integrations over each one of the loops separately.

3.2.2 The Bow-tie topology

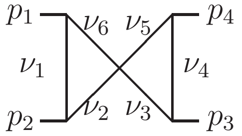

Figure 3.2: The bow-tie topology

A very trivial example is the bow-tie topology of Fig 3.2. The four external legs carry light-like momenta,

$$p_1^2 = p_2^2 = p_3^2 = p_4^2 = 0$$

and the only scale present is

$$s = (p_1+p_2)^2 = (p_3+p_4)^2$$

In fact, due to the absence of a common propagator between the two loops, we just have the multiplication of two disentangled one-loop triangle integrals.

$$I^D_{bow-tie}(\nu_1,\nu_2,\nu_3,\nu_4,\nu_5,\nu_6;s) \;=\; I^D_3(\nu_1,\nu_2,\nu_6;s) I^D_3(\nu_4,\nu_3,\nu_5;s) \tag{3.44}$$

At $D = 4+2n-2\epsilon$ we see that the integrals of the topology are related to the **GLASS** master integral, by

$$I^D_{bow-tie}(\nu_1,\nu_2,\nu_3,\nu_4,\nu_5,\nu_6;s) \;=$$

$$c_{tr}(n,\nu_1,\nu_2,\nu_6)c_{tr}(n,\nu_4,\nu_3,\nu_5)s^{4+2n-\nu_{123456}}$$ 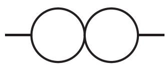 (s) (3.45)

where

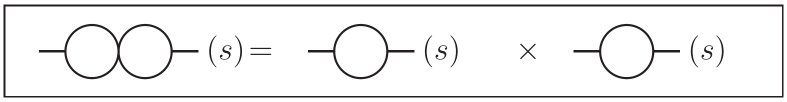

(3.46)

Once more, Eq. 3.45 can be used to reduce the integrals of the subtopologies to the **GLASS** master integral by setting the appropriate powers of the propagators to zero.

3.2.3 The TrianA topology

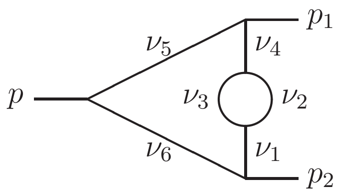

Figure 3.3: The TrianA topology

Unlike the bow-tie topology that we performed the two one-loop integrations independently for the **TrianA** topology of Fig. 3.3 we must perform the two integrations one after the other. Specifically, the integrals of the topology can be written in the form

$$\mathbf{TrianA}^D(\nu_1,\nu_2,\nu_3,\nu_4,\nu_5,\nu_6;M^2) = \int \frac{d^Dk_1}{i\pi^{D/2}} \int \frac{d^Dk_2}{i\pi^{D/2}} \frac{1}{A_1^{\nu_1+\nu_4} A_2^{\nu_2} A_3^{\nu_3} A_5^{\nu_5} A_6^{\nu_6}} \quad (3.47)$$

with

$$\begin{aligned} A_1 &= k_1^2 + i0, \\ A_2 &= (k_1-k_2)^2 + i0, \\ A_3 &= k_2^2 + i0, \\ A_5 &= (k_1+p_1)^2 + i0, \\ A_6 &= (k_1-p_2)^2 + i0, \end{aligned}$$

where $p_1^2 = p_2^2 = 0$ and $p^2 = (p_1+p_2)^2 = M^2$.

We can first perform the integration over k_2, where we get our known one-loop bubble result:

$$\mathbf{TrianA}^D(\nu_1,\nu_2,\nu_3,\nu_4,\nu_5,\nu_6;M^2) = \int \frac{d^Dk_1}{i\pi^{D/2}} \frac{1}{A_1^{\nu_{14}} A_5^{\nu_5} A_6^{\nu_6}} \Pi^D(\nu_2,\nu_3) \frac{1}{A_1^{\nu_{23}-\frac{D}{2}}} \quad (3.48)$$

Finally we are left with the integral over k_1 which belongs to the one-loop Triangle topology yielding

$$\mathbf{TrianA}^D(\nu_1,\nu_2,\nu_3,\nu_4,\nu_5,\nu_6;M^2) = \Pi^D(\nu_2,\nu_3) I_3^D(\nu_{1234}-\frac{D}{2},\nu_5,\nu_6;M^2). \quad (3.49)$$

The **TrianA** topology can be reduced to the **TRI** master integral defined by

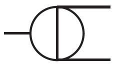

$$(M^2) \;\; = \Pi^{4-2\epsilon}(1,1) I_3^{4-2\epsilon}(\epsilon,1,1;M^2) \quad (3.50)$$

Indeed, the general integral of the topology in $D = 4-2\epsilon+2n$ dimensions is written

$$\mathbf{TrianA}^{4-2\epsilon+2n}(\{\nu_i\};M^2) = C_{\mathbf{TrianA}}(n,\{\nu_i\})(M^2)^{2n+4-\nu_{123456}}$$

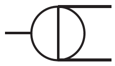

$$(M^2) \quad (3.51)$$

where we use the shorthand notation $\{\nu_i\} = \nu_1,\nu_2,\nu_3,\nu_4,\nu_5,\nu_6$ and

$$\begin{aligned} C_{\mathbf{TrianA}}(n,\{\nu_i\}) &= (-1)^n c_{tr}(n,0,\nu_2,\nu_3) \\ &\times \frac{(1-2\epsilon,3+2n-\nu_{12346})\,(1-2\epsilon,3+2n-\nu_{12345})\,(2\epsilon,\nu_{123456}-4-2n)}{(1,\nu_5-1)\,(1,\nu_6-1)\,(2-3\epsilon,4+3n-2\nu_{123456})} \end{aligned} \quad (3.52)$$

3.2.4 The TrianB topology

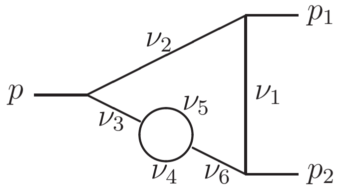

Figure 3.4: The TrianB topology

We now study the two-loop triangle topology with a bubble insertion in the propagator next to the massive external leg, which we name **TrianB**. The general integral of the topology is defined by

$$\mathbf{TrianB}^D(\nu_1,\nu_2,\nu_3,\nu_4,\nu_5,\nu_6;M^2) = \int \frac{d^D k_1}{i\pi^{D/2}} \int \frac{d^D k_2}{i\pi^{D/2}} \frac{1}{A_1^{\nu_1} A_2^{\nu_2} A_3^{\nu_{36}} A_4^{\nu_4} A_5^{\nu_4}} \quad (3.53)$$

with

$$\begin{aligned} A_1 &= k_1^2 + i0, \\ A_2 &= (k_1+p_1)^2 + i0, \\ A_3 &= (k_1-p_2)^2 + i0, \\ A_4 &= (k_1-k_2-p_2)^2 + i0, \\ A_5 &= (k_2-p_2)^2 + i0, \end{aligned}$$

where $p_1^2 = p_2^2 = 0$ and $p^2 = (p_1+p_2)^2 = M^2$. As before, we can successively integrate out the two-loop momenta

$$\mathbf{TrianB}^D(\{\nu_i\}; M^2) = \Pi^D(\nu_4, \nu_5) I_3^D(\nu_1, \nu_2, \nu_{3456-\frac{D}{2}}; M^2). \qquad (3.54)$$

Finally, the topology is reduced to the **SUNSET** master integral

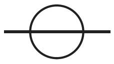

$$\boxed{\quad (M^2) \;\; = \Pi^{4-2\epsilon}(1,1) I_2^{4-2\epsilon}(1, \epsilon; M^2)} \qquad (3.55)$$

via the relation

$$\mathbf{TrianB}^{4-2\epsilon+2n}(\{\nu_i\}; M^2) = C_{\mathbf{TrianB}}(n, \nu_i)(M^2)^{3+2n-\nu_{123456}}$$

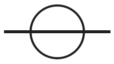

$$(M^2) \qquad (3.56)$$

with

$$\begin{aligned} C_{\mathbf{TrianB}}(n, \nu_i) &= -(-1)^n c_{tr}(n, 0, \nu_4, \nu_5) \\ &\times \frac{(1-\epsilon, 1+n-\nu_{12})\,(1-2\epsilon, 3+2n-\nu_{13456})\,(2\epsilon, \nu_{123456}-4-2n)}{(\epsilon, \nu_{3456}-2-n)\,(1, \nu_2-1)\,(3-3\epsilon, 3+3n-\nu_{123456})} \end{aligned} \qquad (3.57)$$

3.3 Mellin-Barnes representations

With Feynman parameters we solved certain one and two-loop integrals. It turns out, that as we increase the number of external legs or the number of loops or the number of off-shell external particles the same task becomes more and more complicated. We can improve the situation with the introduction of Mellin-Barnes integrals. In this way, the integrations over the Feynman parameters become trivial. Instead we now need to calculate integrals over parameters lying on straight lines parallel to the imaginary axis of the complex plane. Cauchy's residue theorem is then employed and it can be used to solve the problem in two different directions; either to provide hypergeometric representations of the Feynman integral or to separate (by shifting the contours of integrations) the poles in ϵ from the finite part of the integral.

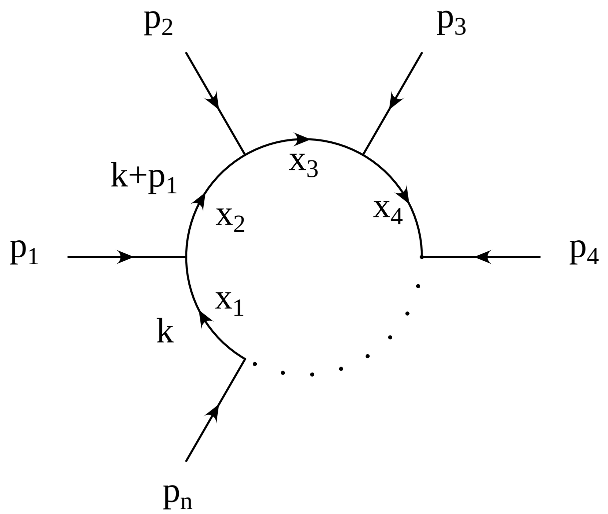

Figure 3.5: The generic one-loop graph

3.3.1 Representation of one-loop integrals

The generic n-point one-loop integral with massless propagators in D-dimensional Minkowski space with loop momentum k is given by

$$\mathcal{I}_n^D(\nu_1, \ldots \nu_n; \{Q_i^2\}) = \int \frac{d^D k}{i\pi^{D/2}} \frac{1}{A_1^{\nu_1} \ldots A_n^{\nu_n}}, \tag{3.58}$$

where, as indicated in Fig. 3.5, the external momenta p_i are all incoming so that $\sum_{i=1}^n p_i^\mu = 0$ and the propagators have the form

$$A_i = (k + q_i)^2 + i0 \qquad , \tag{3.59}$$

with

$$q_1^\mu = 0 \quad \text{and} \quad q_i^\mu = q_{i-1}^\mu + p_{i-1}^\mu.$$

The external momentum scales are indicated with $\{Q_i^2\}$. Due to momentum conservation we have

$$\sum_{i=1}^n p_i^\mu = 0.$$

Let us now detail the terms of the Feynman representation of the generic one-loop diagram (Eq. 3.27). $\mathcal{P}$ is now the sum of all Feynman parameters,

$$\mathcal{P} = \sum_{i=1}^n x_i$$

which, due to the constraint of the δ function, is equal to one and

$$\mathcal{Q} = f\mathcal{P} - d^2$$

where

$$f = \sum_{i=1}^{n} x_i q_i^2$$

and

$$d^\mu = \sum_{i=1}^{n} x_i q_i^\mu .$$

Thus,

$$\begin{aligned}
\mathcal{Q} &= \left(\sum_{i=1}^{n} x_i q_i^2\right)\left(\sum_{j=1}^{n} x_j\right) - \left(\sum_{i=1}^{n} x_i q_i\right)\left(\sum_{j=1}^{n} x_j q_j\right) \\
&= \sum_{i,j=1}^{n} x_i x_j \left(q_i^2 - q_i \cdot q_j\right) \\
&= \frac{1}{2}\sum_{i,j=1}^{n} x_i x_j \left(q_i^2 - 2q_i \cdot q_j + q_j^2\right) \\
&= \frac{1}{2}\sum_{i,j=1}^{n} x_i x_j \left(q_i - q_j\right)^2 \\
&= \sum_{j=2}^{n}\sum_{i<j} x_i x_j s_{ij}
\end{aligned} \tag{3.60}$$

with

$$s_{ij} = (q_i - q_j)^2 = \left(\sum_{m=i}^{j-1} p_m^\mu\right)^2 .$$

The maximum numbers of terms in Q is

$$\mathcal{N}_\mathcal{Q} = \frac{1}{2} n\,(n-1)$$

and increases rapidly with the number of propagators n. It is in general hard to find the appropriate change of variables (if such exists) that disentangles the integrations over the Feynman parameters. Mellin-Barnes (MB) integrals serve in order to decompose the dangerous term $\mathcal{Q}^{D-\sum \nu_i}$ into a product. The main tool will be the MB representation of a power of a sum as a contour integral,

$$(A_1 + A_2)^{-N} = \frac{1}{2\pi i}\int_{-i\infty}^{i\infty} d\xi\, A_1^\xi A_2^{-N-\xi} \frac{\Gamma(-\xi)\Gamma(N+\xi)}{\Gamma(N)}. \tag{3.61}$$

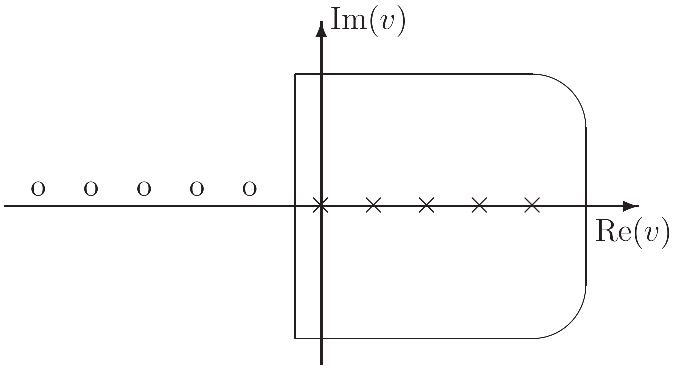

Figure 3.6: The contour of integration for Mellin-Barnes integrals separates the poles coming from $\Gamma(\ldots - v)$ from the poles due to $\Gamma(\ldots + v)$. We can close the contour either to the right or to the left picking one of the two series of residues.

where the integration contour (see Fig. 3.6) separates the poles of $\Gamma(-\xi)$ from the poles of $\Gamma(N+\xi)$, and $A_{1,2}$ are complex numbers such that $|arg(A_1) - arg(A_2) < \pi|$. By iteration of the same formula we generally find

$$\begin{aligned}(A_1 + \ldots + A_m)^{-N} &= \frac{1}{(2\pi i)^{m-1}} \int_{-i\infty}^{i\infty} d\xi_1 \cdots d\xi_{m-1} A_1^{\xi_1} \cdots A_{m-1}^{\xi_{m-1}} A_m^{-N-\xi_1-\ldots-\xi_{m-1}} \\ &\times \frac{\Gamma(-\xi_1)\cdots\Gamma(-\xi_{m-1})\Gamma(N+\xi_1+\ldots\xi_{m-1})}{\Gamma(N)}. \end{aligned} \tag{3.62}$$

It is easy to verify the correctness of the above MB representations. Starting from the r.h.s of Eq. 3.61, we notice that the integrand exhibits poles at

$$\xi = n$$

(due to $\Gamma(-\xi)$) and at

$$\xi = -N - n$$

(due to $\Gamma(N + \xi)$), where $n = 0, 1, 2, \ldots$ We can decide to close the contour of integration to the right. In this case, we sum only the first series of residues. We are now in position to employ Cauchy's residue theorem

$$\oint dy f(y) = 2\pi i \sum_i Res\{f(y_i)\}. \tag{3.63}$$

The only thing we need to know is the residue of the Γ function at $-n = 0, -1, -2, \ldots$.

$$Res\{\Gamma(x)\}_{x=-n} = Res\{\Gamma\,(y-n)\}_{y=0} = Res\{\frac{\Gamma\,(1+y)}{y(y-1)\cdots(y-n)}\}_{y=0} = \frac{(-1)^n}{n!},$$

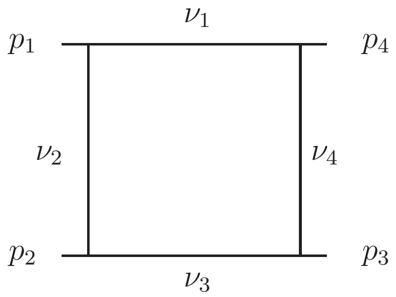

Figure 3.7: The one-loop box topology

where we used the basic property of the Γ function $x\Gamma(x) = \Gamma(1+x)$. Summing up all the residues we obtain:

$$\begin{aligned}
&\frac{1}{2\pi i}\int_{-i\infty}^{i\infty} d\xi A_1^{\xi} A_2^{-N-\xi}\frac{\Gamma(-\xi)\Gamma(N+\xi)}{\Gamma(N)} \\
&= A_2^{-N}\sum_{n=0}^{\infty}\frac{\Gamma(N+n)}{\Gamma(N)}\frac{(-A_1/A_2)^n}{n!} \\
&= A_2^{-n}\frac{(N,n)}{n!}\left(-A_1/A_2\right)^n ,
\end{aligned} \tag{3.64}$$

which is the Taylor expansion of the l.h.s of Eq. 3.61 around $A_1 = 0$. Closing the contour to the left produces an analogous result equivalent to the Taylor expansion of the l.h.s of Eq. 3.61 around $A_2 = 0$.

We can now use Eq. 3.62 to facilitate the integrations over the Feynman parameters in Eq 3.27. We shall demonstrate how this works only for the case of the one-loop box with two adjacent massive external legs (Fig. 3.7) which is difficult to evaluate from the Feynman parameters representation. The same procedure can be repeated for any one-loop diagram.

3.3.2 The adjacent-mass box

The generic massless one-loop box integral in D-dimensional Minkowski space with loop momentum k is given by

$$I_4^d(\nu_1,\nu_2,\nu_3,\nu_4;\{s_{ij}\}) = \int \frac{d^D k}{i\pi^{D/2}}\frac{1}{A_1^{\nu_1}\dots A_4^{\nu_4}}, \tag{3.65}$$

where the propagators are defined in Eq. (3.58) and the external momenta p_i are all incoming so that $\sum_{i=1}^{4} p_i^{\mu} = 0$. The external momentum scales are indicated with

$\{s_{ij}\}$. Following the terminology of the last section, we have

$$\begin{aligned}
s_{12} &= p_1^2 = 0,\\
s_{13} &= (p_1+p_2)^2 = s,\\
s_{14} &= (p_1+p_2+p_3)^2 = p_4^2 = M_2^2,\\
s_{23} &= p_2^2 = 0,\\
s_{24} &= (p_2+p_3)^2 = t,\\
s_{34} &= p_3^2 = M_1^2.
\end{aligned}$$

The Feynman representation of the integral is

$$\begin{aligned}
&\mathcal{I}_4^D(\{\nu_i\};\{s_{ij}\}) = \\
&(-1)^{\frac{D}{2}}\frac{\Gamma(N-D/2)}{\prod\Gamma(\nu_i)}\int_0^1 \frac{\left(\prod dx_l x_l^{\nu_l-1}\right)\delta(1-\Sigma x_l)}{(x_1x_3s+x_2x_4t+x_3x_4M_1^2+x_4x_1M_2^2)^{N-\frac{D}{2}}}
\end{aligned} \tag{3.66}$$

with

$$\{\nu_i\} = \{\nu_1,\nu_2,\nu_3,\nu_4\},$$
$$\{s_{ij}\} = \{s,t,M_1^2,M_2^2\}$$

and

$$N = \nu_1+\nu_2+\nu_3+\nu_4.$$

Performing the MB decomposition of the denominator, we get

$$\begin{aligned}
&\mathcal{I}_4^D(\{\nu_i\};\{s_{ij}\}) = \\
&\frac{(-1)^{\frac{D}{2}}}{\prod\Gamma(\nu_i)}\int_0^1 \left(\prod dx_l x_l^{\nu_l-1}\right)\delta(1-\Sigma x_l)\times \\
&\times\frac{1}{(2\pi i)^3}\int_{-i\infty}^{+i\infty} d\xi_1 d\xi_2 d\xi_3 \Gamma(-\xi_1)\Gamma(-\xi_2)\Gamma(-\xi_3)\Gamma(N-\frac{D}{2}+\xi_{123})\times \\
&\qquad\times(x_1x_3s)^{\frac{D}{2}-N-\xi_{123}}(x_2x_4t)^{\xi_3}\left(x_3x_4M_1^2\right)^{\xi_1}\left(x_4x_1M_2^2\right)^{\xi_2}
\end{aligned} \tag{3.67}$$

and interchanging the order of the MB integrals with the integrals over the Feynman parameters,

$$\begin{aligned}
\mathcal{I}_4^D(\{\nu_i\};\{s_{ij}\}) &= \frac{(-1)^{\frac{D}{2}}s^{\frac{D}{2}-N}}{\prod\Gamma(\nu_i)}\frac{1}{(2\pi i)^3} \\
&\int_{-i\infty}^{+i\infty} d\xi_1 d\xi_2 d\xi_3 \Gamma(-\xi_1)\Gamma(-\xi_2)\Gamma(-\xi_3)\Gamma(N-\frac{D}{2}+\xi_{123})\left(\frac{M_1^2}{s}\right)^{\xi_1}\left(\frac{M_2^2}{s}\right)^{\xi_2}\left(\frac{t}{s}\right)^{\xi_3}\times \\
&\times\int_0^1 dx_1dx_2dx_3dx_4\delta(1-\Sigma x_l)x_1^{\frac{D}{2}-\nu_{234}-\xi_{13}-1}x_2^{\nu_2+\xi_3-1}x_3^{\frac{D}{2}-\nu_{124}-\xi_{23}-1}x_4^{\nu_4+\xi_{123}-1}
\end{aligned} \tag{3.68}$$

It is easy to prove the general formula

$$\int_0^1 \left(\prod_{i=1}^n dx_i x_i^{\alpha_i-1}\right)\delta(1-\sum_i x_i) = \frac{\Gamma(\alpha_1)\cdots\Gamma(\alpha_n)}{\Gamma(\alpha_1+\ldots\alpha_n)} \tag{3.69}$$

by performing the transformation on the integrals of the l.h.s,

$$\begin{aligned} x_1 &= \rho_1, \\ x_2 &= \rho_2(1-\rho_1), \\ x_3 &= \rho_3(1-\rho_2)(1-\rho_1), \\ &\ldots \\ x_{n-1} &= \rho_{n-1}(1-\rho_{n-2})\cdots(1-\rho_1), \\ x_n &= (1-\rho_{n-1})(1-\rho_{n-2})\cdots(1-\rho_1), \end{aligned}$$

The Jacobian is

$$J = (1-\rho_1)^{n-1}(1-\rho_2)^{n-2}\cdots(1-\rho_{n-1}).$$

and we end up with the expression

$$\begin{aligned} \int_0^1 \left(\prod_{i=1}^n dx_i x_i^{\alpha_i-1}\right)\delta(1-\sum_i x_i) &= \left(\int_0^1 d\rho_1 \rho_1^{\alpha_1-1}(1-\rho_1)^{\alpha_2+\ldots\alpha_n-1}\right) \\ \times\left(\int_0^1 d\rho_2\rho_2^{\alpha_2-1}(1-\rho_2)^{\alpha_3+\ldots\alpha_n-1}\right)&\cdots\left(\int_0^1 d\rho_n\rho_n^{\alpha_1-1}(1-\rho_n)^{\alpha_n-1}\right) \end{aligned} \tag{3.70}$$

where all integrations can be done using

$$\int_0^1 d\rho\rho^{\mu-1}(1-\rho)^{\nu-1} = \frac{\Gamma(\mu)\Gamma(\nu)}{\Gamma(\mu+\nu)},$$

and yielding the r.h.s of Eq. (3.69). Inserting Eq. 3.69 in Eq. 3.68 we finally obtain the Mellin-Barnes representation

$$\begin{aligned} \mathcal{I}_4^D(\nu_1,\nu_2,\nu_3,\nu_4;s,t,M_1^2,M_2^2) &= \frac{(-1)^N(-s)^{\frac{D}{2}-N}}{(2\pi i)^3\Gamma(D-N)}\left(\prod_{i=1}^4\frac{1}{\Gamma(\nu_i)}\right) \\ &\times\int_{-i\infty}^{+i\infty} d\xi_1 d\xi_2 d\xi_3 \Gamma(-\xi_1)\Gamma(-\xi_2)\Gamma(-\xi_3)\Gamma(N-\frac{D}{2}+\xi_{123}) \\ &\times\Gamma(\nu_2+\xi_3)\Gamma(\nu_4+\xi_{123})\Gamma(\frac{D}{2}-\nu_{234}-\xi_{13})\Gamma(\frac{D}{2}-\nu_{124}-\xi_{23}) \\ &\times\left(\frac{M_1^2}{s}\right)^{\xi_1}\left(\frac{M_2^2}{s}\right)^{\xi_2}\left(\frac{t}{s}\right)^{\xi_3} \end{aligned} \tag{3.71}$$

This is a result that we will use in two different ways. First we will explore various kinematic limits and we will obtain MB representations for some of the subtopologies. Second, and more important, we will use it as a building block to obtain MB representations for more complicated two-loop diagrams.

3.3.3 The box with one leg off-shell and the on-shell box

We wish to set one of the masses (for example M_1^2) to zero in the representation of Eq. 3.71. We notice that the mass is raised to the integration variable ξ_1, therefore it is necessary to integrate this variable out. The first decision we have to make is how to close the contour. It turns out that we have to close it to the right, otherwise we would yield a series representation of the form

$$I_4^D(\{\nu_i\}; s, t, M_1^2, M_2^2) \sim \sum_n a_n \left(\frac{s}{M_1^2}\right)^n,$$

where the mass is in the denominator and the limit cannot be taken in a straightforward manner. Now we should find which of the residues have non-vanishing contributions at the zero mass limit. We observe that the only way for a residue to survive is to result in raising the mass to the zero power so that it gets eliminated before we take the limit.

$$\sum_{n=0}^{\infty} a_n \left(\frac{M_1^2}{s}\right)^n = a_0 \left(\frac{M_1^2}{s}\right)^0 + \sum_{n=1}^{\infty} a_n \left(\frac{M_1^2}{s}\right)^n \to a_0$$

It is now obvious how to take the vanishing limit of a kinematic variable.

- We first look at the power of the variable and check for which value of the integration variables it vanishes.
- The limit is the contribution of the residue of the representation at this value.

For example, we can symbolically write,

$$I_4^D(\{\nu_i\}; s, t, M_2^2) = 2\pi i \mathrm{Res}\{I_4^D(\{\nu_i\}; s, t, M_1^2, M_2^2)\}_{\xi_1=0} \qquad (3.72)$$

yielding

$$\begin{aligned}
\mathcal{I}_4^D(\nu_1,\nu_2,\nu_3,\nu_4;s,t,M^2) &= \frac{(-1)^N(-s)^{\frac{D}{2}-N}}{(2\pi i)^2\Gamma(D-N)}\left(\prod_{i=1}^{4}\frac{1}{\Gamma(\nu_i)}\right)\\
&\times\int_{-i\infty}^{+i\infty} d\xi_2 d\xi_3\Gamma(-\xi_2)\Gamma(-\xi_3)\Gamma(N-\frac{D}{2}+\xi_{23})\\
&\times\Gamma(\nu_2+\xi_3)\Gamma(\nu_4+\xi_{23})\Gamma(\frac{D}{2}-\nu_{234}-\xi_3)\Gamma(\frac{D}{2}-\nu_{124}-\xi_{23})\\
&\times\left(\frac{M^2}{s}\right)^{\xi_2}\left(\frac{t}{s}\right)^{\xi_3}
\end{aligned}\tag{3.73}$$

In the same manner we can derive the MB representation of the on-shell one-loop box

$$\begin{aligned}
\mathcal{I}_4^D(\nu_1,\nu_2,\nu_3,\nu_4;s,t) &= \frac{(-1)^N(-s)^{\frac{D}{2}-N}}{2\pi i\Gamma(D-N)}\left(\prod_{i=1}^{4}\frac{1}{\Gamma(\nu_i)}\right)\\
&\times\int_{-i\infty}^{+i\infty} d\xi\Gamma(-\xi)\Gamma(N-\frac{D}{2}+\xi)\Gamma(\nu_2+\xi)\Gamma(\nu_4+\xi)\Gamma(\frac{D}{2}-\nu_{234}-\xi)\\
&\times\Gamma(\frac{D}{2}-\nu_{124}-\xi)\left(\frac{t}{s}\right)^{\xi}
\end{aligned}\tag{3.74}$$

3.3.4 The one-loop triangle with MB

We are now interested in taking the limit where one propagator of the adjacent two-mass box is missing. For example we can pinch the second propagator, and set $\nu_2 = 0$. A problem arises from the existence of the factor $\frac{1}{\Gamma(\nu_2)}$ which becomes infinite. This is because one should take the limit of the power of the propagator to zero together with the appropriate kinematic limit. In our case we have the transition from the box topology depending on both s and t, to the triangle topology with only s dependence. Therefore, one should take both $t\to 0$ and $\nu_2\to 0$ in Eq. 3.71, in order to derive a valid expression for the one-loop triangle with massive external legs,

$$I^D_{3,3m}(\nu_4,\nu_1,\nu_3;s,M_1^2,M_2^2) = \mathcal{I}_4^D(\nu_1,0,\nu_3,\nu_4;s,0,M_1^2,M_2^2)\tag{3.75}$$

with

$$
\begin{aligned}
\mathcal{I}_4^D(\nu_1,0,\nu_3,\nu_4;s,0,M_1^2,M_2^2) &= \frac{(-1)^N(-s)^{\frac{D}{2}-\nu_{134}}}{(2\pi i)^2\Gamma(D-\nu_{134})}\frac{1}{\Gamma(\nu_1)\Gamma(\nu_3)\Gamma(\nu_4)} \\
&\times\int_{-i\infty}^{+i\infty} d\xi_1 d\xi_2 \Gamma(-\xi_1)\Gamma(-\xi_2)\Gamma(\nu_{134}-\frac{D}{2}+\xi_{12}) \\
&\times\Gamma(\nu_4+\xi_{12})\Gamma(\frac{D}{2}-\nu_{34}-\xi_1)\Gamma(\frac{D}{2}-\nu_{14}-\xi_2) \\
&\times\left(\frac{M_1^2}{s}\right)^{\xi_1}\left(\frac{M_2^2}{s}\right)^{\xi_2}
\end{aligned} \tag{3.76}
$$

We can continue and set $s \to 0$. Now we have to close the contour to the left, and the only contributing residue comes from $\xi_1 = \frac{D}{2} - \nu_{134} - \xi_2$.

$$
\begin{aligned}
\mathcal{I}_{3,3m}^D(\nu_4,\nu_1,\nu_3;0,M_1^2,M_2^2) &= \frac{(-1)^{\nu_{134}}(-M_2^2)^{\frac{D}{2}-\nu_{134}}}{2\pi i\Gamma(D-\nu_{134})}\frac{\Gamma(\frac{D}{2}-\nu_{13})}{\Gamma(\nu_1)\Gamma(\nu_3)\Gamma(\nu_4)} \\
\times\int_{-i\infty}^{+i\infty} d\xi \Gamma(-\xi)\Gamma(\nu_{134}&-\frac{D}{2}+\xi)\Gamma(\nu_3+\xi)\Gamma(\frac{D}{2}-\nu_{34}-\xi)\left(\frac{M_1^2}{M_2^2}\right)^{\xi}
\end{aligned} \tag{3.77}
$$

We should emphasize that from the MB representations it is straightforward to obtain representations in terms of hypergeometric functions. If we close the contour to the right in Eq. 3.77, we have to sum up the residues at

$$
\begin{aligned}
\xi &= n, \\
\xi &= \frac{D}{2} - \nu_{34} + n,
\end{aligned}
$$

with $n = 0, 1, 2, \ldots$. After we form Pochhammer symbols from the ratios of Γ functions and make use of the inversion formula

$$
(z,-n) = \frac{(-1)^n}{(1-z,n)} \tag{3.78}
$$

so that the summation index in the Pochhammers occurs always with a positive sign, we obtain the sum of two series

$$
\begin{aligned}
\mathcal{I}_{3,3m}^D(\nu_4,\nu_1,\nu_3;0,M_1^2,M_2^2) &= \frac{(-1)^{\nu_{134}}(-M_2^2)^{\frac{D}{2}-\nu_{134}}\Gamma(\frac{D}{2}-\nu_{13})}{\Gamma(D-\nu_{134})\Gamma(\nu_4)} \\
\times\Bigg\{\frac{\Gamma(\frac{D}{2}-\nu_{34})\Gamma(\nu_{134}-\frac{D}{2})}{\Gamma(\nu_1)}&\sum_{n=0}^{\infty}\frac{(\nu_3,n)\left(\nu_{134}-\frac{D}{2},n\right)}{\left(1+\nu_{34}-\frac{D}{2},n\right)n!}\left(-\frac{M_1^2}{M_2^2}\right)^n \\
+\frac{\Gamma(\frac{D}{2}-\nu_4)\Gamma(\nu_{34}-\frac{D}{2})}{\Gamma(\nu_3)}\left(\frac{M_1^2}{M_2^2}\right)^{\frac{D}{2}-\nu_{34}}&\sum_{n=0}^{\infty}\frac{(\nu_1,n)\left(\frac{D}{2}-\nu_4,n\right)}{\left(1-\nu_{34}+\frac{D}{2},n\right)n!}\left(-\frac{M_1^2}{M_2^2}\right)^n\Bigg\}
\end{aligned}
$$

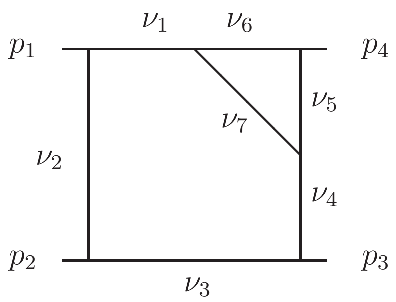

Figure 3.8: The penta-box topology

which can be identified as hypergeometric functions (see Appendix A), yielding

$$\begin{aligned}\mathcal{I}^D_{3,3m}(\nu_4,\nu_1,\nu_3;0,M_1^2,M_2^2) \;=\; & \frac{(-1)^{\nu_{134}}\,(-M_2^2)^{\frac{D}{2}-\nu_{134}}\,\Gamma(\frac{D}{2}-\nu_{13})}{\Gamma(D-\nu_{134})\Gamma(\nu_4)}\times \\ \times\Bigg\{ & \frac{\Gamma(\frac{D}{2}-\nu_{34})\Gamma(\nu_{134}-\frac{D}{2})}{\Gamma(\nu_1)}{}_2F_1(\nu_3,\nu_{134}-\frac{D}{2},1+\nu_{34}-\frac{D}{2};\frac{M_1^2}{M_2^2}) \\ + & \frac{\Gamma(\frac{D}{2}-\nu_4)\Gamma(\nu_{34}-\frac{D}{2})}{\Gamma(\nu_3)}\left(\frac{M_1^2}{M_2^2}\right)^{\frac{D}{2}-\nu_{34}}{}_2F_1(\nu_1,-\nu_4+\frac{D}{2},1-\nu_{34}+\frac{D}{2};\frac{M_1^2}{M_2^2})\Bigg\}\end{aligned} \tag{3.79}$$

For unit powers of propagators at $D=4-2\epsilon$ the hypergeometric functions simplify, giving

$$\mathcal{I}^{4-2\epsilon}_{3,3m}(1,1,1;0,M_1^2,M_2^2)=\frac{\Gamma(1-\epsilon)^2\Gamma(1+\epsilon)}{\epsilon^2\Gamma(1-2\epsilon)}\frac{(-M_1^2)^{-\epsilon}-(-M_2^2)^{-\epsilon}}{M_1^2-M_2^2}. \tag{3.80}$$

Finally, we can set one more scale to zero $M_1^2=0$ eliminating the only remaining MB integral in Eq. 3.77, and retrieve our result of Eq. 3.35,

$$\mathcal{I}^D_{3,3m}(\nu_4,\nu_1,\nu_3;0,0,M^2)=I^D_3(\nu_3,\nu_4,\nu_1;M^2). \tag{3.81}$$

We now turn our attention to the derivation of MB representations for two-loop Feynman integrals.

3.3.5 The Penta-box topology

We start from the penta-box topology of Fig. 3.8 which is defined as

$$\mathbf{PentaB}^D(\{\nu_i\};s,t)=\int\frac{d^Dk_1}{i\pi^{D/2}}\int\frac{d^Dk_2}{i\pi^{D/2}}\frac{1}{A_1^{\nu_1}A_2^{\nu_2}A_3^{\nu_3}A_4^{\nu_4}A_5^{\nu_5}A_6^{\nu_6}A_7^{\nu_7}} \tag{3.82}$$

with $\{\nu_i\} = \nu_1, \nu_2, \nu_3, \nu_4, \nu_5, \nu_6, \nu_7$, and

$$\begin{aligned}
A_1 &= k_1^2 + i0, \\
A_2 &= (k_1 + p_1)^2 + i0, \\
A_3 &= (k_1 + p_1 + p_2)^2 + i0, \\
A_4 &= (k_1 + p_1 + p_2 + p_3)^2 + i0, \\
A_5 &= (k_2 + p_1 + p_2 + p_3)^2 + i0, \\
A_6 &= k_2^2 + i0, \\
A_7 &= (k_2 - k_1)^2 + i0.
\end{aligned} \tag{3.83}$$

The external momenta are incoming with $\sum_i p_i^\mu = 0$ and they form the scales

$$p_1^2 = p_2^2 = p_3^2 = p_4^2 = 0,$$

$$(p_1 + p_2)^2 = s, \qquad (p_2 + p_3)^2 = t, \qquad u = (p_1 + p_3)^2 = -s - t.$$

We want to find a MB representation of the r.h.s of Eq 3.82. In general, it is hard to make a MB decomposition of the $\mathcal{P}$ and $\mathcal{Q}$ terms in the Feynman representation of the two-loop integral (see Eq. 3.26). Instead we view the graph as a composition of one-loop diagrams and use their MB representations as building blocks for the representation of the total graph. For the pentabox, the integration over k_2 yields the triangle function

$$\mathbf{PentaB}^D(\{\nu_i\}; s, t) = \int \frac{d^D k_1}{i\pi^{D/2}} \frac{1}{A_1^{\nu_1} A_2^{\nu_2} A_3^{\nu_3} A_4^{\nu_4}} I_{3,3m}^D(\nu_7, \nu_6, \nu_5; 0, A_1, A_4) \tag{3.84}$$

which, inserting Eq. 3.77, becomes

$$\begin{aligned}
\mathbf{PentaB}^D(\{\nu_i\}; s, t) &= \frac{(-1)^{\frac{D}{2}}}{2\pi i\, \Gamma(D - \nu_{567})} \frac{\Gamma(\frac{D}{2} - \nu_{56})}{\Gamma(\nu_5)\Gamma(\nu_6)\Gamma(\nu_7)} \\
\times \int_{-i\infty}^{+i\infty} & d\xi \Gamma(-\xi)\Gamma(\nu_{567} - \frac{D}{2} + \xi)\Gamma(\nu_5 + \xi)\Gamma(\frac{D}{2} - \nu_{57} - \xi) \\
&\times \int \frac{d^D k_1}{i\pi^{D/2}} \frac{1}{A_1^{\nu_1 - \xi} A_2^{\nu_2} A_3^{\nu_3} A_4^{\nu_{4567} - \frac{D}{2} + \xi}}
\end{aligned} \tag{3.85}$$

The integral over k_1 is the one-loop box function with light-like legs, and its MB representation is given by Eq. 3.74. Substituting in Eq. 3.85 we finally obtain a double Mellin-Barnes integral representation of the pentabox topology,

$$\mathbf{PentaB}^D(\{\nu_i\};s,t) = \frac{(-1)^N(-s)^{D-N}}{(2\pi i)^2\Gamma(\frac{3D}{2}-N)\Gamma(D-\nu_{567})}\frac{\Gamma(\frac{D}{2}-\nu_{56})}{\Gamma(\nu_2)\Gamma(\nu_3)\Gamma(\nu_5)\Gamma(\nu_6)\Gamma(\nu_7)}$$
$$\times\int_{-i\infty}^{+i\infty} d\xi d\alpha\Gamma(-\alpha)\Gamma(\nu_2+\alpha)\frac{\Gamma(-\xi)\Gamma(\nu_5+\xi)\Gamma(\nu_{567}-\frac{D}{2}+\xi)\Gamma(\frac{D}{2}-\nu_{57}-\xi)}{\Gamma(\nu_1-\xi)\Gamma(\nu_{4567}-\frac{D}{2}+\xi)}$$
$$\times\Gamma(N-D+\alpha)\Gamma(\nu_{4567}-\frac{D}{2}+\xi+\alpha)\Gamma(D+\nu_1-N-\xi-\alpha)$$
$$\times\Gamma(D+\nu_3-N-\alpha)\left(\frac{t}{s}\right)^{\alpha} \tag{3.86}$$

with $N=\nu_{1234567}$ the sum of the powers of the propagators.

We want to emphasize that by inserting one graph into another we can write down MB representations for any multi-loop integral. The insertion method economizes in the number of Mellin-Barnes integrals needed for the decomposition of the Feynman representations since, using one-loop graphs as building blocks, $\mathcal{P}$ is always equal to unity and the number of terms in the $\mathcal{Q}$'s are typically less than the ones of the total multi-loop graph. The method is easily automatized and it guarantees a fairly small number of final integrals.

If we had started from Eq. 3.26 a brute force MB decomposition of the two-loop $\mathcal{P}$ and $\mathcal{Q}$ terms would produce a big number of MB integrals. To minimize the number of the final integrals one has to find transformations of the Feynman parameters that simplify the Feynman representation by practically eliminating the $\mathcal{P}$ term, before the MB decomposition. This is not always easy to do and we have found cases (e.g. the double-box topology) that the number of final MB integrals obtained with this method, is bigger than the ones obtained with the insertion method. We shall later show how to derive a MB representation for a two-loop diagram starting from the Feynman representation of the total graph, for the case of the cross-triangle topology.

3.3.6 The TrianC topology

If we set $\nu_2=0,\nu_1=0$ together with $t=0$ in Eq. (3.86) then we obtain what we call the TrianC subtopology of the pentabox graph (see Fig. 3.9). At a first step we

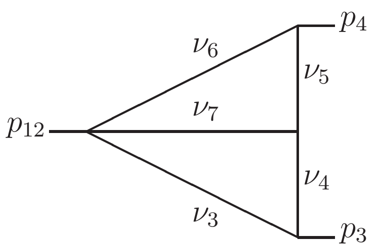

Figure 3.9: The TrianC topology

are left with an one-dimensional Mellin-Barnes integral

$$\begin{aligned}\mathbf{TrianC}^D(\{\nu_i\};s) &= \frac{(-1)^D s^{D-\nu_{34567}}\Gamma(D+\nu_{4567})}{2\pi i\ \Gamma(\frac{3D}{2}-N)\Gamma(D-\nu_{567})}\frac{\Gamma(\nu_{34567}-D)\Gamma(\frac{D}{2}-\nu_{56})}{\Gamma(\nu_3)\Gamma(\nu_5)\Gamma(\nu_6)\Gamma(\nu_7)} \\ &\times\int_{-i\infty}^{+i\infty} d\xi\Gamma(\nu_5+\xi)\Gamma(\nu_{567}-\frac{D}{2}+\xi)\Gamma(\frac{D}{2}-\nu_{57}-\xi)\Gamma(D+\nu_{34567}-\xi)\end{aligned} \tag{3.87}$$

with $\{\nu_i\}=\nu_3,\nu_4,\nu_5,\nu_6,\nu_7$. This integral is an application of Barnes' first lemma, which states

$$\frac{1}{2\pi i}\int_{-i\infty}^{+i\infty} d\xi\Gamma(\alpha+\xi)\Gamma(\beta+\xi)\Gamma(\gamma-\xi)\Gamma(\delta-\xi) = \frac{\Gamma(\alpha+\gamma)\Gamma(\alpha+\delta)\Gamma(\beta+\gamma)\Gamma(\beta+\delta)}{\Gamma(\alpha+\beta+\gamma+\delta)} \tag{3.88}$$

with the contour of integration separating the residues of the $\Gamma(\ldots+\xi)$ from the residues of the $\Gamma(\ldots-\xi)$. So we finally have

$$\begin{aligned}\mathbf{TrianC}^D(\{\nu_i\};s) &= (-1)^D s^{D-N} \\ &\times\frac{\Gamma(N-D)\Gamma(\frac{D}{2}-\nu_{56})\Gamma(\frac{D}{2}-\nu_{34})\Gamma(\frac{D}{2}-\nu_7)\Gamma(D+\nu_3-N)\Gamma(D+\nu_5-N)}{\Gamma(\frac{3D}{2}-N)\Gamma(D-\nu_{347})\Gamma(D-\nu_{567})\Gamma(\nu_3)\Gamma(\nu_5)\Gamma(\nu_7),}\end{aligned} \tag{3.89}$$

with N being the sum of the powers of the propagators. The TrianC topology has only the SUNSET master integral, according to the relation

$\mathbf{TrianC}^{4+2n-2\epsilon}(\{\nu_i\};s) = s^{2n-N}c_{\mathbf{TrianC}}(n,\{\nu_i\})$ 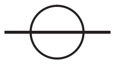 (s) (3.90)

with

$$\begin{aligned}c_{\mathbf{TrianC}}(n,\{\nu_i\}) &= \\ &\frac{(1-\epsilon,1+n-\nu_{56})\,(1-\epsilon,1+n-\nu_{34})\,(2\epsilon,N-4-2n)\,(-\epsilon,2+n-\nu_7)}{(2-3\epsilon,4+3n-N)\,(\nu_3-1,1)\,(\nu_5-1,1)\,(\nu_7-1,1)}\times \\ &\times\frac{(2-2\epsilon,2+2n-N+\nu_3)\,(1-2\epsilon,3+2n-N+\nu_5)}{(2-2\epsilon,2+2n-N+\nu_{567})\,(2-2\epsilon,2+2n-N+\nu_{347})}\end{aligned} \tag{3.91}$$

3.3.7 The Cross-triangle topology

We finally discuss the Mellin-Barnes representation of the cross-triangle topology of Fig. 3.10 which is defined through

$$\mathbf{TrianX}^D(\{\nu_i\};s,t) = \int \frac{d^Dk_1}{i\pi^{D/2}} \int \frac{d^Dk_2}{i\pi^{D/2}} \frac{1}{A_1^{\nu_1} A_2^{\nu_2} A_3^{\nu_3} A_4^{\nu_4} A_5^{\nu_5} A_6^{\nu_6}} \tag{3.92}$$

with $\{\nu_i\} = \nu_1, \nu_2, \nu_3, \nu_4, \nu_5, \nu_6$, and

$$\begin{aligned}
A_1 &= (k_1 + k_2 + p_1 + p_2)^2 + i0, \\
A_2 &= (k_1 + k_2)^2 + i0, \\
A_3 &= k_1^2 + i0, \\
A_4 &= (k_1 + p_1)^2 + i0, \\
A_5 &= k_2^2 + i0, \\
A_6 &= (k_2 + p_2)^2 + i0,
\end{aligned} \tag{3.93}$$

The external momenta are incoming with $\sum_i p_i^\mu = 0$ and they form the scales

$$p_1^2 = p_2^2 = 0,$$

$$p^2 = (p_1 + p_2)^2 = s.$$

We start from the Feynman representation of the integral (Eq. 3.26). We have

$$\begin{aligned}
a &= x_1 + x_2 + x_3 + x_4 \\
b &= x_1 + x_2 + x_5 + x_6 \\
c &= x_1 + x_2 \\
d^\mu &= (x_1 + x_4) p_1^\mu + x_1 p_2^\mu \\
e^\mu &= x_1 p_1^\mu + (x_1 + x_6) p_2^\mu \\
f &= x_1 s.
\end{aligned} \tag{3.94}$$

and

$$\mathcal{P} = ab - c^2 = (x_1 + x_2)(x_3 + x_4 + x_5 + x_6) + (x_3 + x_4)(x_5 + x_6), \tag{3.95}$$

$$\begin{aligned}
\mathcal{Q} &= -a\, e^2 - b\, d^2 + 2\, c\, e \cdot d + f\, \mathcal{P} \\
&= s \left[x_1 x_2 (x_3 + x_4 + x_5 + x_6) + x_2 x_4 x_6 + x_1 x_3 x_5 \right].
\end{aligned} \tag{3.96}$$

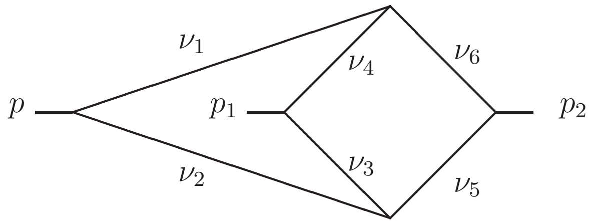

Figure 3.10: The cross-triangle topology

We instantly get discouraged from attempting a MB decomposition of $\mathcal{P}$ (12 terms) and $\mathcal{Q}$ (6 terms) as they stand, since we would end up with 16 integrals in total. Instead we try out some transformation to exploit the existence of the constraint due to the δ function, with the hope of simplifying the Feynman representation of the graph before the decomposition.

We notice that the sum $x_3+x_4+x_5+x_6$ appears in both $\mathcal{P}$ and $\mathcal{Q}$ and it would be nice to eliminate it, if possible. Let us try the transformation

$$x_i = \frac{a_i}{1+a_1}, \qquad i = 1\dots 6$$

Now a_1 runs from 0 to ∞ while the rest of the a_i run from 0 to 1. What is more, the δ function becomes

$$\delta(1-\sum_{i=1}^{6} x_i) = \delta\left(\frac{1}{1+a_1}\left[1-a_2-\ldots-a_6\right]\right) = (1+a_1)\delta\left(1-a_2-\ldots-a_6\right)$$

Applying the transformation, various factors and the Jacobian conspire together and practically recast the representation in the same form, apart from the δ function missing a_1 in its argument and a_1 itself running from 0 to ∞. So we have

$$\begin{aligned}\mathbf{TrianX}^D(\{\nu_i\};s) \;=\; & (-1)^D s^{D-N}\frac{\Gamma(N-D)}{\prod\Gamma(\nu_i)}\int_0^\infty da_1 a_1^{\nu_1-1} \\ & \times\int_0^1\left(\prod_{i=2}^{6} dx_i x_i^{\nu_i-1}\right)\left[(a_1+x_2)(x_3+x_4+x_5+x_6)+(x_3+x_4)(x_5+x_6)\right]^{N-\frac{3D}{2}} \\ & \times\left[a_1x_2(x_3+x_4+x_5+x_6)+x_2x_4x_6+a_1x_3x_5\right]^{D-N}\delta(1-\sum_{i=2}^{6}x_i) \qquad (3.97)\end{aligned}$$

where, for convenience, we relabeled with x_i the variables that range from 0 to 1. Of course, we can repeat the same transformation as many times as we wish, changing the boundaries of some variables and the form of the constraint. An obvious choice is now the variable x_2, giving

$$\begin{aligned}\mathbf{TrianX}^D(\{\nu_i\};s) &= (-1)^D s^{D-N}\frac{\Gamma(N-D)}{\prod\Gamma(\nu_i)}\int_0^\infty da_1 da_2 a_1^{\nu_1-1}a_2^{\nu_2-1}\\ &\times\int_0^1\left(\prod_{i=3}^6 dx_i x_i^{\nu_i-1}\right)[a_1+a_2+(x_3+x_4)(x_5+x_6)]^{N-\frac{3D}{2}}\\ &\times[a_1a_2+a_2x_4x_6+a_1x_3x_5]^{D-N}\,\delta(1-\sum_{i=3}^6 x_i)\end{aligned} \tag{3.98}$$

We can now decompose the $\mathcal{Q}^{D-N}$ term introducing a two-fold Mellin-Barnes integral. Then, the integrations over $a_{1,2}$ can be done easily using

$$\int_0^\infty du\frac{u^{A-1}}{(1+u)^{A+B}} = \frac{\Gamma(A)\Gamma(B)}{\Gamma(A+B)} \tag{3.99}$$

and, furthermore, we can integrate out the remaining Feynman parameters with the change of variables

$$\begin{aligned}x_3 &= \lambda y\\ x_4 &= (1-\lambda)y\\ x_5 &= \mu(1-y)\\ x_6 &= (1-\mu)(1-y).\end{aligned}$$

At the end we obtain the two dimensional MB representation

$$\begin{aligned}\mathbf{TrianX}^D(\{\nu_i\};s) &= \frac{(-1)^N(-s)^{D-N}\Gamma(\frac{D}{2}-\nu_{34})\Gamma(\frac{D}{2}-\nu_{56})}{\Gamma(\frac{3D}{2}-N)\Gamma(D-\nu_{3456})}\left(\prod_{i=1}^6\frac{1}{\Gamma(\nu_i)}\right)\frac{1}{(2\pi i)^2}\\ &\times\int_{-i\infty}^{+i\infty} dudv\Gamma(-v)\Gamma(-u)\Gamma(\nu_3+v)\Gamma(\nu_5+v)\Gamma(\nu_4+u)\Gamma(\nu_6+u)\\ &\times\frac{\Gamma(D+\nu_2-N-v)\Gamma(D+\nu_1-N-u)\Gamma(N-D+u+v)\Gamma(\nu_{3456}-\frac{D}{2}+u+v)}{\Gamma(\nu_{34}+u+v)\Gamma(\nu_{56}+u+v)}.\end{aligned} \tag{3.100}$$

3.4 Laurent expansion in ϵ of MB representations

It is interesting to obtain an analytic expansion in ϵ for the Feynman integrals from their MB representations. This method has been very successful in calculating very complicated integrals, like the double-box [21] and the cross-box [22] with light-like legs. We will work on the MB representation of the cross-triangle (see Eq. 3.100) with unit powers of propagators at $D = 4-2\epsilon$ dimensions. The integral in question, symbolically represented as

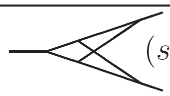

$$\boxed{(s) \quad = \mathbf{TrianX}^{4-2\epsilon}(1,1,1,1,1,1;s)} \tag{3.101}$$

turns out to be a master integral of the cross-triangle topology. It has also been calculated from an expansion of its Feynman representation in Ref. [35, 36], but we recalculate it here as it is a very good example to illustrate the strength of Mellin-Barnes representations in isolating the divergences. From Eq. (3.100), we obtain the following MB representation

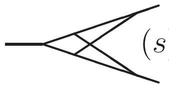

$$(s) \quad = \quad \frac{6(-s)^{-2-2\epsilon}\Gamma(1-\epsilon)^2}{\Gamma(1-2\epsilon)\Gamma(1-3\epsilon)}\,\mathcal{A}(\epsilon), \tag{3.102}$$

where, isolating a trivial factor, we can concentrate on the two-fold MB integral

$$\mathcal{A}(\epsilon) = \frac{1}{(2\pi i)^2}\int_{-i\infty}^{+i\infty} dvdu \frac{\Gamma_1\Gamma_2\Gamma_3\Gamma_4\Gamma_5\Gamma_6\Gamma_7^2\Gamma_8^2}{\Gamma_9^2}, \tag{3.103}$$

with

$$\begin{aligned}
\Gamma_1 &= \Gamma(-v) \\
\Gamma_2 &= \Gamma(-u) \\
\Gamma_3 &= \Gamma(-1-2\epsilon-v) \\
\Gamma_4 &= \Gamma(-1-2\epsilon-u) \\
\Gamma_5 &= \Gamma(2+2\epsilon+u+v) \\
\Gamma_6 &= \Gamma(2+\epsilon+u+v) \\
\Gamma_7 &= \Gamma(1+v) \\
\Gamma_8 &= \Gamma(1+u) \\
\Gamma_9 &= \Gamma(2+u+v).
\end{aligned} \tag{3.104}$$

We intend to calculate this integral using Cauchy's theorem of residues. It is useful to distinguish between the poles produced by Γ functions of the type $\Gamma(\ldots - v)$ and the ones by $\Gamma(\ldots + v)$. The first series of poles spreads up to $+\infty$ in the positive axis and, following Smirnov's convention, we call them Infra-Red poles (IR). Equivalently we shall refer to the second type of poles as Ultra-Violet (UV).

It is important that the contour of integration should be such that it separates the IR from the UV poles and, in addition, there should be no pole sitting on it. For the construction of the MB representations of Feynman integrals with arbitrary powers of propagators and dimension (see Eq. 3.61), we require that all Γ functions have positive real parts and therefore the integral has a finite value. It is easy to satisfy the above condition by tuning the values of the arbitrary parameters (powers of propagators and dimension), since we can practically regulate all the Γ functions with them. At least for the integrals we have studied this was always possible. We would like to retain well defined integrals when taking the limits of the powers of propagators being integers, or the dimension equal to four.

Let us now focus on the double MB integral of Eq. 3.103. This is well defined if, for example, we choose the contours to be straight lines parallel to the imaginary axis with $\mathrm{Re}(u) = \mathrm{Re}(v) = -0.04$ and a value for $\epsilon = -0.7$, then the integrals are well defined. It is also important to notice that there is no contour choice that makes the integral finite at $\epsilon = 0$. Looking, for example at the arguments of Γ_3 and Γ_7 with $\epsilon = 0$, we get the conflicting constraints $-1 - v > 0$ and $1 + v > 0$.

3.4.1 Isolation of the poles

Our purpose is to obtain an analytic expression for $\mathcal{A}(\epsilon)$ that can be expanded around $\epsilon = 0$, after we have isolated the singularities. We perform the two integrations one at a time, starting with v, and we choose to close the contour to the right. It is necessary to analytically continue the value of ϵ from our initial choice $\epsilon = -0.7$ to $\epsilon = 0$. We slowly increase ϵ taking it to zero, and at the same time we observe the behavior of the poles of the Γ functions. The position of the poles of the Γ functions which do not depend on ϵ does not change so we don't worry about them. The remaining Γ functions have residues at

$$\Gamma_3 : \qquad v = -1 - 2\epsilon,\ -2\epsilon,\ 1 - 2\epsilon, \dots \tag{3.105}$$

$$\Gamma_5 : \qquad v = -2 - 2\epsilon - \mathrm{Re}(u),\ -3 - 2\epsilon - \mathrm{Re}(u), \dots \tag{3.106}$$

$$\Gamma_6 : \qquad v = -2 - \epsilon - \mathrm{Re}(u),\ -3 - \epsilon - \mathrm{Re}(u), \dots \tag{3.107}$$

As we increase ϵ the poles of $\Gamma_{5,6}$ move away from the contour of integration, remaining in the UV region. On the contrary, the poles of Γ_3 move towards the

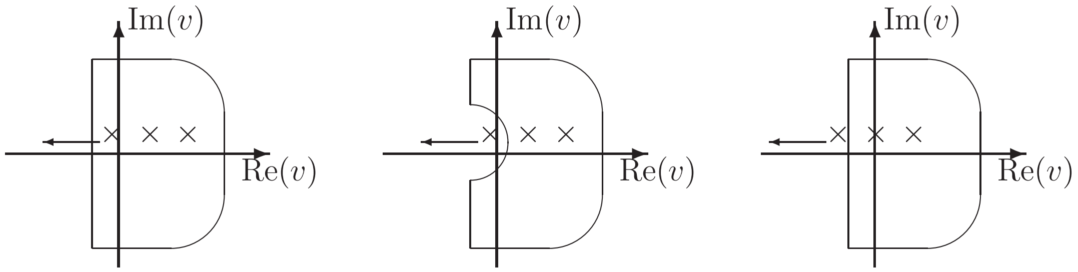

Figure 3.11: When a pole crosses the contour c_1 (left) it produces a singular residue which is isolated by deforming to the contour c_2 (center). The contour can be restored after the dangerous residue moves further away with increasing ϵ (right)

contour. Actually, when $\epsilon = -\frac{1+\mathrm{Re}(u)}{2} = -0.48$ the first residue sits on the contour of integration making the integral infinite and producing a discontinuity in passing to larger values of ϵ.

The residue theorem will help us to do this transition by deforming the contour of integration so that the singular term is excluded and expressed in terms of a single residue. Indeed, just before the pole crosses the contour we can rewrite the original integral as

$$\int_{c_1} dv f(v) = 2\pi i \mathrm{Res}(v_0(\epsilon)) + \int_{c_2} dv f(v) \tag{3.108}$$

where c_1 is the original contour and c_2 is the deformed contour which now excludes the residue at $v = v_0(\epsilon)$ (see Fig. 3.11). The pole is now UV with respect to the new deformed contour, which can be finally restored to its original shape as the pole moves away by continuing to increase ϵ. Of course, we need to repeat the same procedure for every pole crossing the contour until we arrive at $\epsilon = 0$. When we finish isolating the residues that give rise to singularities for all integration variables, we can make a series expansion around $\epsilon = 0$ at the integrands of the produced integrals. It has to be noted that when a crossing happens from the left, we should subtract the residue contribution instead of adding it in Eq. 3.108.

Returning to $A(\epsilon)$, as we said the first residue to cross the contour for the v integration is the first IR residue of Γ_3. According to Eq. 3.108,

$$\mathcal{A}(\epsilon) = \mathcal{A}_3(\epsilon) + \mathcal{A}_0(\epsilon) \tag{3.109}$$

where on the r.h.s $\mathcal{A}_3$ is the residue term

$$\mathcal{A}_3(\epsilon) = \frac{\Gamma(1-2\epsilon)^2\Gamma(1+2\epsilon)}{4\epsilon^2} I(\epsilon) \tag{3.110}$$

with

$$I(\epsilon) = \frac{1}{2\pi i}\int_{-i\infty}^{+i\infty} \frac{\Gamma(-u)\Gamma(-1-2\epsilon-u)\Gamma(1-\epsilon+u)\Gamma(1+u)^3}{\Gamma(1-2\epsilon+u)^2} \tag{3.111}$$

and $\mathcal{A}_0$ is the original integral free of the dangerous singularity in the v integration. The subscript 3 denotes that the first residue of Γ_3 is taken and the subscript 0 denotes that the integrand for the first integration is unchanged but now ϵ can take the value 0 (for this integration only). There is no other pole crossing the contour for ϵ up to zero, so we can continue by resolving the singularities for the u integration.

Once again the pole crossing the contour is at $u = -1-2\epsilon$. We therefore get,

$$\mathcal{A}(\epsilon) = \mathcal{A}_{35}(\epsilon) + \mathcal{A}_{30}(\epsilon) + \mathcal{A}_{05}(\epsilon) + \mathcal{A}_{00}(\epsilon) \tag{3.112}$$

where because, the starting integral is symmetric in u and v,

$$\mathcal{A}_{30}(\epsilon) = \mathcal{A}_{05}(\epsilon) = A_3(\epsilon)|_{\epsilon\longrightarrow 0}$$

where the integral in Eq. 3.111 is now meant to be defined for values of ϵ close to zero. Similarly,

$$\mathcal{A}_{00}(\epsilon) = \mathcal{A}(\epsilon)|_{\epsilon\longrightarrow 0}$$

is now the original integral free of the dangerous residues in both integration variables and we can make an expansion around $\epsilon = 0$. The difference between $\mathcal{A}(\epsilon)$ of Eq. 3.103 and $\mathcal{A}_{00}(\epsilon)$ is that while for the first we have insisted that the UV residues should be separated by the contour from the IR (forcing ϵ to be away from zero), in the latter this condition is not valid. Therefore the $\epsilon = 0$ limit is allowed and the initially UV residues at $v = -1-2\epsilon$ and $u = -1-2\epsilon$ lie on the left half-planes defined by the complex u and v integration contours. Inevitably, some Γ functions take arguments with negative real parts when $\epsilon = 0$, but since the real parts of the complex integration variables u, v are fixed to non-integer values, the Γ functions are well defined yielding a finite result.

Finally, the deepest divergence is given by the double residue term

$$\mathcal{A}_{35}(\epsilon) = \frac{\Gamma(1-2\epsilon)^5\Gamma(1+2\epsilon)^2\Gamma(1-3\epsilon)}{6\epsilon^4\Gamma(1-4\epsilon)^2} \tag{3.113}$$

3.4.2 Evaluating the finite integrals

As we already said, the integrals $I(\epsilon)$ and $\mathcal{A}_{00}(\epsilon)$ are well defined at $\epsilon = 0$, so we can make an expansion around this point. I is multiplied by $1/\epsilon^2$ therefore it needs to be expanded through to $\mathcal{O}(\epsilon^2)$ and for $\mathcal{A}_{00}$ we just need the first term of the series. In simplifying the Γ functions and its derivatives (ψ functions) after the expansion of the integrands it is very convenient to use the formula

$$\Gamma(1-x)\Gamma(x) = g(x) \equiv \frac{\pi}{\sin(\pi x)}. \tag{3.114}$$

The ψ function is defined through

$$\psi(x) = \frac{d \log \Gamma(x)}{dx} \tag{3.115}$$

and it is straightforward to prove that

$$\psi(x+n) = \psi(x) + \sum_{i=0}^{n-1} \frac{1}{x+i} \tag{3.116}$$

and

$$\psi(1-x) - \psi(x) = \pi \cot(\pi x). \tag{3.117}$$

With the above identities we can write the terms of the expansion of the integrals in ϵ at each order in the form

$$J(m,f) = \int_{-i\infty}^{+i\infty} du f(u) g(u)^m \tag{3.118}$$

where m is a positive integer and g is defined through Eq. 3.114. f is an analytic function with no poles lying on the half-plane of the positive real axis. For the separation of the poles we decided to close both contours to the right, and we stick to that choice until the end of the evaluation of the integrals. It is then easy to prove the identities

$$
\begin{aligned}
J(1,f) &= \sum_{n=0}^{\infty}(-1)^n f(n) \\
J(2,f) &= \sum_{n=0}^{\infty}\partial f(n) \\
J(3,f) &= \frac{1}{2!}\sum_{n=0}^{\infty}\left[\partial^2+\pi^2\right] f(n)(-1)^n \\
J(4,f) &= \frac{1}{3!}\sum_{n=0}^{\infty}\left[\partial^3+4\pi^2\partial\right] f(n) \\
J(5,f) &= \frac{1}{4!}\sum_{n=0}^{\infty}\left[\partial^4+10\pi^2\partial^2+9\pi^4\right] f(n)(-1)^n \\
J(6,f) &= \frac{1}{5!}\sum_{n=0}^{\infty}\left[\partial^5+20\pi^2\partial^3+64\pi^4\partial\right] f(n) \qquad (3.119)
\end{aligned}
$$

where ∂^m is the m-th derivative operator acting on the function f and evaluated at the point n. The produced sums are typically harmonic sums and there are several related studies in the literature [37, 38, 39, 40, 41]. They are often expressed in terms of generalized harmonic polylogarithms,

$$
\mathrm{S}_{n,p}(x) = \frac{(-1)^{n+p-1}}{(n-1)!p!}\int_0^1 dz\,\frac{\log(z)^{n-1}\log(1-xz)^p}{z} \qquad x \leq 1\,, \qquad (3.120)
$$

where n, p are positive integers. We retrieve the definition of the common polylogarithms in the special case

$$
\mathrm{Li}_n(x) = \mathrm{S}_{n-1,1}(x). \qquad (3.121)
$$

x is typically a ratio of kinematic variables. In one scale problems, as in our case, $x = 1$ gives rise to the generation of the Riemann zeta functions

$$
\zeta_p = \sum_{n=1}^{\infty}\frac{1}{n^p} \qquad Re(p) > 1. \qquad (3.122)
$$

Finally, we quote the result of our evaluation, which agrees with the known result of Ref. [36],

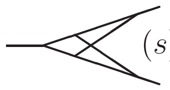

$$
(s) \quad = c_\Gamma^2 \times \left\{\frac{1}{\epsilon^4} - \frac{5\zeta_2}{\epsilon^2} - \frac{23\zeta_3}{\epsilon} - 206\zeta_4\right\} + \mathcal{O}(\epsilon) \qquad (3.123)
$$

where we have factorized the commonly found combination of Γ functions in loop-integral calculations

$$
c_\Gamma = \frac{\Gamma(1-\epsilon)^2\Gamma(1+\epsilon)}{\Gamma(1-2\epsilon)}. \qquad (3.124)
$$

3.5 Summary

In this chapter we discussed the Schwinger and Feynman representations of Feynman integrals. The first provided an algorithm to express tensor integrals in terms of scalar integrals in higher dimension and extra powers of propagators. With the second we managed to solve simple one and two-loop integrals, limiting ourselves in the cases with a single scale dependence and the results were analytic expressions in terms of Gamma functions.

In order to obtain information on more difficult integrals we used the Mellin-Barnes representation. We obtained representations of one-loop diagrams in a general manner, and we showed how to find similar representations for multi-loop diagrams using the insertion method. We were able to express the integrals as a sum of residues making manifest their hypergeometric structure. In addition, we were able to isolate the infrared and ultraviolet singularities by identifying the poles that would cross the contours of integration when an analytic continuation of ϵ to zero was performed.

We can now see a strategy to be formed for the calculation of the one and two-loop integrals of our interest.

- Rewrite the tensor integrals in terms of scalar integrals from their Schwinger parametric representation.

- Reduce the number of scalar integrals to a set of linearly independent "master" integrals. This can be done trivially for some topologies (TrianA, TrianB, TrianC...), that can be expressed in terms of Γ functions. For the rest we resort to more sophisticated methods based on Integration By Parts and they will be described in Chapter 5.

- Find the analytic expansions in ϵ of the master integrals. This will be done either by direct evaluation of the Feynman representation in terms of Γ functions or by their hypergeometric series representation or, for the most difficult cases, by an ϵ expansion of the Mellin-Barnes representation.

Before we continue to the reduction of the scalar integrals to master integrals we shall explore the Negative Dimension Integration Method which provides useful insight for the representation of Feynman integrals in terms of hypergeometric functions.

Chapter 4

Negative Dimensions Integration Method

In Chapter 3, we found an algorithm to relate tensor integrals to scalar integrals with extra-powers of propagators and higher dimension. Therefore we can concentrate on the problem of evaluating the scalar integrals only.

It is possible to represent Feynman integrals in terms of hypergeometric functions. This has several advantages. First, these hypergeometric functions often have integral representations themselves, in which an expansion in ϵ can be made, yielding expressions in logarithms, dilogarithms etc.. Second, because the series is convergent and well behaved in a particular region of phase space, it can be numerically evaluated [42, 43]. In fact, each hypergeometric representation immediately allows an asymptotic expansion of the integral in terms of ratios of momentum and mass scales. Third, through analytic continuation formulae, the hypergeometric functions valid in one kinematic domain can be re-expressed in a different kinematic region.

In the previous chapter we showed how to obtain hypergeometric series representations from the MB representations. An alternative technique which makes immediate connection to the hypergeometric structure of Feynman integrals is the Negative Dimension Integration Method (NDIM). It was originally developed by Halliday and Ricotta [44, 45] in 1987 who suggested that it would be useful to calculate the loop integral considering D as a negative number. Because loop integrals are analytic in the number of dimensions D (and also in the powers of the propagators) they proposed to calculate the integral in negative dimensions and return to positive dimensions, and specifically $D = 4-2\epsilon$, after the integrations have been performed. As we will discuss more fully later on, integration over the loop momentum and/or the parameters introduced to do the loop integration is replaced with infinite series, which again can be identified as generalised hypergeometric functions. Recently this idea has been picked up again by Suzuki and Schmidt who have evaluated a number of one-loop, two-loop and three-loop integrals [46, 47, 48, 49, 50, 51, 52, 53, 54].

In this chapter we wish to explore the negative-dimension approach (NDIM) further. In particular we focus on one-loop integrals with general powers of the propagators and arbitrary dimension D. There are several reasons for doing this. First, it allows connection with the general tensor-reduction program of the previous chapter. Second, we can imagine inserting the one-loop results into a two-loop integral by closing up external legs. This is trivial for most bubble integrals, but more complicated for vertex and box graphs. Broadhurst [55] has shown that this is possible for the non-trivial two-loop self-energy graph. Third, it actually simplifies the calculation. As we will show, by keeping the parameters general, it is easier to identify the regions of convergence of the hypergeometric series and therefore which hypergeometric functions to group together. For specific values of the parameters, the hypergeometric functions often collapse to simpler functions.

We demonstrate the method using as example the one-loop box with massless propagators and at most one external leg off-shell. With NDIM we derive the expressions for the integrals in different kinematic regions in terms of hypergeometric functions of one or two variables for the on-shell and off-shell case respectively. In both cases, D is arbitrary and the propagators are raised to arbitrary powers. As an application of the general formulae, in Sec. 4.2 we consider a particular class of two-loop box integrals which are one-loop box graphs with bubble insertions on one of the legs.

We give general formulae for the general scalar integral of the topology with light-like legs in terms of hypergeometric functions. Finally, we calculate the ϵ-expansion of the master integral of the topology in two kinematic regions, the one where both independent Mandelstam variables are negative and the one where they have opposite sign.

4.1 The general massless one-loop box integral

The generic massless one-loop box (Fig. 3.7) integral in D-dimensional Minkowski space with loop-momentum k is given by Eq. 3.65. In Section 3.3.2 we considered the integral with two light-like and two adjacent massive external legs

$$p_1^2 = p_2^2 = 0, \quad p_3^2 = M_1^2, \quad p_4^2 = M_2^2.$$

To avoid complications which obscure the explanation of the basic principles of the method due to the presence of many scales, we study the limit

$$M_1 = 0, \quad M_2 = M.$$

Therefore the set of scales present in our problem are

$$\{Q_i^2\} = \{s, t, M^2\} \tag{4.1}$$

where $s = (p_1 + p_2)^2$ and $t = (p_2 + p_3)^2$ are the usual Mandelstam variables. In the physical region $t < 0$ and $s > 0$. For standard integrals, the powers ν_i to which each propagator is raised are usually unity. However, we wish to leave the powers as general as possible. Later on we will use these general expressions to derive some results for two-loop box integrals with one-loop insertions on the propagators.

We can rewrite Eq. (3.65) in the Schwinger parameters (x_i) representation

$$I_4^D\left(\nu_1, \nu_2, \nu_3, \nu_4; \{Q_i^2\}\right) = \int \mathcal{D}x \int \frac{d^D k}{i\pi^{D/2}} \exp\left(\sum_{i=1}^{4} x_i A_i\right), \tag{4.2}$$

with

$$\int \mathcal{D}x = (-1)^N \left(\prod_{i=1}^{4} \frac{1}{\Gamma(\nu_i)} \int_0^\infty dx_i x_i^{\nu_i - 1}\right), \tag{4.3}$$

and

$$N = \nu_1 + \nu_2 + \nu_3 + \nu_4. \tag{4.4}$$

After integrating out the loop-momentum k, we obtain our known result

$$I_4^D\left(\nu_1, \nu_2, \nu_3, \nu_4; \{Q_i^2\}\right) = \int \mathcal{D}x \frac{1}{\mathcal{P}^{D/2}} \exp(\mathcal{Q}/\mathcal{P}), \tag{4.5}$$

with

$$\mathcal{P} = x_1 + x_2 + x_3 + x_4, \tag{4.6}$$

and

$$\mathcal{Q} = x_1 x_3\, s + x_2 x_4\, t + x_1 x_4\, M^2. \tag{4.7}$$

4.1.1 The negative-dimension approach

To evaluate the integral further, we treat the number of dimensions D as a negative integer. This is valid because the loop integral is an analytic function of D. Let us start from Eqs. (4.2) and (4.5) and make a series expansion of the exponentials. Eq. (4.2) becomes

$$I_4^D\left(\nu_1,\nu_2,\nu_3,\nu_4;\{Q_i^2\}\right) \;=\; \int \mathcal{D}x \sum_{n_1,\ldots,n_4=0}^{\infty} \int \frac{d^Dk}{i\pi^{D/2}} \prod_{i=1}^{4} \frac{(x_iA_i)^{n_i}}{n_i!} \tag{4.8}$$

where the n_i are positive integers. Likewise, we expand the exponential in Eq. (4.5)

$$I_4^D\left(\nu_1,\nu_2,\nu_3,\nu_4;\{Q_i^2\}\right) = \int \mathcal{D}x \sum_{n=0}^{\infty} \frac{\mathcal{Q}^n\mathcal{P}^{-n-\frac{D}{2}}}{n!}, \tag{4.9}$$

We are again in the familiar situation that we need to decompose the $\mathcal{P}$ and $\mathcal{Q}$ terms. In the last chapter we introduced Mellin-Barnes integrals to achieve the decomposition. Here, we do a multinomial expansion. In general, if we have a sum of terms raised to a power we can write

$$(x_1+x_2+\ldots+x_m)^n = \sum_{n_1,n_2,\ldots n_m=0}^{\infty} \frac{n!}{n_1!n_2!\ldots n_m!} x_1^{n_1}x_2^{n_2}\cdots x_m^{n_m}\delta_{n,n_1+\ldots n_m} \tag{4.10}$$

where the presence of the Kronecker delta fixes the sum of the summation indices to the power n. To make the multinomial expansions of $\mathcal{Q}$ and $\mathcal{P}$ we introduce the integers l_1, l_2, l_3, and m_1, m_2, m_3, m_4, so that

$$\begin{aligned} \mathcal{Q}^n &= \sum_{l_1,\ldots,l_3=0}^{\infty} \frac{(x_1x_3s)^{l_1}}{l_1!}\frac{(x_2x_4t)^{l_2}}{l_2!}\frac{(x_1x_4M^2)^{l_3}}{l_3!}(l_1+l_2+l_3)! \\ \mathcal{P}^{-n-\frac{D}{2}} &= \sum_{m_1,\ldots,m_4=0}^{\infty} \frac{x_1^{m_1}}{m_1!}\cdots\frac{x_4^{m_4}}{m_4!}(m_1+\ldots+m_4)! \end{aligned}$$

with the constraints

$$\sum_{i=1}^{3} l_i = n, \qquad \sum_{i=1}^{4} m_i = -n-\frac{D}{2}. \tag{4.11}$$

By adding together the two equations in (4.11), we obtain an additional constraint, that is

$$l_1+l_2+l_3+m_1+m_2+m_3+m_4 = -\frac{D}{2}, \tag{4.12}$$

which ensures that the powers of $\mathcal{Q}$ and $\mathcal{P}$ match up correctly. The name of the method as integration in Negative Dimensions is now justified, since for Eq. 4.12 to be valid, the dimension D must be a negative even number.

Equating Eqs. (4.8) and (4.9), we have

$$
\begin{aligned}
& I_4^D(\nu_1,\nu_2,\nu_3,\nu_4;s,t,M^2) \\
&= \int \mathcal{D}x \sum_{n_1,\ldots,n_4=0}^{\infty} \int \frac{d^Dk}{i\pi^{D/2}} \frac{(x_1A_1)^{n_1}}{n_1!} \frac{(x_2A_2)^{n_2}}{n_2!} \frac{(x_3A_3)^{n_3}}{n_3!} \frac{(x_4A_4)^{n_4}}{n_4!} \\
&= \int \mathcal{D}x \sum_{\substack{m_1,\ldots,m_4=0 \\ l_1,\ldots,l_3=0}}^{\infty} \frac{(x_1x_3s)^{l_1}\,(x_2x_4t)^{l_2}\,(x_1x_4M^2)^{l_3}}{l_1!l_2!l_3!} \frac{x_1^{m_1}\ldots x_4^{m_4}}{m_1!\ldots m_4!} \times (m_1+m_2+m_3+m_4)!,
\end{aligned}
\tag{4.13}
$$

If more than one leg is off shell, then there will be additional terms in $\mathcal{Q}$ leading to more summation variables. Similarly, if we take the $M^2 \to 0$ limit, this is the same as fixing $l_3 = 0$ in Eq. (4.13).

The x_i are independent variables so that for the equality (4.13) to hold, the integrands themselves must be equal. Therefore, by selecting the coefficient of the powers of $x_i^{-\nu_i}$, where $\nu_i = -n_i$, on both sides of the equality we find

$$
\begin{aligned}
& I_4^D(\nu_1,\nu_2,\nu_3,\nu_4;s,t,M^2) \\
&= \sum_{\substack{m_1,\ldots,m_4=0 \\ l_1,\ldots,l_3=0}}^{\infty} \frac{\Gamma(1+m_1+m_2+m_3+m_4)}{\Gamma(1+l_1)\,\Gamma(1+l_2)\,\Gamma(1+l_3)} \left(\prod_{i=1}^{4} \frac{\Gamma(1-\nu_i)}{\Gamma(1+m_i)} \right) s^{l_1} t^{l_2} \left(M^2\right)^{l_3},
\end{aligned}
\tag{4.14}
$$

subject to the system of constraints

$$
\begin{aligned}
l_1 + l_3 + m_1 &= -\nu_1, \\
l_2 + m_2 &= -\nu_2, \\
l_1 + m_3 &= -\nu_3, \\
l_2 + l_3 + m_4 &= -\nu_4, \\
l_1 + l_2 + l_3 + m_1 + m_2 + m_3 + m_4 &= -D/2.
\end{aligned}
\tag{4.15}
$$

There are seven summation variables and five constraints so that two variables will be unconstrained. There are fifteen solutions of the system of constraints. Each one is inserted into the template solution (4.14). For example, solving with respect to the indices $\{l_1, l_2\}$, we find

$$\begin{aligned}
m_1 &= \nu_2 + \nu_3 + \nu_4 + l_2 - D/2, \\
m_2 &= -\nu_2 - l_2, \\
m_3 &= -\nu_3 - l_1, \\
m_4 &= \nu_1 + \nu_2 + \nu_3 + l_1 - D/2, \\
l_3 &= -l_1 - l_2 + D/2 - \nu_1 - \nu_2 - \nu_3 - \nu_4,
\end{aligned}$$

which is then applied to (4.14). Γ functions that depend on the unconstrained variables l_1 and l_2 are converted into Pochhammer symbols

$$(z, n) \equiv \frac{\Gamma(z+n)}{\Gamma(z)}, \tag{4.16}$$

because they are the most suitable way to write generalized hypergeometric functions. Denoting this solution as $I^{\{l_1,l_2\}}$ and using the shorthand notation

$$\nu_{ij} = \nu_i + \nu_j, \qquad \nu_{ijk} = \nu_i + \nu_j + \nu_k, \tag{4.17}$$

we have

$$\begin{aligned}
I^{\{l_1,l_2\}} &= \left(M^2\right)^{\frac{D}{2}-N} \frac{\Gamma\left(1-\nu_1\right)\Gamma\left(1-\nu_4\right)\Gamma\left(1+N-D\right)}{\Gamma\left(1+\frac{D}{2}-N\right)\Gamma\left(1+\nu_{123}-\frac{D}{2}\right)\Gamma\left(1+\nu_{234}-\frac{D}{2}\right)} \\
&\times \sum_{l_1,l_2=0}^{\infty} \frac{\left(N-\frac{D}{2}, l_1+l_2\right)\left(\nu_3, l_1\right)\left(\nu_2, l_2\right)}{\left(1+\nu_{123}-\frac{D}{2}, l_1\right)\left(1+\nu_{234}-\frac{D}{2}, l_2\right)} \frac{\left(s/M^2\right)^{l_1}}{l_1!} \frac{\left(t/M^2\right)^{l_2}}{l_2!}.
\end{aligned} \tag{4.18}$$

Each solution of the system of constraints, once inserted into the template of Eq. (4.14), has the same generic form

$$\mathcal{PRE} \times \mathcal{SUM}, \tag{4.19}$$

where we have introduced the following notation:

- $\mathcal{SUM}$ is the sum over the terms that contain unconstrained indices of summation. As in the example solution (4.18), instead of dealing with Γ functions, we form Pochhammer symbols. In most cases, $\mathcal{SUM}$ can be directly identified as a generalized hypergeometric function, in the region of convergence of the series. In general, these hypergeometric functions are analytic and may be evaluated at positive values of D and ν_i. In our example, the $\mathcal{SUM}$ term, can be immediately identified as Appell's F_2 function (see Eq. (A.4))

- The prefactor $\mathcal{PRE}$ contains all the rest of the terms that are not included in $\mathcal{SUM}$. More precisely, it is a product of external scales raised to fixed powers, and Γ functions that do not depend on the summation variables. These may be produced either directly from the particular solution of the system, or in the generation of the Pochhammer symbols. For physical loop integrals with positive powers of propagators, we need to evaluate $\mathcal{PRE}$ at positive values of the ν_i and positive D. A problem is immediately obvious: the numerator of $\mathcal{PRE}$ contains $\Gamma(1-\nu_i)$, so that, for positive integer values ν_i, it appears that we need to evaluate the Γ functions for negative arguments, where they are singular. However, $\mathcal{PRE}$ is an analytic function and these singularities cancel between the numerator and denominator.

  In fact, it can be easily shown that, starting from the identity

$$\Gamma\left(z+1\right) = z\,\Gamma\left(z\right), \tag{4.20}$$

  we have

$$\frac{\Gamma\left(z\right)}{\Gamma\left(z-n\right)} = \left(-1\right)^{-n}\frac{\Gamma\left(n+1-z\right)}{\Gamma\left(1-z\right)}, \tag{4.21}$$

  where z is a real (or complex) number, and n is a positive integer.

  In the product of Γ functions in the numerator and denominator of the $\mathcal{PRE}$ term, we can make an iterated use of the identity (4.21), provided we treat $D/2$ as an integer, as we have already done in the multinomial expansion. We can then rewrite the Γ-function prefactor in a more amenable way by flipping all of the Γ functions from numerator to denominator and vice versa

$$\prod_{i=1}^{n+1}\frac{\Gamma(\alpha_i)}{\Gamma(\beta_i)} = (-1)^{\sum_{i=1}^{n+1}(\beta_i-\alpha_i)}\prod_{i=1}^{n+1}\frac{\Gamma(1-\beta_i)}{\Gamma(1-\alpha_i)}, \tag{4.22}$$

  where the index i runs over all Γ functions in the numerator and denominator of $\mathcal{PRE}$.

Applying (4.22) to (4.18) we find that

$$\begin{aligned} I^{\{l_1,l_2\}} &= (-1)^{\frac{D}{2}}\,\left(M^2\right)^{\frac{D}{2}-N}\frac{\Gamma\left(N-\frac{D}{2}\right)\Gamma\left(\frac{D}{2}-\nu_{123}\right)\Gamma\left(\frac{D}{2}-\nu_{234}\right)}{\Gamma\left(\nu_1\right)\Gamma\left(\nu_4\right)\Gamma\left(D-N\right)} \\ &\times\; F_2\left(N-\frac{D}{2},\nu_3,\nu_2,1+\nu_{123}-\frac{D}{2},1+\nu_{234}-\frac{D}{2},\frac{s}{M^2},\frac{t}{M^2}\right). \end{aligned} \tag{4.23}$$

Similarly, the other fourteen solutions are given by:

$$
\begin{aligned}
I_4^{\{m_1,m_4\}} &= (-1)^{\frac{D}{2}}\; s^{\frac{D}{2}-\nu_{123}} t^{\frac{D}{2}-\nu_{234}} \left(M^2\right)^{\nu_{23}-\frac{D}{2}} \\
&\times \frac{\Gamma\left(\nu_{123}-\frac{D}{2}\right)\Gamma\left(\nu_{234}-\frac{D}{2}\right)\Gamma\left(\frac{D}{2}-\nu_{12}\right)\Gamma\left(\frac{D}{2}-\nu_{34}\right)\Gamma\left(\frac{D}{2}-\nu_{23}\right)}{\Gamma\left(\nu_1\right)\Gamma\left(\nu_2\right)\Gamma\left(\nu_3\right)\Gamma\left(\nu_4\right)\Gamma\left(D-N\right)} \\
&\times F_2\left(\frac{D}{2}-\nu_{23}, \frac{D}{2}-\nu_{12}, \frac{D}{2}-\nu_{34}, 1+\frac{D}{2}-\nu_{123}, 1+\frac{D}{2}-\nu_{234}, \frac{s}{M^2}, \frac{t}{M^2}\right),
\end{aligned}
$$

$$
\begin{aligned}
I_4^{\{m_1,l_1\}} &= (-1)^{\frac{D}{2}}\; t^{\frac{D}{2}-\nu_{234}} \left(M^2\right)^{-\nu_1} \frac{\Gamma\left(\nu_{234}-\frac{D}{2}\right)\Gamma\left(\frac{D}{2}-\nu_{123}\right)\Gamma\left(\frac{D}{2}-\nu_{34}\right)}{\Gamma\left(\nu_2\right)\Gamma\left(\nu_4\right)\Gamma\left(D-N\right)} \\
&\times F_2\left(\nu_1, \nu_3, \frac{D}{2}-\nu_{34}, 1+\nu_{123}-\frac{D}{2}, 1+\frac{D}{2}-\nu_{234}, \frac{s}{M^2}, \frac{t}{M^2}\right),
\end{aligned}
$$

$$
\begin{aligned}
I_4^{\{m_4,l_2\}} &= (-1)^{\frac{D}{2}}\; s^{\frac{D}{2}-\nu_{123}} \left(M^2\right)^{-\nu_4} \frac{\Gamma\left(\nu_{123}-\frac{D}{2}\right)\Gamma\left(\frac{D}{2}-\nu_{12}\right)\Gamma\left(\frac{D}{2}-\nu_{234}\right)}{\Gamma\left(\nu_1\right)\Gamma\left(\nu_3\right)\Gamma\left(D-N\right)} \\
&\times F_2\left(\nu_4, \frac{D}{2}-\nu_{12}, \nu_2, 1+\frac{D}{2}-\nu_{123}, 1+\nu_{234}-\frac{D}{2}, \frac{s}{M^2}, \frac{t}{M^2}\right), \\
I_4^{\{m_2,m_4\}} &= (-1)^{\frac{D}{2}}\; s^{\frac{D}{2}-\nu_{123}} t^{-\nu_2} \left(M^2\right)^{\nu_2-\nu_4} \frac{\Gamma\left(\nu_{123}-\frac{D}{2}\right)\Gamma\left(\nu_4-\nu_2\right)\Gamma\left(\frac{D}{2}-\nu_{12}\right)\Gamma\left(\frac{D}{2}-\nu_{34}\right)}{\Gamma\left(\nu_1\right)\Gamma\left(\nu_3\right)\Gamma\left(\nu_4\right)\Gamma\left(D-N\right)}
\end{aligned}
$$

$$
\begin{aligned}
&\times H_2\left(\nu_4-\nu_2, \frac{D}{2}-\nu_{12}, \nu_2, \frac{D}{2}-\nu_{34}, 1+\frac{D}{2}-\nu_{123}, \frac{s}{M^2}, -\frac{M^2}{t}\right), \\
I_4^{\{m_2,l_1\}} &= (-1)^{\frac{D}{2}}\; t^{-\nu_2} \left(M^2\right)^{\frac{D}{2}-\nu_{134}} \frac{\Gamma\left(\nu_{134}-\frac{D}{2}\right)\Gamma\left(\frac{D}{2}-\nu_{123}\right)\Gamma\left(\frac{D}{2}-\nu_{34}\right)}{\Gamma\left(\nu_1\right)\Gamma\left(\nu_4\right)\Gamma\left(D-N\right)} \\
&\times H_2\left(\nu_{134}-\frac{D}{2}, \nu_3, \nu_2, \frac{D}{2}-\nu_{34}, 1+\nu_{123}-\frac{D}{2}, \frac{s}{M^2}, -\frac{M^2}{t}\right),
\end{aligned}
$$

$$
\begin{aligned}
I_4^{\{m_4,l_3\}} &= (-1)^{\frac{D}{2}}\; s^{\frac{D}{2}-\nu_{123}} t^{-\nu_4} \frac{\Gamma\left(\nu_{123}-\frac{D}{2}\right)\Gamma\left(\nu_2-\nu_4\right)\Gamma\left(\frac{D}{2}-\nu_{12}\right)\Gamma\left(\frac{D}{2}-\nu_{23}\right)}{\Gamma\left(\nu_1\right)\Gamma\left(\nu_2\right)\Gamma\left(\nu_3\right)\Gamma\left(D-N\right)} \\
&\times S_1\left(\nu_4, \frac{D}{2}-\nu_{23}, \frac{D}{2}-\nu_{12}, 1-\nu_2+\nu_4, 1+\frac{D}{2}-\nu_{123}, -\frac{s}{t}, \frac{M^2}{t}\right), \\
I_4^{\{l_1,l_3\}} &= (-1)^{\frac{D}{2}}\; t^{\frac{D}{2}-N} \frac{\Gamma\left(N-\frac{D}{2}\right)\Gamma\left(\frac{D}{2}-\nu_{123}\right)\Gamma\left(\frac{D}{2}-\nu_{134}\right)}{\Gamma\left(\nu_2\right)\Gamma\left(\nu_4\right)\Gamma\left(D-N\right)} \\
&\times S_1\left(N-\frac{D}{2}, \nu_1, \nu_3, 1+\nu_{134}-\frac{D}{2}, 1+\nu_{123}-\frac{D}{2}, -\frac{s}{t}, \frac{M^2}{t}\right),
\end{aligned}
$$

$$
\begin{aligned}
I_4^{\{m_2,m_3\}} &= (-1)^{\frac{D}{2}}\; s^{-\nu_3} t^{-\nu_2} \left(M^2\right)^{\frac{D}{2}-\nu_{14}} \frac{\Gamma\left(\nu_{14}-\frac{D}{2}\right)\Gamma\left(\frac{D}{2}-\nu_{12}\right)\Gamma\left(\frac{D}{2}-\nu_{34}\right)}{\Gamma\left(\nu_1\right)\Gamma\left(\nu_4\right)\Gamma\left(D-N\right)} \\
&\times F_3\left(\nu_2, \nu_3, \frac{D}{2}-\nu_{34}, \frac{D}{2}-\nu_{12}, 1+\frac{D}{2}-\nu_{14}, \frac{M^2}{t}, \frac{M^2}{s}\right),
\end{aligned}
$$

$$
\begin{aligned}
I_4^{\{m_2,l_3\}} &= (-1)^{\frac{D}{2}}\, s^{\frac{D}{2}-\nu_{134}} t^{-\nu_2} \frac{\Gamma\left(\nu_{134}-\frac{D}{2}\right)\Gamma\left(\nu_4-\nu_2\right)\Gamma\left(\frac{D}{2}-\nu_{34}\right)\Gamma\left(\frac{D}{2}-\nu_{14}\right)}{\Gamma\left(\nu_1\right)\Gamma\left(\nu_3\right)\Gamma\left(\nu_4\right)\Gamma\left(D-N\right)} \\
&\times\; S_2\left(\nu_{134}-\frac{D}{2}, \nu_4-\nu_2, \frac{D}{2}-\nu_{34}, \nu_2, 1+\nu_{14}-\frac{D}{2}, \frac{M^2}{s}, \frac{s}{t}\right),
\end{aligned}
$$

$$
\begin{aligned}
I_4^{\{m_1,m_3\}} &= I_4^{\{m_2,m_4\}}\left(s\leftrightarrow t,\ \nu_1\leftrightarrow\nu_4,\ \nu_2\leftrightarrow\nu_3\right), \\
I_4^{\{m_3,l_2\}} &= I_4^{\{m_2,l_1\}}\left(s\leftrightarrow t,\ \nu_1\leftrightarrow\nu_4,\ \nu_2\leftrightarrow\nu_3\right), \\
I_4^{\{m_1,l_3\}} &= I_4^{\{m_4,l_3\}}\left(s\leftrightarrow t,\ \nu_1\leftrightarrow\nu_4,\ \nu_2\leftrightarrow\nu_3\right), \\
I_4^{\{l_2,l_3\}} &= I_4^{\{l_1,l_3\}}\left(s\leftrightarrow t,\ \nu_1\leftrightarrow\nu_4,\ \nu_2\leftrightarrow\nu_3\right), \\
I_4^{\{m_3,l_3\}} &= I_4^{\{m_2,l_3\}}\left(s\leftrightarrow t,\ \nu_1\leftrightarrow\nu_4,\ \nu_2\leftrightarrow\nu_3\right).
\end{aligned} \tag{4.24}
$$

The definitions of the functions F_3, H_2, S_1 and S_2 are given in Sec. A.1 together with a table of their regions of convergence.

4.1.2 Classification of the groups of solutions from their region of convergence

We now have to classify the zoo of the solutions of the system of constraints, and more important, we need to answer the practical question of which of them together consist a valid representation of the integral. Within NDIM the answer to this is very simple. One has to add together the solutions that converge in the same kinematic region. For the one-loop box with one leg off-shell, we divide the kinematic regions up as shown in Fig. 4.1:

$$
\begin{aligned}
&\text{region I}: && M^2 > |s|+|t|, \\
&\text{region II(a)}: && |t| > M^2+|s| \text{ and } M^2>|s|, \\
&\text{region II(b)}: && |t| > M^2+|s| \text{ and } |s|>M^2, \\
&\text{region III(a)}: && |s| > M^2+|t| \text{ and } M^2>|t|, \\
&\text{region III(b)}: && |s| > M^2+|t| \text{ and } |t|>M^2,
\end{aligned}
$$

and, applying the convergence criteria of Table A.1 to each of the fifteen solutions, we find that they are distributed as follows:

in region I

$$
I_4^D(\nu_1,\nu_2,\nu_3,\nu_4;s,t,M^2) = I_4^{\{l_1,l_2\}} + I_4^{\{m_1,m_4\}} + I_4^{\{m_4,l_2\}} + I_4^{\{m_1,l_1\}}, \tag{4.26}
$$

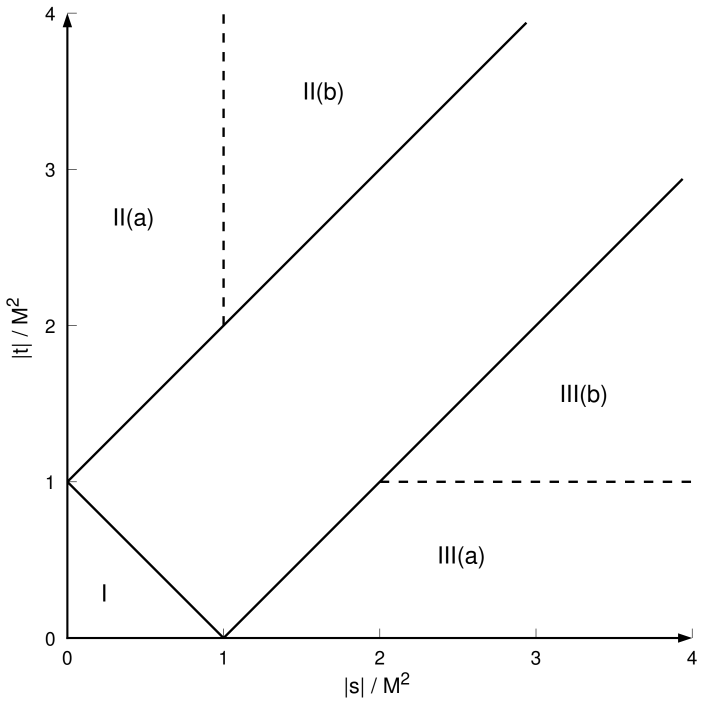

Figure 4.1: The kinematic regions for the one-loop box with one off-shell leg. The solid line shows the phase-space boundary $|s|+|t| = M^2$, together with the reflections $|s| = |t| + M^2$ and $|t| = |s| + M^2$. The reflections are relevant for the convergence properties of the hypergeometric functions which only involve the absolute values of ratios of the scales. The dashed lines show the boundaries $|s| = M^2$ and $|t| = M^2$.

in region II(a)

$$I_4^D(\nu_1,\nu_2,\nu_3,\nu_4;s,t,M^2) = I_4^{\{m_2,m_4\}} + I_4^{\{m_2,l_1\}} + I_4^{\{m_4,l_3\}} + I_4^{\{l_1,l_3\}}, \quad (4.27)$$

in region II(b)

$$I_4^D(\nu_1,\nu_2,\nu_3,\nu_4;s,t,M^2) = I_4^{\{m_2,m_3\}} + I_4^{\{m_2,l_3\}} + I_4^{\{m_4,l_3\}} + I_4^{\{l_1,l_3\}}, \quad (4.28)$$

in region III(a)

$$I_4^D(\nu_1,\nu_2,\nu_3,\nu_4;s,t,M^2) = I_4^{\{m_1,m_3\}} + I_4^{\{m_3,l_2\}} + I_4^{\{m_1,l_3\}} + I_4^{\{l_2,l_3\}}, \quad (4.29)$$

in region III(b)

$$I_4^D(\nu_1,\nu_2,\nu_3,\nu_4;s,t,M^2) = I_4^{\{m_2,m_3\}} + I_4^{\{m_3,l_3\}} + I_4^{\{m_1,l_3\}} + I_4^{\{l_2,l_3\}}. \quad (4.30)$$

Some solutions are convergent in more than one region. For example, $I_4^{\{m_4,l_3\}}$ and $I_4^{\{l_1,l_3\}}$ are convergent in both regions II(a) and II(b) while $I_4^{\{m_2,m_3\}}$ is convergent in both II(b) and III(b). We also see that in region II(a), two of the solutions $\left(I_4^{\{m_2,m_4\}}\right.$ and $\left.I_4^{\{m_4,l_3\}}\right)$ contain dangerous Γ functions when $\nu_2 = \nu_4$. These divergences indicate the region of a logarithmic analytic continuation and can be regulated by letting $\nu_2 = \nu_4 + \delta$, canceling the divergence, and then setting $\delta \to 0$. Similarly, the two divergent contributions in region II(b) $\left(I_4^{\{m_2,l_3\}}\right.$ and $\left.I_4^{\{m_4,l_3\}}\right)$ must be combined in this way.

The above results agree with these obtained starting from the Mellin-Barnes representation (3.73). Closing the contours either to the left or to the right and summing up the enclosed residues, we obtain the same hypergeometric series representations as with NDIM.

4.1.3 Analytic Continuations-Limiting cases

We can perform several checks of these results.

- **Analytic continuation**

  The solutions in the different regions are related by analytic continuations of the hypergeometric functions. We can verify that starting from one region and applying the analytic continuations of the hypergeometric functions we find the solutions in the other kinematic regions

- **The $\nu_i = 0$ limit**

  By pinching out one or more of the propagators (which corresponds to setting $\nu_i = 0$) we obtain results for triangle or bubble integrals. For example, if we set $\nu_2 = \nu_3 = 0$, then any term containing $1/\Gamma(\nu_2)$ or $1/\Gamma(\nu_3)$ is eliminated. In fact, only five solutions survive, one in each group. In each case, the hypergeometric function collapses to unity and we obtain the expected result for the massless-bubble integral with off-shellness M^2 in each of the five kinematic regions thereby spanning the whole of phase space

$$I_2^D\left(\nu_1, \nu_4; M^2\right) = \left(M^2\right)^{\frac{D}{2}-\nu_1-\nu_4} \Pi^D(\nu_1, \nu_4), \tag{4.31}$$

  where the Π^D functon was defined in Eq. 3.37

- **The massless box: $I_4^D\left(\nu_1, \nu_2, \nu_3, \nu_4; s, t\right)$**

  The limit $M^2 \to 0$ can be taken whenever the kinematic region allows it, that is to say, in regions II(b) and III(b), where $M^2 < |s|$, $M^2 < |t|$. These two regions are related by the symmetry $(s \leftrightarrow t,\ \nu_1 \leftrightarrow \nu_4,\ \nu_2 \leftrightarrow \nu_3)$, so we focus only on region II(b). Only three of the solutions survive, and we have:

  if $|s| < |t|$

$$\begin{aligned}
I_4^D\left(\nu_1, \nu_2, \nu_3, \nu_4; s, t\right) &= I_4^{\{l_1,l_3\}}\Big|_{M^2=0} + I_4^{\{m_2,l_3\}}\Big|_{M^2=0} + I_4^{\{m_4,l_3\}}\Big|_{M^2=0} \\
= &\ (-1)^{\frac{D}{2}}\ t^{\frac{D}{2}-N} \frac{\Gamma\left(N-\frac{D}{2}\right)\Gamma\left(\frac{D}{2}-\nu_{134}\right)\Gamma\left(\frac{D}{2}-\nu_{123}\right)}{\Gamma\left(\nu_2\right)\Gamma\left(\nu_4\right)\Gamma\left(D-N\right)} \\
\times &\ {}_3F_2\left(\nu_1, \nu_3, N-\frac{D}{2}, 1+\nu_{134}-\frac{D}{2}, 1+\nu_{123}-\frac{D}{2}, -\frac{s}{t}\right) \\
+ &\ (-1)^{\frac{D}{2}}\ s^{\frac{D}{2}-\nu_{123}} t^{-\nu_4} \frac{\Gamma\left(\nu_{123}-\frac{D}{2}\right)\Gamma\left(\nu_2-\nu_4\right)\Gamma\left(\frac{D}{2}-\nu_{23}\right)\Gamma\left(\frac{D}{2}-\nu_{12}\right)}{\Gamma\left(\nu_1\right)\Gamma\left(\nu_2\right)\Gamma\left(\nu_3\right)\Gamma\left(D-N\right)} \\
\times &\ {}_3F_2\left(\nu_4, \frac{D}{2}-\nu_{12}, \frac{D}{2}-\nu_{23}, 1+\nu_4-\nu_2, 1+\frac{D}{2}-\nu_{123}, -\frac{s}{t}\right) \\
+ &\ (-1)^{\frac{D}{2}}\ s^{\frac{D}{2}-\nu_{134}} t^{-\nu_2} \frac{\Gamma\left(\nu_{134}-\frac{D}{2}\right)\Gamma\left(\nu_4-\nu_2\right)\Gamma\left(\frac{D}{2}-\nu_{14}\right)\Gamma\left(\frac{D}{2}-\nu_{34}\right)}{\Gamma\left(\nu_1\right)\Gamma\left(\nu_3\right)\Gamma\left(\nu_4\right)\Gamma\left(D-N\right)} \\
\times &\ {}_3F_2\left(\nu_2, \frac{D}{2}-\nu_{14}, \frac{D}{2}-\nu_{34}, 1-\nu_4+\nu_2, 1+\frac{D}{2}-\nu_{134}, -\frac{s}{t}\right).
\end{aligned} \tag{4.32}$$

  Similarly, taking the same $M^2 \to 0$ limit for solution (4.30) in region III(b), we find the result valid when $|s| > |t|$, which is also obtained by applying the exchanges $(s \leftrightarrow t,\ \nu_1 \leftrightarrow \nu_4,\ \nu_2 \leftrightarrow \nu_3)$ to Eq. (4.32). Note that we could have obtained the same result by returning to the template solution (4.14) with the system of constraints (4.15) and, after setting $l_3 = 0$, solved the on-shell box directly. In this case, there are two external scales, s and t, so that there will be six summation variables ($m_1, \ldots, m_4$ and l_1, l_2) and five constraints yielding six solutions, three of which converge when $|s| < |t|$, again yielding Eq. (4.32).

As before, there are apparent divergences in the Γ functions when $\nu_2 = \nu_4$ that must be regulated. This is straightforwardly achieved for particular values of the parameters by setting $\nu_2 = \nu_4 + \delta$ and making a Taylor expansion.

- **The $\nu_i = 1$ limit: $I_4^D(1,1,1,1; s,t,M^2)$**

If we set the propagator power equal to one, then all the groups (4.26)–(4.30) give the correct answer

$$I_4^D(1,1,1,1;s,t,M^2) = \frac{2}{\epsilon^2}\frac{\Gamma^2(1-\epsilon)\,\Gamma(1+\epsilon)}{\Gamma(1-2\epsilon)}\frac{1}{st}\Bigg[(-t)^{-\epsilon}{}_2F_1\left(1,-\epsilon,1-\epsilon,-\frac{u}{s}\right)$$
$$+(-s)^{-\epsilon}{}_2F_1\left(1,-\epsilon,1-\epsilon,-\frac{u}{t}\right) - (-M^2)^{-\epsilon}{}_2F_1\left(1,-\epsilon,1-\epsilon,-\frac{M^2u}{st}\right)\Bigg], \tag{4.33}$$

where u is defined by $s+t+u = M^2$ and $\epsilon = (4-D)/2$. To obtain this result we have returned to the series representation of the hypergeometric function and manipulated the series by repeatedly summing with respect to one summation index to obtain an ${}_2F_1$ function, applied identities to change the arguments of the ${}_2F_1$ and rewritten the ${}_2F_1$ as a series. Then we sum with respect to the other index, and repeat if necessary. Eventually all of the hypergeometric functions of two variables can be reduced to ${}_2F_1$ functions.

4.2 Application to two-loop box graphs: The Abox topology

The general results for one-loop box graphs presented in the previous section may be applied to give analytic results for two-loop box integrals with one-loop bubble insertions in one of the propagators. As is well known, the effect of such insertions

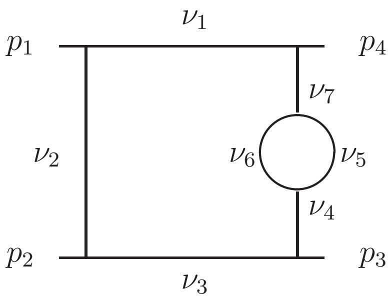

Figure 4.2: A one-loop insertion into a one-loop box diagram.

is to modify the power to which that propagator is raised. For example, we consider the two-loop **Abox** topology shown in Fig. 4.2, with massless external legs

$$\mathbf{Abox}^D(\nu_1,\nu_2,\nu_3,\nu_4,\nu_5,\nu_6,\nu_7;s,t) = \int \frac{d^Dk_1}{i\pi^{D/2}} \int \frac{d^Dk_2}{i\pi^{D/2}} \frac{1}{A_1^{\mu_1}A_2^{\mu_2}A_3^{\mu_3}A_4^{\mu_4}B_1^{\mu_5}B_2^{\mu_6}A_4^{\mu_7}}, \tag{4.34}$$

where the A_i are independent of the second loop momentum k_2 and are given by

$$\begin{aligned} A_1 &= k_1^2 + i0, \\ A_2 &= (k_1+p_1)^2 + i0, \\ A_3 &= (k_1+p_1+p_2)^2 + i0, \\ A_4 &= (k_1+p_1+p_2+p_3)^2 + i0. \end{aligned} \tag{4.35}$$

while

$$\begin{aligned} B_1 &= k_2^2 + i0 \\ B_2 &= (k_2+k_1+p_1+p_2+p_3)^2 + i0. \end{aligned} \tag{4.36}$$

The kinematic variables present are

$$s = (p_1+p_2)^2, \quad t = (p_2+p_3)^2, \quad u = (p_1+p_3)^2 = -s-t$$

while

$$p_1^2 = p_2^2 = p_3^2 = p_4^2 = 0$$

and

$$p_4 = -p_1 - p_2 - p_3.$$

The momentum flowing through the bubble is $k_1+p_1+p_2+p_3$ so that the result of the integration over k_2 is

$$\int \frac{d^Dk_2}{i\pi^{D/2}} \frac{1}{B_1^{\mu_5}B_2^{\mu_6}} = I_2^D(\nu_5,\nu_6;A_4) = \Pi^D(\nu_5,\nu_6)\; A_4^{\frac{D}{2}-\nu_5-\nu_6}, \tag{4.37}$$

where Π^D is defined in Eq. (3.37). In this way, the overall power to which A_4 is raised to, in the two-loop diagram (4.34), is $\nu_4+\nu_5+\nu_6+\nu_7-\frac{D}{2}$. Inserting Eq. (4.37) into (4.34) we find

$$\mathbf{Abox}^D(\nu_1,\nu_2,\nu_3,\nu_4,\nu_5,\nu_6,\nu_7;s,t) = \Pi^D(\nu_5,\nu_6)\; I_4^D\left(\nu_1,\nu_2,\nu_3,\nu_{4567}-\frac{D}{2};s,t\right). \tag{4.38}$$

We can immediately obtain a hypergeometric series representation of the **Abox** topology using the representation (4.32).

In Chapter 5 we will see that the every integral of the topology can be written in terms of integrals belonging to subtopologies and the **ABOX** master integral which is defined as

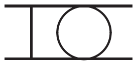

$$(s,t) = \mathbf{Abox}^{4-2\epsilon}(1,1,1,0,1,1,0;s,t) \tag{4.39}$$

By direct substitution in Eq. 4.38 and trivial manipulations of the hypergeometric functions we obtain

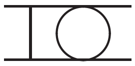

$$\begin{aligned}(s,t) &= (-t)^{-2\epsilon}\frac{K_1}{2\,s\,\epsilon^3}\;{}_2F_1\left(1,-\epsilon,1-\epsilon,\frac{s+t}{s}\right)\\ &+ (-s)^{-2\epsilon}\frac{K_2}{2\,s\,\epsilon^3}\;{}_2F_1\left(1,\epsilon,1-\epsilon,\frac{s+t}{s}\right),\end{aligned} \tag{4.40}$$

where the constants K_1 and K_2 are given by

$$K_1 = \frac{\Gamma(1+2\epsilon)\,\Gamma(1-\epsilon)^3}{(1-2\epsilon)\,\Gamma(1-3\epsilon)} \tag{4.41}$$

$$K_2 = \frac{\Gamma(1+2\epsilon)\,\Gamma(1-2\epsilon)\,\Gamma(1+\epsilon)\,\Gamma(1-\epsilon)^2}{(1-2\epsilon)\,\Gamma(1-3\epsilon)}. \tag{4.42}$$

Note that by starting off with the NDIM approach, we have not actually had to perform any integrations to reach this result or make any assumptions about the smallness of ϵ. The hypergeometric functions have one-dimensional integral representations (see Eq. (A.10)) and can be expanded around $\epsilon=0$ in terms of polylogarithms. The necessary integrals are easily done

$$ {}_2F_1\left(1,-\epsilon,1-\epsilon,x\right) = 1+\epsilon\log(1-x)-\epsilon^2\,\mathrm{Li}_2\left(x\right)-\epsilon^3\,\mathrm{Li}_3\left(x\right)-\epsilon^4\,\mathrm{Li}_4\left(x\right)+\mathcal{O}\left(\epsilon^5\right) \tag{4.43} $$

$$ \begin{aligned} {}_2F_1\left(1,\epsilon,1-\epsilon,x\right) &= (1-x)^{-2\epsilon}\Big\{1+\log(1-x)\epsilon+\left[\,\mathrm{Li}_2\left(x\right)+\log^2(1-x)\right]\epsilon^2 \\ &+\left[\mathrm{Li}_3\left(x\right)-2\,\mathrm{S}_{1,2}\left(x\right)+\frac{2}{3}\log^3(1-x)\right]\epsilon^3 \\ &+\left[\mathrm{Li}_4\left(x\right)+4\,\mathrm{S}_{1,3}\left(x\right)-2\,\mathrm{S}_{2,2}\left(x\right)+\frac{1}{3}\log^4(1-x)\right]\epsilon^4+\mathcal{O}\left(\epsilon^5\right)\Big\}. \end{aligned} \tag{4.44} $$

where $x<1$ so that the polylogarithms are real. For $x>1$ we have to use the inversion formulae of Appendix B.2 producing imaginary parts.

We finally obtain

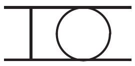

$$ (s,t) = \frac{\Gamma^3\left(1-\epsilon\right)\Gamma\left(1+2\epsilon\right)}{2\,s\,\left(1-2\epsilon\right)\,\epsilon^3\,\Gamma\left(1-3\epsilon\right)}\left[(-s)^{-2\epsilon}\,A_1\left(s,t\right)+(-t)^{-2\epsilon}\,A_2\left(s,t\right)\right] \tag{4.45} $$

where $A_1\left(s,t\right)$ and $A_2\left(s,t\right)$ are given respectively by:

1) in the physical region $s>0$, $t<0$:

$$ \begin{aligned} A_1\left(s,t\right) &= \left(-\frac{t}{s}\right)^{-\epsilon}\Big\{1-\epsilon^2\left[\mathrm{Li}_2\left(\frac{s+t}{t}\right)-2\zeta_2\right]-\epsilon^3\Big[\mathrm{Li}_3\left(\frac{s+t}{t}\right)+\,\mathrm{S}_{1,2}\left(\frac{s+t}{t}\right) \\ &-2\zeta_3\Big]-\epsilon^4\Big[\mathrm{Li}_4\left(\frac{s+t}{t}\right)+\,\mathrm{S}_{2,2}\left(\frac{s+t}{t}\right)+\,\mathrm{S}_{1,3}\left(\frac{s+t}{t}\right) \\ &+2\zeta_2\,\mathrm{Li}_2\left(\frac{s+t}{t}\right)-9\zeta_4\Big]\Big\}+\mathcal{O}\left(\epsilon^5\right), \end{aligned} \tag{4.46} $$

$$ \begin{aligned} A_2\left(s,t\right) &= 1+\epsilon\log\left(-\frac{t}{s}\right)-\epsilon^2\,\mathrm{Li}_2\left(\frac{s+t}{s}\right)-\epsilon^3\,\mathrm{Li}_3\left(\frac{s+t}{s}\right)-\epsilon^4\,\mathrm{Li}_4\left(\frac{s+t}{s}\right) \\ &+\mathcal{O}\left(\epsilon^5\right), \end{aligned} \tag{4.47} $$

2) while in the region $s < 0$, $t < 0$:

$$\begin{aligned}
A_1(s,t) &= \left(\frac{t}{s}\right)^{-\epsilon}\left\{1+\epsilon^2\left[\mathrm{Li}_2\left(\frac{t}{s+t}\right)+\frac{1}{2}\log^2\left(\frac{s+t}{t}\right)-\frac{\pi^2}{2}\right]-\epsilon^3\left[2\,\mathrm{Li}_3\left(\frac{t}{s+t}\right)\right.\right.\\
&\quad \left.-\,\mathrm{S}_{1,2}\left(\frac{t}{s+t}\right)-\zeta_3+\log\left(\frac{s+t}{t}\right)\left(\mathrm{Li}_2\left(\frac{t}{s+t}\right)+\frac{5}{6}\pi^2\right)\right]\\
&\quad +\epsilon^4\left[\mathrm{S}_{1,3}\left(\frac{t}{s+t}\right)-2\,\mathrm{S}_{2,2}\left(\frac{t}{s+t}\right)+4\,\mathrm{Li}_4\left(\frac{t}{s+t}\right)-\frac{23}{180}\pi^4\right.\\
&\quad \left.+\frac{1}{24}\log^4\left(\frac{s+t}{t}\right)+\log\left(\frac{s+t}{t}\right)\left(2\,\mathrm{Li}_3\left(\frac{t}{s+t}\right)-\mathrm{S}_{1,2}\left(\frac{t}{s+t}\right)-\zeta_3\right)\right]\\
&\quad \left.+\frac{\pi^2}{3}\mathrm{Li}_2\left(\frac{t}{s+t}\right)-\frac{\pi^2}{4}\log^2\left(\frac{s+t}{t}\right)+\frac{1}{2}\log^2\left(\frac{s+t}{t}\right)\mathrm{Li}_2\left(\frac{t}{s+t}\right)\right\}\\
&\quad +\mathcal{O}\left(\epsilon^5\right), \qquad (4.48)\\
A_2(s,t) &= 1+\epsilon\log\left(\frac{t}{s}\right)+\epsilon^2\left[\mathrm{Li}_2\left(\frac{s}{s+t}\right)+\frac{1}{2}\log^2\left(\frac{s+t}{s}\right)-\frac{\pi^2}{3}\right]\\
&\quad -\epsilon^3\left[\mathrm{Li}_3\left(\frac{s}{s+t}\right)+\frac{\pi^2}{3}\log\left(\frac{s+t}{s}\right)-\frac{1}{6}\log^3\left(\frac{s+t}{s}\right)\right]\\
&\quad +\epsilon^4\left[\mathrm{Li}_4\left(\frac{s}{s+t}\right)-\frac{\pi^4}{45}-\frac{\pi^2}{6}\log^2\left(\frac{s+t}{s}\right)+\frac{1}{24}\log^4\left(\frac{s+t}{s}\right)\right]\\
&\quad +\mathcal{O}\left(\epsilon^5\right). \qquad (4.49)
\end{aligned}$$

4.3 Discussion

In this chapter we have evaluated one-loop massless box integrals with arbitrary powers of the propagators and with up to one off-shell leg as combinations of hypergeometric functions. The method we used (NDIM), first suggested by Halliday and Ricotta, has its roots in the analytic properties of loop integrals and, in particular, the possibility of treating the space-time dimensions D as a negative integer in intermediate steps.

One can trivially apply NDIM and derive representations in terms of hypergeometric functions for other one-loop diagrams. In general it should be expected that one-loop diagrams with q mass or momentum scales and arbitrary powers of propagators can be expressed, in a straightforward manner, in terms of hypergeometric functions with $q-1$ summation variables. This makes NDIM an extremely efficient method at one-loop level. Nevertheless, for practical purposes, we are interested in calculating the analytic expansions in ϵ of the integrals in terms of logarithms and generalised polylogarithms. As shown for the one-loop massless on-shell box, it may be done through the integral representations of the hypergeometric functions. Unfortunately, although many results have been obtained in this way, it turns out that in various cases expanding the hypergeometric integral representation is very hard if not impossible. Furthermore hypergeometric functions of many variables do not always have known integral representations.

At two-loop level, NDIM has a very limited success where practical difficulties arise from many sources. The terms $\mathcal{P}$ and $\mathcal{Q}$ have in general a much bigger number of terms. Therefore, for their multinomial expansion more indices are required, and due to the small number of constraints, one is left with a big number of indices that should be summed over. Typically, the summations are not easy to perform and very few mathematical tools have been developed in this direction. What is more, the number of solutions is large (typically a few thousands), and it seems impractical at present to identify the region of convergence of all individual solutions.

One could try to avoid having a big number of solutions and many sums to perform by viewing a two-loop integral as the insertion of one-loop into the other, where the second integration is meant to be performed over a one-loop function. With the insertion approach we are always dealing with one loop diagrams and hope to gain better control over the number of solutions and the number of summations. As shown in this chapter, this approach is straightforward when the inserted one-loop graph is a bubble. However this approach becomes very demanding when we have to insert a triangle or a box graph into a second loop using the representations in terms of hypergeometric functions which converge in a specific kinematic domain. A problem arises, since the second integration has to be performed over all kinematic domains, and a systematic way of doing this, unlike the Mellin-Barnes method, is not yet understood for a completely analytic approach.

To summarise, NDIM is very efficient for one-loop integrals with many scales, at least for the cases that we know the integral representations of the hypergeometric functions involved. We could also expect to work in two-loop integrals of the bubble-insertion type, or with dependence on only one mass or momentum scale (propagator-type graphs or triangle graphs with two on-shell external legs). For other integrals appearing in QCD 2→2 scattering we will have to employ more powerful and specialized methods, like Integration By Parts (IBP) and Mellin-Barnes representations.

Chapter 5

Integration by Parts

So far we have been able to relate tensor integrals to scalar integrals with higher powers of propagators and higher dimension. Our attempt to deal with the scalar integrals using the Negative Dimensions Integration Method, provided useful results for one-loop topologies but had problems at two-loops.

In this chapter we shall attack the problem of the multitude of the scalar integrals that we produce from the tensor reduction program of Chapter 3 in a more efficient way. Our aim is to find relations that their recursive application connects scalar integrals with arbitrary powers of propagators and dimension to a minimal set of "master" integrals which are independent of each other i.e they consist a basis in the space of scalar integrals.

It is practical to separate this task into two steps. First we find an algorithm which systematically decreases the power of the propagators achieving the reduction to the scalar integrals of the basis but still in higher dimensions. The algorithm is based on identities derived from Integration by Parts (IBP) or exploiting the invariance of the scalar integrals under Lorentz transformations of the loop momenta. IBP was first introduced by Tkachov and Chetyrkin in 1980 (Ref. [56, 57]). Recently, Gehrmann and Remiddi [25] used the property of Lorentz invariance of scalar integrals to extend the set of identities among the different integrals of a topology. The identities are specific to each topology, though there are many common relations between parent topologies and their sub-topologies.

As a second step, we must find relations reducing the dimension of the scalar integrals of the basis in $D = 4 - 2\epsilon$ dimensions. We start from the Schwinger representation of the master integrals in D, rewrite them as scalar integrals in $D+2$ and extra powers of propagators, and use the algorithm of step one to reduce the extra powers. We therefore end up with a system of equations between the integrals of the basis in D and $D+2$ dimensions. Inverting the system, we obtain relations for the dimensional shift from the basis-integrals in higher dimensions to the master integrals in $D = 4 - 2\epsilon$.

The reduction of tensor integrals to master integrals is a great simplification of the initial problem since the only ingredient missing is to find the analytic expansions in ϵ of the few master integrals only. For the simple ones, Feynman parameters are sufficient and two-loop box integrals with bubble insertions can be calculated with NDIM. For more complicated integrals the ϵ expansion of their Mellin-Barnes representation has provided some remarkable breakthroughs. Finally, there are some remaining master integrals that can be related to the rest with the aid of differential equations that we obtain from the application of the same algorithm as for the tensor reduction. They are calculated by differentiation of other known master integrals.

In this chapter we will describe how IBP and Lorentz-Invariance (LI) identities can be derived. We will then use them to find the algorithms of reduction to master integrals for all one and two-loop integrals which appear at $2 \to 2$ massless QCD scattering which do not have a simple analytic form in terms of Γ-functions. The rest have already been studied in Chapter 3, and they were related to master integrals by exploiting the basic property of Γ-functions

$$\Gamma(1+x) = x\Gamma(x).$$

We will finally define the basis of master integrals and we will provide their analytic expansions in the different kinematic regions completing the program for a general evaluation of integrals for NNLO matrix elements in $2 \to 2$ massless scattering.

5.1 Integration by Parts and Lorentz Invariance identities

We consider the general scalar m-loop diagram in D dimensions with n propagators $1/A_i$ raised to arbitrary powers ν_i and $p_1, \ldots p_r$ external momenta

$$\mathcal{J}^D = \int \frac{d^D k_1}{i\pi^{D/2}} \cdots \int \frac{d^D k_m}{i\pi^{D/2}} \frac{1}{A_1^{\nu_1} \cdots A_n^{\nu_n}}. \tag{5.1}$$

Our immediate goal is to find relations between the scalar integrals with different ν_i's. We can start from

$$\int \frac{d^D k_1}{i\pi^{D/2}} \cdots \int \frac{d^D k_m}{i\pi^{D/2}} \frac{\partial}{\partial a_\mu} \frac{b_\mu}{A_1^{\nu_1} \cdots A_n^{\nu_n}} \equiv 0, \tag{5.2}$$

where we integrate a total derivative with respect to one of the loop momenta

$$a^\mu = k_1^\mu, \ldots, k_m^\mu. \tag{5.3}$$

In the numerator we can contract with either one of the m loop momenta or one of the $r-1$ independent momenta (due to momentum conservation) of the r external legs

$$b^\mu = k_1^\mu, \ldots, k_m^\mu, p_1^\mu, \cdots p_{r-1}^\mu. \tag{5.4}$$

The total number of independent IBP identities is therefore

$$\mathcal{N}_{IBP} = m \times (m + r - 1). \tag{5.5}$$

The total derivative will be acting on each of the terms of the integrand yielding two types of terms:

A

$$\frac{\partial b^\mu}{\partial a^\mu} \frac{1}{A_1 \cdots A_n}, \tag{5.6}$$

B

$$\frac{b^\mu}{A_1 \cdots A_{i-1} A_{i+1} \cdots A_n} \frac{\partial}{\partial a^\mu} \left(\frac{1}{A_i} \right) \tag{5.7}$$

The **Type A** terms are zero unless $a = b$ where, in this case only, $\partial b^\mu / \partial a^\mu = D$. The **Type B** terms are more interesting because the derivative acts on one of the propagators. Assuming the general form of the propagator (see Eq. 3.2) in the massless limit

$$\frac{1}{A} = \frac{1}{(\sum \xi_j k_j + q)^2 + i0} \tag{5.8}$$

we find that

$$b^\mu \frac{\partial}{\partial a^\mu} \left(\frac{1}{A^\nu} \right) = -\nu \frac{\sum \xi_j k_j \cdot b + q \cdot b}{A^{\nu+1}}, \tag{5.9}$$

where we have increased the power ν by one in the denominator and, at the same, we have produced scalar products in the numerator.

The scalar products can be formed either exclusively between external momenta $p_i \cdot p_j$ and are then trivially associated with the external kinematic scales, or with at least one loop-momentum $k_i \cdot p_j$. We divide the latter into **reducible numerators**, if they can be re-written in terms of inverse propagators of the integral, or **irreducible** otherwise.

The creation of reducible numerators leads to cancellations between numerator and denominator decreasing the powers of some propagators and linking the original integral with simpler integrals. The presence of irreducible numerators is a problem, because the resulting integrals are more complicated. In this case one can take linear combinations of two or more IBP identities in order to eliminate them. In general, we have

$$\mathcal{N}_{irr} = \frac{1}{2} m \times (m+1) + m \times (r-1) - n \tag{5.10}$$

irreducible numerators.

After the elimination of the irreducible numerators we are left with identities which in principle relate integrals with increased powers of propagators to integrals with decreased powers of propagators or integrals with one of the powers increased while another is decreased at the same time. For convenience, we shall denote with $\mathbf{i}^+$ ($\mathbf{i}^-$) an integral with the power of the i-th propagator increased(decreased) by one. For example

$$\nu_5(\nu_5 + 1)\mathbf{5}^{++}\mathbf{3}^-$$

represents an integral with the power of the fifth propagator increased by two and the power of the third propagator decreased by one. The multiplicative factor $(-1)^k \nu_i \ldots (\nu_i + k - 1)$ is always present whenever the power of the **i**-th propagator has been increased by $k = 1, 2, \ldots$.

For an algorithm which reduces a topology to master integrals is often sufficient to use appropriate linear combinations of a subset of the IBP identities. Nevertheless, we have found topologies, e.g. the massless two-loop cross-box topology with light-like legs, for which it is necessary to complement the IBP identities with more identities originating from the Lorentz Invariance of the scalar integrals [25].

In fact, since the Feynman integral is a function only of scalar products of the external momenta, it is invariant under the (infinitesimal) rotation

$$p_i'^{\mu} = \Lambda^{\mu}{}_{\nu}\, p_i^{\nu}, \qquad \Lambda_{\mu\nu} = g_{\mu\nu} + \delta\, \epsilon_{\mu\nu}, \qquad \epsilon_{\mu\nu} = -\epsilon_{\nu\mu}. \tag{5.11}$$

where δ is a very small parameter. We can then write

$$\int \frac{d^D k_1}{i\pi^{D/2}} \cdots \int \frac{d^D k_m}{i\pi^{D/2}}\, f(k_j, p_i) = \int \frac{d^D k_1}{i\pi^{D/2}} \cdots \int \frac{d^D k_m}{i\pi^{D/2}}\, f(k_j, p_i'). \tag{5.12}$$

where f is the function of the product of propagators and depends on the loop-momenta $k_j, \quad j = 1, \ldots, m$ and the external momenta $p_a, \quad a = 1..r-1$. Expanding in a Taylor series around $\delta = 0$ the right-hand side of Eq. (5.12), we obtain

$$\int \frac{d^D k}{i\pi^{D/2}} \int \frac{d^D l}{i\pi^{D/2}} \sum_{a=1}^{r-1} \frac{\partial f(k_j, p_i)}{\partial p_a^{\mu}}\, \epsilon^{\mu}{}_{\nu}\, p_a^{\nu} = 0. \tag{5.13}$$

With the $r-1$ independent external momenta, we can build

$$\mathcal{N}_{LI} = \frac{1}{2}(r-1) \times (r-2) \tag{5.14}$$

independent second rank antisymmetric tensors that, once inserted into Eq. (5.13), give rise to equal number of LI identities. For graphs with four legs we can choose

$$\begin{aligned}
\epsilon_1^{\mu\nu} &= p_1^{\mu}\, p_2^{\nu} - p_2^{\mu}\, p_1^{\nu}, \\
\epsilon_2^{\mu\nu} &= p_1^{\mu}\, p_3^{\nu} - p_3^{\mu}\, p_1^{\nu}, \\
\epsilon_3^{\mu\nu} &= p_2^{\mu}\, p_3^{\nu} - p_3^{\mu}\, p_2^{\nu}.
\end{aligned}$$

5.2 Dimensional shift

IBP and LI identities suffice to reduce the extra powers of propagators of the scalar integrals generated from the tensor decomposition of Section 3.1. Therefore we obtain a minimal basis of integrals required which cannot be reduced any further.

The integrals of the basis appear in many different dimensions $D = 4 - 2\epsilon + 2n$ and it is rather hard to attempt a direct evaluation for all possible n. Instead we can find recurrence relations, similar to the ones reducing the powers of propagators, which reduce the dimension of the basis-integrals as well.

Let as assume that we have an IBP and LI algorithm G for the power reduction of a topology $\mathcal{T}$ with powers of propagators $\{\nu_i\}$. Schematically,

$$\mathcal{T}^D(\{\nu_i\}) \xrightarrow{G} \sum_j C_{ij}^D B_j^D \tag{5.15}$$

where each of the integrals of the topology characterized by the $\{\nu_i\}$ powers in D dimensions can be written in terms of the integrals of the basis B_j^D in the same dimension. We pick one of the integrals of the basis and we express it in the Schwinger representation

$$B_i^D = \int \mathcal{D}x \frac{1}{\mathcal{P}^{D/2}} \exp\left(\frac{\mathcal{Q}}{\mathcal{P}}\right). \tag{5.16}$$

where Q, P, and $\int \mathcal{D}x$ are defined in Section 3.1. We rewrite the above equation as

$$B_i^D = \int \mathcal{D}x \frac{\mathcal{P}}{\mathcal{P}^{(D+2)/2}} \exp\left(\frac{\mathcal{Q}}{\mathcal{P}}\right). \tag{5.17}$$

multiplying and dividing the integrand with P. We remember that for an $m - loop$ integral P is an m-degree polynomial in the Schwinger parameters x_i,

$$P = \sum_{l_1 \ldots l_m} d_{l_1 \ldots l_m} x_{l_1} \cdots x_{l_m}$$

where $d_{i_1 \ldots i_m}$ depends on the topology. As usual, we absorb the x_i's of P in the numerator into $\int \mathcal{D}x$, increasing the powers of the propagators, while the extra P in the denominator increases the dimension of the integral. Therefore, we can express the integral of the basis in D dimensions in terms of integrals of the topology in $D + 2$ dimensions with the cost of increasing the powers of the propagators.

$$B_i^D = \sum_j d_j T^{D+2}(\{\nu_j\})$$

With the algorithm G each of the $D + 2$ dimensional integrals of the r.h.s. reduces to the integrals of the basis in the same dimension. So the last equation now reads

$$B_i^D = \sum_j A_{ij}^D B_j^{D+2} \tag{5.18}$$

where the coefficients A_{ij}^D is an $n \times n$ matrix, where n is the number of master integrals, and depends on the topology and the dimension.

The system of Eqs. 5.18 expresses integrals of the basis in lower dimension in terms of integrals of the basis in higher dimensions with step two. In practice, we are interested in shifting the dimension in the opposite direction since our tensor reduction program produces integrals in higher dimensions. Therefore we need to invert the system (5.18), yielding

$$B_i^{D+2} = \sum_j (A^{-1})_{ij}^D B_j^D. \tag{5.19}$$

We can now have a rough picture of the basic steps that are needed for the calculation of the tensor integrals in terms of master integrals.

- Rewrite tensors to scalar integrals with extra powers of propagators and higher dimension
- Apply IBP and LI identities in order to reduce the extra powers of the propagators
- Apply dimensional-shift (Eqs. 5.19) arriving to master integrals in $D = 4 - 2\epsilon$ dimensions.
- Evaluate the analytic expansions in ϵ of the master integrals (with Feynman parameters, NDIM, MB representations, etc.)

5.3 The one-loop box topology

In Chapters 3, 4 we studied the one-loop box topology, shown in Fig. 5.1. We now concentrate on the limit where all external legs are massless. With NDIM we found an analytic expression for the one-loop box with arbitrary powers of propagators in this limit (Eq. 4.32) in terms of hypergeometric functions. In principle, it is possible to calculate analytic expansions in ϵ for all integrals with different powers of propagators and dimensions through their hypergeometric representation but it is very tedious and we would rather reduce the general scalar integral to master integrals with the application of IBP.

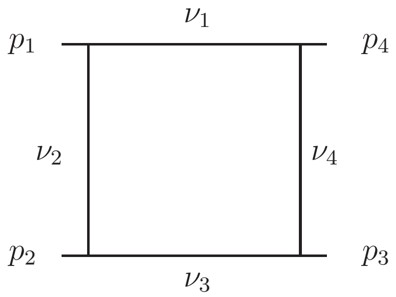

Figure 5.1: The one-loop box topology

The number of independent IBP identities for the one-loop box topology is $\mathcal{N}_{IBP} = 4$, and the number of irreducible numerators $\mathcal{N}_{irr} = 0$. The IBP identities can be cast in the form

$$s\,\nu_1 \mathbf{1}^+ I_4^D = -\left(D - \nu_{12334}\right) I_4^D + \left(\nu_1 \mathbf{1}^+ + \nu_2 \mathbf{2}^+ + \nu_4 \mathbf{4}^+\right) \mathbf{3}^- I_4^D, \tag{5.20}$$

$$t\,\nu_2 \mathbf{2}^+ I_4^D = -\left(D - \nu_{12344}\right) I_4^D + \left(\nu_1 \mathbf{1}^+ + \nu_2 \mathbf{2}^+ + \nu_3 \mathbf{3}^+\right) \mathbf{4}^- I_4^D, \tag{5.21}$$

$$s\,\nu_3 \mathbf{3}^+ I_4^D = -\left(D - \nu_{11234}\right) I_4^D + \left(\nu_2 \mathbf{2}^+ + \nu_3 \mathbf{3}^+ + \nu_4 \mathbf{4}^+\right) \mathbf{1}^- I_4^D, \tag{5.22}$$

$$t\,\nu_4 \mathbf{4}^+ I_4^D = -\left(D - \nu_{12234}\right) I_4^D + \left(\nu_1 \mathbf{1}^+ + \nu_3 \mathbf{3}^+ + \nu_4 \mathbf{4}^+\right) \mathbf{2}^- I_4^D, \tag{5.23}$$

where we have used the shorthand notation $I_4^D = I_4^D(\nu_1, \nu_2, \nu_3, \nu_4; s, t)$ and $\nu_{ijjk} = \nu_i + 2\nu_j + \nu_k$, etc. Starting from integrals in D dimensions with extra powers of propagators, repeated application of these identities reduces ν_1, ν_2, ν_3 and ν_4 to unity, resulting in the simplest integral of the topology which we call **BOX**. It is a basic integral, in the sense that any other integral of the topology is linearly dependent on this one. We introduce the following notation to describe it

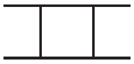

$$\boxed{(D, s, t) \equiv \mathrm{BOX}^D(s,t) = I_4^D(1,1,1,1,s,t)}\,. \tag{5.24}$$

At the same time, in the right hand side of Eqs. (5.20)- (5.23) we observe that the $\mathbf{i}^-$ operators can pinch one of the legs of the topology yielding integrals of the one-loop triangle topology (see Eq. 3.35)

$$I_4^D\left(\nu_1, \nu_2, 0, \nu_4; s, t\right) = I_3^D\left(\nu_1, \nu_2, \nu_4; t\right), \tag{5.25}$$

$$I_4^D\left(\nu_1, 0, \nu_3, \nu_4; s, t\right) = I_3^D\left(\nu_4, \nu_1, \nu_3; s\right), \tag{5.26}$$

$$I_4^D\left(0, \nu_2, \nu_3, \nu_4; s, t\right) = I_3^D\left(\nu_3, \nu_4, \nu_2; t\right), \tag{5.27}$$

$$I_4^D\left(\nu_1, \nu_2, \nu_3, 0; s, t\right) = I_3^D\left(\nu_2, \nu_3, \nu_1; s\right). \tag{5.28}$$

which, in their own turn, can be written in terms of the **BUB** master integral defined in Eq. (3.38).

Finally, we derive the dimensional shift formula

$-u$ 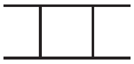 $(D+2,s,t) \;=\; \frac{st}{2(D-3)}$ 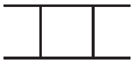 (D,s,t)

$+\frac{2}{D-4}\Big\{$ 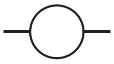 $(D,s) \;+$ 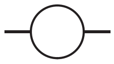 $(D,t)\Big\}$ (5.29)

where $u = -s-t$. This completes the tensor reduction program for the one-loop box topology reducing it to the following set of master integrals in $D = 4-2\epsilon$

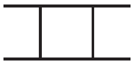 $(s,t),$ 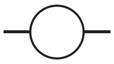 (s) , 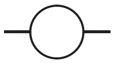 (t) . (5.30)

We can easily obtain an analytic expression which can be expanded in ϵ, for the **BUB** master integral from Eq. 3.35 with the substitution $\nu_1 = 0,\ \nu_2 = 1,\ \nu_3 = 1,\ D = 4-2\epsilon$, yielding

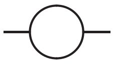 $(s) \;=\; \frac{\Gamma(1+\epsilon)\,\Gamma(1-\epsilon)^2}{\Gamma(2-2\epsilon)\,\epsilon}(-s)^{-\epsilon}.$ (5.31)

The **BOX** master integral can be calculated from Eq. 4.33 with $M = 0$ and expanding the hypergeometric functions according to Eq. 4.43. We can see that the leading term in the series expansion is $1/\epsilon^2$ divergent. Another observation we can make with simple substitutions in Eq. 5.29, is that the one-loop box function is finite in $D = 6-2\epsilon$ dimensions. It is useful to change our basis of master integrals replacing the divergent box in $4-2\epsilon$ dimensions with the finite box in $6-2\epsilon$ dimensions so that we will be able to isolate the singular parts of the one-loop amplitudes in terms of **BUB** functions only. Therefore our favorite basis of Master integrals for the one-loop box topology and the sub-topologies becomes

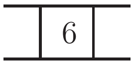 (s,t) 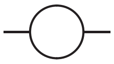 (s) 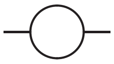 (t) (5.32)

For $s > 0$, $t < 0$ and $u = -s-t < 0$ we need to know the analytic expansion in ϵ of the **BOX** in $D = 4-2\epsilon$ dimensions for arguments (u,t), (s,t) and (s,u). When both arguments are negative we have no imaginary parts and the expansion can be cast in the form

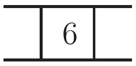

$$
\begin{aligned}
(u,t) \;=\;& \frac{\Gamma(1+\epsilon)\,\Gamma(1-\epsilon)^2}{2s\Gamma(1-2\epsilon)\,(1-2\epsilon)}\left(\frac{\mu^2}{s}\right)^{\epsilon}\Bigg\{\frac{1}{2}\left[(L_x-L_y)^2+\pi^2\right] \\
&+2\epsilon\left[\mathrm{Li}_3(x)-L_x\mathrm{Li}_2(x)-\frac{1}{3}L_x^3-\frac{\pi^2}{2}L_x\right] \\
&-2\epsilon^2\Bigg[\mathrm{Li}_4(x)+L_y\mathrm{Li}_3(x)-\frac{1}{2}L_x^2\mathrm{Li}_2(x)-\frac{1}{8}L_x^4-\frac{1}{6}L_x^3L_y+\frac{1}{4}L_x^2L_y^2 \\
&\qquad-\frac{\pi^2}{4}L_x^2-\frac{\pi^2}{3}L_xL_y-\frac{\pi^4}{45}\Bigg]+(u\leftrightarrow t)\Bigg\}+\mathcal{O}(\epsilon^3),
\end{aligned}
\tag{5.33}
$$

while when one argument is positive we find,

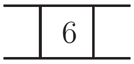

$$
\begin{aligned}
(s,t) \;=\;& \frac{\Gamma(1+\epsilon)\Gamma(1-\epsilon)^2}{2u\Gamma(1-2\epsilon)(1-2\epsilon)}\left(-\frac{\mu^2}{u}\right)^{\epsilon}\Bigg\{\left(L_x^2+2i\pi L_x\right) \\
&+\epsilon\Bigg[\left(-2\mathrm{Li}_3(x)+2L_x\mathrm{Li}_2(x)-\frac{2}{3}L_x^3+2L_yL_x^2-\pi^2L_x+2\zeta_3\right) \\
&\qquad+i\pi\left(2\mathrm{Li}_2(x)+4L_yL_x-L_x^2-\frac{\pi^2}{3}\right)\Bigg] \\
&+\epsilon^2\Bigg[\Bigg(2\mathrm{Li}_4\left(\frac{x-1}{x}\right)+2\mathrm{Li}_4(y)-2L_y\mathrm{Li}_3(x)-2L_x\mathrm{Li}_3(y)+(2L_xL_y-L_x^2-\pi^2)\mathrm{Li}_2(x) \\
&\quad+\frac{1}{3}L_x^4-\frac{5}{3}L_x^3L_y+\frac{3}{2}L_x^2L_y^2+\frac{2}{3}\pi^2L_x^2-2\pi^2L_xL_y+2L_y\zeta_3+\frac{1}{6}\pi^4\Bigg) \\
&\qquad+i\pi\Bigg(-2\mathrm{Li}_3(x)-2\mathrm{Li}_3(y)+2L_y\mathrm{Li}_2(x)+\frac{1}{3}L_x^3-2L_x^2L_y+3L_xL_y^2 \\
&\qquad\qquad-\frac{\pi^2}{3}L_y+2\zeta_3\Bigg)\Bigg]\Bigg\}+\mathcal{O}(\epsilon^3),
\end{aligned}
\tag{5.34}
$$

where

$$x=-\frac{t}{s} \tag{5.35}$$

and

$$L_x=\log\left(\frac{-t}{s}\right),\qquad L_y=\log\left(\frac{-u}{s}\right), \tag{5.36}$$

Finally, (s,u) is obtained from Eq. (5.34) by exchanging u and t.

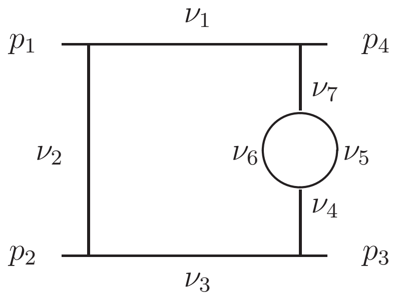

Figure 5.2: The Abox topology .

5.4 IBP algorithm for the bubble-box (Abox) topology

We now want to extend the results of the previous section to the case where we have a one-loop bubble insertion in one of the legs of the one-loop box topology. This is the **Abox** topology (see Fig 5.2) defined in Eq. (4.34) This integral is related by a factor to the ordinary one-loop box integral

$$\mathbf{Abox}^D(\nu_1,\nu_2,\nu_3,\nu_4,\nu_5,\nu_6,\nu_7;s,t) = \Pi^D(\nu_5,\nu_6)\, I_4^D\left(\nu_1,\nu_2,\nu_3,\nu_{4567}-\frac{D}{2};s,t\right), \tag{5.37}$$

where $\Pi^D(\nu_5,\nu_6)$ is given in Eq. 3.37. For arbitrary D we have the relation

$$\Pi^D(\nu_5,\nu_6) = c_{tr}(0,0,\nu_5,\nu_6)\Pi^D(1,1) \tag{5.38}$$

where the function $c_{tr}(n,\nu_1,\nu_2,\nu_3)$ is defined in Eq. (3.41). The propagators of the associated one-loop box, according to Eq. 5.37, have powers

$$\mu_1 = \nu_1, \quad \mu_2 = \nu_2, \quad \mu_3 = \nu_2, \quad \mu_4 = \nu_{4567} - \frac{D}{2}. \tag{5.39}$$

Expressions for the one-loop box integral with general powers of the propagators were obtained with NDIM in the previous chapter. Again, we will first try to reduce the extra powers of the propagators finding the minimum set of integrals required for the calculation of the one-loop box in Eq. (5.37).

A vital difference between the power reduction of the ordinary one-loop box with integer powers of propagators and the one-loop box function in Eq. (5.37) is that the power of the fourth propagator is regulated by the dimension which is not an integer in dimensional regularisation. Therefore it is impossible to pinch this propagator out since its power can never take the integer value zero. Instead, we need to modify the IBP identity of Eq. (5.21) eliminating the $\mathbf{4}^-$ terms. If we act with $\mu_4\mathbf{4}^+$ on Eq. (5.21) and with $\mu_2\mathbf{2}^+$ on Eq. (5.23), and subtract the two equations we obtain the identity

$$(D-2-\mu_{1223})\,\mu_2\mathbf{2}^+I_4^D \;=\; (D-2-\mu_{1344})\,\mu_4\mathbf{4}^+I_4^D+(\mu_2-\mu_4)\left(\mu_1\mathbf{1}^+ +\mu_3\mathbf{3}^+\right)I_4^D, \tag{5.40}$$

which reduces μ_2 to one while at the same time increases μ_1, μ_3 and μ_4. On their own turn, μ_1 and μ_3 are decreased to unity with the known identities,

$$s\,\mu_1\mathbf{1}^+I_4^D \;=\; -(D-\mu_{12334})\,I_4^D+\left(\mu_1\mathbf{1}^+ +\mu_2\mathbf{2}^+ +\mu_4\mathbf{4}^+\right)\mathbf{3}^-I_4^D, \tag{5.41}$$

$$s\,\mu_3\mathbf{3}^+I_4^D \;=\; -(D-\mu_{11234})\,I_4^D+\left(\mu_2\mathbf{2}^+ +\mu_3\mathbf{3}^+ +\mu_4\mathbf{4}^+\right)\mathbf{1}^-I_4^D. \tag{5.42}$$

We should note that with the repeated application of the above identities we produce integrals with the first or the third propagator pinched out, belonging to the one-loop triangle topology (see Eq. 3.35)

$$I_4^D\left(\mu_1,\mu_2,0,\mu_4;s,t\right)=I_3^D\left(\mu_1,\mu_2,\mu_4;t\right), \tag{5.43}$$

$$I_4^D\left(0,\mu_2,\mu_3,\mu_4;s,t\right)=I_3^D\left(\mu_3,\mu_2,\mu_4;t\right). \tag{5.44}$$

The above triangles reinserted in Eq. 5.37 correspond to integrals of the two-loop **TrianB** topology which in turn reduces to the **SUNSET** master integral

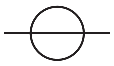 (t)

according to the formulae of Section 3.2.4. Subsequent application of

$$t\,\mu_4\mathbf{4}^+I_4^D \;=\; -(D-\mu_{12234})\,I_4^D+\left(\mu_1\mathbf{1}^+ +\mu_3\mathbf{3}^+ +\mu_4\mathbf{4}^+\right)\mathbf{2}^-I_4^D, \tag{5.45}$$

can be used to control the power of μ_4 and form the pinched triangle integral

$$I_4^D(\mu_1,0,\mu_3,\mu_4;s,t)=I_3^D(\mu_4,\mu_1,\mu_3;s). \tag{5.46}$$

which (inserted in Eq. 5.37) corresponds to the **TrianA** topology that can be reduced to the **TRI** master integral

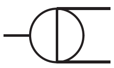 (s) ,

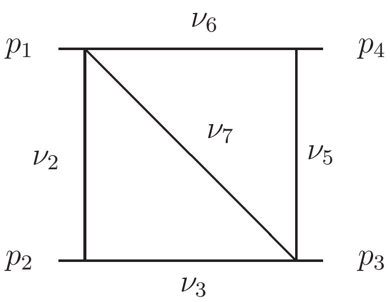

Figure 5.3: The propagators are labelled according and are each raised to the ν_i power.

through application of the algorithm of Section 3.2.3.

Equation (5.45) should be used until $\mu_4 = 2-D/2$, corresponding to $\nu_4 = 0,\ \nu_5 = \nu_6 = 1,\ \nu_7 = 0$. This last integral cannot be reduced any further and is defined as the **ABOX** master integral

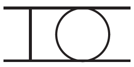

$$\boxed{(D, s, t) \quad = \mathbf{Abox}^D(1,1,1,0,1,1,0;s,t)} \tag{5.47}$$

Finally, we find the dimensional shift identity

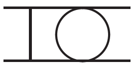

$$(D+2, s, t) = \frac{(D-4)st^2}{3(D-1)(3D-10)(3D-8)(t+s)}$$

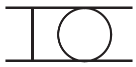

$$(D, s, t)$$

$$+ \frac{s\left[(D-4)t+(2D-6)s\right]}{3(D-2)(D-1)(3D-8)(t+s)}$$

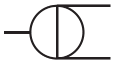

$$(D, s)$$

$$+ \frac{t}{3(D-4)(D-1)(t+s)}$$

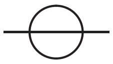

$$(D, s)\,, \tag{5.48}$$

which allows the reduction of the dimension to $D = 4-2\epsilon$. The analytic expansion of the **ABOX** master integral is given in Section 4.2 for the various kinematic regions.

5.5 The diagonal-box (Cbox) topology

The diagonal-box topology is shown in Fig. 5.5 and it is a sub-topology of the Penta-box topology (see Section 3.3.5) with $\nu_1 = \nu_4 = 0$.

Starting from the MB representation of the Penta-box of Eq. (3.86) and setting $\nu_1 = \nu_4 = 0$ the two-fold integral is reduced, with the aid of Barnes first lemma

(Eq. 3.88), to the single MB integral representation for the **Cbox** topology

$$\begin{aligned}\mathbf{Cbox}^D(\{\nu_i\};s,t) &= \frac{(-1)^D\ s^{D-\nu_{23567}}}{\Gamma(\nu_2)\Gamma(\nu_3)\Gamma(\nu_5)\Gamma(\nu_6)\Gamma(\nu_7)} \\ \times\frac{\Gamma\left(\frac{D}{2}-\nu_7\right)\Gamma\left(\frac{D}{2}-\nu_{56}\right)\Gamma\left(\frac{D}{2}-\nu_{23}\right)}{\Gamma(D-\nu_{237})\Gamma(D-\nu_{567})\Gamma\left(\frac{3}{2}D-\nu_{23567}\right)} & \int_{-i\infty}^{i\infty}\frac{d\alpha}{2\pi i}\Gamma(-\alpha)\Gamma(D-\nu_{3567}-\alpha) \\ \times\Gamma(D-\nu_{2367}-\alpha)\Gamma(\nu_{23567}-D+\alpha)\Gamma(\nu_3+\alpha)\Gamma(\nu_6+\alpha)\left(\frac{t}{s}\right)^{\alpha}, \end{aligned} \tag{5.49}$$

where the path of integration over α must be chosen so that to separate the poles coming from $\Gamma(\ldots-\alpha)$ from those coming from $\Gamma(\ldots+\alpha)$ and $\{\nu_i\}=\nu_2,\nu_3,\nu_5,\nu_6,\nu_7$.

In the kinematic region $|t|<|s|$ the contour at infinity must be closed to the right and we then obtain an expression in terms of hypergeometric functions

$$\begin{aligned}\mathbf{Cbox}^D(\{\nu_i\};s,t) &= (-1)^D\ s^{D-\nu_{23567}}\ \frac{\Gamma\left(\frac{D}{2}-\nu_{23}\right)\Gamma\left(\frac{D}{2}-\nu_{56}\right)\Gamma\left(\frac{D}{2}-\nu_7\right)}{\Gamma(\nu_7)\Gamma\left(\frac{3}{2}D-\nu_{23567}\right)} \\ &\times\Bigg[\frac{\Gamma(\nu_{23567}-D)\Gamma(D-\nu_{2367})\Gamma(D-\nu_{3567})}{\Gamma(\nu_2)\Gamma(\nu_5)\Gamma(D-\nu_{567})\Gamma(D-\nu_{237})} \\ &\times{}_3F_2\left(\nu_3,\nu_6,\nu_{23567}-D,1-D+\nu_{2367},1-D+\nu_{3567},-\frac{t}{s}\right) \\ &+\frac{\Gamma(\nu_2-\nu_5)\Gamma(D-\nu_{267})\Gamma(\nu_{2367}-D)}{\Gamma(\nu_2)\Gamma(\nu_3)\Gamma(\nu_6)\Gamma(D-\nu_{567})} \\ &\times\left(\frac{t}{s}\right)^{D-\nu_{2367}}{}_3F_2\left(\nu_5,D-\nu_{267},D-\nu_{237},1+D-\nu_{2367},1+\nu_5-\nu_2,-\frac{t}{s}\right) \\ &+\frac{\Gamma(\nu_5-\nu_2)\Gamma(D-\nu_{357})\Gamma(\nu_{3567}-D)}{\Gamma(\nu_3)\Gamma(\nu_5)\Gamma(\nu_6)\Gamma(D-\nu_{237})} \\ &\times\left(\frac{t}{s}\right)^{D-\nu_{3567}}{}_3F_2\left(\nu_2,D-\nu_{357},D-\nu_{567},1+D-\nu_{3567},1+\nu_2-\nu_5,-\frac{t}{s}\right)\Bigg]. \end{aligned} \tag{5.50}$$

The solution valid when $|s|<|t|$ can be obtained from Eq. (5.50) by the exchanges

$$s\leftrightarrow t,\qquad \nu_2\leftrightarrow\nu_3,\qquad \nu_5\leftrightarrow\nu_6. \tag{5.51}$$

The expression for the diagonal box (5.50) has an apparent singularity when $\nu_2-\nu_5$ is an integer which cancels in the actual evaluation of the diagram.

Following our operational recipe, we first try to simplify the evaluation of the integrals of the topology using IBP and then we calculate the ϵ expansions of the master integrals. We can write down $N_{IBP}=10$ identities which have $N_{irr}=4$

irreducible numerators. Taking appropriate linear combinations of the identities, we eliminate the irreducible numerators. We finally produce the following relations

$$\begin{aligned}(D-2-2\nu_{23})\,\nu_2\mathbf{2}^+ &= (D-2-2\nu_7)\,\nu_7\mathbf{7}^+ - (D-2-2\nu_{23})\,\nu_3\mathbf{3}^+, &(5.52)\\ (D-2-2\nu_{56})\,\nu_6\mathbf{6}^+ &= (D-2-2\nu_7)\,\nu_7\mathbf{7}^+ - (D-2-2\nu_{56})\,\nu_5\mathbf{5}^+, &(5.53)\end{aligned}$$

so that we can reduce both ν_2 and ν_6 to unity at the expense of increasing ν_3 and ν_5 together with ν_7. Eqs. 5.52 and 5.53, are meant to act on the general integral of the topology $\mathbf{Cbox}^D(\nu_2,\nu_3,\nu_5,\nu_6,\nu 7;s,t)$. Similarly, for ease of notation, all IBP and LI identities presented in the rest of this Chapter will implicitly refer to the general integral of the topology in question.

We now reduce ν_3 and ν_5 to unity using the relations

$$\begin{aligned}s\,(D-2-2\nu_{23})\,\nu_3\mathbf{3}^+ &= -\,(D-1-\nu_{237})\,(3D-2\nu_{235667}) &(5.54)\\ &\quad +2\,(D-1-\nu_{237})\,\nu_5\mathbf{5}^+\mathbf{6}^- + (D-2-2\nu_7)\,\nu_7\mathbf{7}^+\mathbf{6}^-,\\ t\,(D-2-2\nu_{56})\,\nu_5\mathbf{5}^+ &= -\,(D-1-\nu_{567})\,(3D-2\nu_{223567}) &(5.55)\\ &\quad +2\,(D-1-\nu_{567})\,\nu_3\mathbf{3}^+\mathbf{2}^- + (D-2-2\nu_7)\,\nu_7\mathbf{7}^+\mathbf{2}^-,\end{aligned}$$

which, because ν_2 and ν_6 are already unity, produces simpler pinched integrals of the form

$$\begin{aligned}\mathbf{Cbox}^D(0,\nu_3,\nu_5,\nu_6,\nu_7;s,t) &= \mathbf{TrianA}^D(\nu_5,\nu_6,0,\nu_3,\nu_7,0;s)\\ \mathbf{Cbox}^D(\nu_2,\nu_3,\nu_5,0,\nu_7;s,t) &= \mathbf{TrianA}^D(\nu_3,\nu_2,0,\nu_5,\nu_7,0;t) \qquad (5.56)\end{aligned}$$

which collapse to the

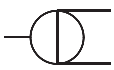 (s) , 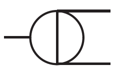 (t)

master integrals.

When the outer propagators have unit powers, we can reduce ν_7 using

$$\begin{aligned}st\,(D-2-2\nu_7)\,\nu_7\mathbf{7}^+ &= -(s+t)\,(D-3-\nu_7)\,(3D-10-2\nu_7) &(5.57)\\ &\quad +2\,(D-3-\nu_7)\left(t\mathbf{5}^+\mathbf{6}^- + s\mathbf{6}^+\mathbf{5}^-\right)\\ &\quad +(D-2-2\nu_7)\left(t\nu_7\mathbf{7}^+\mathbf{6}^- + s\nu_7\mathbf{7}^+\mathbf{5}^-\right).\end{aligned}$$

This equation is only valid when $\nu_2=\nu_3=\nu_5=\nu_6=1$. The integral with unit powers of propagators cannot be reduced any further and it is a master integral

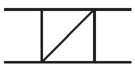 $\boxed{(D,s,t) \;=\mathbf{Cbox}^D(1,1,1,1,1;s,t)}$ (5.58)

We can shift its dimension down to $D = 4 - 2\epsilon$ with the identity

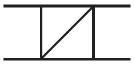

$$(D+2, s, t) =$$

$$\frac{(D-4)^2 s^2 t^2}{3(D-3)(D-2)(3D-10)(3D-8)(t+s)^2}$$

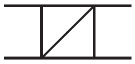

$$(D, s, t)$$

$$+\frac{s\left[(2D-5)t + (D-3)s\right]}{3(D-3)(D-2)^2(t+s)^2}$$

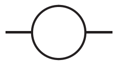

$$(D, s)$$

$$+\frac{t\left[(D-3)t + (2D-5)s\right]}{3(D-3)(D-2)^2(t+s)^2}$$

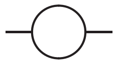

$$(D, t)\,. \qquad (5.59)$$

With the propagator powers equal to unity, all of the ${}_3F_2$ functions of Eq. (5.50) reduce to ${}_2F_1$. To deal with the pole in $(\nu_2 - \nu_5)$ we set $\nu_2 = \nu_5 + \delta$, and, after performing an appropriate analytical continuation, we take the limit $\delta \to 0$. The final expression is given by

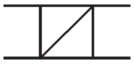

$$\begin{aligned}(D, s, t) \quad = \quad & -\frac{\Gamma\left(\frac{D}{2}-1\right)\Gamma\left(3-D\right)\Gamma^2\left(\frac{D}{2}-2\right)}{\Gamma\left(\frac{3}{2}D-5\right)} \\ & \times \left[(-t)^{D-5}\, {}_2F_1\left(1, 1, D-2, \frac{s+t}{t}\right)\right. \\ & \left. + (-s)^{D-5}\, {}_2F_1\left(1, 1, D-2, \frac{s+t}{s}\right)\right]. \qquad (5.60)\end{aligned}$$

If we make a series expansion in $\epsilon = 2 - \frac{D}{2}$, we obtain

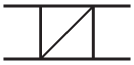

$$(s, t) = \frac{\Gamma^3\left(1-\epsilon\right)\Gamma\left(1+2\epsilon\right)}{2\left(s+t\right)\Gamma\left(1-3\epsilon\right)\,\epsilon^3}\left[(-s)^{-2\epsilon}\, C\left(s, t\right) + (-t)^{-2\epsilon}\, C\left(t, s\right)\right], \qquad (5.61)$$

where $C\left(s, t\right)$ is given respectively by:

1) in the physical region $s > 0$, $t < 0$:

$$\begin{aligned} C\left(s, t\right) \quad = \quad & \log\left(-\frac{t}{s}\right) + 2\epsilon\, \mathrm{Li}_2\left(\frac{s+t}{t}\right) + 4\epsilon^2\, \mathrm{Li}_3\left(\frac{s+t}{t}\right) + 8\epsilon^3\, \mathrm{Li}_4\left(\frac{s+t}{t}\right) \\ & + \mathcal{O}\left(\epsilon^4\right), \qquad (5.62)\end{aligned}$$

2) while in the region $s < 0$, $t < 0$:

$$\begin{aligned} C\left(s, t\right) \quad = \quad & \log\left(\frac{t}{s}\right) - 2\epsilon\left[\mathrm{Li}_2\left(\frac{t}{s+t}\right) + \frac{1}{2}\log^2\left(\frac{s+t}{t}\right) - \frac{\pi^2}{3}\right] \\ & + 4\epsilon^2\left[\mathrm{Li}_3\left(\frac{t}{s+t}\right) - \frac{1}{6}\log^3\left(\frac{s+t}{t}\right) + \frac{\pi^2}{3}\log\left(\frac{s+t}{t}\right)\right] \\ & - 8\epsilon^3\left[\mathrm{Li}_4\left(\frac{t}{s+t}\right) + \frac{1}{24}\log^4\left(\frac{s+t}{t}\right) - \frac{\pi^2}{6}\log^2\left(\frac{s+t}{t}\right) - \frac{\pi^4}{45}\right] \\ & + \mathcal{O}\left(\epsilon^4\right). \qquad (5.63)\end{aligned}$$

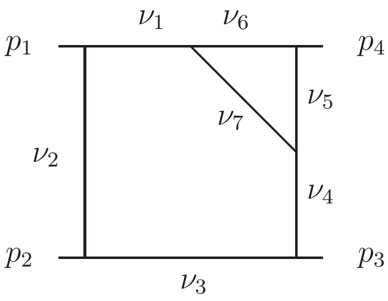

Figure 5.4: The penta-box topology. It is reducible to simpler topologies due to the presence of the triangle sub-graph.

Note that the prefactor of Eq. (5.60) indicates that the integral diverges as $1/\epsilon^3$. However, the hypergeometric functions conspire to remove the leading divergence and we reproduce the result quoted in Ref.[58].

5.6 IBP algorithm for topologies with a triangle subgraph

Topologies with massless external legs and a triangle subgraph reduce trivially to simpler sub-topologies with IBP. For integrals of this kind, one of the external legs of the triangle is always an external leg of the total graph. This is defined for our purposes as a "good" external leg of the triangle subgraph. Another possibility is that an external leg of the triangle is a propagator of the total graph and it is a "good" external leg as well. Finally, if an external leg of the subgraph is neither an external leg of the total graph nor a propagator it is a "bad" external leg. Accordingly, if a propagator of the triangle is connected to two "good" external legs, then it is a "good" propagator otherwise a "bad" one. For example, all the propagators of the triangle in the pentabox graph (Figure 5.6) are good ones while all of them in the diagonal-box graph (Figure 5.5) are "bad" ones.

It is easy to find IBP identities that reduce the graph to simpler integrals when the triangle subgraph has at least one "good" propagator. We pick a "good" propagator and define b^μ to be its momentum and a^μ the loop-momentum flowing through

Figure 5.5: The **TrianD** (left) and **TrianE** (right) topologies. They can be reduced to simpler topologies with the IBP triangle rule

it. We then write down the corresponding identity of Eq. 5.2 with the a^μ and b^μ that we have just chosen. The produced terms will either "pinch" the propagators of the triangle or the propagators of the rest of the graph.

As an example we consider the penta-box topology of Section 3.3.5. shown in Figure 5.6. The momenta carried by each of the propagators are defined in Eq. (3.82). We start from

$$\int \frac{d^D k_1}{i\pi^{D/2}} \int \frac{d^D k_2}{i\pi^{D/2}} \frac{\partial}{\partial k_2^\mu} \frac{[(k_2+p_1+p_2+p_3)^\mu\,;\; k_2^\mu]}{A_1^{\nu_1} A_2^{\nu_2} A_3^{\nu_3} A_4^{\nu_4} A_5^{\nu_5} A_6^{\nu_6} A_7^{\nu_7}} = 0, \tag{5.64}$$

yielding the identities

$$(D - 2\nu_5 - \nu_6 - \nu_7) = \left(\nu_6 \mathbf{6}^+\mathbf{5}^- + \nu_7 \mathbf{7}^+\mathbf{5}^- - \nu_7 \mathbf{7}^+\mathbf{4}^-\right), \tag{5.65}$$

$$(D - \nu_5 - 2\nu_6 - \nu_7) = \left(\nu_5 \mathbf{5}^+\mathbf{6}^- + \nu_7 \mathbf{7}^+\mathbf{6}^- - \nu_7 \mathbf{7}^+\mathbf{1}^-\right), \tag{5.66}$$

By repeated application of Eq. (5.65), we can reduce either of ν_4 or ν_5 to zero. Similarly, by applying Eq. (5.66) we can lower (and eventually eliminate) the power of either ν_1 or ν_6. The pinched integrals belong to the **Abox** or **Cbox** topologies which we already know how to evaluate. Using the same identities we can reduce the subtopology **TrianD** of the pentabox topology with $\nu_2 = 0$ (see Figure 5.6), to triangles that they belong to the known **TrianA**, **TrianB** and **TrianC** topologies. With the same method Kramer and Lampe [36] evaluated the integrals of the **TrianE** topology (see Figure 5.6).

5.7 Reduction algorithm for the Cross-Triangle topology

The cross-triangle topology (**TrianX**) (Figure 3.10) is defined in Section 3.3.7. In this section we want to find an algorithm for the reduction of the topology to master integrals. For this particular topology, though IBP identities are sufficient on their own for the reduction, we find it easier to complement them with the one LI identity one can write for a graph with three external legs. For an alternative solution to this reduction problem, exploiting a connection with massless three-loop propagator integrals, see Ref. [59]

Some of the eight IBP identities and the single Lorentz-invariance identity depend on one irreducible scalar product in the numerator, that we choose to be $(l\cdot p_2)$:

$$s\nu_1\mathbf{1}^+ + (2D-2\nu_{235}-\nu_{146}) - \nu_4\mathbf{4}^+\mathbf{3}^- - \nu_1\mathbf{1}^+\mathbf{2}^- - \nu_6\mathbf{6}^+\mathbf{5}^- = 0 \quad (5.67)$$

$$s\nu_2\mathbf{2}^+ + (2D-2\nu_{146}-\nu_{235}) - \nu_3\mathbf{3}^+\mathbf{4}^- - \nu_2\mathbf{2}^+\mathbf{1}^- - \nu_5\mathbf{5}^+\mathbf{6}^- = 0 \quad (5.68)$$

$$\begin{aligned}2\,(l\cdot p_2)\,\nu_1\mathbf{1}^+ - (D-\nu_{24}-2\nu_3) + \nu_1\mathbf{1}^+\left(\mathbf{2}^- + \mathbf{4}^- - \mathbf{5}^-\right)&\\ + \nu_2\mathbf{2}^+\left(\mathbf{3}^- - \mathbf{5}^-\right) + \nu_4\mathbf{4}^+\mathbf{3}^- = 0&\end{aligned} \quad (5.69)$$

$$\begin{aligned}2\,(l\cdot p_2)\,\nu_2\mathbf{2}^+ - (D-\nu_{125}-2\nu_6) + \nu_2\mathbf{2}^+\left(\mathbf{6}^- - \mathbf{3}^-\right)&\\ - \nu_1\mathbf{1}^+\left(\mathbf{6}^- - \mathbf{4}^-\right) - \nu_5\mathbf{5}^+\mathbf{6}^- = 0&\end{aligned} \quad (5.70)$$

$$\begin{aligned}2\,(l\cdot p_2)\,\nu_3\mathbf{3}^+ + (D-\nu_{345}-\nu_6) + \nu_3\mathbf{3}^+\left(\mathbf{2}^- - \mathbf{5}^-\right) + \nu_4\mathbf{4}^+\left(\mathbf{1}^- - \mathbf{6}^-\right)&\\ - \nu_5\mathbf{5}^+\mathbf{6}^- = 0&\end{aligned} \quad (5.71)$$

$$\begin{aligned}2\,(l\cdot p_2)\,\nu_4\mathbf{4}^+ + s\nu_4\mathbf{4}^+ - (D-\nu_{346}-2\nu_5) + \nu_3\mathbf{3}^+\left(\mathbf{5}^- - \mathbf{2}^-\right)&\\ + \nu_4\mathbf{4}^+\left(\mathbf{6}^- - \mathbf{1}^-\right) + \nu_6\mathbf{6}^+\mathbf{5}^- = 0&\end{aligned} \quad (5.72)$$

$$\begin{aligned}2\,(l\cdot p_2)\,\nu_5\mathbf{5}^+ + s\nu_5\mathbf{5}^+ - (D-\nu_{36}-2\nu_4) + \nu_5\mathbf{5}^+\left(\mathbf{4}^- + \mathbf{6}^- - \mathbf{1}^-\right)&\\ + \nu_6\mathbf{6}^+\left(\mathbf{4}^- - \mathbf{1}^-\right) + \nu_3\mathbf{3}^+\mathbf{4}^- = 0&\end{aligned} \quad (5.73)$$

$$\begin{aligned}2\,(l\cdot p_2)\,\nu_6\mathbf{6}^+ - (D-\nu_{45}-2\nu_3) - \nu_6\mathbf{6}^+\left(\mathbf{3}^- + \mathbf{5}^- - \mathbf{2}^-\right)&\\ + \nu_5\mathbf{5}^+\left(\mathbf{2}^- - \mathbf{3}^-\right) + \nu_4\mathbf{4}^+\mathbf{3}^- = 0&\end{aligned} \quad (5.74)$$

$$2\,(l\cdot p_2)\,\nu_1\mathbf{1}^+ - (D-\nu_{2356}) + \nu_1\mathbf{1}^+\left(\mathbf{2}^- + \mathbf{6}^- - \mathbf{5}^-\right) + \nu_4\mathbf{4}^+\mathbf{3}^- = 0. \quad (5.75)$$

The identity

$$s\nu_1\mathbf{1}^+ = -(2D-2\nu_{235}-\nu_{146}) + \nu_4\mathbf{4}^+\mathbf{3}^- + \nu_1\mathbf{1}^+\mathbf{2}^- + \nu_6\mathbf{6}^+\mathbf{5}^-, \quad (5.76)$$

together with the symmetric one for $\nu_2\mathbf{2}^+$, can reduce ν_1 and ν_2 to unity. By eliminating the irreducible scalar product in the numerator, we obtain

$$\begin{aligned}\nu_3\mathbf{3}^+ \quad &= \quad \frac{1}{D-2-\nu_{3456}}\left(\nu_4\mathbf{4}^+\nu_6\mathbf{6}^+\mathbf{1}^- - \nu_3\mathbf{3}^+\nu_5\mathbf{5}^+\mathbf{2}^-\right) \\ &\quad + \frac{1}{D-2-2\nu_{34}}\left[(D-2-2\nu_{46})\,\nu_6\mathbf{6}^+ + 2\,(\nu_3-\nu_6)\,\nu_5\mathbf{5}^+\right], \quad (5.77)\end{aligned}$$

and the symmetric one for $\nu_4\mathbf{4}^+$, which reduce ν_3 and ν_4 to one. To complete the reduction, we use

$$(\nu_{56}-\nu_{34}) = \nu_2\mathbf{2}^+\left(\mathbf{3}^- - \mathbf{5}^-\right) + \nu_1\mathbf{1}^+\left(\mathbf{4}^- - \mathbf{6}^-\right), \qquad (5.78)$$

that can be re-iterated until $(\nu_{56}-\nu_{34}) = 0$. Since we are applying this identity to scalar integrals where ν_3 and ν_4 have already been reduced to one, the reduction procedure will stop when $\nu_5 = \nu_6 = 1$. This integral cannot be reduced any further, and we choose the crossed master triangle (**XTRI**) to be

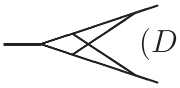

$$\boxed{\ (D,s) \quad = \mathbf{TrianX}^D(1,1,1,1,1,1;s).} \qquad (5.79)$$

During the application of the above algorithm, we produce pinched integrals belonging to the **TrianC** and **TrianD** topologies, which in their own turn are reduced to the

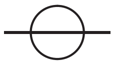 (s) , 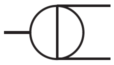 (s)

master integrals.

Finally, the dimensional-shift formula for the cross-triangle master integral reads

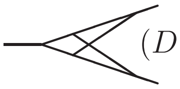

$$(D+2,s) \quad = \quad -\frac{(D-4)s^2}{4(D-2)(2D-7)(2D-5)}$$

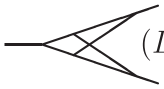

$$(D,s)$$

$$-\frac{37D^3-313D^2+858D-752}{2(D-4)(D-2)(2D-7)(2D-5)(3D-8)}$$

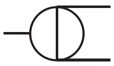

$$(D,s)$$

$$+\frac{43D^4-478D^3+1963D^2-3530D+2352}{2(D-4)^2(D-3)(D-2)(2D-7)(2D-5)s}$$

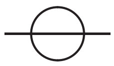

$$(D,s)\,. \qquad (5.80)$$

The expression of the master integral of Eq. (5.79) in $D = 4-2\epsilon$ has been computed in Refs. [35, 36], and we recalculated it by expanding the MB representation of the integral in Eq. 3.123.

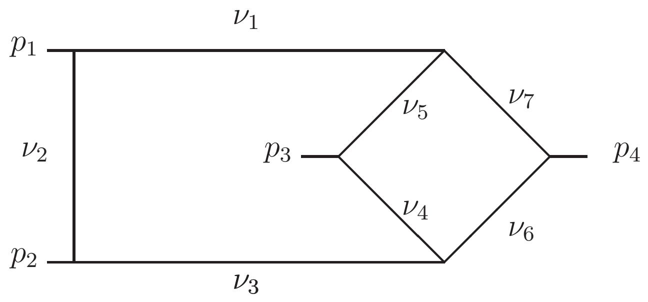

Figure 5.6: The two-loop cross-box graph with arbitrary powers of propagators

5.8 The Cross-Box topology

In this section we deal with the reduction of the Cross-Box (**Xbox**) topology to master integrals. We denote the generic two-loop scalar crossed (or non-planar) four-point function in D dimensions of Fig. 5.8 with seven propagators A_i raised to arbitrary powers ν_i as

$$\mathbf{Xbox}^D(\{\nu_i\}; s,t) = \int \frac{d^D k_1}{i\pi^{D/2}} \int \frac{d^D k_2}{i\pi^{D/2}} \frac{1}{A_1^{\nu_1} A_2^{\nu_2} A_3^{\nu_3} A_4^{\nu_4} A_5^{\nu_5} A_6^{\nu_6} A_7^{\nu_7}}, \tag{5.81}$$

where $\{\nu_i\} = \nu_1, \nu_2, \nu_3, \nu_4, \nu_5, \nu_6, \nu_7$ and the propagators are

$$\begin{aligned}
A_1 &= (k_1 + k_2 + p_3 + p_4)^2 + i0, \\
A_2 &= (k_1 + k_2 + p_1 + p_3 + p_4)^2 + i0, \\
A_3 &= (k_1 + k_2)^2 + i0, \\
A_4 &= k_2^2 + i0, \\
A_5 &= (k_2 + p_3)^2 + i0, \\
A_6 &= k_1^2 + i0, \\
A_7 &= (k_1 + p_4)^2 + i0.
\end{aligned} \tag{5.82}$$

The external momenta p_j are in-going and light-like, $p_j^2 = 0$, $j = 1 \ldots 4$, so that the only momentum scales are the usual Mandelstam variables $s = (p_1 + p_2)^2$ and $t = (p_2 + p_3)^2$, together with $u = (p_1 + p_3)^2 = -s - t$.

5.8.1 IBP and LI identities

As usual, we aim to find an algorithm to reduce the powers of the propagators. So far, IBP identities were sufficient for the reduction of the topologies we have encountered. In the cross-triangle topology, we used a LI identity in order to simplify the reduction algorithm, but one could still achieve the reduction without it. It turns out, that for the cross-box topology LI identities are indispensable. We can write 10 IBP and 3 LI identities and we expect the presence of $N_{irr} = 2$ irreducible numerators. The identities can be cast in the form

$$s\nu_1\mathbf{1}^+ - \nu_7\mathbf{7}^+\mathbf{6}^- - \nu_5\mathbf{5}^+\mathbf{4}^- - \left(\nu_2\mathbf{2}^+ + \nu_1\mathbf{1}^+\right)\mathbf{3}^- - \nu_{1257} - 2\nu_{346} + 2D = 0 \quad (5.83)$$

$$s\nu_3\mathbf{3}^+ - \nu_6\mathbf{6}^+\mathbf{7}^- - \nu_4\mathbf{4}^+\mathbf{5}^- - \left(\nu_3\mathbf{3}^+ + \nu_2\mathbf{2}^+\right)\mathbf{1}^- - \nu_{2346} - 2\nu_{157} + 2D = 0 \quad (5.84)$$

$$\begin{aligned} &2\left(l\cdot p_4\right)\nu_4\mathbf{4}^+ - \left(\nu_6\mathbf{6}^+ + \nu_5\mathbf{5}^+\right)\mathbf{7}^- + \nu_5\mathbf{5}^+\mathbf{1}^- + \nu_4\mathbf{4}^+\left(\mathbf{3}^- - \mathbf{6}^-\right) \\ &\qquad - \nu_{456} - 2\nu_7 + D = 0 \end{aligned} \quad (5.85)$$

$$\begin{aligned} &2\left(l\cdot p_4\right)\nu_5\mathbf{5}^+ + \nu_7\mathbf{7}^+\mathbf{6}^- + \nu_5\mathbf{5}^+\left(\mathbf{7}^- - \mathbf{1}^- + s\right) + \nu_4\mathbf{4}^+\left(\mathbf{6}^- - \mathbf{3}^-\right) \\ &\qquad + \nu_{457} + 2\nu_6 - D = 0 \end{aligned} \quad (5.86)$$

$$\begin{aligned} &2\left(l\cdot p_4\right)\nu_6\mathbf{6}^+ + \nu_7\mathbf{7}^+\left(\mathbf{5}^- - \mathbf{1}^-\right) + \nu_6\mathbf{6}^+\left(\mathbf{7}^- + \mathbf{5}^- - \mathbf{1}^- + s\right) + \nu_4\mathbf{4}^+\mathbf{5}^- \\ &\qquad + \nu_{47} + 2\nu_5 - D = 0 \end{aligned} \quad (5.87)$$

$$\begin{aligned} &2\left(l\cdot p_4\right)\nu_7\mathbf{7}^+ + \nu_6\mathbf{6}^+\left(\mathbf{3}^- - \mathbf{4}^-\right) - \nu_7\mathbf{7}^+\left(\mathbf{6}^- + \mathbf{4}^- - \mathbf{3}^-\right) - \nu_5\mathbf{5}^+\mathbf{4}^- \\ &\qquad - \nu_{56} - 2\nu_4 + D = 0 \end{aligned} \quad (5.88)$$

$$\begin{aligned} &2s\left(l\cdot p_4\right)\nu_2\mathbf{2}^+ + 4s\left(l\cdot p_4\right)\nu_3\mathbf{3}^+ + \nu_2\mathbf{2}^+\left[(t+s)\left(s+\mathbf{1}^-\right) - t\mathbf{3}^-\right] \\ &\qquad + s\left(2\nu_6\mathbf{6}^+ + 2\nu_3\mathbf{3}^+ + \nu_2\mathbf{2}^+\right)\mathbf{7}^- - s\left(2\nu_3\mathbf{3}^+ + \nu_2\mathbf{2}^+\right)\mathbf{6}^- \\ &\qquad - \left(2D - 2\nu_{13457} - \nu_2\right)s = 0 \end{aligned} \quad (5.89)$$

$$\begin{aligned} &2s\left(l\cdot p_4\right)\nu_3\mathbf{3}^+ - 2s\left(l\cdot p_4\right)\nu_1\mathbf{1}^+ + (t+s)\nu_2\mathbf{2}^+\left(\mathbf{1}^- - \mathbf{3}^-\right) + s\left(\nu_1\mathbf{1}^+ - \nu_3\mathbf{3}^+\right)\mathbf{6}^- \\ &\qquad + s\left(\nu_6\mathbf{6}^+ + \nu_3\mathbf{3}^+ - \nu_1\mathbf{1}^+\right)\mathbf{7}^- - s\nu_5\mathbf{5}^+\mathbf{4}^- - s\nu_1\mathbf{1}^+\mathbf{3}^- \\ &\qquad - \left(\nu_6 - \nu_{15}\right)s = 0 \end{aligned} \quad (5.90)$$

$$\begin{aligned} &2\left(l\cdot p_4\right)\nu_3\mathbf{3}^+ - 2\left(l\cdot p_1\right)\nu_2\mathbf{2}^+ + (t+s)\nu_2\mathbf{2}^+ + \left(\nu_6\mathbf{6}^+ + \nu_3\mathbf{3}^+ + \nu_2\mathbf{2}^+ + \nu_1\mathbf{1}^+\right)\mathbf{7}^- \\ &\qquad - \left(\nu_2\mathbf{2}^+ + \nu_1\mathbf{1}^+\right)\mathbf{5}^- - \nu_3\mathbf{3}^+\mathbf{4}^- + \nu_{1236} + 2\nu_7 - D = 0 \end{aligned} \quad (5.91)$$

$$\begin{aligned} &2s\left(l\cdot p_4\right)\nu_3\mathbf{3}^+ - 2s\left(l\cdot p_1\right)\nu_7\mathbf{7}^+ + \nu_7\mathbf{7}^+\left[(t+s)\left(s-\mathbf{1}^-\right) + t\mathbf{5}^- + s\mathbf{2}^-\right] \\ &\qquad + \nu_6\mathbf{6}^+\left(t\mathbf{4}^- - t\mathbf{3}^- + s\mathbf{7}^-\right) + s\nu_3\mathbf{3}^+\left(\mathbf{7}^- - \mathbf{6}^-\right) + (t+s)\nu_2\mathbf{2}^+\mathbf{1}^- + s\nu_1\mathbf{1}^+\mathbf{2}^- \\ &\qquad + s\left(\nu_{126} + 2\nu_{3457} - 2D\right) - t\left(D - \nu_{67} + \nu_2 - 2\nu_{45}\right) = 0 \end{aligned} \quad (5.92)$$

$$2s\,(l\cdot p_4)\,\nu_3\mathbf{3}^+ - 2s\,(l\cdot p_1)\,\nu_5\mathbf{5}^+ + (t+s)\,\nu_5\mathbf{5}^+\left(\mathbf{7}^- - \mathbf{1}^- + s\right) + (t+s)\nu_2\mathbf{2}^+\mathbf{1}^-$$
$$+ (t+s)\nu_4\mathbf{4}^+\left(\mathbf{6}^- - \mathbf{3}^-\right) + s\left(\nu_6\mathbf{6}^+ + \nu_3\mathbf{3}^+\right)\mathbf{7}^- - s\nu_3\mathbf{3}^+\mathbf{6}^- - s\nu_1\mathbf{1}^+\mathbf{2}^-$$
$$+ s\,(\nu_{1456} - \nu_2 + 2\nu_7 - D) + t\,(2\nu_{67} + \nu_{45} - \nu_2 - D) = 0 \tag{5.93}$$
$$2s\,(l\cdot p_4)\,\nu_3\mathbf{3}^+ + 2s\,(l\cdot p_1)\,\nu_6\mathbf{6}^+ + \nu_6\mathbf{6}^+\left[t\left(\mathbf{4}^- - \mathbf{3}^-\right) - s\left(\mathbf{2}^- - \mathbf{1}^- + s\right)\right] - s\nu_4\mathbf{4}^+\mathbf{5}^-$$
$$+ s\nu_3\mathbf{3}^+\left(\mathbf{7}^- - \mathbf{6}^- - \mathbf{2}^-\right) + t\nu_7\mathbf{7}^+\left(\mathbf{5}^- - \mathbf{1}^-\right) + (t+s)\nu_2\mathbf{2}^+\mathbf{1}^-$$
$$+ s\,(\nu_{34} - \nu_2) + t\,(\nu_{67} + 2\nu_{45} - \nu_2 - D) = 0 \tag{5.94}$$
$$2s\,(l\cdot p_4)\,\nu_3\mathbf{3}^+ + 2s\,(l\cdot p_1)\,\nu_4\mathbf{4}^+ + \nu_4\mathbf{4}^+\left[(t+s)\left(\mathbf{6}^- - \mathbf{3}^-\right) + s\mathbf{5}^-\right] + 2s\nu_6\mathbf{6}^+\mathbf{7}^-$$
$$+ (t+s)\nu_5\mathbf{5}^+\left(\mathbf{7}^- - \mathbf{1}^-\right) + (t+s)\nu_2\mathbf{2}^+\mathbf{1}^- + s\nu_3\mathbf{3}^+\left(\mathbf{7}^- - \mathbf{6}^- + \mathbf{2}^-\right)$$
$$+ s\,(\nu_{23} + 2\nu_{146} + 3\nu_5 + 4\nu_7 - 3D) + t\,(\nu_{45} - \nu_2 + 2\nu_{67} - D) = 0, \tag{5.95}$$

where we use the shorthand $\nu_{ij} = \nu_i + \nu_j$, $\nu_{ijk} = \nu_i + \nu_j + \nu_k$, etc.

Equations (5.83) and (5.84) of the system, being independent of the two irreducible scalar products, need no further manipulation, and can be rewritten in the form

$$s\nu_1\mathbf{1}^+ = \nu_7\mathbf{7}^+\mathbf{6}^- + \nu_5\mathbf{5}^+\mathbf{4}^- + \left(\nu_2\mathbf{2}^+ + \nu_1\mathbf{1}^+\right)\mathbf{3}^- + \nu_{1257} + 2\nu_{346} - 2D, \tag{5.96}$$
$$s\nu_3\mathbf{3}^+ = \nu_6\mathbf{6}^+\mathbf{7}^- + \nu_4\mathbf{4}^+\mathbf{5}^- + \left(\nu_3\mathbf{3}^+ + \nu_2\mathbf{2}^+\right)\mathbf{1}^- + \nu_{2346} + 2\nu_{157} - 2D. \tag{5.97}$$

By repeated application of these two identities, we can reduce ν_1 and ν_3 to one. During this process, the generic scalar box is expressed as a linear combination of crossed-box diagrams with $\nu_1 = \nu_3 = 1$ and diagrams belonging to simpler topologies, that originate when powers of propagators are reduced (pinched) to zero by the decreasing operators. We will deal with the pinched diagrams later, concentrating now on the reduction of the remaining propagators.

In order to use the other equations of the system, we have to eliminate the irreducible scalar products in the numerator.

For example, applying the operator $\nu_7\mathbf{7}^+$ to Eq. (5.85) and $\nu_4\mathbf{4}^+$ to Eq. (5.88), and taking the difference, we get

$$(D - 2\nu_7 - \nu_{56} - 2)\,\nu_7\mathbf{7}^+ - (D - \nu_{56} - 2\nu_4 - 2)\,\nu_4\mathbf{4}^+ - (\nu_7 - \nu_4)\left(\nu_5\mathbf{5}^+ + \nu_6\mathbf{6}^+\right)$$
$$+ \nu_5\mathbf{5}^+\nu_7\mathbf{7}^+\mathbf{1}^- - \nu_4\mathbf{4}^+\nu_6\mathbf{6}^+\mathbf{3}^- = 0. \tag{5.98}$$

In the same way, we can apply $\nu_6\mathbf{6}^+$ to Eq. (5.86) and $\nu_5\mathbf{5}^+$ to Eq. (5.87) and take the difference, to obtain

$$(D-\nu_{47}-2\nu_5-2)\,\nu_5\mathbf{5}^+ - (D-\nu_{47}-2\nu_6-2)\,\nu_6\mathbf{6}^+ + (\nu_6-\nu_5)\left(\nu_4\mathbf{4}^+ + \nu_7\mathbf{7}^+\right) + \nu_5\mathbf{5}^+\nu_7\mathbf{7}^+\mathbf{1}^- - \nu_4\mathbf{4}^+\nu_6\mathbf{6}^+\mathbf{3}^- = 0. \tag{5.99}$$

Combining Eq. (5.98) and (5.99) to eliminate $\nu_5\mathbf{5}^+$, we have

$$\begin{aligned}\nu_4\mathbf{4}^+ &= \frac{(D-2\nu_{57}-2)}{(D-2\nu_{45}-2)}\nu_7\mathbf{7}^+ - 2\frac{(\nu_7-\nu_4)}{(D-2\nu_{45}-2)}\nu_6\mathbf{6}^+ \\ &\quad + \frac{1}{(D-\nu_{4567}-2)}\left(\nu_5\mathbf{5}^+\nu_7\mathbf{7}^+\mathbf{1}^- - \nu_4\mathbf{4}^+\nu_6\mathbf{6}^+\mathbf{3}^-\right),\end{aligned} \tag{5.100}$$

that can be used to reduce ν_4 to one, at the expense of increasing ν_6 and ν_7. If, on the other hand, we eliminate $\nu_4\mathbf{4}^+$, we obtain the symmetric equation that can reduce ν_5 to one. At this point, all the powers of the propagators except ν_2, ν_6 and ν_7 have been reduced to one.

In the same spirit we can derive

$$\begin{aligned}st\nu_2\mathbf{2}^+\nu_6\mathbf{6}^+ &= (2\nu_{1567}+\nu_2+2-2D)\,s\nu_6\mathbf{6}^+ + (\nu_{467}+2\nu_5-D)\,s\nu_2\mathbf{2}^+ \\ &\quad - 2\,(D-\nu_{467}-2\nu_5)\left(\nu_6\mathbf{6}^+\mathbf{7}^- + \nu_4\mathbf{4}^+\mathbf{5}^- + \nu_3\mathbf{3}^+\mathbf{1}^- + \nu_2\mathbf{2}^+\mathbf{1}^-\right) \\ &\quad + s\left(2\nu_3\mathbf{3}^+ + \nu_2\mathbf{2}^+\right)\left[\left(\nu_7\mathbf{7}^+ + \nu_6\mathbf{6}^+ + \nu_4\mathbf{4}^+\right)\mathbf{5}^- - \nu_7\mathbf{7}^+\mathbf{1}^-\right] \\ &\quad + t\nu_2\mathbf{2}^+\nu_6\mathbf{6}^+\left(\mathbf{3}^- - \mathbf{1}^-\right) + 2s\nu_4\mathbf{4}^+\nu_6\mathbf{6}^+\mathbf{5}^- \\ &\quad + 2\,(D-\nu_{467}-2\nu_5)\,(2D-2\nu_{157}-\nu_{2346}),\end{aligned} \tag{5.101}$$

that, together with the symmetric one for $\nu_2\mathbf{2}^+\nu_7\mathbf{7}^+$ and with

$$\begin{aligned}s\nu_6\mathbf{6}^+\nu_7\mathbf{7}^+ &= (D-\nu_{567}-2\nu_4-1)\,\nu_6\mathbf{6}^+ + (D-\nu_{467}-2\nu_5-1)\,\nu_7\mathbf{7}^+ \\ &\quad + \nu_6\mathbf{6}^+\nu_7\mathbf{7}^+\left(\mathbf{3}^- + \mathbf{1}^- - \mathbf{5}^- - \mathbf{4}^-\right) - \nu_4\mathbf{4}^+\nu_7\mathbf{7}^+\mathbf{5}^- - \nu_5\mathbf{5}^+\nu_6\mathbf{6}^+\mathbf{4}^- \\ &\quad + \nu_7(\nu_7+1)\mathbf{7}^{++}\left(\mathbf{1}^- - \mathbf{5}^-\right) + \nu_6(\nu_6+1)\mathbf{6}^{++}\left(\mathbf{3}^- - \mathbf{4}^-\right),\end{aligned} \tag{5.102}$$

reduces all powers except one (ν_2 or ν_6 or ν_7) to unity.

We can decrease ν_2 at the expense of increasing ν_6 and ν_7 using

$$
\begin{aligned}
&[(\nu_4 - \nu_7 + 2\nu_{23} + 2 - D)\, s + (\nu_{45} - \nu_{67})\, t]\, \nu_2 \mathbf{2}^+ = (\nu_5 - \nu_3)\, s\nu_4 \mathbf{4}^+ + (\nu_7 - \nu_3)\, s\nu_6 \mathbf{6}^+ \\
&\quad - (D - 2\nu_7 - \nu_{16} - 2)\, s\nu_7 \mathbf{7}^+ - (D - 2\nu_5 - \nu_{14} - 2)\, s\nu_5 \mathbf{5}^+ \\
&\quad + (t+s)\nu_2 \mathbf{2}^+ \left[\nu_7 \mathbf{7}^+ \left(\mathbf{1}^- - \mathbf{5}^-\right) + \nu_4 \mathbf{4}^+ \left(\mathbf{6}^- - \mathbf{3}^-\right)\right] \\
&\quad + t\nu_2 \mathbf{2}^+ \left[\nu_5 \mathbf{5}^+ \left(\mathbf{7}^- - \mathbf{1}^-\right) + \nu_6 \mathbf{6}^+ \left(\mathbf{3}^- - \mathbf{4}^-\right)\right] \\
&\quad - s\nu_1 \mathbf{1}^+ \left(\nu_7 \mathbf{7}^+ \mathbf{5}^- + \nu_5 \mathbf{5}^+ \mathbf{7}^-\right) \\
&\quad + s\nu_3 \mathbf{3}^+ \left[\left(2\nu_7 \mathbf{7}^+ + \nu_4 \mathbf{4}^+\right) \mathbf{6}^- + \left(2\nu_5 \mathbf{5}^+ + \nu_6 \mathbf{6}^+\right) \mathbf{4}^-\right] \\
&\quad - (2D - 2\nu_{57} - 3\nu_{46}) \left[\nu_6 \mathbf{6}^+ \mathbf{7}^- + \nu_4 \mathbf{4}^+ \mathbf{5}^- + \left(\nu_3 \mathbf{3}^+ + \nu_2 \mathbf{2}^+\right) \mathbf{1}^-\right] \\
&\quad + (\nu_{57} - 2\nu_2) \left[\nu_7 \mathbf{7}^+ \mathbf{6}^- + \nu_5 \mathbf{5}^+ \mathbf{4}^- + \left(\nu_2 \mathbf{2}^+ + \nu_1 \mathbf{1}^+\right) \mathbf{3}^-\right] \\
&\quad + 4D^2 - 2\,(5\nu_{57} + 4\nu_{46} + \nu_3 - \nu_2 + 2\nu_1)\, D + \nu_7\,(5\nu_{17} + 10\nu_{456} + 4\nu_3 + \nu_2) \\
&\quad + \nu_6\,(3\nu_6 + 10\nu_5 + 6\nu_{14} + 3\nu_3 - \nu_2) + \nu_5\,(5\nu_5 + 10\nu_4 + 4\nu_3 + \nu_2 + 5\nu_1) \\
&\quad + \nu_4\,(3\nu_4 + 3\nu_3 - \nu_2 + 6\nu_1) - 2\nu_2\,(2\nu_3 + \nu_{12})\,.
\end{aligned} \tag{5.103}
$$

The power of the seventh propagator can be reduced with

$$
\begin{aligned}
&s(t+s)\nu_7(\nu_7+1)\mathbf{7}^{++} = \sigma\nu_7 \mathbf{7}^+ - (\nu_7 - 1)\frac{(D-6)\,t + (5D - 2\nu_7 - 26)\,s}{D - 2\nu_7 - 6}\mathbf{6}^+ \\
&\quad + \rho\frac{(2D - \nu_7 - 11)\,t + (3D - 2\nu_7 - 15)\,s}{D - \nu_7 - 5}\mathbf{5}^+ \nu_7 \mathbf{7}^+ \mathbf{1}^- \\
&\quad + \rho\frac{(D - 2\nu_7 - 4)\,t + (5 - D)\,s}{D - \nu_7 - 5}\mathbf{4}^+ \mathbf{6}^+ \mathbf{3}^- + \rho(t+s)\Big\{-\nu_7(\nu_7+1)\mathbf{7}^{++}\mathbf{6}^- \\
&\quad + \mathbf{5}^+ \nu_7 \mathbf{7}^+ \left(\mathbf{3}^- - \mathbf{4}^- - \mathbf{6}^-\right) + \mathbf{4}^+ \nu_7 \mathbf{7}^+ \left[2\left(\mathbf{3}^- - \mathbf{6}^-\right) + \mathbf{1}^-\right] \\
&\quad - \mathbf{2}^+ \left(\nu_7 \mathbf{7}^+ + \mathbf{4}^+\right) \mathbf{1}^- + \mathbf{5}^+ \mathbf{6}^+ \mathbf{3}^- - 2\,\mathbf{5}^{++}\mathbf{4}^-\Big\} \\
&\quad - 2\nu_7 \frac{t+s}{D - 2\nu_7 - 6}\left(\mathbf{4}^+ \nu_7 \mathbf{7}^+ \mathbf{5}^- + \mathbf{5}^+ \mathbf{6}^+ \mathbf{4}^-\right) + (t+s)\Big[2\,\mathbf{6}^{++}\left(\mathbf{4}^- - \mathbf{3}^-\right) \\
&\quad + \nu_7(\nu_7+1)\mathbf{7}^{++}\left(\mathbf{5}^- - \mathbf{1}^-\right) + \mathbf{6}^+ \nu_7 \mathbf{7}^+ \left(\mathbf{5}^- + \mathbf{4}^- - \mathbf{3}^- - \mathbf{1}^-\right)\Big] \\
&\quad + \rho s\Big[\mathbf{3}^+ \mathbf{5}^+ \left(\mathbf{1}^- - \mathbf{4}^- - \mathbf{7}^-\right) - \mathbf{3}^+ \mathbf{6}^+ \left(\mathbf{4}^- + \mathbf{7}^-\right) - \mathbf{3}^+ \nu_7 \mathbf{7}^+ \left(\mathbf{4}^- + \mathbf{2}^-\right) \\
&\quad - \mathbf{4}^+ \left(\nu_7 \mathbf{7}^+ \mathbf{2}^- + \mathbf{6}^+ \mathbf{7}^- + \mathbf{1}^+ \mathbf{2}^- + \mathbf{3}^+ \mathbf{7}^-\right)\Big] \\
&\quad + (2D - 3\nu_7 - 7)\rho\Big[\mathbf{6}^+ \mathbf{7}^- + \mathbf{4}^+ \mathbf{5}^- + \left(\mathbf{3}^+ + \mathbf{2}^+\right) \mathbf{1}^- - 2(D - \nu_7 - 4)\Big],
\end{aligned} \tag{5.104}
$$

where we have introduced the shorthands

$$
\begin{aligned}
\rho &= \frac{D-6}{D - 2\nu_7 - 6} \\
\sigma &= \frac{(5D^2 - 8\nu_7 D - 50D + 2\nu_7^2 + 42\nu_7 + 124)\,s + (2D^2 - 3\nu_7 D - 21D + 18\nu_7 + 54)\,t}{D - 2\nu_7 - 6}.
\end{aligned}
$$

Equation (5.104) is not as general as the previous ones since we have set all the powers of the other propagators to unity. In addition, since this equation contains $\mathbf{7}^{++}$, we cannot always reduce ν_7 to one, and are left with integrals where $\nu_7 = 2$. A similar identity can be obtained by symmetry for $\mathbf{6}^{++}$, so that we are left with three integrals: $\mathbf{Xbox}^D(1,1,1,1,1,1,1;s,t)$, $\mathbf{Xbox}^D(1,1,1,1,1,1,2;s,t)$ and $\mathbf{Xbox}^D(1,1,1,1,1,2,1;s,t)$.

The last step is to write the integral with $\nu_6 = 2$ as a combination of the other two. This can be done with the identity that links $\mathbf{6}^+$ with $\mathbf{7}^+$. We can derive such an identity, equating the expressions obtained by acting with $\nu_7\mathbf{7}^+$ on $\nu_2\mathbf{2}^+\nu_4\mathbf{4}^+$

and by acting with $\nu_2\mathbf{2}^+$ on $\nu_4\mathbf{4}^+\nu_7\mathbf{7}^+$

$$
\begin{aligned}
&(D-6)(D-5)\frac{t}{t+s}\mathbf{6}^+ = (D-6)(D-5)\mathbf{7}^+ - 4\frac{(D-5)^3}{t+s} \\
&\quad -\Big(\mathbf{5}^+\mathbf{7}^+ + \mathbf{1}^+\mathbf{7}^+ + \mathbf{1}^+\mathbf{5}^+ + \mathbf{1}^+\mathbf{4}^+\Big)\mathbf{6}^- - \Big(\mathbf{3}^+\mathbf{7}^+ + \mathbf{4}^+\mathbf{6}^+ + \mathbf{3}^+\mathbf{6}^+ + \mathbf{3}^+\mathbf{4}^+\Big)\mathbf{5}^- \\
&\quad +\Big(\mathbf{3}^+\mathbf{4}^+ + \mathbf{4}^+\mathbf{6}^+ + \mathbf{5}^+\mathbf{6}^+ + \mathbf{3}^+\mathbf{6}^+\Big)\mathbf{1}^- - (D-7)\mathbf{4}^+\mathbf{7}^+\mathbf{1}^- \\
&\quad -\frac{1}{2}\Big(\mathbf{2}^+\mathbf{7}^+\mathbf{6}^- + \mathbf{2}^+\mathbf{5}^+\mathbf{6}^- + \mathbf{4}^+\mathbf{7}^+\mathbf{5}^- + \mathbf{2}^+\mathbf{6}^+\mathbf{5}^- - \mathbf{1}^+\mathbf{4}^+\mathbf{3}^-\Big) \\
&\quad -\frac{t+s}{2}\Big[\mathbf{2}^+\mathbf{4}^+\mathbf{7}^+\left(\mathbf{6}^- + \mathbf{5}^-\right) + 2\left(\mathbf{2}^{++}\mathbf{7}^+ - \mathbf{2}^+\mathbf{4}^+\mathbf{7}^+ + \mathbf{2}^{++}\mathbf{4}^+\right)\mathbf{1}^-\Big] \\
&\quad -\frac{s}{2}\Big\{\mathbf{2}^+\Big[\mathbf{3}^+\left(\mathbf{6}^+ + \mathbf{5}^+ + \mathbf{4}^+\right)\mathbf{7}^- + \mathbf{4}^+\mathbf{6}^+\mathbf{7}^- + \mathbf{3}^+\left(\mathbf{7}^+ + \mathbf{6}^+ + \mathbf{5}^+\right)\mathbf{4}^-\Big] \\
&\quad +\mathbf{3}^+\mathbf{5}^+\left(2\,\mathbf{7}^+ - \mathbf{2}^+\right)\mathbf{1}^-\Big\} - (D-6)\frac{(t+2s)}{2(t+s)}\Big[\mathbf{2}^+\left(\mathbf{7}^+\mathbf{4}^- + \mathbf{4}^+\mathbf{7}^- + \mathbf{5}^+\mathbf{4}^-\right) \\
&\quad +2\Big(\mathbf{1}^+\mathbf{7}^+ + \mathbf{5}^+\mathbf{7}^+ + \mathbf{1}^+\mathbf{6}^+ + \mathbf{1}^+\mathbf{5}^+\Big)\mathbf{4}^- - 2\,\mathbf{1}^+\mathbf{6}^+\mathbf{3}^-\Big] - \frac{2(D-5)t+s}{2s}\mathbf{2}^+\mathbf{7}^+\mathbf{5}^- \\
&\quad -(D-6)\Big[\mathbf{4}^+\mathbf{7}^+\mathbf{3}^- + \left(\mathbf{3}^+\mathbf{4}^+ + \mathbf{4}^+\mathbf{6}^+ + \mathbf{3}^+\mathbf{6}^+ + \mathbf{3}^+\mathbf{5}^+\right)\mathbf{7}^-\Big] \\
&\quad +(D-6)\frac{s}{t+s}\Big[\mathbf{7}^+\mathbf{3}^+\mathbf{4}^- + \Big(\mathbf{7}^+\mathbf{3}^+ + \mathbf{7}^+\mathbf{4}^+ + \mathbf{1}^+\mathbf{4}^+\Big)\mathbf{2}^-\Big] + \frac{2D-13}{2}\mathbf{4}^+\mathbf{7}^+\mathbf{6}^- \\
&\quad +(D-5)\frac{(D-5)t+(2D-11)s}{s(t+s)}\Big[\left(\mathbf{2}^+ + \mathbf{1}^+\right)\mathbf{3}^- + \mathbf{7}^+\mathbf{6}^-\Big] \\
&\quad +(D-5)\frac{t}{t+s}\Big[2\,\mathbf{3}^+\mathbf{7}^+\mathbf{6}^- + \mathbf{3}^+\mathbf{4}^+\mathbf{6}^- - \mathbf{1}^+\mathbf{7}^+\mathbf{5}^- - \mathbf{1}^+\mathbf{5}^+\mathbf{7}^-\Big] + \frac{t}{2s}\mathbf{2}^+\mathbf{5}^+\mathbf{3}^- \\
&\quad -(D-5)\frac{(D-5)t-s}{s(t+s)}\Big[\mathbf{4}^+\mathbf{5}^- + \mathbf{2}^+\mathbf{1}^- + \mathbf{6}^+\mathbf{7}^- + \mathbf{3}^+\mathbf{1}^-\Big] - \frac{2D-15}{2}\mathbf{3}^+\mathbf{7}^+\mathbf{1}^- \\
&\quad +(D-5)\Big[\mathbf{1}^-\left(\mathbf{3}^+\mathbf{5}^+ + 2\,\mathbf{2}^{++} + \mathbf{2}^+\mathbf{3}^+\right)\Big] + \frac{t}{2}\Big[\mathbf{2}^+\left(\mathbf{5}^+\mathbf{7}^+\mathbf{1}^- + \mathbf{4}^+\mathbf{6}^+\mathbf{3}^-\right)\Big] \\
&\quad +\frac{5t-2(D-7)s}{2(t+s)}\mathbf{5}^+\mathbf{7}^+\mathbf{1}^- - \frac{(2D-9)t^2-(D-5)st-2(D-5)s^2}{2s(t+s)}\mathbf{2}^+\mathbf{5}^+\mathbf{1}^- \\
&\quad -(D-6)\frac{t+2s}{2s}\mathbf{2}^+\mathbf{7}^+\mathbf{3}^- - \frac{2(D-5)t^2+(D-6)st+2(D-6)s^2}{2s(t+s)}\mathbf{2}^+\mathbf{6}^+\mathbf{4}^- \\
&\quad +\frac{(3D-16)t+2(D-5)s}{2s}\mathbf{2}^+\mathbf{7}^+\mathbf{1}^- + \frac{(D-4)t+2s}{2(t+s)}\mathbf{2}^+\mathbf{6}^+\mathbf{7}^- \\
&\quad +\frac{2(D-5)t^2-(D-6)st-2(D-6)s^2}{2s(t+s)}\mathbf{2}^+\mathbf{5}^+\mathbf{7}^- - (4D-21)\frac{t}{2(t+s)}\mathbf{4}^+\mathbf{6}^+\mathbf{3}^- \\
&\quad +\frac{(D-5)t+(D-6)s}{t+s}\mathbf{3}^+\mathbf{6}^+\mathbf{4}^- - \frac{(D-4)t-2(D-6)s}{2s}\mathbf{2}^+\mathbf{4}^+\mathbf{3}^- \\
&\quad +\frac{(2D-11)t^2+(D-7)st+2(D-6)s^2}{2s(t+s)}\mathbf{2}^+\mathbf{6}^+\mathbf{3}^- + \frac{t+2s}{2s}\mathbf{2}^+\mathbf{6}^+\mathbf{1}^- \\
&\quad +\frac{2(D-5)t+(D-6)s}{t+s}\mathbf{3}^+\mathbf{5}^+\mathbf{4}^- + (D-5)\frac{(D-5)t+(2D-11)s}{s(t+s)}\mathbf{5}^+\mathbf{4}^- \\
&\quad +\frac{2D-11}{2}\mathbf{2}^+\mathbf{4}^+\mathbf{5}^- - \frac{(D-6)t-2s}{2s}\mathbf{2}^+\mathbf{4}^+\mathbf{1}^- + \frac{2(D-5)t-s}{2s}\mathbf{2}^+\mathbf{4}^+\mathbf{6}^-,
\end{aligned}
\tag{5.105}
$$

where we have set all the powers of the propagators to unity.

At the end of this reduction program, we are left with the following two crossed-box integrals: $\mathbf{Xbox}^D(1,1,1,1,1,1,1;s,t)$ and $\mathbf{Xbox}^D(1,1,1,1,1,1,2;s,t)$, plus simpler diagrams that can always be expressed as a combination of master integrals:

- the master crossed triangle of

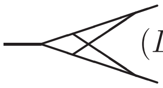

$$(D,s) \quad = \quad \mathbf{Xbox}^D\,(1,0,1,1,1,1,1;s,t) = \mathbf{XTRI}^D(s), \tag{5.106}$$

- the master diagonal box produced by

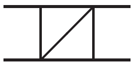

$$\begin{aligned}(D,s,t) \quad &= \quad \mathbf{Xbox}^D\,(0,1,1,0,1,1,1;s,t) = \mathbf{Xbox}^D\,(1,1,0,1,1,1,0;s,t)\\ &= \quad \mathbf{CBOX}^D(s,t),\end{aligned} \tag{5.107}$$

together with

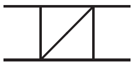

$$\begin{aligned}(D,s,u) \quad &= \quad \mathbf{Xbox}^D\,(1,1,0,1,0,1,1;s,t) = \mathbf{Xbox}^D\,(0,1,1,1,1,0,1;s,t)\\ &= \quad \mathbf{CBOX}^D(s,u),\end{aligned} \tag{5.108}$$

and

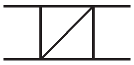

$$(D,t,u) \quad = \mathbf{Xbox}^D\,(0,1,0,1,1,1,1;s,t) = \mathbf{CBOX}^D(t,u), \tag{5.109}$$

- the master box with a bubble insertion produced by

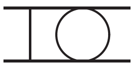

$$(D,s,t) \quad = \mathbf{Xbox}^D\,(1,1,1,0,1,1,0;s,t)\,, \tag{5.110}$$

together with

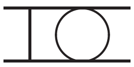

$$(D,s,u) \quad = \mathbf{Xbox}^D\,(1,1,1,1,0,0,1;s,t) = \mathbf{ABOX}^D(s,u), \tag{5.111}$$

- the master triangle with a bubble insertion produced by

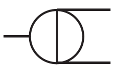

$$\begin{aligned}(D,s) \quad &= \quad \mathbf{Xbox}^D\,(1,0,1,0,1,1,0;s,t) = \mathbf{Xbox}^D\,(1,0,1,1,0,0,1;s,t)\\ &= \quad \mathbf{TRI}^D(s),\end{aligned} \tag{5.112}$$

- the master sunset diagram produced by

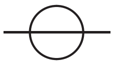

$$(D,s) = \mathbf{Xbox}^{D}\,(0,0,1,0,1,0,1;s,t) = \mathbf{Xbox}^{D}\,(1,0,0,1,0,1,0;s,t) = \mathbf{SUNS}^{D}(s), \tag{5.113}$$

together with

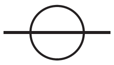

$$(D,t) = \mathbf{Xbox}^{D}\,(0,1,0,0,1,1,0;s,t) = \mathbf{SUNS}^{D}(t), \tag{5.114}$$

and finally

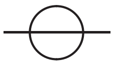

$$(D,u) = \mathbf{Xbox}^{D}\,(0,1,0,1,0,0,1;s,t) = \mathbf{SUNS}^{D}(u). \tag{5.115}$$

In this point we have derived a basis of master integrals for the cross-box topology. It is of our freedom to choose a different but equivalent more symmetric basis. Instead of keeping $\mathbf{Xbox}^{D}(1,1,1,1,1,1,2;s,t)$ as one of the two cross-box integrals members of the basis, we prefer to switch to $\mathbf{Xbox}^{D}(1,2,1,1,1,1,1;s,t)$. The expression for this one, in terms of the master integrals of the old basis, can be easily obtained through the application of the reduction algorithm outlined above. This allows us to define the two cross-box master integrals as

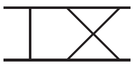

$$\boxed{(D,s,t) = \mathbf{Xbox}^{D}(1,1,1,1,1,1,1;s,t)} \tag{5.116}$$

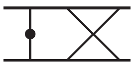

$$\boxed{(D,s,t) = \mathbf{Xbox}^{D}(1,2,1,1,1,1,1;s,t)}, \tag{5.117}$$

which are symmetric under the exchange $t \leftrightarrow u$.

Finally, given the reduction algorithm for the extra powers of propagators developed here, it is straightforward to apply the procedure of Section 5.2 in order to relate the cross-box master integrals in higher dimensions to the master integrals in $D = 4 - 2\epsilon$ dimensions. The relative expressions are rather lengthy and we do not present them here.

With the dimensional-shift at hand we have completed the tensor reduction of the cross-box topologies to master integrals in $4-2\epsilon$ dimensions. All master integrals belonging in subtopologies were calculated earlier. The calculation of the cross-box master integrals is a hard and laborious problem. Tausk [22] calculated the

$$\mathbf{XBOX}_1^{4-2\epsilon}\,(s,t) \equiv$$

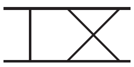

$$(s,t)$$

master integral by performing an ϵ-expansion of the MB-representation of the integral. Fortunately, we can avoid a direct evaluation of the second cross-box master integral

$$\mathbf{XBOX}_2^{4-2\epsilon}(s,t) \equiv$$ 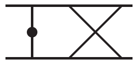 (s,t)

since the two integrals are related by a simple differential equation. Differential equations for scalar integrals can be obtained in a straightforward manner starting from the Schwinger parametric form of the integrals, and this will be the subject of the following paragraph.

5.8.2 Differential equations for the master integrals of the cross-box topology

We consider the Schwinger representation of the general scalar two-loop box with arbitrary powers of propagators,

$$\mathbf{Xbox}^D(\{\nu_i\};s,t) = \int \mathcal{D}x \, \frac{1}{\mathcal{P}^{D/2}} \, \exp\left(\frac{\mathcal{Q}}{\mathcal{P}}\right), \tag{5.118}$$

where

$$\int \mathcal{D}x = \prod_{i=1}^{7} \frac{(-1)^{\nu_i}}{\Gamma(\nu_i)} \int_0^\infty dx_i \, x_i^{\nu_i - 1}, \tag{5.119}$$

$$\mathcal{P} = (x_7 + x_6 + x_5 + x_4)(x_3 + x_2 + x_1) + (x_5 + x_4)(x_7 + x_6), \tag{5.120}$$

and

$$\mathcal{Q} = x_2(x_5x_6 - x_4x_7)t + [x_1x_3(x_7 + x_6 + x_5 + x_4) + x_3x_5x_7 - x_2x_4x_7 + x_1x_4x_6]\, s. \tag{5.121}$$

It is straightforward to differentiate both sides of Eq. 5.118 with respect to the kinematic variables s and t. The only dependence on these variables comes from Q, we therefore have

$$\frac{\partial}{\partial t}\mathbf{Xbox}^D(\{\nu_i\};s,t) = \int \mathcal{D}x \, \frac{x_2(x_5x_6 - x_4x_7)}{\mathcal{P}} \frac{1}{\mathcal{P}^{D/2}} \, \exp\left(\frac{\mathcal{Q}}{\mathcal{P}}\right), \tag{5.122}$$

which we rewrite in terms of integrals in $D+2$ dimensions and extra powers of propagators

$$\frac{\partial}{\partial t}\mathbf{Xbox}^D(\{\nu_i\};s,t) = -\nu_2\mathbf{2}^+(\nu_5\mathbf{5}^+\nu_6\mathbf{6}^+ - \nu_4\mathbf{4}^+\nu_7\mathbf{7}^+)\mathbf{Xbox}^{D+2}(\{\nu_i\};s,t) \tag{5.123}$$

The integrals of the r.h.s can be reduced to the master integrals in D dimensions with the algorithm of Section 5.8.1.

In the special case of differentiating the cross-box master integrals with respect to t, we obtain the following two equations

$\frac{\partial}{\partial t}$ 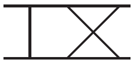 $(D,s,t) = \frac{1}{t-u}\left[H(t,u)+H(u,t)\right],$ (5.124)

$\frac{\partial}{\partial t}$ 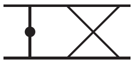 $(D,s,t) = \frac{1}{t-u}\left[K(t,u)+K(u,t)\right],$ (5.125)

where

$H(t,u) = h_1$ 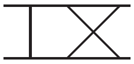 $(D,s,t) + h_2$ 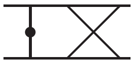 (D,s,t)

$+\, h_3$ 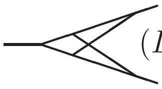 $(D,s) + h_4$ 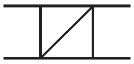 (D,s,t)

$+\, h_5$ 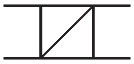 $(D,t,u) + h_6$ 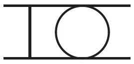 (D,s,t)

$+\, h_7$ 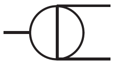 $(D,s) + h_8$ 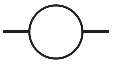 (D,s)

$+\, h_9$ 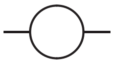 $(D,t)\,,$ (5.126)

$K(t,u) = k_1$ 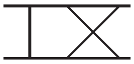 $(D,s,t) + k_2$ 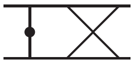 (D,s,t)

$+\, k_3$ 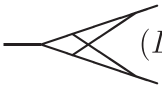 $(D,s) + k_4$ 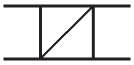 (D,s,t)

$+\, k_5$ 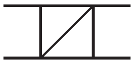 $(D,t,u) + k_6$ 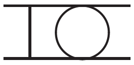 (D,s,t)

$+\, k_7$ 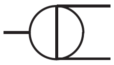 $(D,s) + k_8$ 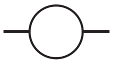 (D,s)

$+\, k_9$ 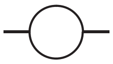 $(D,t)\,.$ (5.127)

The coefficients are given by

$$
\begin{aligned}
h_1 &= \frac{(D-4)s^2-4tu}{4tu} \quad h_2 = -\frac{(D-6)s}{4(D-5)} \quad h_3 = \frac{(D-4)(2D-9)s}{4(D-5)tu} \\
h_4 &= \frac{3}{2}\frac{(D-4)(3D-14)u}{(D-5)st^2} \quad h_5 = \frac{3}{2}\frac{(D-4)(3D-14)s^2}{(D-6)t^2u^2} \quad h_6 = 3\frac{(D-3)(3D-14)}{(D-5)t^2} \\
h_7 &= \frac{3}{4}\frac{(D-3)(3D-10)\left[(3D-14)\left(u^2+t^2\right)+2(D-4)tu\right]}{(D-5)(D-4)st^2u^2} \\
h_8 &= \frac{3}{4}\frac{(D-3)(3D-10)(3D-8)\left[(D-5)(3D-14)\left(u^2+t^2\right)-(D-6)(D-4)tu\right]}{(D-5)^2(D-4)^2s^2t^2u^2} \\
h_9 &= \frac{3}{2}\frac{(D-3)(3D-14)(3D-10)(3D-8)}{(D-6)(D-5)^2(D-4)^2st^3u^2}\Big[(2D-9)(3D-16)u^2 \\
&\quad + \left(7D^2-68D+164\right)tu + 2(D-5)^2t^2\Big],
\end{aligned}
\tag{5.128}
$$

and by

$$
\begin{aligned}
k_1 &= \frac{(D-5)^2 s}{tu} \quad k_2 = -\frac{(D-6)(u^2+t^2)}{2tu} \quad k_3 = \frac{(D-4)(2D-9)}{tu} \\
k_4 &= 6\frac{(D-4)(3D-14)u\,[(5-D)u+(2D-11)t]}{(D-6)s^2t^3} \quad k_5 = \frac{3}{2}\frac{(D-5)(D-4)(3D-14)s^3}{(D-6)t^3u^3} \\
k_6 &= 3\frac{(D-3)(3D-14)}{(D-6)st^3u}\left[(5D-28)tu+(D-6)t^2-2(D-5)u^2\right] \\
k_7 &= \frac{3}{2}\frac{(D-3)(3D-10)}{(D-6)(D-4)s^2t^3u^3}\Big[2(D-6)(3D-14)tu\left(u^2+t^2\right) \\
&\quad -(D-5)(3D-14)\left(u^4+t^4\right)+2\left(5D^2-49D+118\right)t^2u^2\Big] \\
k_8 &= 3\frac{(D-3)(3D-10)(3D-8)}{(D-6)(D-5)(D-4)^2s^3t^3u^3}\Big[3(D-5)^2(3D-14)tu\left(u^2+t^2\right) \\
&\quad -(D-5)^2(3D-14)\left(u^4+t^4\right)-(D-4)\left(7D^2-70D+176\right)t^2u^2\Big] \\
k_9 &= 3\frac{(D-3)(3D-14)(3D-10)(3D-8)}{(D-6)^2(D-5)(D-4)^2s^2t^4u^3}\Big[(D-5)^2(D-2)u^4 \\
&\quad +(D-6)\left(13D^2-129D+318\right)tu^3+2\left(5D^3-80D^2+422D-734\right)t^2u^2 \\
&\quad +(D-6)(D-5)(5D-24)t^3u+(D-6)(D-5)^2t^4\Big]. \qquad (5.129)
\end{aligned}
$$

Differential equations with respect to s can be obtained with the same method.

The differential equations for the master integrals are a very useful tool. Finding an appropriate boundary condition we could try to solve them and calculate the master integrals. For example, Gehrmann and Remiddi [28, 27, 25] have developed a technique to solve the differential equations order by order in ϵ, and they have evaluated integrals even more complicated than the ones involved in the above system. In our case, given the original calculation of Tausk for $\mathbf{XBOX}_1^{4-2\epsilon}(s,t)$ from its Mellin-Barnes representation, we will use the differential equations to verify it and guess the solution for $\mathbf{XBOX}_2^{4-2\epsilon}(s,t)$.

5.8.3 Analytic expansion of the second master integral

Taking a closer look in Eq. 5.124 we see that in order to evaluate the master integral $\mathbf{XBOX}_2^{4-2\epsilon}(s,t)$ one needs the ϵ-expansion of the master integral $\mathbf{XBOX}_1^{4-2\epsilon}(s,t)$ (which has already been calculated in Ref [22]) together with its derivative and the ϵ expansions of the master integrals of the sub-topologies which we calculated in previous sections.

Solving the equation with respect to $\mathbf{XBOX}_2^{4-2\epsilon}(s,t)$, we obtain, in the physical region $s>0$, $t,u<0$,

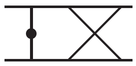

$$(s,t) = \Gamma^2(1+\epsilon)\left\{\frac{G_1(t,u)}{s^3 t} + \frac{G_2(t,u)}{s^2 t^2} + \frac{G_1(u,t)}{s^3 u} + \frac{G_2(u,t)}{s^2 u^2}\right\}, \tag{5.130}$$

where

$$\begin{aligned}
G_1(t,u) = s^{-2\epsilon}\Bigg\{ & \frac{6}{\epsilon^3} + \frac{1}{\epsilon^2}\left(32 - 6\,L_x - 6\,L_y\right) \\
& + \frac{1}{\epsilon}\left(1 - 12\,\pi^2 - 24\,L_x + L_x^2 - 24\,L_y + 16\,L_x\,L_y + L_y^2\right) - 43 - 18\,L_x + 13\,L_x^2 + \frac{8}{3}\,L_x^3 \\
& - 18\,L_y + 16\,L_x\,L_y + 11\,L_x^2\,L_y + 13\,L_y^2 - 20\,L_x\,L_y^2 + \frac{8}{3}\,L_y^3 + \pi^2\left(17\,L_x + 17\,L_y - \frac{112}{3}\right) \\
& - 122\,\zeta(3) + 62\,L_x\,\mathrm{Li}_2\left(-\frac{t}{s}\right) - 62\,\mathrm{Li}_3\left(-\frac{t}{s}\right) + 62\,\mathrm{S}_{1,2}\left(-\frac{t}{s}\right) \\
& + i\pi\left[\frac{1}{\epsilon}\left(16 + 6\,L_x + 6\,L_y\right) - 34 - 9\,\pi^2 - 6\,L_x - 10\,L_x^2 - 6\,L_y + 14\,L_x\,L_y - 10\,L_y^2\right]\Bigg\},
\end{aligned} \tag{5.131}$$

$$\begin{aligned}
G_2(t,u) = s^{-2\epsilon}\Bigg\{ & -\frac{2}{\epsilon^4} + \frac{1}{\epsilon^3}\left(-8 + \frac{5}{2}\,L_x + \frac{7}{2}\,L_y\right) \\
& + \frac{1}{\epsilon^2}\left(-\frac{29}{2} - \frac{5}{12}\,\pi^2 + 7\,L_x - L_x^2 + 20\,L_y - 4\,L_x\,L_y - L_y^2\right) \\
& + \frac{1}{\epsilon}\Bigg[-\frac{1}{2} + 17\,L_x + 2\,L_x^2 - \frac{L_x^3}{3} + \frac{\pi^2}{6}\left(14 + 5\,L_x - 29\,L_y\right) + 13\,L_y - 28\,L_x\,L_y - 4\,L_y^2 \\
& \quad + 3\,L_x\,L_y^2 - L_y^3 + \frac{19}{2}\,\zeta(3) - 2\,L_x\,\mathrm{Li}_2\left(-\frac{t}{s}\right) + 2\,\mathrm{Li}_3\left(-\frac{t}{s}\right) - 2\,\mathrm{S}_{1,2}\left(-\frac{t}{s}\right)\Bigg] \\
& + \frac{37}{2} + \frac{37}{40}\,\pi^4 + 7\,L_x - 5\,L_x^2 - \frac{22}{3}\,L_x^3 + \frac{2}{3}\,L_x^4 + 5\,L_y - 20\,L_x\,L_y + \frac{8}{3}\,L_x^3\,L_y - 2\,L_y^2 \\
& + 24\,L_x\,L_y^2 - L_x^2\,L_y^2 - 8\,L_y^3 - \frac{4}{3}\,L_x\,L_y^3 + \frac{4}{3}\,L_y^4 \\
& + \frac{\pi^2}{6}\left(79 - 22\,L_x - 5\,L_x^2 - 200\,L_y + 76\,L_x\,L_y + 25\,L_y^2\right) + \left(68 - 13\,L_x - 33\,L_y\right)\zeta(3) \\
& + \left(10\,\pi^2 - 32\,L_x + 17\,L_x^2 + 12\,L_x\,L_y\right)\mathrm{Li}_2\left(-\frac{t}{s}\right) + \left(32 - 60\,L_x - 12\,L_y\right)\mathrm{Li}_3\left(-\frac{t}{s}\right) \\
& + \left(28\,L_x - 6\,L_y - 32\right)\mathrm{S}_{1,2}\left(-\frac{t}{s}\right) - 26\,\mathrm{S}_{1,3}\left(-\frac{t}{s}\right) - 36\,\mathrm{S}_{2,2}\left(-\frac{t}{s}\right) + 86\,\mathrm{Li}_4\left(-\frac{t}{s}\right) \\
& + i\pi\Bigg[\frac{2}{\epsilon^3} + \frac{1}{\epsilon^2}\left(11 - L_x + L_y\right) + \frac{1}{\epsilon}\left(1 - \frac{31}{6}\,\pi^2 - 10\,L_x - 2\,L_x^2 + 4\,L_y - 2\,L_x\,L_y - 2\,L_y^2\right) \\
& \quad + 11 + 4\,L_x - 2\,L_x^2 + \frac{10}{3}\,L_x^3 + \frac{\pi^2}{3}\left(-65 + 28\,L_x - L_y\right) + 2\,L_y - 8\,L_x\,L_y - 8\,L_y^2 \\
& \quad + 2\,L_y^3 - 89\,\zeta(3) + \left(14\,L_x + 18\,L_y\right)\mathrm{Li}_2\left(-\frac{t}{s}\right) - 32\,\mathrm{Li}_3\left(-\frac{t}{s}\right) + 44\,\mathrm{S}_{1,2}\left(-\frac{t}{s}\right)\Bigg]\Bigg\},
\end{aligned} \tag{5.132}$$

and $L_x = \log(-t/s)$, $L_y = \log(-u/s)$.

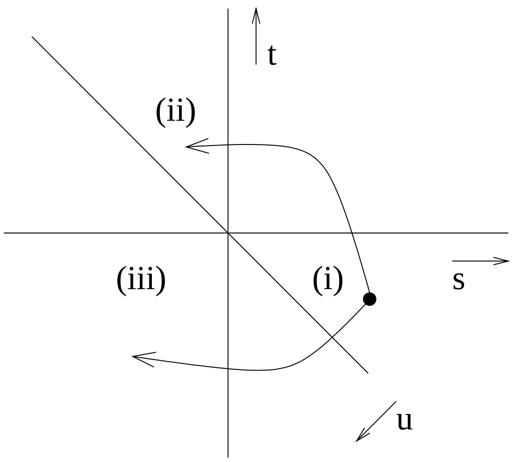

Figure 5.7: The physical regions (i), (ii) and (iii) in the (s, t, u)-plane.

The three kinematically accessible regions of the phase-space are depicted in Fig. 5.8.3.

(i) $\boldsymbol{s > 0,\ t, u < 0}$. All logarithms and polylogarithms occurring in Eqs. (5.131) and (5.132) are real in this region.

Formulae for the other two regions, (ii) and (iii), can be derived by analytic continuation, starting from region (i) and following the paths indicated in the figure.

The analytic continuation can be performed through a few simple steps. recalling the $+i0$ prescription associated with the external kinematic scales.

(ii) $\boldsymbol{t > 0,\ s, u < 0}$. Going from region (i) to region (ii), we have to pass through two branches: $t = 0$ and $s = 0$. We can then split the analytic continuation into two steps:

- we first split the logarithm $T = \log(-t) - \log(s)$. At $t = 0$, nothing happens to the polylogarithms $\mathrm{S}_{n,p}(-t/s)$, but $\log(-t)$ gets an imaginary part: $\log(-t) \to \log(t) - i\pi$.

  We are now in an unphysical region, where both s and t are positive and u is negative. Using the transformation formulae for $x \to 1/x$ (see, Appendix B.2), we can express $\mathrm{S}_{n,p}(-t/s)$ in terms of $\mathrm{S}_{n,p}(-s/t)$ and $\log(t/s)$.

- To enter region (ii), we have to pass now the branch point at $s = 0$. We split $\log(t/s) = \log(t) - \log(s)$ and $U = \log(s+t) - \log(s)$ and we analytically continue $\log(s) \to \log(-s) + i\pi$.

In this way, for example, the logarithms in Eqs. (5.131) and (5.132) undergo the transformation

$$\log\left(-\frac{t}{s}\right) \quad \to \quad \log\left(-\frac{t}{s}\right) - 2\,i\,\pi, \tag{5.133}$$

$$\log\left(-\frac{u}{s}\right) \quad \to \quad \log\left(\frac{u}{s}\right) - i\,\pi. \tag{5.134}$$

(iii) $\boldsymbol{u > 0,\ s, t < 0}$. The procedure to go from region (i) to region (iii) is similar to the previous one, but it requires an additional step.

- We rewrite $\mathrm{S}_{n,p}\left(-t/s\right)$ in terms of $\mathrm{S}_{n,p}\left((s+t)/s\right)$, $\log(-t/s)$ and $\log((s+t)/s)$, using the transformation $x \to 1-x$, and we split the logarithms as before. In passing the first branch point at $u = 0$, the polylogarithms are well defined while $\log(s+t) \to \log(-s-t) - i\pi$.
- We invert now the argument of the polylogarithms, expressing $\mathrm{S}_{n,p}\left((s+t)/s\right)$ in terms of $\mathrm{S}_{n,p}\left(s/(s+t)\right)$ and $\log((-s-t)/s) = \log(-s-t) - \log(s)$. Finally, $\log(s) \to \log(-s) + i\pi$, as we pass the branch point at $s = 0$ and enter region (iii).

The logarithms in Eqs. (5.131) and (5.132) undergo the transformation

$$\log\left(-\frac{t}{s}\right) \quad \to \quad \log\left(\frac{t}{s}\right) - i\,\pi, \tag{5.135}$$

$$\log\left(-\frac{u}{s}\right) \quad \to \quad \log\left(-\frac{u}{s}\right) - 2\,i\,\pi. \tag{5.136}$$

The expression for $G_1(t,u)$ and $G_2(t,u)$ in this region can also be obtained directly from the expressions in region (ii), using the symmetry $t \leftrightarrow u$.

A non-trivial check of the correctness of the expressions of $\mathbf{XBOX}_1^D\,(s,t)$ and $\mathbf{XBOX}_2^D\,(s,t)$ comes from Eq. (5.125), that must be identically satisfied, once the respective ϵ expansions are used.

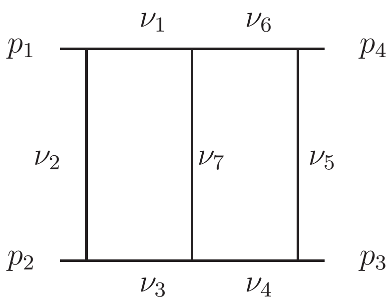

Figure 5.8: The planar double-box topology.

5.9 The planar double-box topology

We denote the generic two-loop scalar planar double-box function in D dimensions of Fig. 5.9 with seven propagators A_i raised to arbitrary powers ν_i as

$$\mathbf{Pbox}^D(\{\nu_i\}; s, t) = \int \frac{d^D k_1}{i\pi^{D/2}} \int \frac{d^D k_2}{i\pi^{D/2}} \frac{1}{A_1^{\nu_1} A_2^{\nu_2} A_3^{\nu_3} A_4^{\nu_4} A_5^{\nu_5} A_6^{\nu_6} A_7^{\nu_7}}, \tag{5.137}$$

where $\{\nu_i\} = \nu_1, \nu_2, \nu_3, \nu_4, \nu_5, \nu_6, \nu_7$ and the propagators are

$$\begin{aligned}
A_1 &= k_1^2 + i0, \\
A_2 &= (k_1 + p_1)^2 + i0, \\
A_3 &= (k_1 + p_1 + p_2)^2 + i0, \\
A_4 &= (k_2 + p_1 + p_2)^2 + i0, \\
A_5 &= (k_2 + p_1 + p_2 + p_3)^2 + i0, \\
A_6 &= k_2^2 + i0, \\
A_7 &= (k_1 - k_2)^2 + i0.
\end{aligned} \tag{5.138}$$

The external momenta p_j are in-going and light-like, $p_j^2 = 0$, $j = 1 \ldots 4$, so that the only momentum scales are the usual Mandelstam variables $s = (p_1 + p_2)^2$ and $t = (p_2 + p_3)^2$, together with $u = (p_1 + p_3)^2 = -s - t$.

5.9.1 IBP algorithm for the planar double-box

Smirnov and Veretin [58] found an algorithm based on IBP for the reduction of the double-box to master integrals. Here we give a synopsis of their algorithm.

We first decrease the power of the first propagator ν_1 to unity with the identity

$$s\nu_1 \mathbf{1}^+ = \left(\nu_1 \mathbf{1}^+ + \nu_2 \mathbf{2}^+ + \nu_7 \mathbf{7}^+\right) \mathbf{3}^- - \nu_7 \mathbf{7}^+ \mathbf{4}^- - (D - \nu_{12337}) \tag{5.139}$$

Three similar relations obtained by symmetry reduce the powers of ν_3, ν_4 and ν_6. We can now reduce the power of ν_2 to one with the identity

$$\begin{aligned}(D-2-\nu_{1223})\nu_2\mathbf{2}^+ &= (D-2-\nu_{1377})\nu_7\mathbf{7}^+ + (\nu_2-\nu_7)(\nu_1\mathbf{1}^+ + \nu_3\mathbf{3}^+) \\ &\quad +\nu_7\mathbf{7}^+(\nu_1\mathbf{1}^+\mathbf{6}^- + \nu_3\mathbf{3}^+\mathbf{4}^-) \qquad (5.140)\end{aligned}$$

and with its symmetric we reduce ν_5 to unity as well. Now all powers of propagators have been reduced to one except ν_7. The identity for the reduction of this last power reads

$$\begin{aligned} t(D-6-2\nu_7)\nu_7(\nu_7+1)\mathbf{7}^{++} &= \\ -(D-5-\nu_7)&\left[3D-14-2\nu_7+2\nu_7\frac{t}{s}\right]\nu_7\mathbf{7}^+ + \frac{2}{s}(D-4-\nu_7)^2(D-5-\nu_7) \\ +\Bigg\{&(\mathbf{5}^+ + \mathbf{6}^+)\left[-\frac{2}{s}(D-4-\nu_7)(D-5-\nu_7) + 2\frac{t}{s}\nu_7^2\mathbf{7}^+\right] \\ &- \left[2t\nu_7(\nu_7+1)\mathbf{7}^{++} + 2(D-4-\nu_7)\nu_7\mathbf{7}^+\right]\mathbf{3}^+\Bigg\}\mathbf{4}^- \\ +(D-6)\Bigg\{&\nu_7\mathbf{7}^+(\mathbf{1}^+ + \mathbf{2}^+ + \mathbf{3}^+ + \mathbf{4}^+ + \mathbf{6}^+\ ) \\ &+(\mathbf{4}^+ + \mathbf{6}^+)(\mathbf{1}^+ + \mathbf{2}^+ + \mathbf{3}^+)\Bigg\}\mathbf{5}^- \qquad (5.141)\end{aligned}$$

which is valid only when all the powers are equal to unit. The reduction will stop when ν_7 becomes one or two, leading to the two master double planar box integrals

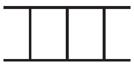

$$\boxed{(D,s,t) \quad = \mathbf{PBOX_1}^D(s,t) = \mathbf{Pbox}^D(1,1,1,1,1,1,1;s,t)}, \qquad (5.142)$$

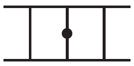

$$\boxed{(D,s,t) \quad = \mathbf{PBOX_2}^D(s,t) = \mathbf{Pbox}^D(1,1,1,1,1,1,2;s,t)}. \qquad (5.143)$$

During the application of the above algorithm integrals with pinched propagators are produced and they belong to the topologies that we have already studied earlier in this thesis.

It is again possible to obtain the dimensional shift identities for the reduction of the dimension of the master integrals in Eq. 5.142 by direct application of the method described in Section 5.2.

The first master integral was calculated by Smirnov[21] from its MB representation. The second master integral was calculated by Smirnov and Veretin [58], through a differential equation which expressed it in terms of the first master integral its derivative with respect to the one of the kinematic variables and simpler master integrals of the subtopologies.

It appeared that the algorithm described in ref. [58] completely solved the problem of calculating on-shell double box diagrams. However, as was reported by Glover and Tejeda-Yeomans [60], it often happens that in the reduction of a given tensor integral, the coefficients in front of the master integrals are of order $\mathcal{O}(1/\epsilon)$. This is a consequence of the fact that in the reduction of these integrals it is necessary to reduce the dimension down to $D = 4 - 2\epsilon$ from at least $D = 6 - 2\epsilon$, and in the system of equations for the dimensional shift, there are factors of $1/(D-6)$ sitting in front of the two master integrals. Thus, in order to calculate such tensor integrals to $\mathcal{O}(\epsilon)$, one would need to know them to one order higher in ϵ than they are given in Refs. [21, 58].

A typical example is the following integral with an irreducible numerator:

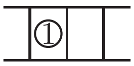

$$(D,s,t) \quad = \mathbf{PBOX_3} \equiv \int \frac{d^D k_1}{i\pi^{D/2}} \int \frac{d^D k_2}{i\pi^{D/2}} \frac{A_8}{A_1^{\nu_1} A_2^{\nu_2} A_3^{\nu_3} A_4^{\nu_4} A_5^{\nu_5} A_6^{\nu_6} A_7^{\nu_7}}, \tag{5.144}$$

where we have an irreducible numerator

$$A_8 = (k_1 + p_1 + p_2 + p_3)^2 + i0. \tag{5.145}$$

The reduction to master integrals reads:

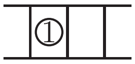 $(D,s,t) \;= -\frac{1}{2}\frac{(3D-14)s}{D-4}$ 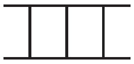 (D,s,t)

$-\frac{1}{2}\frac{(D-6)st}{(D-4)(D-5)}$ 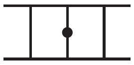 $(D,s,t) \; +24\frac{(D-3)}{(D-6)t}$ 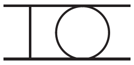 (D,s,t)

$-3\frac{(s+t)}{(D-5)(D-6)s^2t}\big[(7D^2-68D+164)s$

$+(3D-14)(3D-16)t\big]$ 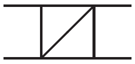 (D,s,t)

$-4\frac{(D-3)^2(2D-9)}{(D-4)^2(D-5)s^2}$ 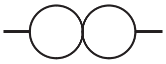 $(D,s) \; + \frac{3}{2}\frac{(D-3)(3D-10)}{(D-4)^2(D-5)^2(D-6)s^2t}$

$\times\big[8(D-4)(D-5)^2s + (-11D^3+158D^2-754D+1196)t\big]$ 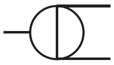 (D,s)

$+3\frac{(D-3)(3D-8)(3D-10)}{(D-4)^3(D-5)^2(D-6)s^3t}\big[(D-5)(7D^2-68D+164)s$

$+(23D^3-337D^2+1640D-2652)t\big]$ 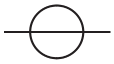 (D,s)

$+3\frac{(D-3)(3D-8)(3D-10)}{(D-4)^3(D-5)^2(D-6)s^2t^2}\big[(16D^3-229D^2+1088D-1716)s$

$+(D-5)(3D-14)(3D-16)t\big]$ 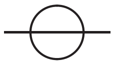 $(D,t)\;,$ (5.146)

The factors of $(D-4)$ in the denominators of the first two terms on the right hand side of eq. (5.146) are the ones which cause the problem.

To circumvent the problem we calculate the integral with the irreducible numerator directly from a Mellin-Barnes representation. It then can be used instead of the second master integral $\mathbf{PBOX_2}$ as a new master integral. We check our result in two different ways: firstly, by verifying that the new basis of master integrals satisfy a system of differential equations, and secondly, by using them to compute the integrals of the old basis in $D=6$ dimensions, both of which are finite, and comparing the result with a numerical integration.

5.9.2 Calculation by Mellin-Barnes contour integrals of a master integral

The analytic structure of the on-shell double box is rather simple, since it only depends on two scales, and its only thresholds are at $s=0$ and $t=0$. The main difficulty in calculating this diagram is to find a way to isolate its infrared and collinear divergences. For the analytical calculation it is convenient to use a Mellin-Barnes representation, which enables us to isolate the poles in ϵ in a very natural way.

We shall consider the following class of Feynman integrals

$$I^D(\nu_1,\nu_2,\nu_3,\nu_4,\nu_5,\nu_6,\nu_7,\nu_8;) = \int \frac{d^D k_1}{i\pi^{D/2}} \int \frac{d^D k_2}{i\pi^{D/2}} \frac{1}{A_1^{\nu_1} A_2^{\nu_2} A_3^{\nu_3} A_4^{\nu_4} A_5^{\nu_5} A_6^{\nu_6} A_7^{\nu_7} A_8^{\nu_8}}, \tag{5.147}$$

where we have kept the powers of the propagators arbitrary. At the end we will specialize at the values $\nu_1 = \ldots = \nu_7 = 1$ and $\nu_8 = -1$ corresponding to the tensor integral of Eq. (5.144).

We derive our Mellin-Barnes representation for the two-loop integrals (5.147) by doing the loop integrations one by one. In terms of Feynman parameters, the k_2-loop can be written as

$$\begin{aligned} \int \frac{d^D k_2}{i\pi^{D/2}} \frac{1}{A_4^{\nu_4} A_5^{\nu_5} A_6^{\nu_6} A_7^{\nu_7}} &= (-1)^{\nu_{4567}} \frac{\Gamma(\nu_{4567} - \frac{D}{2})}{\Gamma(\nu_4)\Gamma(\nu_5)\Gamma(\nu_6)\Gamma(\nu_7)} \\ &\times \int_0^\infty \prod_{j=4}^{7} \mathrm{d}x_j \, x_j^{\nu_j - 1} \delta(1 - x_4 - x_5 - x_6 - x_7) \, \mathcal{Q}^{\frac{D}{2} - \nu_{4567}}, \end{aligned} \tag{5.148}$$

where $\nu_{4567} = \nu_4 + \nu_5 + \nu_6 + \nu_7$ (similar abbreviations will be used below), and

$$\mathcal{Q} = -A_1 x_6 x_7 - A_3 x_4 x_7 - A_8 x_5 x_7 - s x_4 x_6. \tag{5.149}$$

By introducing three Mellin-Barnes parameters, α, β and τ, we split the polynomial $\mathcal{Q}$ into factors:

$$\begin{aligned} \Gamma(\nu_{4567} - D/2)\, \mathcal{Q}^{d/2 - \nu_{4567}} &= \int_{-i\infty}^{i\infty} \frac{\mathrm{d}\alpha \, \mathrm{d}\beta \, \mathrm{d}\tau}{(2\pi i)^3} (-A_1 x_6 x_7)^\alpha (-A_3 x_4 x_7)^\beta (-A_8 x_5 x_7)^\tau \\ &\times (-s x_4 x_6)^{\frac{D}{2} - \nu_{4567} - \alpha - \beta - \tau} \Gamma(-\alpha)\Gamma(-\beta)\Gamma(-\tau)\Gamma(\nu_{4567} - d/2 + \alpha + \beta + \tau). \end{aligned} \tag{5.150}$$

After inserting Eq. (5.150) into Eq. (5.148), we evaluate the Feynman parameter integrals in terms of Γ functions, which gives us the following Mellin-Barnes representation for the k_2-loop:

$$\int \frac{d^D k_2}{i\pi^{D/2}} \frac{1}{A_4^{\nu_4} A_5^{\nu_5} A_6^{\nu_6} A_7^{\nu_7}} = \frac{(-1)^{\nu_{4567}}}{\Gamma(\nu_4)\Gamma(\nu_5)\Gamma(\nu_6)\Gamma(\nu_7)}$$
$$\times \frac{1}{\Gamma(D-\nu_{4567})} \int\limits_{-i\infty}^{i\infty} \frac{\mathrm{d}\alpha\,\mathrm{d}\beta\,\mathrm{d}\tau}{(2\pi i)^3} (-A_1)^{\alpha}(-A_3)^{\beta}(-A_8)^{\tau}(-s)^{\frac{D}{2}-\nu_{4567}-\alpha-\beta-\tau}$$
$$\times \Gamma(-\alpha)\Gamma(-\beta)\Gamma(-\tau)\Gamma(\nu_{4567} - \frac{D}{2} + \alpha + \beta + \tau)$$
$$\times \Gamma(\frac{D}{2} - \nu_{567} - \alpha - \tau)\Gamma(\frac{D}{2} - \nu_{457} - \beta - \tau)\Gamma(\nu_5 + \tau)\Gamma(\nu_7 + \alpha + \beta + \tau). \tag{5.151}$$

When this result is inserted into (5.147), the remaining k_1-integral has the form of an on-shell massless one-loop box diagram with indices $\nu_1 - \alpha$, ν_2, $\nu_3 - \beta$, $\nu_8 - \tau$. We repeat the above steps for this k-integral, using a further Mellin-Barnes parameter, σ, and finally obtain

$$I(\nu_1, \nu_2, \nu_3, \nu_4, \nu_5, \nu_6, \nu_7, \nu_8; d) = \frac{(-1)^N}{\Gamma(\nu_2)\Gamma(\nu_4)\Gamma(\nu_5)\Gamma(\nu_6)\Gamma(\nu_7)\Gamma(D-\nu_{4567})} \frac{1}{(2\pi i)^4}$$
$$\times \int\limits_{-i\infty}^{i\infty} \mathrm{d}\alpha\,\mathrm{d}\beta\,\mathrm{d}\tau\,\mathrm{d}\sigma (-t)^{-\sigma}(-s)^{D-N+\sigma} \frac{\Gamma(-\alpha)\Gamma(-\beta)\Gamma(-\tau)\Gamma(\nu_{4567} - \frac{D}{2} + \alpha + \beta + \tau)}{\Gamma(\nu_1 - \alpha)\Gamma(\nu_3 - \beta)\Gamma(\nu_8 - \tau)}$$
$$\times \frac{\Gamma(\sigma)\Gamma(\nu_{1238} - \frac{D}{2} - \alpha - \beta - \tau - \sigma)}{\Gamma(D - \nu_{1238} + \alpha + \beta + \tau)} \Gamma(\frac{D}{2} - \nu_{567} - \alpha - \tau)\Gamma(\frac{D}{2} - \nu_{457} - \beta - \tau)$$
$$\times \Gamma(\nu_5 + \tau)\Gamma(\nu_7 + \alpha + \beta + \tau)\Gamma(\frac{D}{2} - \nu_{128} + \alpha + \tau + \sigma)\Gamma(\nu_8 - \tau - \sigma)$$
$$\times \Gamma(\frac{D}{2} - \nu_{238} + \beta + \tau + \sigma)\Gamma(\nu_2 - \sigma). \tag{5.152}$$

In deriving this formula, we have assumed that the various parameters are such, that all the manipulations we performed are justified. This is certainly true if we are able to find a set of straight lines, parallel to the imaginary axis, for the integration variables α, β, σ, and τ, such that the arguments of all the Γ functions in it have positive real parts. We then define the integrals (5.147) for values of the parameters where such contours do not exist by analytic continuation.

Let us now consider the case with the irreducible numerator,

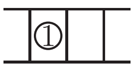 $(s,t) = I^{4-2\epsilon}(1,1,1,1,1,1,1,-1).$

On the one hand, from the definition (5.144), $\nu_5 + \nu_8 = 1 - 1 = 0$. On the other hand, if the real parts of the arguments of all gamma functions are positive, then in particular $Re(\nu_5 + \tau)$, $Re(\sigma)$ and $Re(\nu_8 - \tau - \sigma)$ are positive, and therefore $Re(\nu_5+\nu_8) > 0$. Since this does not depend on D, it means that in order to calculate the integral using the Mellin-Barnes representation (5.152), we must perform an analytic continuation not only in D, but also in ν_5 or ν_8. We choose ν_8. Setting $\nu_8 = -1 + \eta$ and all other ν's equal to one, we get

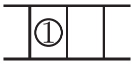

$$
\begin{aligned}
(s,t) \;&=\; \lim_{\eta\downarrow 0} I^{4-2\epsilon}(1,1,1,1,1,1,-1+\eta) = \\
&\frac{1}{\Gamma(-2\epsilon)} \lim_{\eta\downarrow 0} \frac{1}{(2\pi i)^4} \int_{-i\infty}^{i\infty} d\alpha\, d\beta\, d\tau\, d\sigma (-t)^{-\sigma} (-s)^{-2-\eta-2\epsilon+\sigma}\, \Gamma(\sigma)\Gamma(1-\sigma) \\
&\times \frac{\Gamma(-\alpha)\Gamma(-\beta)\Gamma(-\tau)\Gamma(1+\tau)\Gamma(-1+\eta-\tau-\sigma)}{\Gamma(1-\alpha)\Gamma(1-\beta)\Gamma(-1+\eta-\tau)} \Gamma(1-\eta-\epsilon+\alpha+\tau+\sigma) \\
&\times \frac{\Gamma(1+\alpha+\beta+\tau)\Gamma(2+\epsilon+\alpha+\beta+\tau)}{\Gamma(2-\eta-2\epsilon+\alpha+\beta+\tau)} \Gamma(-1-\epsilon-\beta-\tau) \\
&\times \Gamma(\eta+\epsilon-\alpha-\beta-\tau-\sigma).\Gamma(1-\eta-\epsilon+\beta+\tau+\sigma) \\
&\times \Gamma(-1-\epsilon-\alpha-\tau)
\end{aligned} \tag{5.153}
$$

We can make the real parts of the arguments of all *Gamma* functions in Eq. 5.153 positive by picking, for example, $\eta = 12y$ and $\epsilon = -12y$, where y is some positive number much smaller than one, and choosing contours for the Mellin-Barnes variables defined by: $Re(\alpha) = Re(\beta) = -y$, $Re(\tau) = -1 + 4y$ and $Re(\sigma) = 4y$.

Starting from these values, we first perform an analytic continuation in η to $\eta = 0$, keeping ϵ fixed, and then another one in ϵ to the vicinity of $\epsilon = 0$. The procedure for both continuations is straightforward: keeping the integration contours fixed, we simply have to keep track of the poles of the Γ functions, and whenever one of them crosses an integration contour, add its residue to a list of terms that will contribute to the final answer. For example, with the above choice of contours, the first crossing happens at $\eta = 8y$, when the pole at $\tau = -1 + \eta - \sigma$ crosses the τ-contour. After taking a residue in one integration variable, we continue to follow the poles in the remaining variables, building up a tree of single and multiple residue terms. By this procedure, poles in ϵ are automatically expressed through singular Γ functions multiplying integrals that can safely be expanded under the integral sign.

To $\mathcal{O}(\epsilon^0)$, it turns out that, along with terms where there is no integral left, only single and two-fold integrals contribute, because terms with more integrals are killed by the factor $1/\Gamma(-2\epsilon)$ in Eq. (5.153). In the two-fold integrals, one integration can be done by Barnes's first lemma. The single integrals that are left can all be calculated by closing the contour and summing harmonic series. In the kinematic region $s, t < 0$ the integral has no imaginary part and we find the following result:

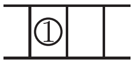

$$
\begin{aligned}
(s,t) \quad = \quad & \frac{\Gamma(1+\epsilon)^2}{s^2(-s)^{2\epsilon}} \left\{ \frac{9}{4\,\epsilon^4} - \frac{2}{\epsilon^3}\ell - \frac{7\pi^2}{3\,\epsilon^2} \right. \\
& + \frac{1}{\epsilon}\left[\frac{4}{3}\ell^3 + \frac{14}{3}\pi^2\ell - 4\left(\ell^2+\pi^2\right)L + 8\,\mathrm{Li}_3\left(-t/s\right) - 8\,\ell\,\mathrm{Li}_2\left(-t/s\right) - 16\,\zeta(3)\right] \\
& - \frac{4}{3}\ell^4 - \frac{13}{3}\pi^2\ell^2 + \left(\frac{16}{3}\ell^3 + \frac{26}{3}\pi^2\ell\right)L - 5\left(\ell^2+\pi^2\right)L^2 \\
& + \left(6\,\ell^2 - 20\,\ell L - \frac{4}{3}\pi^2\right)\mathrm{Li}_2\left(-t/s\right) + \left(8\,\ell + 20L\right)\mathrm{Li}_3\left(-t/s\right) \\
& \left. + 20\,\mathrm{S}_{2,2}\left(-t/s\right) - 20\,\ell\,\mathrm{S}_{1,2}\left(-t/s\right) - 28\,\mathrm{Li}_4\left(-t/s\right) + \left(28\,\ell - 20L\right)\zeta(3) - \frac{7\pi^4}{45} \right\},
\end{aligned}
\tag{5.154}
$$

with $\ell = \log(t/s)$ and $L = \log(1 + t/s)$. Expressions in other kinematic regions can be obtained with the analytic continuations described in Section 5.8.3.

5.9.3 Differential equations for double-box master integrals

It is possible to construct a system of differential equations satisfied by the double box master integrals. In terms of the new basis, these differential equations are :

$\frac{\partial}{\partial t}$ 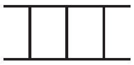 $(D,s,t) \quad = \quad \frac{[(D-5)s-t}{(s+t)t}$ 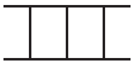 (D,s,t)

$+\frac{(D-4)}{(s+t)t}$ 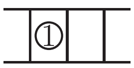 $(D,s,t) \quad -6\frac{(D-4)}{st^2}$ 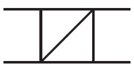 (D,s,t)

$+12\frac{(D-3)}{(s+t)t^2}$  $(D,s,t) \quad +4\frac{(D-3)^2}{(D-4)s^2t(s+t)}$ 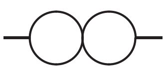 (D,s)

$+3\frac{(D-3)(3D-10)(2s+t)}{(D-4)s^2t^2(s+t)}$ 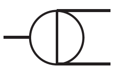 (D,s)

$+6\frac{(D-3)(3D-8)(3D-10)(s-t)}{(D-4)^2s^3t^2(s+t)}$ 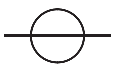 (D,s)

$+6\frac{(D-3)(3D-8)(3D-10)}{(D-4)^2st^3(s+t)}$ 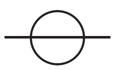 (D,t) (5.155)

$\frac{\partial}{\partial t}$ 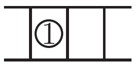 $(D,s,t) \quad = \quad -\frac{1}{2}\frac{(D-4)s}{(s+t)t}$ 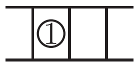 (D,s,t)

$+\frac{1}{2}\frac{(D-4)s}{s+t}$ 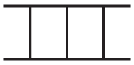 $(D,s,t) \quad -9\frac{(D-4)}{st}$ 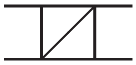 (D,s,t)

$+12\frac{(D-3)}{(s+t)t}$ 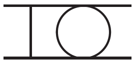 $(D,s,t) \quad +2\frac{(D-3)^2(s+2t)}{(D-4)s^2t(s+t)}$ 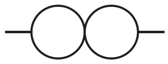 (D,s)

$+\frac{15}{2}\frac{(D-3)(3D-10)}{(D-4)st(s+t)}$ 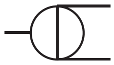 (D,s)

$+6\frac{(D-3)(3D-8)(3D-10)}{(D-4)^2s^2t(s+t)}$ 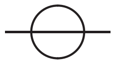 (D,s)

$+9\frac{(D-3)(3D-8)(3D-10)}{(D-4)^2st^2(s+t)}$ 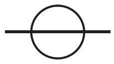 (D,t) (5.156)

Expanding eqs. (5.155,5.156) in ϵ, and inserting the expansion of $\mathbf{PBOX_1}$ from ref. [21], of the pinched diagrams from previous sections, and the result of Eq. (5.154) for $\mathbf{PBOX_3}$ we find that they are indeed satisfied.

Inspecting the right hand sides of the differential equations, one notices that in Eq. (5.155), the coefficient of $\mathbf{PBOX_3}$, and in Eq. (5.156), those of $\mathbf{PBOX_1}$ and $\mathbf{PBOX_3}$, are all proportional to $D-4$. This means that, if $\mathbf{PBOX_1}$ is known to $\mathcal{O}(\epsilon^0)$, the $\mathcal{O}(\epsilon^0)$ part of $\mathbf{PBOX_3}$ is, a priori, only determined by the system of equations up to a t-independent constant.

One also observes that the system of differential equations has a singular point at $s+t=0$. This corresponds to the special kinematic configuration where $p_1+p_3=0$. At this point, the numerator of $\mathbf{PBOX_3}$ becomes reducible:

$$\begin{aligned} A_8 &= (k+p_1+p_2+p_3)^2 \\ &= (k+p_2)^2 = P_1 - P_2 + P_3 - s, \end{aligned} \tag{5.157}$$

so

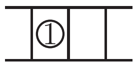 (s,t)

collapses to a linear combination of $\mathbf{PBOX_1}$ and pinched diagrams. This singular point can be used for the calculation of the t-independent constant. In this way Gehrmann and Remiddi [26] calculated an equivalent combination to $\mathbf{PBOX_3}$ of the $\mathbf{PBOX_1}$ and $\mathbf{PBOX_2}$ master integrals, which is in agreement with the result of Eq. (5.154).

5.9.4 Master integrals in D=6 dimensions

The master integrals $\mathbf{PBOX_1}$ and $\mathbf{PBOX_2}$ are both finite in $D = 6$ dimensions. This can be deduced from power counting considerations in momentum space; it is also easy to see by examining the arguments of the Γ functions in the Mellin-Barnes representation (5.152). With the dimensional shift equations that can be derived from the Schwinger parametric form of the integrals and the IBP algorithm to reduce the extra powers of propagators, we relate these master integrals in $D = 6 - 2\epsilon$ dimensions to master integrals of the new basis in $D = 4 - 2\epsilon$ dimensions. Substituting ϵ-expansions for the latter, we find that all pole terms indeed cancel, and the finite parts are

$$\mathbf{PBOX_1}^{D=6} = \left\{ \frac{a_1}{(s+t)} + \frac{b}{t} \right\}, \tag{5.158}$$

$$\mathbf{PBOX_2}^{D=6} = \left\{ \frac{a_2}{s(s+t)} + \frac{b}{s\,t} \right\}, \tag{5.159}$$

where

$$a_1 = t\,\frac{\partial a_2}{\partial t} - 6\,\zeta(3), \tag{5.160}$$

while

$$a_2 = \frac{\pi^4}{10} + 6\,\mathrm{Li}_4\,(-t/s) + \left(\ell^2 + \pi^2\right)\,\mathrm{Li}_2\,(-t/s) + 4\,\ell\,(\zeta(3) - \mathrm{Li}_3\,(-t/s)) + \frac{\pi^2}{6}\ell^2, \tag{5.161}$$

and

$$\begin{aligned} b = {} & \left(2\,\zeta(3) - 2\,\mathrm{Li}_3\,(-t/s) - \frac{\pi^2}{3}\ell\right) L + \frac{1}{2}(\ell^2 + \pi^2)L^2 + \left(2\,\ell\,L - \frac{\pi^2}{3}\right)\,\mathrm{Li}_2\,(-t/s) \\ & + 2\,\ell\,\mathrm{S}_{1,2}\,(-t/s) - 2\,\mathrm{S}_{2,2}\,(-t/s)\,. \end{aligned} \tag{5.162}$$

The Feynman representations of the $\mathbf{PBOX_1}$ and $\mathbf{PBOX_2}$ master integrals in six dimensions are finite and can be calculated numerically. We have tested that the numerical results are in agreement with the expressions of this section.

We note that this set of master integrals has been used by Bern, Dixon and Ghinculov for the calculation of the two-loop corrections to Bhabha scattering [19].

5.10 Synopsis: The Master Integrals

Here we summarize the operational procedure for the calculation of the scalar and tensor one and two-loop Feynman integrals appearing in 2→2 massless QCD scattering.

- **Tensor Reduction:** From their Schwinger representation, tensor integrals are related to scalar integrals of the same topology with extra powers of propagators and higher dimension.

- **Reduction Algorithm:** IBP and LI recursive identities reduce all one and two-loop topologies encountered in 2→2 massless QCD scattering to master integrals.

- **Master integrals:**

  We find the following master integrals

  - The box in six dimensions and the bubble master integrals for the one loop topologies

    $\mathbf{BOX^6}(s,t) =$ 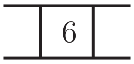 (s,t), $\mathbf{BUB}(s) =$ 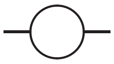 (s) ,

  - The two master cross-box integrals

    $\mathbf{XBOX_1}(s,t) =$ 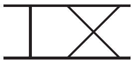 (s,t), $\mathbf{XBOX_2}(s,t) =$ 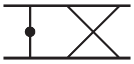 (s,t)

  - The two master double-box integrals

    $\mathbf{PBOX_1}(s,t) =$ 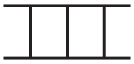 (s,t), $\mathbf{PBOX_3}(s,t) =$ 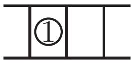 (s,t)

  - The cross-triangle master integral

    $\mathbf{XTRI}(s) =$ 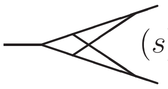 (s)

  - The diagonal-box and the bubble-box master integrals

    $\mathbf{CBOX}(s,t) =$ 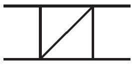 (s,t), $\mathbf{ABOX}(s,t) =$ 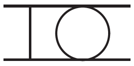 (s,t)

  - The sunset and Tri master integrals

    $\mathbf{SUNSET}(s) =$ 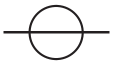 (s) , $\mathbf{TRI}(s) =$ 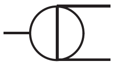 (s)

  The analytic expansions in ϵ of the master integrals are all calculated, therefore we can continue with the main task of evaluating matrix elements at NNLO.

Chapter 6

NNLO virtual corrections for quark scattering

In hadron-hadron collisions, the most basic hard process is parton-parton scattering to form a large transverse momentum jet. The single jet inclusive transverse energy distribution observed at the TEVATRON and CERN S$p\bar{p}$S shows good agreement with theoretical next-to-leading order $\mathcal{O}(\alpha_s^3)$ perturbative predictions over a wide range of jet transverse energies and tests the point-like nature of the partons down to distance scales of 10^{-17} m. However, data collected in Run I by the CDF collaboration at the TEVATRON indicated possible new physics at large transverse energy [61]. Data obtained by the D0 collaboration [62] was more consistent with next-to-leading order expectations. However, because of both theoretical and experimental uncertainties no definite conclusion could be drawn. The experimental situation may be clarified in the forthcoming Run II starting in 2001 where increased statistics and improved detectors may lead to a reduction in both the statistical and systematic errors.

The theoretical prediction may be improved by including the next-to-next-to-leading order perturbative predictions. This has the effect of (a) reducing the renormalisation scale dependence and (b) improving the matching of the parton level theoretical jet algorithm with the hadron level experimental jet algorithm because the jet structure can be modeled by the presence of a third parton. Varying the renormalisation scale up and down by a factor of two about the jet transverse energy leads to a 20% (10%) renormalisation scale uncertainty at leading order (next-to-leading order) for jets with $E_T \sim 100$ GeV. The improvement in accuracy expected at next-to-next-to-leading order can be estimated using the renormalisation group equations together with the known leading and next-to-leading order coefficients and is at the 1-2% level.

The full next-to-next-to-leading order prediction requires a knowledge of the two-loop 2→2 matrix elements as well as the contributions from the one-loop 2→3 and tree-level 2→4 processes. Helicity amplitudes for the one-loop 2→3 parton sub-processes $gg \to ggg$, $\bar{q}q \to ggg$, $\bar{q}q \to \bar{q}'q'g$, and processes related to these by crossing symmetry, have been computed in [63, 64, 65] respectively. The amplitudes for the six gluon $gg \to gggg$, four gluon-two quark $\bar{q}q \to gggg$, two gluon-four quark $\bar{q}q \to \bar{q}'q'gg$ and six quark $\bar{q}q \to \bar{q}'q'\bar{q}''q''$ 2→4 processes and the associated crossed processes computed at tree-level are also known and are available in [66, 67, 68, 69, 70, 71, 72, 73].

The calculation of the two-loop amplitudes for the 2→2 scattering processes

$$q + \bar{q} \to q' + \bar{q}' \tag{6.1}$$

$$q + \bar{q} \to q + \bar{q}, \tag{6.2}$$

$$q + \bar{q} \to g + g, \tag{6.3}$$

$$g + g \to g + g, \tag{6.4}$$

has proved more intractable due mainly to the difficulty of evaluating the planar and non-planar two-loop graphs. This issue has been completely resolved with the techniques described in previous chapters and generic two-loop massless 2→2 processes can in principle be expressed in terms of the two-loop master integrals of Section 5.10.

The first to address such a calculation were Bern, Dixon and Kosower [74] with the maximal helicity violating two loop amplitude for $gg \to gg$[1]. The whole set of NNLO virtual corrections for the processes (6.1)- (6.4) were presented in references [4, 3, 2, 1, 5]. Bern, Dixon and Ghinculov [19] have recently completed the first full two-loop calculation of physical 2→2 scattering amplitudes, the QED processes $e^+e^- \to \mu^+\mu^-$ and $e^+e^- \to e^-e^+$.

[1]This amplitude vanishes at tree level and does therefore not contribute to 2→2 scattering at next-to-next-to-leading order $\mathcal{O}(\alpha_s^4)$.

In this chapter we present dimensionally regularized and renormalized analytic expressions for the NNLO matrix elements of the quark scattering processes (6.1)-(6.2). As is common in QCD calculations, we use the $\overline{\mathrm{MS}}$ renormalisation scheme and conventional dimensional regularisation where all external particles are treated in D dimensions. There is an overlap between the QED calculation of [19] and the QCD results presented here and we expect that the analytic expressions presented here will therefore provide a useful check of some of their results.

Catani has described the pole structure of generic renormalised two-loop amplitudes [17] and we use his techniques to isolate the poles in the $\overline{\mathrm{MS}}$ scheme. We find that the pole structure expected in the $\overline{\mathrm{MS}}$ scheme on general grounds is indeed reproduced by direct evaluation of the Feynman diagrams. Ultimately these poles must be canceled by infrared singularities from tree level $2\to4$ and one-loop $2\to3$ processes.

6.1 Notation

We consider the unlike-quark scattering process

$$q(p_1) + \bar{q}(p_2) + q'(p_3) + \bar{q}'(p_4)\to 0, \tag{6.5}$$

and the like-quark scattering process

$$q(p_1) + \bar{q}(p_2) + q(p_3) + \bar{q}(p_4)\to 0, \tag{6.6}$$

where particles are incoming and carry light-like momenta (shown in parentheses). Their total momentum is conserved, satisfying

$$p_1^\mu + p_2^\mu + p_3^\mu + p_4^\mu = 0,$$

and the associated Mandelstam variables are given by

$$s = (p_1+p_2)^2, \qquad t = (p_2+p_3)^2, \qquad u = (p_1+p_3)^2. \tag{6.7}$$

We use conventional dimensional regularisation and treat the external quark states in D space-time dimensions and renormalise the ultraviolet divergences in the $\overline{\mathrm{MS}}$

scheme. The bare coupling α_0 is related to the running coupling $\alpha_s \equiv \alpha_s(\mu^2)$, at renormalisation scale μ, by

$$\alpha_0 \, S_\epsilon = \alpha_s \left[1 - \frac{\beta_0}{\epsilon}\left(\frac{\alpha_s}{2\pi}\right) + \left(\frac{\beta_0^2}{\epsilon^2} - \frac{\beta_1}{2\epsilon}\right)\left(\frac{\alpha_s}{2\pi}\right)^2 + \mathcal{O}(\alpha_s^3)\right], \tag{6.8}$$

where

$$S_\epsilon = (4\pi)^\epsilon e^{-\epsilon\gamma}, \qquad \gamma = 0.5772\ldots = \text{Euler constant}, \tag{6.9}$$

is the typical phase-space volume factor in $D = 4 - 2\epsilon$ dimensions. As usual, the first two coefficients of the QCD beta function, β_0 and β_1 for N_F (massless) quark flavours are

$$\beta_0 = \frac{11 C_A - 4 T_R \, N_F}{6}, \qquad \beta_1 = \frac{17 C_A^2 - 10 C_A T_R \, N_F - 6 C_F T_R \, N_F}{6}. \tag{6.10}$$

where N is the number of colours, and

$$C_F = \frac{N^2-1}{2N}, \qquad C_A = N, \qquad T_R = \frac{1}{2}. \tag{6.11}$$

The renormalised amplitude for the unlike-quark process is given by

$$|\mathcal{M}\rangle_{unlike} = 4\pi\alpha_s \left[|\mathcal{M}^{(0)}\rangle + \left(\frac{\alpha_s}{2\pi}\right)|\mathcal{M}^{(1)}\rangle + \left(\frac{\alpha_s}{2\pi}\right)^2 |\mathcal{M}^{(2)}\rangle + \mathcal{O}\left(\alpha_s^3\right)\right], \tag{6.12}$$

with $|\mathcal{M}^{(i)}\rangle$ representing the i-loop amplitude in colour-space. For the like-quark scattering we have the related expression

$$\begin{aligned} |\mathcal{M}\rangle_{like} \;=\; 4\pi\alpha_s \Bigg[& \left(|\mathcal{M}^{(0)}\rangle - |\overline{\mathcal{M}}^{(0)}\rangle\right) + \left(\frac{\alpha_s}{2\pi}\right)\left(|\mathcal{M}^{(1)}\rangle - |\overline{\mathcal{M}}^{(1)}\rangle\right) \\ & + \left(\frac{\alpha_s}{2\pi}\right)^2 \left(|\mathcal{M}^{(2)}\rangle - |\overline{\mathcal{M}}^{(2)}\rangle\right) + \mathcal{O}(\alpha_s^3)\Bigg]. \end{aligned} \tag{6.13}$$

Here $|\overline{\mathcal{M}}^{(i)}\rangle$ describes the t-channel graphs which can be obtained from the s-channel diagrams by exchanging the roles of particles 2 and 4

$$|\overline{\mathcal{M}}^{(i)}\rangle = |\mathcal{M}^{(i)}\rangle(2 \leftrightarrow 4). \tag{6.14}$$

Both $|\mathcal{M}^{(i)}\rangle$ and $|\overline{\mathcal{M}}^{(i)}\rangle$ are renormalisation scale and renormalisation scheme dependent.

In squaring the amplitudes and summing over colours and spins we find two types of terms,

- the self-interference of the graphs in a single channel, described by the function $\mathcal{A}(s,t,u)$ for the s-channel and $\mathcal{A}(t,s,u)$ for the t-channel, and
- the interference of the s-channel graphs with the t-channel graphs, described by the function $\mathcal{B}(s,t,u)$.

Thus, for distinct quark scattering we have

$$\langle\mathcal{M}|\mathcal{M}\rangle_{unlike} = \sum |\mathcal{M}(q+\bar{q}\to\bar{q}'+q')|^2 = \mathcal{A}(s,t,u), \tag{6.15}$$

while for identical quarks

$$\begin{aligned}\langle\mathcal{M}|\mathcal{M}\rangle_{like} &= \sum |\mathcal{M}(q+\bar{q}\to\bar{q}+q)|^2 \\ &= \mathcal{A}(s,t,u)+\mathcal{A}(t,s,u)+\mathcal{B}(s,t,u).\end{aligned} \tag{6.16}$$

Similarly, for the crossed and time-reversed processes we obtain

$$\sum |\mathcal{M}(q+q'\to q+q')|^2 = \mathcal{A}(u,t,s) \tag{6.17}$$
$$\sum |\mathcal{M}(q+\bar{q}'\to q+\bar{q}')|^2 = \mathcal{A}(t,s,u) \tag{6.18}$$
$$\sum |\mathcal{M}(\bar{q}+\bar{q}'\to \bar{q}+\bar{q}')|^2 = \mathcal{A}(u,t,s) \tag{6.19}$$
$$\sum |\mathcal{M}(q+\ q\to q+\ q)|^2 = \mathcal{A}(u,t,s)+\mathcal{A}(t,u,s)+\mathcal{B}(u,t,s). \tag{6.20}$$

The function $\mathcal{A}$ can be expanded perturbatively to yield

$$\mathcal{A}(s,t,u) = 16\pi^2\alpha_s^2\left[\mathcal{A}^4(s,t,u)+\left(\frac{\alpha_s}{2\pi}\right)\mathcal{A}^6(s,t,u)+\left(\frac{\alpha_s}{2\pi}\right)^2\mathcal{A}^8(s,t,u)+\mathcal{O}(\alpha_s^3)\right], \tag{6.21}$$

where

$$\mathcal{A}^4(s,t,u) = \langle\mathcal{M}^{(0)}|\mathcal{M}^{(0)}\rangle \equiv 2(N^2-1)\left(\frac{t^2+u^2}{s^2}-\epsilon\right), \tag{6.22}$$
$$\mathcal{A}^6(s,t,u) = \left(\langle\mathcal{M}^{(0)}|\mathcal{M}^{(1)}\rangle+\langle\mathcal{M}^{(1)}|\mathcal{M}^{(0)}\rangle\right), \tag{6.23}$$
$$\mathcal{A}^8(s,t,u) = \left(\langle\mathcal{M}^{(1)}|\mathcal{M}^{(1)}\rangle+\langle\mathcal{M}^{(0)}|\mathcal{M}^{(2)}\rangle+\langle\mathcal{M}^{(2)}|\mathcal{M}^{(0)}\rangle\right). \tag{6.24}$$

In the same manner

$$\mathcal{B}(s,t,u) = 16\pi^2\alpha_s^2\left[\mathcal{B}^4(s,t,u)+\left(\frac{\alpha_s}{2\pi}\right)\mathcal{B}^6(s,t,u)+\left(\frac{\alpha_s}{2\pi}\right)^2\mathcal{B}^8(s,t,u)+\mathcal{O}(\alpha_s^3)\right], \tag{6.25}$$

where, in terms of the amplitudes, we have

$$\begin{aligned}
\mathcal{B}^4(s,t,u) &= -\left(\langle\overline{\mathcal{M}}^{(0)}|\mathcal{M}^{(0)}\rangle + \langle\mathcal{M}^{(0)}|\overline{\mathcal{M}}^{(0)}\rangle\right) \\
&\equiv -4\left(\frac{N^2-1}{N}\right)(1-\epsilon)\left(\frac{u^2}{st}+\epsilon\right), \qquad (6.26) \\
\mathcal{B}^6(s,t,u) &= -\left(\langle\overline{\mathcal{M}}^{(1)}|\mathcal{M}^{(0)}\rangle + \langle\mathcal{M}^{(0)}|\overline{\mathcal{M}}^{(1)}\rangle + \langle\overline{\mathcal{M}}^{(0)}|\mathcal{M}^{(1)}\rangle + \langle\mathcal{M}^{(1)}|\overline{\mathcal{M}}^{(0)}\rangle\right) \\
& \qquad (6.27) \\
\mathcal{B}^8(s,t,u) &= -\left(\langle\overline{\mathcal{M}}^{(1)}|\mathcal{M}^{(1)}\rangle + \langle\mathcal{M}^{(1)}|\overline{\mathcal{M}}^{(1)}\rangle\right. \\
&\quad \left.+\langle\overline{\mathcal{M}}^{(0)}|\mathcal{M}^{(2)}\rangle + \langle\mathcal{M}^{(2)}|\overline{\mathcal{M}}^{(0)}\rangle + \langle\mathcal{M}^{(0)}|\overline{\mathcal{M}}^{(2)}\rangle + \langle\overline{\mathcal{M}}^{(2)}|\mathcal{M}^{(0)}\rangle\right). \\
& \qquad (6.28)
\end{aligned}$$

Expressions for $\mathcal{A}^6$ and $\mathcal{B}^6$, valid in dimensional regularisation, are given in Ref. [75]. The main goal of this thesis is to give analytic expressions for the functions $\mathcal{A}^8$ and $\mathcal{B}^8$. We first concentrate on the contributions to both $\mathcal{A}^8$ and $\mathcal{B}^8$ due to the interference of one-loop amplitudes with one-loop amplitudes, namely

$$\mathcal{A}^{8\,(1\times1)}(s,t,u) = \langle\mathcal{M}^{(1)}|\mathcal{M}^{(1)}\rangle, \qquad (6.29)$$

and

$$\mathcal{B}^{8\,(1\times1)}(s,t,u) = -\left(\langle\overline{\mathcal{M}}^{(1)}|\mathcal{M}^{(1)}\rangle + \langle\mathcal{M}^{(1)}|\overline{\mathcal{M}}^{(1)}\rangle\right). \qquad (6.30)$$

Even though they are simpler to evaluate than the two loop graphs, they form a vital part of the NNLO virtual corrections. One-loop helicity amplitudes for the $2 \to 2$ quark scattering processes were given in Ref. [76] as truncated expansions in ϵ including their finite part. However, this is only sufficient to obtain the pole structure of $\mathcal{A}^{8\,(1\times1)}$ and $\mathcal{B}^{8\,(1\times1)}$ up to $1/\epsilon^2$. To determine the $1/\epsilon$ and finite parts requires knowledge of the one-loop amplitude through to $\mathcal{O}(\epsilon^2)$.

Next, we give the analytical formulae for the two-loop contribution to $\mathcal{A}^8$

$$\mathcal{A}^{8\,(2\times0)}(s,t,u) = \langle\mathcal{M}^{(0)}|\mathcal{M}^{(2)}\rangle + \langle\mathcal{M}^{(2)}|\mathcal{M}^{(0)}\rangle$$

and $\mathcal{B}^8$

$$\mathcal{B}^{8\,(2\times0)}(s,t,u) = \langle\overline{\mathcal{M}}^{(0)}|\mathcal{M}^{(2)}\rangle + \langle\mathcal{M}^{(2)}|\overline{\mathcal{M}}^{(0)}\rangle + \langle\mathcal{M}^{(0)}|\overline{\mathcal{M}}^{(2)}\rangle + \langle\overline{\mathcal{M}}^{(2)}|\mathcal{M}^{(0)}\rangle$$

which they consistute the core of our calculations.

6.2 Method

As shown in Chapter 5, massless two-loop integrals for 2→2 scattering can be described in terms of a basis set of scalar *master* integrals. The simpler massless master integrals comprise the trivial topologies of single scale integrals which can be written as products of Gamma functions:

Sunset(s) = 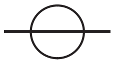 (s)

Glass(s) = 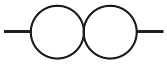 (s)

Tri(s) = 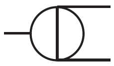 (s)

the less trivial non-planar triangle graph [35, 36],

Xtri(s) = 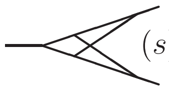 (s)

and two scale integrals that are related to the one-loop box graphs [77, 78],

Abox(s,t) = $e^{2\gamma\epsilon}$ 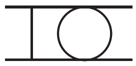 (s,t)

Cbox(s,t) = 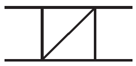 (s,t).

The planar double box and non-planar double box

Pbox$_1(s,t)$ = 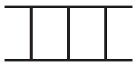 (s,t)

Xbox$_1(s,t)$ = 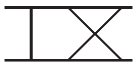 (s,t)

involve multiple Mellin-Barnes integrals and are much more complicated to evaluate as series expansions in ϵ. Expressions for these integrals valid through to $\mathcal{O}(\epsilon^0)$ are given in [21] and [22] respectively.

It turns out that for the two latter topologies, integrals involving loop momenta in the numerator cannot be entirely reduced in terms of the simpler integrals mentioned above and an additional master integral is required in each case. Reference [58] describes the procedure for reducing the tensor integrals down to a basis involving the planar box integral

Pbox$_2(s,t)$ = 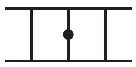 (s,t), where the blob on the middle propagator represents an additional power of that propagator, and provides a series expansion for Pbox_2 to $\mathcal{O}(\epsilon^0)$. However, as was pointed out in [60], knowledge of Pbox_1 and Pbox_2 to $\mathcal{O}(\epsilon^0)$ is not sufficient to determine all tensor loop integrals to the same order. A better basis involves the tensor integral,

$\mathrm{Pbox}_3(s,t) =$ 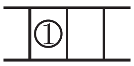 $(s,t),$

where ① represents the planar box integral with one irreducible numerator associated with the left loop. Symmetry of the integral ensures that,

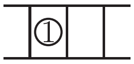 $(s,t) \equiv$ 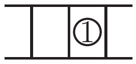 $(s,t).$

Series expansions for Pbox_3 are relatively compact and straightforward to obtain and are detailed in [79, 26]. Pbox_2 can therefore be eliminated in favor of Pbox_3. We note that this choice is not unique. Bern et al. [19] choose to use the Pbox_1 and Pbox_2 basis, but with the integrals evaluated in $D = 6 - 2\epsilon$ dimensions where they are both infrared and ultraviolet finite.

Similarly, the tensor reduction of the non-planar box integrals [78] also requires a second master integral,

$\mathrm{Xbox}_2(s,t) =$ 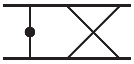 $(s,t),$

where the blob again denotes an additional power of the propagator. For the non-planar graphs there are no complications as in the planar case and all tensors to $\mathcal{O}(\epsilon^0)$ may be described in terms of the series expansions of Xbox_1 and Xbox_2 through to $\mathcal{O}(\epsilon^0)$ [79, 78].

In general tensor integrals are associated with scalar integrals in higher dimension and with higher powers of propagators. This connection can straightforwardly be achieved using the Schwinger parameter form of the integral [80] and the explicit expressions for generic two-loop integrals with up to four powers of loop momenta in the numerator are presented in Chapter 3[2]. Systematic application of the integration-by-parts (IBP) identities [57, 56] and Lorentz invariance (LI) identities [25] is sufficient to reduce these higher-dimension, higher-power integrals to master

[2]A method to reduce tensor integrals constructing differential operators that change the powers of the propagators as well as the dimension of the integral was presented in Ref. [34].

integrals in $D = 4 - 2\epsilon$. Some topologies that occur in Feynman diagrams such as the pentabox [80] are immediately simplified using the IBP identities and collapse to combinations of master integrals. However, the tensor integrals directly associated with the master integrals usually require more care. Explicit identities relevant for the tensor integrals of the Abox and Cbox topologies [80], for Pbox_1 and Pbox_2 integrals [58] and for the Xtri, Xbox_1 and Xbox_2 integrals [78] needed to be worked out. Using these identities, we have constructed MAPLE and FORM programs to rewrite two-loop tensor integrals for massless 2→2 scattering directly in terms of the basis set of master integrals.

The one-loop integrals are much easier to solve. There are only two master integrals, the scalar bubble graph,

$$\mathrm{Bub}(s) = e^{\gamma\epsilon}$$ 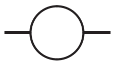 $$(s) \quad ,$$

and the one-loop scalar box graph,

$$\mathrm{Box}(s,t) = e^{\gamma\epsilon}$$ 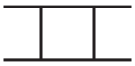 $$(s,t).$$

where we redefined the one-loop master integrals of Chapter 5 with a multiplicative factor $e^{\gamma\epsilon}$ for convenience in renormalising with the $\overline{\mathrm{MS}}$ scheme. We treat the tensor integrals in the same way as the two-loop integrals: shifting both dimension and powers of propagators and then using IBP to rewrite the integrals as combinations of Bub and Box. We note that this is not a unique choice for the master integrals. The one-loop bubble graph is proportional to the one-loop triangle graph with one off-shell leg. Another common choice is to replace the one-loop box in $D = 4 - 2\epsilon$ by the finite one-loop box in $D = 6 - 2\epsilon$, Box^6.

The general procedure for computing the two-loop amplitudes is therefore as follows. First the two-loop Feynman diagrams are generated using `QGRAF` [81]. We then project by tree level, perform the summation over colours and spins and trace over the Dirac matrices in D dimensions using conventional dimensional regularisation. It is then straightforward to identify the scalar and tensor integrals present and replace them with combinations of master integrals using the tensor reduction of two-loop integrals. The final result is a combination of master integrals in $D = 4-2\epsilon$ which can be substituted for the expansions in ϵ. For the interference of one-loop amplitudes with one-loop amplitudes we have a slightly different approach since we first calculate the tensor and scalar integrals of the amplitudes in terms of the one-loop master integrals and then we contract with each other performing the spin and color traces.

6.3 One-loop contributions for unlike-quark scattering

We first present the one-loop contributions to the NNLO virtual corrections. In the unlike-quark case we obtain,

$$\begin{aligned}
\mathcal{A}^{8\,(1\times 1)}(s,t,u) &= \left[|\mathcal{IR}_t+\mathcal{F}_r+\mathcal{F}_g|^2+\left(N^2-1\right)|\mathcal{IR}_{nt}|^2\right]\langle\mathcal{M}_0|\mathcal{M}_0\rangle \\
&+ 2\,\mathrm{Re}\left[\left(\mathcal{IR}_t+\mathcal{F}_r+\mathcal{F}_g\right)^{\dagger}\mathcal{F}_1+\left(N^2-1\right)\mathcal{IR}_{nt}^{\dagger}\mathcal{F}_2\right] \\
&+ \left(N^2-1\right)\Bigg[\frac{N^4-3N^2+3}{N^2}\mathcal{F}_3(s,t,u)+\frac{N^2+3}{N^2}\mathcal{F}_3(s,u,t) \\
&\qquad +\frac{N^2-3}{N^2}\left[\mathcal{F}_4(s,t,u)+\mathcal{F}_4(s,u,t)\right]\Bigg], \qquad (6.31)
\end{aligned}$$

where the infrared poles present in the one-loop amplitude proportional to the tree-level matrix elements are given by

$$\mathcal{IR}_t = \frac{2}{\epsilon(2+\epsilon)}\left[\frac{1}{N}\mathrm{Bub}(s)-\frac{2}{N}\mathrm{Bub}(u)-\frac{(N^2-2)}{N}\mathrm{Bub}(t)\right], \qquad (6.32)$$

$$\mathcal{IR}_{nt} = \frac{2}{\epsilon(2+\epsilon)}\left[\frac{1}{N}\mathrm{Bub}(u)-\frac{1}{N}\mathrm{Bub}(t)\right], \qquad (6.33)$$

which diverge as $1/\epsilon^2$ and $1/\epsilon$ respectively. Both

$$\mathcal{F}_r = \beta_0\left(-\frac{1}{\epsilon}+\frac{3(1-\epsilon)}{3-2\epsilon}\,\mathrm{Bub}(s)\right), \qquad (6.34)$$

and

$$\mathcal{F}_g = \frac{\epsilon\left[N^2(11+2\epsilon)+9-4\epsilon^2\right]}{2(2+\epsilon)(3-2\epsilon)N}\,\mathrm{Bub}(s), \qquad (6.35)$$

are finite terms multiplying the tree-level matrix elements. The functions

$$\mathcal{F}_1 = \frac{N^2-1}{2N}\left[(N^2-2)f(s,t,u)+2f(s,u,t)\right], \qquad (6.36)$$

and

$$\mathcal{F}_2 = \frac{N^2-1}{2N}\Big[f(s,t,u)-f(s,u,t)\Big] \qquad (6.37)$$

are finite and multiplied by the infrared poles of the conjugated one-loop amplitude, with

$$\begin{aligned} f(s,t,u) &= \left[\frac{3s^2+7u^2+9t^2}{s^2} - 4\frac{u^2+t^2+2s^2}{(2+\epsilon)s^2} + \epsilon\frac{5u+7t}{s}\right]\Big[\mathrm{Bub}(t)-\mathrm{Bub}(s)\Big] \\ &\quad + u(1-2\epsilon)\frac{6t^2+2u^2-3\epsilon s^2}{s^2}\ \mathrm{Box}^6(s,t). \end{aligned} \tag{6.38}$$

Finally the square of the finite part of the one-loop amplitude is fixed by the finite functions $\mathcal{F}_3$ and $\mathcal{F}_4$,

$$\begin{aligned} \mathcal{F}_3(s,t,u) &= \left|\mathrm{Box}^6(s,t)\right|^2 \left[\frac{t^4+6t^2u^2+u^4}{2s^2}\right] \\ &+ 2\,\mathrm{Re}\left\{\Big[\mathrm{Bub}(t)-\mathrm{Bub}(s)\Big]^\dagger\ \mathrm{Box}^6(s,t)\right\}\left[\frac{2u^3-tu^2+8t^2u-t^3}{2s^2}\right] \\ &+ |\mathrm{Bub}(t)-\mathrm{Bub}(s)|^2\left[\frac{5t^2-2tu+2u^2}{s^2}\right] + \mathcal{O}(\epsilon), \end{aligned} \tag{6.39}$$

and

$$\begin{aligned} \mathcal{F}_4(s,t,u) &= 2\,\mathrm{Re}\left\{\mathrm{Box}^{6\dagger}(s,t)\mathrm{Box}^6(s,u)\right\}\left[\frac{tu(t^2+u^2)}{s^2}\right] \\ &+2\,\mathrm{Re}\left\{[\mathrm{Bub}(u)-\mathrm{Bub}(s)]^\dagger\ \mathrm{Box}^6(s,t)\right\}\left[\frac{u(7t^2-2tu+3u^2)}{2s^2}\right] \\ &+2\,\mathrm{Re}\left\{[\mathrm{Bub}(u)-\mathrm{Bub}(s)]^\dagger\,[\mathrm{Bub}(t)-\mathrm{Bub}(s)]\right\}\left[\frac{3(t^2-tu+u^2)}{2s^2}\right] + \mathcal{O}(\epsilon). \end{aligned} \tag{6.40}$$

In the latter expressions, we have discarded contributions of $\mathcal{O}(\epsilon)$.

After explicit series expansion in ϵ, the infrared singular terms $\mathcal{IR}_t$ and $\mathcal{IR}_{nt}$ reproduce the pole structure obtained by expanding

$$\mathcal{IR}_{t,C} = \frac{e^{\epsilon\gamma}}{\Gamma(1-\epsilon)}\left(\frac{1}{\epsilon^2}+\frac{3}{2\epsilon}\right)\left[\frac{1}{N}\left(-\frac{\mu^2}{s}\right)^\epsilon - \frac{2}{N}\left(-\frac{\mu^2}{u}\right)^\epsilon - \frac{(N^2-2)}{N}\left(-\frac{\mu^2}{t}\right)^\epsilon\right], \tag{6.41}$$

$$\mathcal{IR}_{nt,C} = \frac{e^{\epsilon\gamma}}{\Gamma(1-\epsilon)}\left(\frac{1}{\epsilon^2}+\frac{3}{2\epsilon}\right)\left[\frac{1}{N}\left(-\frac{\mu^2}{u}\right)^\epsilon - \frac{1}{N}\left(-\frac{\mu^2}{t}\right)^\epsilon\right], \tag{6.42}$$

which is the singular structure obtained by straightforward application of the formalism of [17, 18]. To rewrite Eq. (6.31) directly in terms of $\mathcal{IR}_{t,C}$ and $\mathcal{IR}_{nt,C}$ rather than $\mathcal{IR}_t$ and $\mathcal{IR}_{nt}$ requires the finite difference to be evaluated through to $\mathcal{O}(\epsilon^2)$.

Equation (6.31) is valid in all kinematic regions. Series expansions in ϵ in a particular region can be easily obtained by inserting the appropriate expansions of the master integrals. In this equation, the finite functions are multiplied by poles in ϵ, so they must be expanded through to $\mathcal{O}(\epsilon^2)$.

6.4 One-loop contributions for like-quark scattering

For the like-quark contribution we find a similar expression,

$$\begin{aligned}
\mathcal{B}^{8\,(1\times1)}(s,t,u) \;=&\\
-2\,\mathrm{Re}\Bigg\{ & \left(\overline{\mathcal{IR}}_t + \overline{\mathcal{F}}_r + \overline{\mathcal{F}}_g\right)^\dagger \left(\mathcal{IR}_t + \mathcal{F}_r + \mathcal{F}_g\right) \langle\overline{\mathcal{M}}_0|\mathcal{M}_0\rangle \\
& +(N^2-1)\left(\overline{\mathcal{IR}}_{nt} - \overline{\mathcal{F}}_r - \overline{\mathcal{F}}_g\right)^\dagger \mathcal{IR}_{nt}\,\langle\overline{\mathcal{M}}_0|\mathcal{M}_0\rangle \\
& + \Big[\left(\overline{\mathcal{IR}}_t + \overline{\mathcal{F}}_r + \overline{\mathcal{F}}_g\right)^\dagger \mathcal{F}_1' + (N^2-1)\left(\overline{\mathcal{IR}}_{nt} - \overline{\mathcal{F}}_r - \overline{\mathcal{F}}_g\right)^\dagger \mathcal{F}_2' + (s \leftrightarrow t)\Big] \\
& + \frac{N^2-1}{N}\Bigg[-\frac{N^4-N^2-1}{2N^2}\, f_3^\dagger(s,t,u) f_3(t,s,u) \\
& \qquad + \frac{N^4-2N^2-1}{2N^2}\left[f_3^\dagger(s,t,u) f_4(t,s,u) + (s\leftrightarrow t)\right] \\
& \qquad + \frac{3N^2+1}{2N^2}\, f_4^\dagger(s,t,u) f_4(t,s,u)\Bigg]\Bigg\}. \qquad (6.43)
\end{aligned}$$

The infrared singular functions are given by

$$\overline{\mathcal{IR}}_t = \frac{2}{\epsilon(2+\epsilon)}\left[\frac{1}{N}\mathrm{Bub}(s) + \frac{1}{N}\mathrm{Bub}(t) - \frac{(N^2+1)}{N}\mathrm{Bub}(u)\right], \qquad (6.44)$$

$$\overline{\mathcal{IR}}_{nt} = \frac{2}{\epsilon(2+\epsilon)}\left[\frac{N^2-1}{N}\mathrm{Bub}(s) - \frac{1}{N}\mathrm{Bub}(t) + \frac{1}{N}\mathrm{Bub}(u)\right], \qquad (6.45)$$

which diverge as $1/\epsilon^2$. The finite renormalisation term is

$$\overline{\mathcal{F}}_r = \beta_0\left(-\frac{1}{\epsilon} + \frac{3(1-\epsilon)}{3-2\epsilon}\mathrm{Bub}(t)\right), \qquad (6.46)$$

while the remaining finite contribution multiplying tree-level is given by

$$\overline{\mathcal{F}}_g = \frac{\epsilon\,(N^2(11+2\epsilon)+9-4\epsilon^2)}{2(2+\epsilon)(3-2\epsilon)N}\mathrm{Bub}(t). \qquad (6.47)$$

Once again, the finite part of the crossed one loop amplitude multiplying the infrared divergent terms of the one loop amplitude generates finite functions

$$\mathcal{F}_1' = \frac{N^2-1}{2N^2}\left[\left(N^2-2\right) f_1(s,t,u) + 2f_2(s,t,u)\right], \tag{6.48}$$

and

$$\mathcal{F}_2' = \frac{N^2-1}{2N^2}\left[f_1(s,t,u) - f_2(s,t,u)\right], \tag{6.49}$$

where

$$\begin{aligned} f_1(s,t,u) &= \frac{2u}{st}(1-2\epsilon)\left[t^2+u^2-2\epsilon(t^2+s^2)+\epsilon^2 s^2\right]\mathrm{Box}^6(s,t) \\ &\quad + \frac{2}{st(2+\epsilon)}\left[2u(2u-t)+\epsilon(u^2-tu-4t^2)+\epsilon^2(ts-4u^2)\right. \\ &\qquad \left. +\epsilon^3 us+\epsilon^4 ts\right]\left[\mathrm{Bub}(t)-\mathrm{Bub}(s)\right], \end{aligned} \tag{6.50}$$

and

$$\begin{aligned} f_2(s,t,u) &= \frac{2}{s}(1-2\epsilon)\left[2u^2-\epsilon(t^2+s^2+u^2)+3s^2\epsilon^2+s^2\epsilon^3\right]\mathrm{Box}^6(s,u) \\ &\quad \frac{2}{ts(2+\epsilon)}\left[6u^2-2t^2\epsilon-\epsilon^2(2t^2+5u^2+3tu)-\epsilon^3 s^2\right. \\ &\qquad \left. +\epsilon^4 ts\right]\left[\mathrm{Bub}(u)-\mathrm{Bub}(s)\right]. \end{aligned} \tag{6.51}$$

Finally the square of the finite part of the one-loop amplitude is controlled by the finite functions f_3 and f_4

$$f_3(s,t,u) = \frac{1}{s}\left\{(s^2+u^2)\mathrm{Box}^6(s,t) + (2u-s)\Big[\mathrm{Bub}(s)-\mathrm{Bub}(t)\Big]\right\} + \mathcal{O}(\epsilon), \tag{6.52}$$

and

$$f_4(s,t,u) = \frac{u}{s}\left\{2s\mathrm{Box}^6(t,u) + 3\Big[\mathrm{Bub}(u)-\mathrm{Bub}(t)\Big]\right\} + \mathcal{O}(\epsilon). \tag{6.53}$$

Again, the infrared singular structure obtained by explicit expansion of $\overline{\mathcal{IR}}_t$ and $\overline{\mathcal{IR}}_{nt}$ as series in ϵ, agrees with that obtained using the formalism of [17, 18]

$$\overline{\mathcal{IR}}_{t,C} = \frac{e^{\epsilon\gamma}}{\Gamma(1-\epsilon)}\left(\frac{1}{\epsilon^2}+\frac{3}{2\epsilon}\right)\left\{\frac{1}{N}\left(-\frac{\mu^2}{s}\right)^{\epsilon} + \frac{1}{N}\left(-\frac{\mu^2}{t}\right)^{\epsilon} - \frac{(N^2+1)}{N}\left(-\frac{\mu^2}{u}\right)^{\epsilon}\right\}, \tag{6.54}$$

and

$$\overline{\mathcal{IR}}_{nt,C} = \frac{e^{\epsilon\gamma}}{\Gamma(1-\epsilon)}\left(\frac{1}{\epsilon^2}+\frac{3}{2\epsilon}\right)\left\{\frac{N^2-1}{N}\left(-\frac{\mu^2}{s}\right)^{\epsilon} - \frac{1}{N}\left(-\frac{\mu^2}{t}\right)^{\epsilon} + \frac{1}{N}\left(-\frac{\mu^2}{u}\right)^{\epsilon}\right\}. \tag{6.55}$$

As before, we can rewrite Eq. (6.43) directly in terms of $\overline{\mathcal{IR}}_{t,C}$ and $\overline{\mathcal{IR}}_{nt,C}$ rather than $\overline{\mathcal{IR}}_t$ and $\overline{\mathcal{IR}}_{t,C}$ provided the finite difference is evaluated through to $\mathcal{O}(\epsilon^2)$.

6.5 Unlike-quark scattering two-loop contributions

In this section, we give explicit formulae for the ϵ-expansion of the two-loop contribution to the next-to-next-to-leading order term $\mathcal{A}^8(s,t,u)$. We divide the two-loop contributions into two classes: those that multiply poles in the dimensional regularisation parameter ϵ and those that are finite as $\epsilon \to 0$

$$\mathcal{A}^{8\ (2\times 0)}(s,t,u) = \mathcal{P}oles_a + \mathcal{F}inite_a. \tag{6.56}$$

$\mathcal{P}oles_a$ contains both infrared singularities and ultraviolet divergences. The latter are removed by renormalisation, while the former must be analytically canceled by the infrared singularities occurring in radiative processes of the same order. The structure of these infrared divergences has been widely studied and, as has been demonstrated by Catani [17] and detailed in Chapter 2, can be largely predicted. For the application of the formalism we choose to decompose the tree-level and one-loop amplitudes in terms of the $|h\rangle$ and $|v\rangle$ color vectors in color space of Section 2.7 and in order to isolate the singular part of the two-loop amplitude we make use of the expression of Eq. 2.38, where the color charge matrix is given by Eq. 2.50. The $\mathcal{P}oles_a$ are then determined up to a process and renormalisation scheme dependent function which contains only single poles and is controlled by the term $\mathbf{H}^{(2)}$ of Eq. 2.39.

For the case of the quark form factor (in the $\overline{\mathrm{MS}}$ scheme) it is given by

$$\boldsymbol{H}^{(2)}(\epsilon) = \frac{1}{4\epsilon}\frac{e^{\epsilon\gamma}}{\Gamma(1-\epsilon)}\left(\frac{\mu^2 e^{-i\lambda_{12}\pi}}{2p_1.p_2}\right)^{2\epsilon} H^{(2)}, \tag{6.57}$$

with

$$H^{(2)} = \left[\frac{1}{4}\gamma_{(1)} + 3C_F K + \frac{5}{2}\zeta_2\beta_0 C_F - \frac{28}{9}\beta_0 C_F - \left(\frac{16}{9} - 7\zeta_3\right) C_F C_A\right] \tag{6.58}$$

where

$$\gamma_{(1)} = (-3 + 24\zeta_2 - 48\zeta_3)\, C_F^2 + \left(-\frac{17}{3} - \frac{88}{3}\zeta_2 + 24\zeta_3\right) C_F C_A + \left(\frac{4}{3} + \frac{32}{3}\zeta_2\right) C_F T_R N_F. \tag{6.59}$$

and the constant K is

$$K = \left(\frac{67}{18} - \frac{\pi^2}{6}\right) C_A - \frac{10}{9} T_R N_F. \tag{6.60}$$

We expect that in the four-quark two loop amplitude, we might obtain contributions from $\boldsymbol{H}^{(2)}$ for each of the six colour antennae.

6.5.1 Infrared pole structure

Applying the formalism to the case at hand, we find that the pole structure of the two-loop amplitude interfered with tree level has the following structure

$$\begin{aligned}\mathcal{P}oles_a = 2\,\mathrm{Re}\Bigg[& \frac{1}{2}\langle\mathcal{M}^{(0)}|\boldsymbol{I}^{(1)}(\epsilon)\boldsymbol{I}^{(1)}(\epsilon)|\mathcal{M}^{(0)}\rangle - \frac{\beta_0}{\epsilon}\langle\mathcal{M}^{(0)}|\boldsymbol{I}^{(1)}(\epsilon)|\mathcal{M}^{(0)}\rangle \\ & + \langle\mathcal{M}^{(0)}|\boldsymbol{I}^{(1)}(\epsilon)|\mathcal{M}^{(1)\,\mathrm{fin}}\rangle \\ & + e^{-\epsilon\gamma}\frac{\Gamma(1-2\epsilon)}{\Gamma(1-\epsilon)}\left(\frac{\beta_0}{\epsilon}+K\right)\langle\mathcal{M}^{(0)}|\boldsymbol{I}^{(1)}(2\epsilon)|\mathcal{M}^{(0)}\rangle \\ & + \langle\mathcal{M}^{(0)}|\boldsymbol{H}^{(2)}(\epsilon)|\mathcal{M}^{(0)}\rangle\Bigg]. \end{aligned} \tag{6.61}$$

The colour algebra is straightforward and we find

$$\begin{aligned}\langle\mathcal{M}^{(0)}|\boldsymbol{I}^{(1)}(\epsilon)|\mathcal{M}^{(0)}\rangle &= \langle\mathcal{M}^{(0)}|\mathcal{M}^{(0)}\rangle \\ \times\frac{e^{\epsilon\gamma}}{\Gamma(1-\epsilon)}&\left(\frac{1}{\epsilon^2}+\frac{3}{2\epsilon}\right)\left[\frac{1}{N}\left(-\frac{\mu^2}{s}\right)^{\epsilon} - \frac{2}{N}\left(-\frac{\mu^2}{u}\right)^{\epsilon} - \frac{N^2-2}{N}\left(-\frac{\mu^2}{t}\right)^{\epsilon}\right]\end{aligned} \tag{6.62}$$

$$\begin{aligned}\langle\mathcal{M}^{(0)}|\boldsymbol{I}^{(1)}(\epsilon)\boldsymbol{I}^{(1)}(\epsilon)|\mathcal{M}^{(0)}\rangle &= \langle\mathcal{M}^{(0)}|\mathcal{M}^{(0)}\rangle \\ \times\frac{e^{2\epsilon\gamma}}{\Gamma(1-\epsilon)^2}\left(\frac{1}{\epsilon^2}+\frac{3}{2\epsilon}\right)^2 &\left[\frac{N^4-3N^2+3}{N^2}\left(-\frac{\mu^2}{t}\right)^{2\epsilon} + \frac{N^2+3}{N^2}\left(-\frac{\mu^2}{u}\right)^{2\epsilon}\right. \\ & - 2\frac{N^2-2}{N^2}\left(-\frac{\mu^2}{s}\right)^{\epsilon}\left(-\frac{\mu^2}{t}\right)^{\epsilon} + 2\frac{N^2-3}{N^2}\left(-\frac{\mu^2}{t}\right)^{\epsilon}\left(-\frac{\mu^2}{u}\right)^{\epsilon} \\ & \left. - \frac{4}{N^2}\left(-\frac{\mu^2}{s}\right)^{\epsilon}\left(-\frac{\mu^2}{u}\right)^{\epsilon} + \frac{1}{N^2}\left(-\frac{\mu^2}{s}\right)^{2\epsilon}\right]\end{aligned} \tag{6.63}$$

$$\begin{aligned}\langle\mathcal{M}^{(0)}|\boldsymbol{I}^{(1)}(\epsilon)|\mathcal{M}^{(1)\,\mathrm{fin}}\rangle &= \frac{e^{\epsilon\gamma}}{\Gamma(1-\epsilon)}\left(\frac{1}{\epsilon^2}+\frac{3}{2\epsilon}\right) \\ \times\Bigg\{&\left[\frac{1}{N}\left(-\frac{\mu^2}{s}\right)^{\epsilon} - \frac{2}{N}\left(-\frac{\mu^2}{u}\right)^{\epsilon} - \frac{N^2-2}{N}\left(-\frac{\mu^2}{t}\right)^{\epsilon}\right]\Phi_1(s,t,u) \\ &+ \left[\frac{1}{N}\left(-\frac{\mu^2}{u}\right)^{\epsilon} - \frac{1}{N}\left(-\frac{\mu^2}{t}\right)^{\epsilon}\right](N^2-1)\,\Phi_2(s,t,u)\Bigg\}\end{aligned} \tag{6.64}$$

and

$$\begin{aligned}\langle\mathcal{M}^{(0)}|\boldsymbol{H}^{(2)}(\epsilon)|\mathcal{M}^{(0)}\rangle &= \langle\mathcal{M}^{(0)}|\mathcal{M}^{(0)}\rangle \\ &\times\frac{e^{\epsilon\gamma}}{2\,\epsilon\,\Gamma(1-\epsilon)}H^{(2)}\left[\left(-\frac{\mu^2}{s}\right)^{2\epsilon} + \left(-\frac{\mu^2}{t}\right)^{2\epsilon} - \left(-\frac{\mu^2}{u}\right)^{2\epsilon}\right],\end{aligned} \tag{6.65}$$

where the square bracket in Eq. (6.65) is a guess simply motivated by summing over the antennae present in the quark-quark scattering process and on dimensional grounds. Different choices only affect the finite remainder.

The functions Φ_1 and Φ_2 appearing in Eq. (6.64) are finite functions and are obtained from projection of $\boldsymbol{I}^{(1)}$ onto the one-loop amplitude. We find

$$\begin{aligned}\Phi_1(s,t,u) = &\frac{N^2-1}{2N}\left[\left(N^2-2\right)\phi(s,t,u)+2\phi(s,u,t)\right]\\ &-\frac{1}{2\epsilon(3-2\epsilon)}\left[\frac{N^2-1}{N}\left(6-7\epsilon-2\epsilon^2\right)-\frac{1}{N}\left(10\epsilon^2-4\epsilon^3\right)\right]\mathrm{Bub}(s)\langle\mathcal{M}^{(0)}|\mathcal{M}^{(0)}\rangle\\ &-\frac{e^{\epsilon\gamma}}{\Gamma(1-\epsilon)}\left(\frac{1}{\epsilon^2}+\frac{3}{2\epsilon}\right)\left[\frac{1}{N}\left(-\frac{\mu^2}{s}\right)^{\epsilon}-\frac{2}{N}\left(-\frac{\mu^2}{u}\right)^{\epsilon}-\frac{N^2-2}{N}\left(-\frac{\mu^2}{t}\right)^{\epsilon}\right]\langle\mathcal{M}^{(0)}|\mathcal{M}^{(0)}\rangle\\ &-\beta_0\left[\frac{1}{\epsilon}-\frac{3(1-\epsilon)}{(3-2\epsilon)}\mathrm{Bub}(s)\right]\langle\mathcal{M}^{(0)}|\mathcal{M}^{(0)}\rangle \qquad (6.66)\end{aligned}$$

$$\begin{aligned}\Phi_2(s,t,u) = &\frac{N^2-1}{2N}\left[\phi(s,t,u)-\phi(s,u,t)\right]\\ &-\frac{e^{\epsilon\gamma}}{\Gamma(1-\epsilon)}\left(\frac{1}{\epsilon^2}+\frac{3}{2\epsilon}\right)\left[\frac{1}{N}\left(-\frac{\mu^2}{u}\right)^{\epsilon}-\frac{1}{N}\left(-\frac{\mu^2}{t}\right)^{\epsilon}\right]\langle\mathcal{M}^{(0)}|\mathcal{M}^{(0)}\rangle \qquad (6.67)\end{aligned}$$

where the function $\phi(s,t,u)$ is written in terms of the one-loop box graph in $D = 6-2\epsilon$ and the one-loop bubble graph in $D = 4-2\epsilon$

$$\begin{aligned}\phi(s,t,u) \;=\; &\frac{4(u^2+t^2)-2\epsilon(3ut+6t^2+5u^2)-\epsilon^2 s(7t+5u)}{s^2}\left[\frac{\mathrm{Bub}(s)-\mathrm{Bub}(t)}{\epsilon}\right]\\ &+u\,(1-2\,\epsilon)\frac{6t^2+2u^2-3\epsilon s^2}{s^2}\,\mathrm{Box}^6(s,t). \qquad (6.68)\end{aligned}$$

Our explicit Feynman diagram reproduces the anticipated pole structure exactly and provides a very stringent check on the calculation. We therefore construct the finite remainder by subtracting Eq. (6.61) from the full result.

6.5.2 Finite contributions

In this subsection, we give explicit expressions for the finite two-loop contribution to $\mathcal{A}^8$, $\mathcal{F}inite_a$, which is given by

$$\mathcal{F}inite_a = 2\,\mathrm{Re}\langle\mathcal{M}^{(0)}|\mathcal{M}^{(2)\,\mathrm{fin}}\rangle. \qquad (6.69)$$

For high energy hadron-hadron collisions, we probe all parton-parton scattering processes simultaneously. We therefore need to be able to evaluate the finite parts in the s-, t- and u-channels corresponding to the processes

$$\begin{aligned} q+\bar{q} &\rightarrow \bar{q}'+q' \\ q+\bar{q}' &\rightarrow \bar{q}'+q \\ q+q' &\rightarrow q+q', \end{aligned}$$

respectively. In principle, the analytic expressions for different channels are related by crossing symmetry. However, the cross-box diagram has cuts in all three channels yielding complex parts in all physical regions. The analytic continuation is therefore rather involved and prone to error. We therefore choose to give expressions describing $\mathcal{A}^8(s,t,u)$, $\mathcal{A}^8(t,s,u)$ and $\mathcal{A}^8(u,t,s)$ which are directly valid in the physical region, $s>0$ and $u,t<0$, and are given in terms of logarithms and polylogarithms that have no imaginary parts.

In general the expansions of the two-loop master integrals contain the generalised polylogarithms of Nielsen

$$\mathrm{S}_{n,p}(x) = \frac{(-1)^{n+p-1}}{(n-1)!\,p!}\int_0^1 dt\,\frac{\log^{n-1}(t)\log^p(1-xt)}{t}, \qquad n,p\geq 1, \quad x\leq 1 \tag{6.70}$$

where the level is $n+p$. Keeping terms up to $\mathcal{O}(\epsilon)$ corresponds to probing level 4 so that only polylogarithms with $n+p\leq 4$ occur. For $p=1$ we find the usual polylogarithms

$$\mathrm{S}_{n-1,1}(z)\equiv \mathrm{Li}_n(z). \tag{6.71}$$

A basis set of 6 polylogarithms (one with $n+p=2$, two with $n+p=3$ and three with $n+p=4$ is sufficient to describe a function of level 4. At level 4, we choose to eliminate the S_{22}, S_{13} and S_{12} functions using the standard polylogarithm identities [82] and retain the polylogarithms with arguments x, $1-x$ and $(x-1)/x$, where

$$x=-\frac{t}{s}, \qquad y=-\frac{u}{s}=1-x, \qquad -\frac{u}{t}=\frac{x-1}{x}. \tag{6.72}$$

For convenience, we also introduce the following logarithms

$$L_x=\log\left(\frac{-t}{s}\right), \qquad L_y=\log\left(\frac{-u}{s}\right), \qquad L_s=\log\left(\frac{s}{\mu^2}\right) \tag{6.73}$$

where μ is the renormalisation scale. The common choice $\mu^2=s$ corresponds to setting $L_s=0$.

For each channel, we choose to present our results by grouping terms according to the power of the number of colours N and the number of light quarks N_F so that in channel c

$$\mathcal{F}inite_{a,c} = 2\Big(N^2-1\Big)\Big(N^2 A_c + B_c + \frac{1}{N^2}C_c + N\,N_F D_c + \frac{N_F}{N}E_c + N_F^2 F_c\Big). \tag{6.74}$$

The s-channel process $q\bar{q}\to\bar{q}'q'$

We first give expressions for the s-channel annihilation process, $q\bar{q}\to\bar{q}'q'$. We find that

$$\begin{aligned}
A_s \;=\; & \Bigg[2\,\mathrm{Li}_4(x) + \Big(-2\,L_x - \frac{11}{3}\Big)\mathrm{Li}_3(x) + \Big(L_x^2 + \frac{11}{3}\,L_x - \frac{2}{3}\,\pi^2\Big)\mathrm{Li}_2(x) \\
& + \frac{121}{18}\,L_s^2 + \Big(-\frac{11}{3}\,L_x^2 + 11\,L_x - \frac{296}{27}\Big)L_s + \frac{1}{6}\,L_x^4 + \Big(\frac{1}{3}\,L_y - \frac{49}{18}\Big)L_x^3 \\
& + \Big(\frac{11}{6}\,L_y - \frac{5}{6}\,\pi^2 + \frac{197}{18}\Big)L_x^2 + \Big(-\frac{2}{3}\,L_y\,\pi^2 - \frac{47}{18}\,\pi^2 + 6\,\zeta_3 - \frac{95}{24}\Big)L_x \\
& + \Big(\frac{11}{24}\,\pi^2 - 7\,\zeta_3 - \frac{409}{216}\Big)L_y + \frac{113}{720}\,\pi^4 - \frac{7}{6}\,\pi^2 + \frac{197}{36}\,\zeta_3 + \frac{23213}{2592}\Bigg]\Bigg[\frac{t^2+u^2}{s^2}\Bigg] \\
& + \Bigg[-3\,\mathrm{Li}_4(y) + 6\,\mathrm{Li}_4(x) - 3\,\mathrm{Li}_4\Big(\frac{x-1}{x}\Big) + \Big(-2\,L_x - \frac{7}{2}\Big)\mathrm{Li}_3(x) \\
& + 3\,L_x\,\mathrm{Li}_3(y) + \Big(\frac{1}{2}\,L_x^2 + \frac{7}{2}\,L_x + \frac{1}{2}\,\pi^2\Big)\mathrm{Li}_2(x) + \Big(-\frac{11}{6}\,L_x^2 + \frac{11}{6}\,L_x\Big)L_s \\
& + \Big(\frac{1}{2}\,L_y\,\pi^2 - \frac{13}{9}\,\pi^2 - \zeta_3 - \frac{32}{9}\Big)L_x + \Big(\frac{7}{4}\,L_y - \frac{3}{4}\,\pi^2 + \frac{44}{9}\Big)L_x^2 \\
& + \Big(\frac{1}{2}\,L_y - \frac{49}{36}\Big)L_x^3 - \frac{7}{120}\,\pi^4 + \frac{47}{36}\,\pi^2 + 2\,\zeta_3\Bigg]\Bigg[\frac{t^2-u^2}{s^2}\Bigg] + \Bigg[3\,L_x^2\Bigg]\frac{t^3}{s^2 u} \\
& + 3\,\mathrm{Li}_4(y) - 3\,\mathrm{Li}_4(x) + 3\,\mathrm{Li}_4\Big(\frac{x-1}{x}\Big) - 3\,L_x\,\mathrm{Li}_3(y) - \frac{5}{2}\,\mathrm{Li}_3(x) \\
& + \Big(\frac{5}{2}\,L_x - \frac{1}{2}\,\pi^2\Big)\mathrm{Li}_2(x) - \frac{11}{6}\,L_x\,L_s + \frac{1}{8}\,L_x^4 + \Big(-\frac{1}{2}\,L_y + \frac{1}{3}\Big)L_x^3 \\
& + \Big(\frac{5}{4}\,L_y + \frac{1}{4}\,\pi^2 + \frac{1}{6}\Big)L_x^2 + \Big(-\frac{1}{2}\,L_y\,\pi^2 - \frac{7}{6}\,\pi^2 + 3\,\zeta_3 + \frac{32}{9}\Big)L_x \\
& + \frac{1}{40}\,\pi^4 - \frac{11}{36}\,\pi^2 + 4\,\zeta_3
\end{aligned} \tag{6.75}$$

$$
\begin{aligned}
B_s \quad &= \Bigg[-6\,\mathrm{Li}_4(x) - \frac{22}{3}\,\mathrm{Li}_3(y) + \left(-3\,L_x^2 - \frac{22}{3}\,L_x - \frac{22}{3}\,L_y + 2\,\pi^2 \right) \mathrm{Li}_2(x) \\
&+ \left(6\,L_x + \frac{22}{3} \right) \mathrm{Li}_3(x) + \left(\frac{22}{3}\,L_x^2 - 22\,L_x - \frac{22}{3}\,L_y^2 + 22\,L_y - \frac{88}{3} \right) L_s \\
&- \frac{1}{2}\,L_x^4 + \left(-L_y + \frac{125}{18} \right) L_x^3 + \left(\frac{1}{2}\,L_y^2 - \frac{31}{6}\,L_y + 3\,\pi^2 - \frac{743}{36} \right) L_x^2 \\
&+ \left(-\frac{31}{6}\,L_y^2 + \left(-\frac{4}{3}\,\pi^2 + \frac{9}{2} \right) L_y + \frac{307}{72}\,\pi^2 + \zeta_3 - \frac{49}{27} \right) L_x \\
&+ \frac{1}{4}\,L_y^4 - \frac{71}{18}\,L_y^3 + \left(-\frac{2}{3}\,\pi^2 + \frac{689}{36} \right) L_y^2 + \left(-\frac{73}{24}\,\pi^2 - \zeta_3 - \frac{275}{27} \right) L_y \\
&+ \frac{79}{720}\,\pi^4 - \frac{55}{72}\,\pi^2 - \frac{443}{36}\,\zeta_3 + \frac{30659}{648} \Bigg] \left[\frac{t^2+u^2}{s^2} \right] \\
&+ \Bigg[-12\,\mathrm{Li}_4(y) + 3\,\mathrm{Li}_4(x) - 8\,\mathrm{Li}_4\left(\frac{x-1}{x} \right) + \left(2\,L_y + 8 \right) \mathrm{Li}_3(y) \\
&+ \left(-\frac{3}{2}\,L_x^2 + \left(-8\,L_y - \frac{11}{2} \right) L_x + 8\,L_y - \frac{4}{3}\,\pi^2 \right) \mathrm{Li}_2(x) - 12\,L_y\,L_x\,\mathrm{Li}_2(y) \\
&+ \left(4\,L_x - 12\,L_y + \frac{11}{2} \right) \mathrm{Li}_3(x) + \left(\frac{11}{3}\,L_x^2 - \frac{11}{3}\,L_x + \frac{11}{3}\,L_y^2 - \frac{11}{3}\,L_y \right) L_s \\
&- \frac{17}{24}\,L_x^4 + \left(L_y + \frac{131}{36} \right) L_x^3 + \left(-\frac{25}{2}\,L_y^2 - \frac{15}{4}\,L_y + \frac{13}{12}\,\pi^2 - \frac{289}{36} \right) L_x^2 \\
&+ \left(\frac{1}{3}\,L_y^3 + 5\,L_y^2 + \frac{5}{3}\,L_y\,\pi^2 + \frac{89}{36}\,\pi^2 + \frac{37}{9} \right) L_x - \frac{1}{6}\,L_y^4 + \frac{17}{9}\,L_y^3 \\
&+ \left(\frac{7}{12}\,\pi^2 - \frac{361}{36} \right) L_y^2 + \left(\frac{59}{36}\,\pi^2 + 6\,\zeta_3 + \frac{64}{9} \right) L_y - \frac{1}{20}\,\pi^4 - \frac{44}{9}\,\pi^2 - 9\,\zeta_3 \Bigg] \left[\frac{t^2-u^2}{s^2} \right] \\
&\left[-7\,L_x^2 \right] \frac{t^3}{s^2 u} + \left[5\,L_y^2 \right] \frac{u^3}{s^2 t} - 12\,\mathrm{Li}_4(y) + 12\,\mathrm{Li}_4(x) - 12\,\mathrm{Li}_4\left(\frac{x-1}{x} \right) \\
&+ \left(6\,L_x - 6 \right) \mathrm{Li}_3(y) + \left(-6\,L_y + \frac{9}{2} \right) \mathrm{Li}_3(x) - 6\,L_y\,L_x\,\mathrm{Li}_2(y) \\
&+ \left(\left(-6\,L_y - \frac{9}{2} \right) L_x - 6\,L_y + 2\,\pi^2 \right) \mathrm{Li}_2(x) + \left(\frac{11}{3}\,L_x - \frac{11}{3}\,L_y \right) L_s \\
&- \frac{1}{2}\,L_x^4 + \left(2\,L_y - \frac{5}{6} \right) L_x^3 + \left(-\frac{15}{2}\,L_y^2 - 2\,L_y - \pi^2 + \frac{17}{12} \right) L_x^2 \\
&+ \left(-\frac{11}{4}\,L_y^2 + \left(3\,\pi^2 + \frac{1}{2} \right) L_y + \frac{25}{12}\,\pi^2 - 6\,\zeta_3 - \frac{37}{9} \right) L_x + \frac{1}{4}\,L_y^3 \\
&+ \frac{7}{12}\,L_y^2 + \left(-\frac{5}{4}\,\pi^2 + 6\,\zeta_3 + \frac{64}{9} \right) L_y - \frac{17}{60}\,\pi^4 - \frac{2}{3}\,\pi^2 + 5\,\zeta_3 \qquad (6.76)
\end{aligned}
$$

$$
\begin{aligned}
C_s \;=\;& \Bigg[16\,\mathrm{Li}_4(y)+8\,\mathrm{Li}_4(x)-16\,L_y\,\mathrm{Li}_3(y)-8\,L_x\,\mathrm{Li}_3(x)+\left(4\,L_x^2+\frac{8}{3}\,\pi^2\right)\mathrm{Li}_2(x)\\
&+8\,L_y^2\,\mathrm{Li}_2(y)+\frac{5}{12}\,L_x^4+\left(\frac{4}{3}\,L_y-\frac{9}{2}\right)L_x^3+\left(-\frac{3}{2}\,L_y^2+\frac{9}{2}\,L_y-\frac{11}{3}\,\pi^2+\frac{1}{4}\right)L_x^2\\
&+\left(\frac{8}{3}\,L_y^3+\frac{9}{2}\,L_y^2+\left(\frac{22}{3}\,\pi^2-\frac{27}{2}\right)L_y+\frac{1}{2}\,\pi^2-6\,\zeta_3+\frac{189}{8}\right)L_x\\
&+\frac{1}{12}\,L_y^4-\frac{9}{2}\,L_y^3+\left(-\frac{7}{3}\,\pi^2+\frac{65}{4}\right)L_y^2+\left(-\frac{1}{2}\,\pi^2+6\,\zeta_3-\frac{189}{8}\right)L_y\\
&-\frac{49}{60}\,\pi^4+\frac{29}{24}\,\pi^2-\frac{15}{2}\,\zeta_3+\frac{511}{32}\Bigg]\left[\frac{t^2+u^2}{s^2}\right]\\
&+\Bigg[12\,\mathrm{Li}_4(y)-24\,\mathrm{Li}_4(x)+24\,\mathrm{Li}_4\left(\frac{x-1}{x}\right)+\left(-18\,L_x+10\,L_y-2\right)\mathrm{Li}_3(y)\\
&+\left(-2\,L_x+18\,L_y+4\right)\mathrm{Li}_3(x)+\left(2\,L_x^2+\left(6\,L_y-4\right)L_x-2\,L_y+4\,\pi^2\right)\mathrm{Li}_2(x)\\
&+\left(18\,L_x\,L_y-4\,L_y^2\right)\mathrm{Li}_2(y)+\frac{4}{3}\,L_x^4+\left(-3\,L_y-\frac{8}{3}\right)L_x^3\\
&+\left(15\,L_y^2+L_y+\frac{1}{12}\,\pi^2-\frac{15}{4}\right)L_x^2+\left(-L_y^3-4\,L_y^2-2\,L_y\,\pi^2+\frac{11}{12}\,\pi^2+8\,\zeta_3+6\right)L_x\\
&-\frac{1}{6}\,L_y^4+\frac{7}{3}\,L_y^3+\left(\frac{7}{12}\,\pi^2-\frac{9}{4}\right)L_y^2+\left(\frac{3}{4}\,\pi^2-16\,\zeta_3+6\right)L_y\\
&+\frac{1}{30}\,\pi^4-\frac{4}{3}\,\pi^2+4\,\zeta_3\Bigg]\left[\frac{t^2-u^2}{s^2}\right]+\left[3\,L_x^2\right]\frac{t^3}{s^2u}+\left[3\,L_y^2\right]\frac{u^3}{s^2t}\\
&+4\,\mathrm{Li}_3(y)+2\,\mathrm{Li}_3(x)+\left(-2\,L_x+4\,L_y\right)\mathrm{Li}_2(x)+\frac{3}{4}\,L_x^3+\left(-\frac{7}{4}\,L_y-\frac{15}{4}\right)L_x^2\\
&+\left(\frac{5}{4}\,L_y^2-\frac{3}{2}\,L_y+\frac{5}{12}\,\pi^2-6\right)L_x+\frac{7}{4}\,L_y^3+\frac{9}{4}\,L_y^2+\left(-\frac{19}{12}\,\pi^2+6\right)L_y\\
&+\pi^2-12\,\zeta_3
\end{aligned}
\tag{6.77}
$$

$$
\begin{aligned}
D_s \;=\; & \Bigg[\frac{2}{3}\,\mathrm{Li}_3(x) - \frac{2}{3}\,L_x\,\mathrm{Li}_2(x) - \frac{22}{9}\,L_s^2 + \Bigg(- 2\,L_x + \frac{2}{3}\,L_x^2 + \frac{389}{54}\Bigg)\,L_s \\
& + \frac{2}{9}\,L_x^3 + \Bigg(- \frac{29}{18} - \frac{1}{3}\,L_y\Bigg)\,L_x^2 + \Bigg(\frac{10}{9}\,\pi^2 + \frac{11}{6}\Bigg)\,L_x \\
& + \Bigg(- \frac{1}{12}\,\pi^2 + \frac{25}{54}\Bigg)\,L_y - \frac{455}{54} + \frac{41}{36}\,\pi^2 - \frac{49}{18}\,\zeta_3\Bigg]\left[\frac{t^2+u^2}{s^2}\right] \\
& + \Bigg[\Bigg(\frac{1}{3}\,L_x^2 - \frac{1}{3}\,L_x\Bigg)\,L_s + \frac{1}{9}\,L_x^3 - \frac{13}{18}\,L_x^2 + \Bigg(\frac{4}{9}\,\pi^2 + \frac{8}{9}\Bigg)\,L_x - \frac{2}{9}\,\pi^2\Bigg]\left[\frac{t^2-u^2}{s^2}\right] \\
& + \frac{1}{3}\,L_x\,L_s - \frac{1}{6}\,L_x^2 - \frac{8}{9}\,L_x + \frac{2}{9}\,\pi^2
\end{aligned}
\tag{6.78}
$$

$$
\begin{aligned}
E_s \;=\; & \Bigg[\frac{4}{3}\,\mathrm{Li}_3(y) - \frac{4}{3}\,\mathrm{Li}_3(x) + \Bigg(\frac{4}{3}\,L_y + \frac{4}{3}\,L_x\Bigg)\,\mathrm{Li}_2(x) - \frac{4}{9}\,L_x^3 + \Bigg(\frac{29}{9} + \frac{2}{3}\,L_y\Bigg)\,L_x^2 \\
& + \Bigg(4\,L_x - 4\,L_y + \frac{4}{3}\,L_y^2 + \frac{29}{6} - \frac{4}{3}\,L_x^2\Bigg)\,L_s + \Bigg(- \frac{223}{54} + \frac{2}{3}\,L_y^2 - \frac{77}{36}\,\pi^2\Bigg)\,L_x \\
& + \frac{4}{9}\,L_y^3 - \frac{29}{9}\,L_y^2 + \Bigg(\frac{223}{54} + \frac{23}{12}\,\pi^2\Bigg)\,L_y - \frac{35}{18}\,\zeta_3 - \frac{685}{81} - \frac{7}{36}\,\pi^2\Bigg]\left[\frac{t^2+u^2}{s^2}\right] \\
& + \Bigg[\Bigg(- \frac{2}{3}\,L_x^2 + \frac{2}{3}\,L_x + \frac{2}{3}\,L_y - \frac{2}{3}\,L_y^2\Bigg)\,L_s - \frac{2}{9}\,L_x^3 + \frac{13}{9}\,L_x^2 \\
& + \Bigg(- \frac{8}{9}\,\pi^2 - \frac{16}{9}\Bigg)\,L_x - \frac{2}{9}\,L_y^3 + \frac{13}{9}\,L_y^2 + \Bigg(- \frac{8}{9}\,\pi^2 - \frac{16}{9}\Bigg)\,L_y + \frac{8}{9}\,\pi^2\Bigg]\left[\frac{t^2-u^2}{s^2}\right] \\
& + \Bigg(- \frac{2}{3}\,L_x + \frac{2}{3}\,L_y\Bigg)\,L_s - \frac{16}{9}\,L_y - \frac{1}{3}\,L_y^2 + \frac{16}{9}\,L_x + \frac{1}{3}\,L_x^2
\end{aligned}
\tag{6.79}
$$

$$
F_s \;=\; \Bigg(- \frac{20}{27}\,L_s + \frac{50}{81} - \frac{2}{9}\,\pi^2 + \frac{2}{9}\,L_s^2\Bigg)\left[\frac{t^2+u^2}{s^2}\right] \tag{6.80}
$$

We can check some of these results by comparing with the analytic expressions presented in Ref. [19] for the QED process $e^+e^-\to\mu^+\mu^-$. Taking the QED limit corresponds to setting $C_A = 0$, $C_F = 1$, $T_R = 1$ as well as setting the cubic Casimir $C_3 = (N^2-1)(N^2-2)/N^2 = 0$. This means that we can directly compare $E_s(\propto C_F T_R\,N_F)$ and $F_s(\propto T_R^2\,N_F^2)$ but *not* C_s which receives contributions from both C_3 and C_F^2. We see that (6.79) and (6.80) agree with Eqs. (2.38) and (2.39) of [19] respectively.

The other coefficients, A_s, B_s, C_s and D_s are new results.

The t-channel process $q + \bar{q}' \to q + \bar{q}'$

The t-channel process, $q + \bar{q}' \to q + \bar{q}'$ is fixed by $\mathcal{A}^8(t,s,u)$. We find that the finite two-loop contribution in the t-channel is given by Eq. (6.74) with

$$
\begin{aligned}
A_t \;=\; & \Bigg[-2\,\mathrm{Li}_4(x) + \left(2\,L_x - \frac{11}{3}\right)\mathrm{Li}_3(x) + \left(\frac{11}{3}\,L_x - L_x^2 + \frac{2}{3}\,\pi^2\right)\mathrm{Li}_2(x) \\
& + \frac{121}{18}\,L_s^2 + \left(\frac{22}{9}\,L_x - \frac{11}{3}\,L_x^2 - \frac{296}{27}\right)L_s + \frac{1}{4}\,L_x^4 + \left(-\frac{14}{9} - \frac{1}{3}\,L_y\right)L_x^3 \\
& + \left(-\frac{7}{6}\,\pi^2 + \frac{20}{3} + \frac{11}{6}\,L_y\right)L_x^2 + \left(\zeta_3 - \frac{46}{9} + \frac{2}{3}\,L_y\,\pi^2 - \frac{373}{72}\,\pi^2\right)L_x \\
& + \left(-\frac{409}{216} + \frac{11}{24}\,\pi^2 - 7\,\zeta_3\right)L_y + \frac{23213}{2592} - \frac{49}{9}\,\pi^2 + \frac{197}{36}\,\zeta_3 - \frac{1}{48}\,\pi^4\Bigg]\left[\frac{s^2+u^2}{t^2}\right] \\
& + \Bigg[-3\,\mathrm{Li}_4\left(\frac{x-1}{x}\right) - 3\,\mathrm{Li}_4(y) - 6\,\mathrm{Li}_4(x) + \left(5\,L_x - \frac{7}{2}\right)\mathrm{Li}_3(x) \\
& + 3\,L_x\,\mathrm{Li}_3(y) + \left(-\frac{1}{2}\,\pi^2 - \frac{1}{2}\,L_x^2 + \frac{7}{2}\,L_x\right)\mathrm{Li}_2(x) + \left(-\frac{11}{6}\,L_x - \frac{11}{6}\,L_x^2\right)L_s \\
& - \frac{1}{6}\,L_x^4 + \left(-\frac{19}{18} + L_y\right)L_x^3 + \left(-\frac{1}{2}\,\pi^2 + \frac{55}{18} + \frac{7}{4}\,L_y\right)L_x^2 \\
& + \left(-\frac{1}{2}\,L_y\,\pi^2 - \frac{20}{9}\,\pi^2 + \frac{32}{9} - 2\,\zeta_3\right)L_x - \frac{19}{36}\,\pi^2 + \frac{29}{120}\,\pi^4 + 2\,\zeta_3\Bigg]\left[\frac{s^2-u^2}{t^2}\right] \\
& + \left[3\,L_x^2\right]\frac{s^3}{t^2 u} + 3\,\mathrm{Li}_4\left(\frac{x-1}{x}\right) + 3\,\mathrm{Li}_4(y) + 3\,\mathrm{Li}_4(x) + \left(-3\,L_x - \frac{5}{2}\right)\mathrm{Li}_3(x) \\
& - 3\,L_x\,\mathrm{Li}_3(y) + \left(\frac{1}{2}\,\pi^2 + \frac{5}{2}\,L_x\right)\mathrm{Li}_2(x) + \frac{11}{6}\,L_x\,L_s + \frac{1}{4}\,L_x^4 + \left(-L_y - \frac{3}{4}\right)L_x^3 \\
& + \left(\frac{5}{4}\,L_y + 2\right)L_x^2 + \left(\frac{1}{2}\,L_y\,\pi^2 - \frac{32}{9} + \frac{7}{6}\,\pi^2\right)L_x - \frac{5}{24}\,\pi^4 + \frac{55}{36}\,\pi^2 + 4\,\zeta_3 \qquad (6.81)
\end{aligned}
$$

$$
\begin{aligned}
B_t \;=\; & \Bigg[6\,\mathrm{Li}_4(x)+\left(-6\,L_x+\frac{44}{3}\right)\mathrm{Li}_3(x)+\left(\frac{22}{3}\,L_y-\frac{44}{3}\,L_x-2\,\pi^2+3\,L_x^2\right)\mathrm{Li}_2(x)\\
&+\frac{22}{3}\,\mathrm{Li}_3(y)+\left(-\frac{88}{3}-\frac{22}{3}\,L_y^2+22\,L_y-\frac{22}{3}\,\pi^2+\frac{44}{3}\,L_x\,L_y\right)L_s-L_y\,L_x^3\\
&+\left(-L_y^3+\frac{29}{3}\,L_y^2+\left(-\frac{187}{9}-\frac{7}{3}\,\pi^2\right)L_y-\frac{52}{3}+\frac{25}{3}\,\pi^2\right)L_x\\
&+\left(4\,\pi^2+2\,L_y^2+3-\frac{16}{3}\,L_y\right)L_x^2+\frac{1}{4}\,L_y^4-\frac{71}{18}\,L_y^3+\left(\frac{5}{6}\,\pi^2+\frac{689}{36}\right)L_y^2\\
&+\left(-\frac{407}{72}\,\pi^2-\zeta_3-\frac{275}{27}\right)L_y+\frac{30659}{648}-\frac{77}{720}\,\pi^4-\frac{707}{36}\,\zeta_3+\frac{183}{8}\,\pi^2\Bigg]\left[\frac{s^2+u^2}{t^2}\right]\\
&+\Bigg[-12\,\mathrm{Li}_4\left(\frac{x-1}{x}\right)-8\,\mathrm{Li}_4(y)-3\,\mathrm{Li}_4(x)+\left(-14\,L_y+10\,L_x-\frac{5}{2}\right)\mathrm{Li}_3(x)\\
&+\left(-8-2\,L_y+2\,L_x\right)\mathrm{Li}_3(y)+\left(-\frac{5}{2}\,L_x^2+\left(4\,L_y+\frac{5}{2}\right)L_x-8\,L_y-\frac{8}{3}\,\pi^2\right)\mathrm{Li}_2(x)\\
&+\left(\frac{22}{3}\,L_x^2+\left(-\frac{22}{3}\,L_y+\frac{22}{3}\right)L_x+\frac{11}{3}\,\pi^2-\frac{11}{3}\,L_y+\frac{11}{3}\,L_y^2\right)L_s-\frac{5}{12}\,L_x^4\\
&+\left(\frac{73}{18}+L_y\right)L_x^3+\left(-\frac{41}{12}\,L_y-\frac{3}{2}\,L_y^2-\frac{193}{18}+\frac{11}{6}\,\pi^2\right)L_x^2\\
&+\left(\frac{1}{3}\,L_y^3-7\,L_y^2+\left(\frac{7}{6}\,\pi^2+\frac{295}{18}\right)L_y-\frac{101}{9}-8\,\zeta_3+\frac{92}{9}\,\pi^2\right)L_x-\frac{1}{6}\,L_y^4+\frac{17}{9}\,L_y^3\\
&+\left(-\frac{5}{12}\,\pi^2-\frac{361}{36}\right)L_y^2+\left(\frac{64}{9}+\frac{167}{36}\,\pi^2+8\,\zeta_3\right)L_y-\zeta_3+\frac{29}{90}\,\pi^4-\frac{91}{12}\,\pi^2\Bigg]\left[\frac{s^2-u^2}{t^2}\right]\\
&-\left[7\,L_x^2\right]\frac{s^3}{t^2u}+\left[5\,L_y^2-10\,L_x\,L_y+5\,\pi^2+5\,L_x^2\right]\frac{u^3}{t^2s}-12\,\mathrm{Li}_4\left(\frac{x-1}{x}\right)\\
&-12\,\mathrm{Li}_4(y)-12\,\mathrm{Li}_4(x)+\left(12\,L_x-6\,L_y+\frac{21}{2}\right)\mathrm{Li}_3(x)+\left(6+6\,L_x\right)\mathrm{Li}_3(y)\\
&+\left(-\frac{21}{2}\,L_x-2\,\pi^2+6\,L_y\right)\mathrm{Li}_2(x)-\frac{11}{3}\,L_s\,L_y-\frac{1}{2}\,L_x^4+\left(-\frac{1}{6}+3\,L_y\right)L_x^3\\
&+\left(\frac{5}{2}+\frac{1}{2}\,\pi^2-\frac{3}{4}\,L_y-\frac{3}{2}\,L_y^2\right)L_x^2+\left(-\frac{16}{3}\,L_y-3+2\,L_y^2-\frac{29}{6}\,\pi^2-6\,\zeta_3\right)L_x\\
&+\frac{1}{4}\,L_y^3+\frac{7}{12}\,L_y^2+\left(-2\,\pi^2+6\,\zeta_3+\frac{64}{9}\right)L_y+\frac{5}{12}\,\pi^2+\frac{13}{20}\,\pi^4-\zeta_3
\end{aligned}
\tag{6.82}
$$

$$
\begin{aligned}
C_t \;=\;& \Bigg[16\,\mathrm{Li}_4\left(\frac{x-1}{x}\right) + \left(16\,L_y - 8\,L_x\right)\mathrm{Li}_3(x) + \left(-16\,L_x + 16\,L_y\right)\mathrm{Li}_3(y) \\
& -8\,\mathrm{Li}_4(x) + \left(4\,L_x^2 + 8\,L_y^2 + \frac{16}{3}\,\pi^2 - 16\,L_x\,L_y\right)\mathrm{Li}_2(x) + \frac{2}{3}\,L_x^4 - \frac{4}{3}\,L_y\,L_x^3 \\
& +\left(3 - 5\,L_y^2 - \frac{5}{3}\,\pi^2\right)L_x^2 + \left(5\,L_y^3 + 9\,L_y^2 + \left(\frac{7}{3}\,\pi^2 - 19\right)L_y + 16\,\zeta_3 - 9\,\pi^2\right)L_x \\
& +\frac{1}{12}\,L_y^4 - \frac{9}{2}\,L_y^3 + \left(\frac{65}{4} - \frac{19}{6}\,\pi^2\right)L_y^2 + \left(-\frac{189}{8} - 10\,\zeta_3 - 5\,\pi^2\right)L_y \\
& +\pi^4 - \frac{15}{2}\,\zeta_3 + \frac{511}{32} + \frac{95}{24}\,\pi^2\Bigg]\left[\frac{s^2+u^2}{t^2}\right] \\
& +\Bigg[12\,\mathrm{Li}_4\left(\frac{x-1}{x}\right) + 24\,\mathrm{Li}_4(y) + 24\,\mathrm{Li}_4(x) + \left(-24\,L_x + 8\,L_y + 6\right)\mathrm{Li}_3(x) \\
& +\left(6\,L_x^2 + \left(-6 - 4\,L_y\right)L_x - 4\,L_y^2 + 4\,\pi^2 + 2\,L_y\right)\mathrm{Li}_2(x) \\
& +\left(-10\,L_y - 8\,L_x + 2\right)\mathrm{Li}_3(y) + \frac{5}{6}\,L_x^4 + \left(2\,L_y - 2\,L_y^2 - \frac{7}{3}\,\pi^2 - 6\right)L_x^2 \\
& +\left(-\frac{2}{3}\,L_y + \frac{2}{3}\right)L_x^3 + \left(-\frac{7}{3}\,L_y^3 - 3\,L_y^2 + \left(\frac{9}{2} + \frac{19}{6}\,\pi^2\right)L_y + 16\,\zeta_3 - \frac{19}{3}\,\pi^2 - 12\right)L_x \\
& -\frac{1}{6}\,L_y^4 + \frac{7}{3}\,L_y^3 + \left(\frac{1}{4}\,\pi^2 - \frac{9}{4}\right)L_y^2 + \left(\frac{13}{12}\,\pi^2 + 6 - 6\,\zeta_3\right)L_y \\
& -\frac{43}{12}\,\pi^2 - \frac{7}{4}\,\pi^4 + 2\,\zeta_3\Bigg]\left[\frac{s^2-u^2}{t^2}\right] + \left[3\,L_x^2\right]\frac{s^3}{t^2 u} + \left[3\,\pi^2 - 6\,L_x\,L_y + 3\,L_y^2 + 3\,L_x^2\right]\frac{u^3}{t^2 s} \\
& -2\,\mathrm{Li}_3(x) - 4\,\mathrm{Li}_3(y) + \left(2\,L_x - 4\,L_y\right)\mathrm{Li}_2(x) + \left(-3 + 2\,L_y\right)L_x^2 \\
& +\left(\pi^2 - 3\,L_y - \frac{13}{2}\,L_y^2\right)L_x + \frac{7}{4}\,L_y^3 + \frac{9}{4}\,L_y^2 + \left(6 + \frac{7}{2}\,\pi^2\right)L_y + \frac{7}{4}\,\pi^2 - 8\,\zeta_3
\end{aligned}
\tag{6.83}
$$

$$
\begin{aligned}
D_t \;=\;& \Bigg[\frac{2}{3}\,\mathrm{Li}_3(x) - \frac{2}{3}\,L_x\,\mathrm{Li}_2(x) - \frac{22}{9}\,L_s^2 + \left(-\frac{26}{9}\,L_x + \frac{2}{3}\,L_x^2 + \frac{389}{54}\right)L_s \\
& +\frac{5}{9}\,L_x^3 + \left(-\frac{37}{18} - \frac{1}{3}\,L_y\right)L_x^2 + \left(\frac{265}{54} + \frac{11}{36}\,\pi^2\right)L_x + \left(\frac{25}{54} - \frac{1}{12}\,\pi^2\right)L_y \\
& -\frac{49}{18}\,\zeta_3 - \frac{455}{54} + \frac{25}{36}\,\pi^2\Bigg]\left[\frac{s^2+u^2}{t^2}\right] \\
& +\Bigg[\left(\frac{1}{3}\,L_x^2 + \frac{1}{3}\,L_x\right)L_s + \frac{2}{9}\,L_x^3 - \frac{7}{18}\,L_x^2 + \left(-\frac{8}{9} + \frac{2}{9}\,\pi^2\right)L_x + \frac{1}{9}\,\pi^2\Bigg]\left[\frac{s^2-u^2}{t^2}\right] \\
& -\frac{1}{3}\,L_x\,L_s - \frac{1}{9}\,\pi^2 + \frac{8}{9}\,L_x - \frac{1}{2}\,L_x^2
\end{aligned}
\tag{6.84}
$$

$$
\begin{aligned}
E_t \;=\;& \Bigg[-\frac{8}{3}\,\mathrm{Li}_3(x) - \frac{4}{3}\,\mathrm{Li}_3(y) + \left(-\frac{4}{3}\,L_y + \frac{8}{3}\,L_x \right) \mathrm{Li}_2(x) - \frac{2}{3}\,L_x^2\,L_y \\
&+ \left(-4\,L_y + \frac{4}{3}\,\pi^2 + \frac{4}{3}\,L_y^2 + \frac{29}{6} - \frac{8}{3}\,L_x\,L_y \right) L_s + \left(\frac{29}{6} + \frac{22}{9}\,L_y - \frac{2}{3}\,L_y^2 + \frac{2}{3}\,\pi^2 \right) L_x \\
&+ \frac{4}{9}\,L_y^3 - \frac{29}{9}\,L_y^2 + \left(\frac{223}{54} + \frac{37}{36}\,\pi^2 \right) L_y - \frac{41}{12}\,\pi^2 - \frac{685}{81} - \frac{11}{18}\,\zeta_3 \Bigg] \left[\frac{s^2+u^2}{t^2} \right] \\
&+ \Bigg[\left(-\frac{4}{3}\,L_x^2 + \left(\frac{4}{3}\,L_y - \frac{4}{3} \right) L_x - \frac{2}{3}\,\pi^2 + \frac{2}{3}\,L_y - \frac{2}{3}\,L_y^2 \right) L_s - \frac{8}{9}\,L_x^3 \\
&+ \left(\frac{14}{9} + \frac{2}{3}\,L_y \right) L_x^2 + \left(-\frac{20}{9}\,L_y - \frac{8}{9}\,\pi^2 + \frac{32}{9} \right) L_x - \frac{2}{9}\,L_y^3 + \frac{13}{9}\,L_y^2 \\
&+ \left(-\frac{16}{9} - \frac{2}{9}\,\pi^2 \right) L_y + \pi^2 \Bigg] \left[\frac{s^2-u^2}{t^2} \right] \\
&+ \frac{4}{3}\,L_x\,L_y + \frac{2}{3}\,L_s\,L_y - \frac{1}{3}\,L_y^2 - \frac{1}{3}\,\pi^2 - \frac{16}{9}\,L_y
\end{aligned}
\tag{6.85}
$$

$$
F_t \;=\; \left[\frac{2}{9}\,L_s^2 + \left(\frac{4}{9}\,L_x - \frac{20}{27} \right) L_s + \frac{2}{9}\,L_x^2 - \frac{20}{27}\,L_x + \frac{50}{81} \right] \left[\frac{s^2+u^2}{t^2} \right]
\tag{6.86}
$$

The u-channel process $q + q' \to q + q'$

The u-channel process, $q + q' \to q + q'$ is determined by $A^8(u,t,s)$. We find that the finite two-loop contribution in the u-channel is given by Eq. (6.74) with

$$
\begin{aligned}
A_u \;=\;& \Bigg[-2\,\mathrm{Li}_4\left(\frac{x-1}{x} \right) + \left(2\,L_x + \frac{11}{3} - 2\,L_y \right) \mathrm{Li}_3(x) + \left(2\,L_x + \frac{11}{3} - 2\,L_y \right) \mathrm{Li}_3(y) \\
&+ \left(-L_x^2 + \left(-\frac{11}{3} + 2\,L_y \right) L_x - \frac{1}{3}\,\pi^2 + \frac{11}{3}\,L_y - L_y^2 \right) \mathrm{Li}_2(x) + \frac{121}{18}\,L_s^2
\end{aligned}
$$

$$
\begin{aligned}
&+\left(-\frac{11}{3}L_x^2+\left(11+\frac{22}{3}L_y\right)L_x-\frac{11}{3}\pi^2-\frac{296}{27}+\frac{22}{9}L_y-\frac{11}{3}L_y^2\right)L_s+\frac{1}{12}L_x^4\\
&+\left(-\frac{49}{18}-\frac{2}{3}L_y\right)L_x^3+\left(2L_y^2+\frac{197}{18}+\frac{8}{3}L_y\right)L_x^2+\left(-\frac{5}{3}L_y^3\right.\\
&+\frac{17}{6}L_y^2+\left(-\frac{2}{3}\pi^2-\frac{98}{9}\right)L_y+4\zeta_3-\frac{95}{24}-\frac{31}{9}\pi^2\left.\right)L_x+\frac{1}{4}L_y^4\\
&-\frac{14}{9}L_y^3+\left(\frac{1}{2}\pi^2+\frac{20}{3}\right)L_y^2+\left(-\frac{46}{9}-\frac{25}{8}\pi^2+3\zeta_3\right)L_y+\frac{17}{144}\pi^4+\frac{65}{36}\zeta_3\\
&+\frac{11}{2}\pi^2+\frac{23213}{2592}\left.\right)\left[\frac{t^2+s^2}{u^2}\right]+\left(-6\,\mathrm{Li}_4\left(\frac{x-1}{x}\right)+3\,\mathrm{Li}_4(x)+3\,\mathrm{Li}_4(y)\right.\\
&+\left(2L_x-2L_y+\frac{7}{2}\right)\mathrm{Li}_3(x)+\left(-5L_y+\frac{7}{2}+5L_x\right)\mathrm{Li}_3(y)\\
&+\left(-\frac{1}{2}L_x^2+\left(-\frac{7}{2}+L_y\right)L_x-\pi^2+\frac{7}{2}L_y-\frac{1}{2}L_y^2\right)\mathrm{Li}_2(x)\\
&+\left(-\frac{11}{6}L_x^2+\left(\frac{11}{6}+\frac{11}{3}L_y\right)L_x-\frac{11}{6}\pi^2-\frac{11}{6}L_y-\frac{11}{6}L_y^2\right)L_s-\frac{1}{8}L_x^4\\
&+\left(\frac{1}{2}L_y-\frac{49}{36}\right)L_x^3+\left(-\frac{1}{4}\pi^2+\frac{1}{2}L_y+\frac{3}{4}L_y^2+\frac{44}{9}\right)L_x^2+\left(-\frac{5}{6}L_y^3\right.\\
&+\frac{37}{12}L_y^2+\left(-\frac{5}{6}\pi^2-\frac{143}{18}\right)L_y-\frac{32}{9}-3\zeta_3-\frac{67}{36}\pi^2\left.\right)L_x-\frac{1}{24}L_y^4-\frac{19}{18}L_y^3\\
&+\left(-\frac{5}{12}\pi^2+\frac{55}{18}\right)L_y^2+\left(-\frac{83}{36}\pi^2+3\zeta_3+\frac{32}{9}\right)L_y-\frac{3}{2}\zeta_3-\frac{7}{120}\pi^4+\frac{157}{36}\pi^2\left.\right]\left[\frac{t^2-s^2}{u^2}\right]\\
&+\left[-6L_xL_y+3L_y^2+3\pi^2+3L_x^2\right]\frac{t^3}{u^2s}\\
&+3\,\mathrm{Li}_4\left(\frac{x-1}{x}\right)-3\,\mathrm{Li}_4(x)-3\,\mathrm{Li}_4(y)+\frac{5}{2}\mathrm{Li}_3(x)+\left(\frac{5}{2}-3L_x+3L_y\right)\mathrm{Li}_3(y)\\
&+\left(\frac{5}{2}L_y-\frac{5}{2}L_x+\frac{1}{2}\pi^2\right)\mathrm{Li}_2(x)+\left(\frac{11}{6}L_y-\frac{11}{6}L_x\right)L_s+\frac{1}{8}L_x^4\\
&+\left(\frac{1}{3}-\frac{1}{2}L_y\right)L_x^3+\left(\frac{1}{6}+\frac{1}{4}\pi^2-\frac{9}{4}L_y\right)L_x^2+\left(\frac{7}{2}L_y^2+\left(-\frac{13}{6}+\frac{1}{2}\pi^2\right)L_y\right.\\
&+\frac{32}{9}+3\zeta_3-\frac{1}{6}\pi^2\left.\right)L_x+\frac{1}{8}L_y^4-\frac{3}{4}L_y^3+\left(2+\frac{1}{2}\pi^2\right)L_y^2\\
&+\left(-3\zeta_3-\frac{32}{9}-\frac{3}{2}\pi^2\right)L_y+\frac{3}{2}\zeta_3+\frac{61}{36}\pi^2+\frac{11}{120}\pi^4
\end{aligned}
\tag{6.87}
$$

$$
\begin{aligned}
B_u \;=\; & \Bigg[6\,\mathrm{Li}_4\left(\frac{x-1}{x}\right)+\left(-\frac{22}{3}+6\,L_y-6\,L_x\right)\mathrm{Li}_3(x)+\left(-\frac{44}{3}-6\,L_x+6\,L_y\right)\mathrm{Li}_3(y)\\
&+\left(3\,L_x^2+\left(-6\,L_y+\frac{22}{3}\right)L_x+3\,L_y^2-\frac{44}{3}\,L_y+\pi^2\right)\mathrm{Li}_2(x)+\left(\frac{22}{3}\,L_x^2\right.\\
&\left.+\left(-22-\frac{44}{3}\,L_y\right)L_x-\frac{88}{3}+\frac{22}{3}\,\pi^2\right)L_s-\frac{1}{4}\,L_x^4+\left(2\,L_y+\frac{125}{18}\right)L_x^3\\
&+\left(-\frac{11}{2}\,L_y^2-\frac{743}{36}-\frac{25}{3}\,L_y+\frac{1}{2}\,\pi^2\right)L_x^2+\left(4\,L_y^3-\frac{28}{3}\,L_y^2+\left(\frac{133}{9}+\frac{7}{3}\,\pi^2\right)L_y\right.\\
&\left.+\frac{535}{72}\,\pi^2+7\,\zeta_3-\frac{49}{27}\right)L_x+\left(-\frac{5}{2}\,\pi^2+3\right)L_y^2+\left(-\frac{52}{3}+\frac{1}{9}\,\pi^2-6\,\zeta_3\right)L_y\\
&-\frac{1217}{72}\,\pi^2+\frac{30659}{648}-\frac{437}{720}\,\pi^4-\frac{179}{36}\,\zeta_3\Bigg)\left[\frac{t^2+s^2}{u^2}\right]+\left(-3\,\mathrm{Li}_4\left(\frac{x-1}{x}\right)+8\,\mathrm{Li}_4(x)\right.\\
&+12\,\mathrm{Li}_4(y)+\left(-4\,L_x-8\,L_y-\frac{11}{2}\right)\mathrm{Li}_3(x)+\left(\frac{5}{2}-10\,L_y-4\,L_x\right)\mathrm{Li}_3(y)\\
&+\left(\frac{3}{2}\,L_x^2+\left(\frac{11}{2}+L_y\right)L_x-\frac{5}{2}\,L_y^2+\frac{5}{2}\,L_y-\frac{7}{6}\,\pi^2\right)\mathrm{Li}_2(x)+\left(\frac{11}{3}\,L_x^2+\left(-\frac{11}{3}\right.\right.\\
&\left.\left.-\frac{22}{3}\,L_y\right)L_x+\frac{11}{3}\,\pi^2+\frac{22}{3}\,L_y+\frac{22}{3}\,L_y^2\right)L_s-\frac{1}{2}\,L_x^4+\left(\frac{131}{36}+\frac{7}{3}\,L_y\right)L_x^3\\
&+\left(-\frac{289}{36}-\frac{3}{4}\,\pi^2-\frac{15}{4}\,L_y^2-\frac{7}{2}\,L_y\right)L_x^2+\left(-\frac{11}{6}\,L_y^3+\frac{13}{12}\,L_y^2+\left(\frac{223}{18}+\frac{17}{6}\,\pi^2\right)L_y\right.\\
&\left.+\frac{73}{18}\,\pi^2+\frac{37}{9}+4\,\zeta_3\right)L_x+\frac{1}{12}\,L_y^4+\frac{73}{18}\,L_y^3+\left(\frac{3}{4}\,\pi^2-\frac{193}{18}\right)L_y^2+\left(\frac{191}{36}\,\pi^2\right.\\
&\left.+2\,\zeta_3-\frac{101}{9}\right)L_y-\frac{67}{12}\,\pi^2-\frac{7}{2}\,\zeta_3-\frac{61}{90}\,\pi^4\Bigg]\left[\frac{t^2-s^2}{u^2}\right]\\
&+\left[-7\,\pi^2-7\,L_x^2-7\,L_y^2+14\,L_x\,L_y\right]\frac{t^3}{u^2 s}+5\,\frac{s^3}{u^2 t}\,L_y^2-12\,\mathrm{Li}_4\left(\frac{x-1}{x}\right)+12\,\mathrm{Li}_4(x)\\
&+12\,\mathrm{Li}_4(y)+\left(-\frac{9}{2}-6\,L_y\right)\mathrm{Li}_3(x)+\left(6\,L_x-\frac{21}{2}-12\,L_y\right)\mathrm{Li}_3(y)\\
&+\left(-\frac{21}{2}\,L_y+\frac{9}{2}\,L_x-2\,\pi^2\right)\mathrm{Li}_2(x)+\frac{11}{3}\,L_x\,L_s-\frac{1}{2}\,L_x^4+\left(-\frac{5}{6}+2\,L_y\right)L_x^3\\
&+\left(-\frac{3}{2}\,L_y^2+\frac{17}{12}+\frac{9}{2}\,L_y-\pi^2\right)L_x^2+\left(\frac{1}{12}\,\pi^2-\frac{37}{4}\,L_y^2-6\,\zeta_3+\frac{1}{3}\,L_y-\frac{37}{9}-L_y^3\right)L_x\\
&-\frac{1}{6}\,L_y^3+\left(\frac{5}{2}-\frac{3}{2}\,\pi^2\right)L_y^2+\left(\frac{65}{12}\,\pi^2+6\,\zeta_3-3\right)L_y+\frac{5}{4}\,\pi^2-\frac{11}{20}\,\pi^4+\frac{19}{2}\,\zeta_3
\end{aligned}
\tag{6.88}
$$

$$
\begin{aligned}
C_u \;=\; & \Bigg[-8\,\mathrm{Li}_4\left(\frac{x-1}{x}\right)-16\,\mathrm{Li}_4(y)+\left(8\,L_x-8\,L_y\right)\mathrm{Li}_3(x)+\left(8\,L_x+8\,L_y\right)\mathrm{Li}_3(y)\\
&+\left(8\,L_x\,L_y+4\,L_y^2-4\,L_x^2-\frac{20}{3}\,\pi^2\right)\mathrm{Li}_2(x)+\frac{1}{12}\,L_x^4+\left(-\frac{5}{3}\,L_y-\frac{9}{2}\right)L_x^3\\
&+\left(9\,L_y+\frac{1}{4}+5\,L_y^2-\frac{11}{6}\,\pi^2\right)L_x^2+\left(\frac{8}{3}\,L_y^3+\left(13-3\,\pi^2\right)L_y-4\,\pi^2+\frac{189}{8}-14\,\zeta_3\right)L_x\\
&+\left(3-\frac{11}{3}\,\pi^2\right)L_y^2+\left(-9\,\pi^2+8\,\zeta_3\right)L_y+\frac{9}{5}\,\pi^4-\frac{289}{24}\,\pi^2-\frac{15}{2}\,\zeta_3+\frac{511}{32}\Bigg]\left[\frac{t^2+s^2}{u^2}\right]\\
&+\Bigg[24\,\mathrm{Li}_4\left(\frac{x-1}{x}\right)-24\,\mathrm{Li}_4(x)-12\,\mathrm{Li}_4(y)+\left(-4+16\,L_y+2\,L_x\right)\mathrm{Li}_3(x)\\
&+\left(-6-16\,L_x+24\,L_y\right)\mathrm{Li}_3(y)+\Bigg(-2\,L_x^2+\left(-8\,L_y+4\right)L_x-6\,L_y\\
&+6\,\pi^2+6\,L_y^2\Bigg)\mathrm{Li}_2(x)+\frac{4}{3}\,L_x^4+\left(-\frac{19}{3}\,L_y-\frac{8}{3}\right)L_x^3+\Bigg(7\,L_y+2\,L_y^2-\frac{15}{4}\\
&+\frac{25}{12}\,\pi^2\Bigg)L_x^2+\left(\frac{10}{3}\,L_y^3-10\,L_y^2+\left(\frac{15}{2}-\frac{1}{2}\,\pi^2\right)L_y-\frac{13}{12}\,\pi^2+6\,\zeta_3+6\right)L_x+\frac{1}{3}\,L_y^4\\
&+\frac{2}{3}\,L_y^3+\left(\frac{5}{3}\,\pi^2-6\right)L_y^2+\left(\frac{20}{3}\,\pi^2-8\,\zeta_3-12\right)L_y-\frac{61}{12}\,\pi^2+\frac{21}{20}\,\pi^4+8\,\zeta_3\Bigg]\left[\frac{t^2-s^2}{u^2}\right]\\
&+\left[-6\,L_x\,L_y+3\,L_y^2+3\,\pi^2+3\,L_x^2\right]\frac{t^3}{u^2 s}\\
&+3\,\frac{s^3}{u^2 t}\,L_y^2-2\,\mathrm{Li}_3(x)+2\,\mathrm{Li}_3(y)+\left(2\,L_y+2\,L_x\right)\mathrm{Li}_2(x)+\frac{3}{4}\,L_x^3\\
&+\left(-\frac{1}{2}\,L_y-\frac{15}{4}\right)L_x^2+\left(9\,L_y+\frac{7}{6}\,\pi^2-6\right)L_x+\frac{8}{3}\,L_y\,\pi^2-\frac{17}{4}\,\pi^2-3\,L_y^2-10\,\zeta_3
\end{aligned}
\tag{6.89}
$$

$$
\begin{aligned}
D_u \;=\;& \Bigg[-\frac{2}{3}\,\mathrm{Li}_3(x)-\frac{2}{3}\,\mathrm{Li}_3(y)+\left(\frac{2}{3}\,L_x-\frac{2}{3}\,L_y\right)\mathrm{Li}_2(x)-\frac{22}{9}\,L_s^2\\
&+\left(\frac{2}{3}\,L_x^2+\left(-2-\frac{4}{3}\,L_y\right)L_x+\frac{2}{3}\,L_y^2-\frac{26}{9}\,L_y+\frac{389}{54}+\frac{2}{3}\,\pi^2\right)L_s\\
&+\frac{2}{9}\,L_x^3+\left(\frac{1}{3}\,L_y-\frac{29}{18}\right)L_x^2+\left(\frac{4}{9}\,\pi^2-\frac{4}{3}\,L_y^2+\frac{11}{9}\,L_y+\frac{11}{6}\right)L_x\\
&+\frac{5}{9}\,L_y^3-\frac{37}{18}\,L_y^2+\left(\frac{3}{4}\,\pi^2+\frac{265}{54}\right)L_y-\frac{455}{54}-\frac{11}{12}\,\pi^2-\frac{37}{18}\,\zeta_3\Bigg]\left[\frac{t^2+s^2}{u^2}\right]\\
&+\Bigg[\left(\frac{1}{3}\,L_x^2+\left(-\frac{1}{3}-\frac{2}{3}\,L_y\right)L_x+\frac{1}{3}\,L_y+\frac{1}{3}\,\pi^2+\frac{1}{3}\,L_y^2\right)L_s\\
&+\frac{1}{9}\,L_x^3-\frac{13}{18}\,L_x^2+\left(-\frac{1}{3}\,L_y^2+\frac{1}{9}\,\pi^2+\frac{8}{9}+\frac{10}{9}\,L_y\right)L_x+\frac{2}{9}\,L_y^3\\
&-\frac{7}{18}\,L_y^2+\left(-\frac{8}{9}+\frac{2}{9}\,\pi^2\right)L_y-\frac{11}{18}\,\pi^2\Bigg]\left[\frac{t^2-s^2}{u^2}\right]\\
&+\left(\frac{1}{3}\,L_x-\frac{1}{3}\,L_y\right)L_s-\frac{1}{6}\,L_x^2+\left(-\frac{8}{9}+\frac{2}{3}\,L_y\right)L_x-\frac{5}{18}\,\pi^2+\frac{8}{9}\,L_y-\frac{1}{2}\,L_y^2
\end{aligned}
\tag{6.90}
$$

$$
\begin{aligned}
E_u \;=\;& \Bigg[\frac{4}{3}\,\mathrm{Li}_3(x)+\frac{8}{3}\,\mathrm{Li}_3(y)+\left(-\frac{4}{3}\,L_x+\frac{8}{3}\,L_y\right)\mathrm{Li}_2(x)\\
&+\left(-\frac{4}{3}\,L_x^2+\left(\frac{8}{3}\,L_y+4\right)L_x-\frac{4}{3}\,\pi^2+\frac{29}{6}\right)L_s-\frac{4}{9}\,L_x^3+\left(\frac{29}{9}-\frac{2}{3}\,L_y\right)L_x^2\\
&+\left(\frac{10}{3}\,L_y^2-\frac{223}{54}-\frac{29}{36}\,\pi^2-\frac{22}{9}\,L_y\right)L_x+\left(-\frac{10}{9}\,\pi^2+\frac{29}{6}\right)L_y\\
&-\frac{685}{81}-\frac{59}{18}\,\zeta_3+\frac{109}{36}\,\pi^2\Bigg]\left[\frac{t^2+s^2}{u^2}\right]\\
&+\Bigg[\left(-\frac{2}{3}\,L_x^2+\left(\frac{2}{3}+\frac{4}{3}\,L_y\right)L_x-\frac{4}{3}\,L_y-\frac{2}{3}\,\pi^2-\frac{4}{3}\,L_y^2\right)L_s-\frac{2}{9}\,L_x^3+\frac{13}{9}\,L_x^2\\
&+\left(\frac{2}{3}\,L_y^2-\frac{20}{9}\,L_y-\frac{2}{9}\,\pi^2-\frac{16}{9}\right)L_x-\frac{8}{9}\,L_y^3+\frac{14}{9}\,L_y^2+\left(\frac{32}{9}-\frac{8}{9}\,\pi^2\right)L_y+\pi^2\Bigg]\left[\frac{t^2-s^2}{u^2}\right]\\
&-\frac{2}{3}\,L_x\,L_s+\frac{1}{3}\,L_x^2+\left(-\frac{4}{3}\,L_y+\frac{16}{9}\right)L_x+\frac{1}{3}\,\pi^2
\end{aligned}
\tag{6.91}
$$

$$
F_u \;=\; \left[\frac{2}{9}\,L_s^2+\left(\frac{4}{9}\,L_y-\frac{20}{27}\right)L_s+\frac{2}{9}\,L_y^2-\frac{20}{27}\,L_y+\frac{50}{81}\right]\left[\frac{t^2+s^2}{u^2}\right]
\tag{6.92}
$$

6.6 Like-quark scattering two-loop contributions

In this section, we give explicit formulae for the ϵ-expansion of the two-loop contribution to the next-to-next-to-leading order term $\mathcal{B}^8(s,t,u)$.

As in Section 6.5, we divide the two-loop contributions as in

$$\mathcal{B}^{8\ (2\times 0)}(s,t,u) = \mathcal{P}oles_b + \mathcal{F}inite_b. \tag{6.93}$$

$\mathcal{P}oles_b$ contains infrared singularities that will be analytically canceled by the infrared singularities occurring in radiative processes of the same order (ultraviolet divergences are removed by renormalisation).

6.6.1 Infrared Pole Structure

We find that the pole structure in the $\overline{\mathrm{MS}}$ scheme can be written as

$$\begin{aligned}\mathcal{P}oles_b = -2\,\mathrm{Re}\Bigg[\quad & \frac{1}{2}\langle\overline{\mathcal{M}}^{(0)}|\boldsymbol{I}^{(1)}(\epsilon)\boldsymbol{I}^{(1)}(\epsilon)|\mathcal{M}^{(0)}\rangle - \frac{\beta_0}{\epsilon}\langle\overline{\mathcal{M}}^{(0)}|\boldsymbol{I}^{(1)}(\epsilon)|\mathcal{M}^{(0)}\rangle \\ & + \langle\overline{\mathcal{M}}^{(0)}|\boldsymbol{I}^{(1)}(\epsilon)|\mathcal{M}^{(1)\mathrm{fin}}\rangle \\ & + e^{-\epsilon\gamma}\frac{\Gamma(1-2\epsilon)}{\Gamma(1-\epsilon)}\left(\frac{\beta_0}{\epsilon}+K\right)\langle\overline{\mathcal{M}}^{(0)}|\boldsymbol{I}^{(1)}(2\epsilon)|\mathcal{M}^{(0)}\rangle \\ & + \langle\overline{\mathcal{M}}^{(0)}|\boldsymbol{H}^{(2)}(\epsilon)|\mathcal{M}^{(0)}\rangle + (s\leftrightarrow t)\Bigg],\end{aligned} \tag{6.94}$$

In Eq. (6.94), the symmetrisation under s and t exchange represents the additional effect of the s-channel tree graph interfering with the t-channel two-loop graphs.

The colour algebra is straightforward and we find that the s-t symmetric contributions proportional to

$$\langle\overline{\mathcal{M}}^{(0)}|\mathcal{M}^{(0)}\rangle = 2\left(\frac{N^2-1}{N}\right)(1-\epsilon)\left(\frac{u^2}{st}+\epsilon\right), \tag{6.95}$$

are given by

$$\langle\overline{\mathcal{M}}^{(0)}|\boldsymbol{I}^{(1)}(\epsilon)|\mathcal{M}^{(0)}\rangle = \langle\overline{\mathcal{M}}^{(0)}|\mathcal{M}^{(0)}\rangle \times\frac{e^{\epsilon\gamma}}{\Gamma(1-\epsilon)}\left(\frac{1}{\epsilon^2}+\frac{3}{2\epsilon}\right)\left[\frac{1}{N}\left(-\frac{\mu^2}{s}\right)^{\epsilon}+\frac{1}{N}\left(-\frac{\mu^2}{t}\right)^{\epsilon}-\frac{N^2+1}{N}\left(-\frac{\mu^2}{u}\right)^{\epsilon}\right] \tag{6.96}$$

$$\begin{aligned}\langle\overline{\mathcal{M}}^{(0)}|\boldsymbol{I}^{(1)}(\epsilon)\boldsymbol{I}^{(1)}(\epsilon)|\mathcal{M}^{(0)}\rangle &= \langle\overline{\mathcal{M}}^{(0)}|\mathcal{M}^{(0)}\rangle \\ &\times\frac{e^{2\epsilon\gamma}}{\Gamma(1-\epsilon)^2}\left(\frac{1}{\epsilon^2}+\frac{3}{2\epsilon}\right)^2\left\{\frac{N^4-3N^2-2}{N^2}\left(-\frac{\mu^2}{u}\right)^{\epsilon}\left[\left(-\frac{\mu^2}{s}\right)^{\epsilon}+\left(-\frac{\mu^2}{t}\right)^{\epsilon}\right]\right. \\ &+\frac{3N^2+1}{N^2}\left(-\frac{\mu^2}{u}\right)^{2\epsilon}-\frac{(N^2-2)(N^2+1)}{N^2}\left(-\frac{\mu^2}{s}\right)^{\epsilon}\left(-\frac{\mu^2}{t}\right)^{\epsilon} \\ &\left.+\frac{1}{N^2}\left(-\frac{\mu^2}{s}\right)^{2\epsilon}+\frac{1}{N^2}\left(-\frac{\mu^2}{t}\right)^{2\epsilon}\right\}\end{aligned} \tag{6.97}$$

and

$$\langle\overline{\mathcal{M}}^{(0)}|\boldsymbol{H}^{(2)}(\epsilon)|\mathcal{M}^{(0)}\rangle = \langle\overline{\mathcal{M}}^{(0)}|\mathcal{M}^{(0)}\rangle \times\frac{e^{\epsilon\gamma}}{2\epsilon\Gamma(1-\epsilon)}H^{(2)}\left[\left(-\frac{\mu^2}{s}\right)^{2\epsilon}+\left(-\frac{\mu^2}{t}\right)^{2\epsilon}-\left(-\frac{\mu^2}{u}\right)^{2\epsilon}\right], \tag{6.98}$$

where $H^{(2)}$ is defined in Eq. 6.58 and the constant K is given by Eq. 6.60. The square bracket in Eq. (6.98) is a guess simply motivated by summing over the antennae present in the quark-quark scattering process and on dimensional grounds. Different choices affect only the finite remainder.

The bracket of $\boldsymbol{I}^{(1)}$ between the t-channel tree graph and the finite part of the s-channel one-loop graphs is not symmetric under the exchange of s and t and is given by

$$\begin{aligned}\langle\overline{\mathcal{M}}^{(0)}|\boldsymbol{I}^{(1)}(\epsilon)|\mathcal{M}^{(1)\mathrm{fin}}\rangle &= \frac{e^{\epsilon\gamma}}{\Gamma(1-\epsilon)}\left(\frac{1}{\epsilon^2}+\frac{3}{2\epsilon}\right) \\ \times &\left\{\left[\frac{1}{N}\left(-\frac{\mu^2}{s}\right)^{\epsilon}+\frac{1}{N}\left(-\frac{\mu^2}{t}\right)^{\epsilon}-\frac{N^2+1}{N}\left(-\frac{\mu^2}{u}\right)^{\epsilon}\right]\Xi_1(s,t,u)\right. \\ &\left.+\left[\frac{N^2-1}{N}\left(-\frac{\mu^2}{s}\right)^{\epsilon}-\frac{1}{N}\left(-\frac{\mu^2}{t}\right)^{\epsilon}+\frac{1}{N}\left(-\frac{\mu^2}{u}\right)^{\epsilon}\right](N^2-1)\,\Xi_2(s,t,u)\right\}.\end{aligned} \tag{6.99}$$

The functions Ξ_1 and Ξ_2 appearing in Eq. (6.99) are finite and are given by

$$\begin{aligned}
\Xi_1(s,t,u) &= \frac{N^2-1}{2N^2}\left[\left(N^2-2\right)\xi_1(s,t,u)+2\xi_2(s,t,u)\right] \\
&- \frac{1}{2\epsilon\,(3-2\epsilon)}\left[\frac{N^2-1}{N}\left(6-7\epsilon-2\epsilon^2\right)-\frac{1}{N}\left(10\epsilon^2-4\epsilon^3\right)\right]\mathrm{Bub}(s)\langle\overline{\mathcal{M}}^{(0)}|\mathcal{M}^{(0)}\rangle \\
&- \frac{e^{\epsilon\gamma}}{\Gamma(1-\epsilon)}\left(\frac{1}{\epsilon^2}+\frac{3}{2\epsilon}\right) \\
&\times \left[\frac{1}{N}\left(-\frac{\mu^2}{s}\right)^{\epsilon}-\frac{2}{N}\left(-\frac{\mu^2}{u}\right)^{\epsilon}-\frac{N^2-2}{N}\left(-\frac{\mu^2}{t}\right)^{\epsilon}\right]\langle\overline{\mathcal{M}}^{(0)}|\mathcal{M}^{(0)}\rangle \\
&- \beta_0\left[\frac{1}{\epsilon}-\frac{3(1-\epsilon)}{3-2\epsilon}\mathrm{Bub}(s)\right]\langle\overline{\mathcal{M}}^{(0)}|\mathcal{M}^{(0)}\rangle
\end{aligned} \tag{6.100}$$

and

$$\begin{aligned}
\Xi_2(s,t,u) &= \frac{N^2-1}{2N^2}\Big[\xi_1(s,t,u)-\xi_2(s,t,u)\Big] \\
&-\frac{e^{\epsilon\gamma}}{\Gamma(1-\epsilon)}\left(\frac{1}{\epsilon^2}+\frac{3}{2\epsilon}\right)\left[\frac{1}{N}\left(-\frac{\mu^2}{u}\right)^{\epsilon}-\frac{1}{N}\left(-\frac{\mu^2}{t}\right)^{\epsilon}\right]\langle\overline{\mathcal{M}}^{(0)}|\mathcal{M}^{(0)}\rangle
\end{aligned} \tag{6.101}$$

with

$$\begin{aligned}
\xi_1(s,t,u) &= \frac{2u}{st}(1-2\epsilon)\left[u^2+t^2-2\epsilon\left(t^2+s^2\right)+\epsilon^2 s^2\right]\mathrm{Box}^6(s,t) \\
&+\frac{2}{st}\Big[2u^2-\epsilon\left(5s^2+6t^2+9st\right)+\left(2s^2+4t^2+st\right)\epsilon^2 \\
&\qquad+\left(s^2+3st\right)\epsilon^3-st\epsilon^4\Big]\left[\frac{\mathrm{Bub}(s)-\mathrm{Bub}(t)}{\epsilon}\right],
\end{aligned} \tag{6.102}$$

$$\begin{aligned}
\xi_2(s,t,u) &= \frac{2}{s}(1-2\epsilon)\left[2u^2-\epsilon\left(t^2+s^2+u^2\right)+3\epsilon^2 s^2+s^2\epsilon^3\right]\mathrm{Box}^6(s,u) \\
&+\frac{2}{st}\Big[2u^2-\epsilon\left(6s^2+6t^2+10st\right)+\left(3s^2+4t^2+3st\right)\epsilon^2 \\
&\qquad+\left(s^2+2st\right)\epsilon^3-st\epsilon^4\Big]\left[\frac{\mathrm{Bub}(s)-\mathrm{Bub}(u)}{\epsilon}\right].
\end{aligned} \tag{6.103}$$

The leading infrared singularity is $\mathcal{O}(1/\epsilon^4)$ and it is a very stringent check on the reliability of our calculation that the pole structure obtained by computing the Feynman diagrams agrees with that anticipated by Catani through to $\mathcal{O}(1/\epsilon)$. We therefore construct the finite remainder by subtracting Eq. (6.94) from the full result.

6.6.2 Finite contributions

In this subsection, we give explicit expressions for the finite two-loop contribution to $\mathcal{B}^8$, $\mathcal{F}inite_b$, which is given by

$$\mathcal{F}inite_b = -2\,\mathrm{Re}\left(\langle \mathcal{M}^{(0)}|\overline{\mathcal{M}}^{(2)\,\mathrm{fin}}\rangle + \langle \overline{\mathcal{M}}^{(0)}|\mathcal{M}^{(2)\,\mathrm{fin}}\rangle\right). \tag{6.104}$$

The identical-quark processes probed in high-energy hadron-hadron collisions are the mixed s- and t-channel process

$$q + \bar{q} \rightarrow \bar{q} + q,$$

controlled by $\mathcal{B}(s,t,u)$ (as well as the distinct quark matrix elements $\mathcal{A}(s,t,u)$ and $\mathcal{A}(t,s,u)$ as indicated in Section 6.1)), and the mixed t- and u-channel processes

$$\begin{aligned} q + q &\rightarrow q + q, \\ \bar{q} + \bar{q} &\rightarrow \bar{q} + \bar{q}, \end{aligned}$$

which are determined by the $\mathcal{B}(t,s,u)$. The analytic expressions for different channels are related by crossing symmetry. Once again, because of the complexity of analytic continuations we choose to give expressions describing $\mathcal{B}^8(s,t,u)$ and $\mathcal{B}^8(t,s,u)$ which are directly valid in the physical region $s > 0$ and $u, t < 0$, and are given in terms of logarithms and polylogarithms that have no imaginary parts.

Using the standard polylogarithm identities [82] we retain the polylogarithms with arguments x, $1-x$ and $(x-1)/x$, where

$$x = -\frac{t}{s}, \qquad y = -\frac{u}{s} = 1 - x, \qquad \frac{x-1}{x} = -\frac{u}{t}. \tag{6.105}$$

For convenience, we also introduce the following logarithms

$$L_x = \log\left(\frac{-t}{s}\right), \qquad L_y = \log\left(\frac{-u}{s}\right), \qquad L_s = \log\left(\frac{s}{\mu^2}\right), \tag{6.106}$$

where μ is the renormalisation scale. The common choice $\mu^2 = s$ corresponds to setting $L_s = 0$.

For each channel, we choose to present our results by grouping terms according to the power of the number of colours N and the number of light quarks N_F, so that in channel c

$$\mathcal{F}inite_{b,c} = 2\left(\frac{N^2-1}{N}\right)\left(N^2 A_c + B_c + \frac{1}{N^2}C_c + N\,N_F D_c + \frac{N_F}{N}E_c + N_F^2 F_c\right). \tag{6.107}$$

Here $c = st$ (ut) to denote the mixed s- and t-channel (u- and t-channel) processes respectively.

The process $q\bar{q}\to\bar{q}q$

We first give expressions for the mixed s-channel and t-channel annihilation process, $q\bar{q}\to\bar{q}q$. We find that

$$
\begin{aligned}
A_{st} \;=\;& \Bigg[2\,\mathrm{Li}_4(y) - 2\,\mathrm{Li}_4(x) + 2\,\mathrm{Li}_4\left(\frac{x-1}{x}\right) + \left(-2\,L_x + 12\right)\mathrm{Li}_3(y) + 4\,L_y\,L_x\,\mathrm{Li}_2(y) \\
&+\left(-\frac{23}{3} - 2\,L_x + 4\,L_y\right)\mathrm{Li}_3(x) + \left(\frac{23}{3}\,L_x + 12\,L_y + 2\,L_x^2 + \frac{5}{3}\,\pi^2\right)\mathrm{Li}_2(x) \\
&-\frac{121}{9}\,L_s^2 + \left(\frac{11}{3}\,L_x^2 + \left(-\frac{22}{9} - \frac{22}{3}\,L_y\right)L_x + \frac{11}{3}\,\pi^2 + \frac{22}{3}\,L_y^2 - 22\,L_y + \frac{592}{27}\right)L_s \\
&-\frac{1}{6}\,L_x^4 + \left(\frac{14}{9} + \frac{5}{3}\,L_y\right)L_x^3 + \left(-\frac{11}{12}\,\pi^2 + L_y^2 - \frac{31}{6} + \frac{13}{12}\,L_y\right)L_x^2 \\
&+\left(\frac{1}{3}\,L_y^3 + 6\,L_y^2 + \left(\frac{8}{3}\,\pi^2 + \frac{8}{9}\right)L_y + \frac{89}{36}\,\pi^2 - 6\,\zeta_3 + \frac{695}{216}\right)L_x \\
&-\frac{1}{6}\,L_y^4 + \frac{22}{9}\,L_y^3 + \left(-\frac{169}{18} + \frac{1}{6}\,\pi^2\right)L_y^2 + \left(\frac{61}{18}\,\pi^2 + 12\,\zeta_3 + \frac{1673}{108}\right)L_y \\
&-\frac{347}{18}\,\zeta_3 - \frac{121}{360}\,\pi^4 - \frac{23213}{1296} - \frac{8}{3}\,\pi^2\Bigg]\,\frac{u^2}{st} \\
&+\Bigg[-4\,\mathrm{Li}_4(x) + 24\,\mathrm{Li}_3(y) + \left(2\,L_x + 12\right)\mathrm{Li}_3(x) + \left(-\frac{2}{3}\,\pi^2 + 24\,L_y - 12\,L_x\right)\mathrm{Li}_2(x) \\
&+\frac{1}{12}\,L_x^4 - \frac{19}{12}\,L_x^3 + \left(-\frac{5}{2} + \frac{1}{3}\,\pi^2\right)L_x^2 + \left(-2\,\zeta_3 - \frac{29}{6}\,\pi^2 + 12\,L_y^2 + 5\,L_y\right)L_x \\
&+\frac{7}{45}\,\pi^4 - \frac{5}{2}\,\pi^2 - 12\,\zeta_3 - 4\,L_y\,\pi^2\Bigg]\,\frac{u}{s} + \Bigg[3\,L_x^2 + 3\,\pi^2 + 3\,L_y^2 - 6\,L_x\,L_y\Bigg]\,\frac{t^2}{s^2} + \Bigg[3\,L_y^2\Bigg]\,\frac{s^2}{t^2} \\
&-32\,\mathrm{Li}_4(y) - 32\,\mathrm{Li}_4\left(\frac{x-1}{x}\right) + 8\,L_x\,\mathrm{Li}_3(y) + \left(2 - 28\,L_y + 18\,L_x\right)\mathrm{Li}_3(x) \\
&+\left(-2\,L_x^2 + \left(-2 - 24\,L_y\right)L_x - 2\,\pi^2\right)\mathrm{Li}_2(x) - 28\,L_y\,L_x\,\mathrm{Li}_2(y) - \frac{11}{12}\,L_x^4 \\
&+\left(-\frac{7}{12} + \frac{14}{3}\,L_y\right)L_x^3 + \left(-32\,L_y^2 + \frac{1}{2}\,L_y + 2 + \frac{1}{2}\,\pi^2\right)L_x^2 \\
&+\left(\left(6 + \frac{20}{3}\,\pi^2\right)L_y - \frac{3}{2}\,\pi^2 - 18\,\zeta_3\right)L_x - 2\,\zeta_3 - 3\,\pi^2 - 6\,L_y^2 + 28\,L_y\,\zeta_3 + \frac{1}{3}\,\pi^4, \qquad (6.108)
\end{aligned}
$$

$$
\begin{aligned}
B_{st} \;=\; & \Bigg[-8\,\mathrm{Li}_4(y)-3\,\mathrm{Li}_4(x)-8\,\mathrm{Li}_4\left(\frac{x-1}{x}\right)+8\,L_x\,\mathrm{Li}_3(y)+\left(-6-12\,L_y+12\,L_x\right)\mathrm{Li}_3(x)\\
&+\left(-6\,\pi^2+6\,L_x-\frac{13}{2}\,L_x^2\right)\mathrm{Li}_2(x)-12\,L_y\,L_x\,\mathrm{Li}_2(y)\\
&+\left(-\frac{11}{6}\,L_x^2+\left(-\frac{22}{3}\,L_y+\frac{22}{3}\right)L_x-22\,L_y+\frac{11}{3}\,\pi^2+\frac{22}{3}\,L_y^2+\frac{176}{3}\right)L_s\\
&-\frac{7}{24}\,L_x^4-\frac{7}{9}\,L_x^3+\left(-\frac{17}{2}\,L_y^2+\frac{7}{2}\,L_y-\frac{19}{36}-\frac{1}{6}\,\pi^2\right)L_x^2\\
&+\left(L_y^3-\frac{27}{2}\,L_y^2+\left(-3\,\pi^2+\frac{251}{9}\right)L_y+\frac{181}{9}-\frac{5}{6}\,\pi^2-12\,\zeta_3\right)L_x\\
&-\frac{1}{2}\,L_y^4+\frac{103}{9}\,L_y^3+\left(-\frac{242}{9}+\frac{5}{2}\,\pi^2\right)L_y^2+\left(12\,\zeta_3+\frac{98}{3}+\frac{127}{18}\,\pi^2\right)L_y\\
&+\frac{581}{18}\,\zeta_3-\frac{31}{360}\,\pi^4-\frac{124}{9}\,\pi^2-\frac{30659}{324}\Bigg]\frac{u^2}{st}\\
&+\Bigg[-6\,\mathrm{Li}_4(x)+4\,L_x\,\mathrm{Li}_3(x)-L_x^2\,\mathrm{Li}_2(x)-\frac{22}{3}\,L_x\,L_s-\frac{1}{24}\,L_x^4-\frac{5}{18}\,L_x^3-\frac{47}{3}\,L_x^2\\
&+\left(24\,L_y+\frac{2}{9}\,\pi^2+\frac{128}{9}-4\,\zeta_3\right)L_x+\frac{1}{15}\,\pi^4-\frac{47}{3}\,\pi^2\Bigg]\frac{u}{s}\\
&+\Bigg[-8\,L_x\,L_y+4\,L_x^2+4\,\pi^2+4\,L_y^2\Bigg]\frac{t^2}{s^2}+\Bigg[4\,L_y^2\Bigg]\frac{s^2}{t^2}\\
&+16\,\mathrm{Li}_4(y)+16\,\mathrm{Li}_4\left(\frac{x-1}{x}\right)-16\,L_x\,\mathrm{Li}_3(y)+\left(-12\,L_x+8\,L_y+2\right)\mathrm{Li}_3(x)\\
&+\left(4\,L_x^2+4\,\pi^2-2\,L_x\right)\mathrm{Li}_2(x)+8\,L_y\,L_x\,\mathrm{Li}_2(y)+\frac{11}{3}\,L_x^2\,L_s+\frac{5}{8}\,L_x^4+\left(2-\frac{4}{3}\,L_y\right)L_x^3\\
&+\left(-L_y+4\,L_y^2-\frac{163}{9}\right)L_x^2+\left(\left(\frac{8}{3}\,\pi^2+8\right)L_y+\frac{11}{3}\,\pi^2+12\,\zeta_3\right)L_x\\
&-2\,\zeta_3-\frac{2}{3}\,\pi^4-4\,\pi^2-8\,L_y\,\zeta_3-8\,L_y^2, \qquad (6.109)
\end{aligned}
$$

$$
\begin{aligned}
C_{st} \;=\;& \Bigg[- 2\,\mathrm{Li}_4(y) - 5\,\mathrm{Li}_4(x) - 2\,\mathrm{Li}_4\left(\frac{x-1}{x}\right) + 2\,L_x\,\mathrm{Li}_3(y) + \Big(1 + 6\,L_x - 4\,L_y\Big)\,\mathrm{Li}_3(x) \\
&+\left(- \frac{7}{3}\,\pi^2 - \frac{5}{2}\,L_x^2 - L_x\right)\mathrm{Li}_2(x) - 4\,L_y\,L_x\,\mathrm{Li}_2(y) - \frac{1}{8}\,L_x^4 + \left(\frac{5}{12} - \frac{1}{3}\,L_y\right)L_x^3 + 3\,L_y^3 \\
&+\left(\frac{17}{12}\,\pi^2 + \frac{5}{4} - \frac{3}{4}\,L_y - \frac{5}{2}\,L_y^2\right)L_x^2 + \left(- \frac{9}{2}\,L_y^2 + \left(- \frac{5}{3}\,\pi^2 + 13\right)L_y + \frac{8}{3}\,\pi^2 - \frac{45}{8}\right)L_x \\
&+\left(- \frac{21}{2} + \frac{4}{3}\,\pi^2\right)L_y^2 + \left(\frac{93}{4} + \frac{13}{6}\,\pi^2 - 8\,\zeta_3\right)L_y + 19\,\zeta_3 - \frac{31}{6}\,\pi^2 - \frac{511}{16} - \frac{1}{90}\,\pi^4\Bigg]\,\frac{u^2}{st} \\
&+\Bigg[- 10\,\mathrm{Li}_4(x) + 6\,L_x\,\mathrm{Li}_3(x) + \left(- L_x^2 - \frac{2}{3}\,\pi^2\right)\mathrm{Li}_2(x) + \frac{1}{24}\,L_x^4 - \frac{13}{12}\,L_x^3 \\
&+\left(- \frac{5}{2} + \frac{1}{3}\,\pi^2\right)L_x^2 + \left(5\,L_y + \frac{5}{2}\,\pi^2 - 6\,\zeta_3 + 12\right)L_x + \frac{2}{9}\,\pi^4 - \frac{5}{2}\,\pi^2\Bigg]\,\frac{u}{s} \\
&+\Big[L_x^2 - 2\,L_x\,L_y + \pi^2 + L_y^2\Big]\,\frac{t^2}{s^2} + \Big[L_y^2\Big]\,\frac{s^2}{t^2} \\
&+8\,\mathrm{Li}_4(y) + 8\,\mathrm{Li}_4\left(\frac{x-1}{x}\right) - 8\,L_x\,\mathrm{Li}_3(y) + \Big(- 6\,L_x + 4\,L_y + 4\Big)\,\mathrm{Li}_3(x) \\
&+\Big(- 4\,L_x + 2\,L_x^2 + 2\,\pi^2\Big)\,\mathrm{Li}_2(x) + 4\,L_y\,L_x\,\mathrm{Li}_2(y) + \frac{13}{24}\,L_x^4 + \left(- \frac{5}{12} - \frac{2}{3}\,L_y\right)L_x^3 \\
&+\left(- 9 + 2\,L_y^2 - \frac{7}{6}\,\pi^2 - \frac{1}{2}\,L_y\right)L_x^2 + \left(\left(2 + \frac{4}{3}\,\pi^2\right)L_y - \frac{3}{2}\,\pi^2 + 6\,\zeta_3\right)L_x \\
&-4\,\zeta_3 - \frac{1}{3}\,\pi^4 - 2\,L_y^2 - 4\,L_y\,\zeta_3 - \pi^2, \qquad (6.110)
\end{aligned}
$$

$$
\begin{aligned}
D_{st} \;=\;& \Bigg[\frac{2}{3}\,\mathrm{Li}_3(x) - \frac{2}{3}\,L_x\,\mathrm{Li}_2(x) + \frac{44}{9}\,L_s^2 \\
&+\left(- \frac{2}{3}\,L_x^2 + \left(\frac{4}{3}\,L_y + \frac{26}{9}\right)L_x + 4\,L_y - \frac{4}{3}\,L_y^2 - \frac{389}{27} - \frac{2}{3}\,\pi^2\right)L_s \\
&-\frac{5}{9}\,L_x^3 + \left(\frac{2}{3}\,L_y + \frac{37}{18}\right)L_x^2 + \left(- \frac{13}{18}\,\pi^2 - \frac{11}{9}\,L_y - \frac{40}{9}\right)L_x - \frac{4}{9}\,L_y^3 + \frac{29}{9}\,L_y^2 \\
&+\left(- \frac{11}{9}\,\pi^2 - \frac{149}{27}\right)L_y - \frac{2}{9}\,\pi^2 + \frac{43}{9}\,\zeta_3 + \frac{455}{27}\Bigg]\,\frac{u^2}{st}, \qquad (6.111)
\end{aligned}
$$

$$
\begin{aligned}
E_{st} &= \Bigg[2\,\mathrm{Li}_3(x) - 2\,L_x\,\mathrm{Li}_2(x) + \left(\frac{1}{3}\,L_x^2 + \left(\frac{4}{3}\,L_y - \frac{4}{3}\right)L_x - \frac{2}{3}\,\pi^2 - \frac{4}{3}\,L_y^2 + 4\,L_y - \frac{29}{3}\right)L_s \\
&\quad + \frac{1}{9}\,L_x^3 - \frac{19}{18}\,L_x^2 + \left(-\frac{11}{9}\,L_y + \frac{1}{3}\,\pi^2 - \frac{43}{9}\right)L_x - \frac{4}{9}\,L_y^3 + \frac{29}{9}\,L_y^2 + \left(-\frac{14}{9}\,\pi^2 - \frac{11}{3}\right)L_y \\
&\quad + \frac{29}{9}\,\zeta_3 + \frac{1370}{81} + \frac{22}{9}\,\pi^2\Bigg]\frac{u^2}{st} \\
&\quad + \left[\frac{4}{3}\,L_x\,L_s + \frac{1}{9}\,L_x^3 + \frac{2}{3}\,L_x^2 + \left(-\frac{2}{9}\,\pi^2 - \frac{32}{9}\right)L_x + \frac{2}{3}\,\pi^2\right]\frac{u}{s} \\
&\quad - \frac{1}{3}\,L_x^3 + \frac{16}{9}\,L_x^2 - \frac{2}{3}\,L_x\,\pi^2 - \frac{2}{3}\,L_x^2\,L_s,
\end{aligned}
\tag{6.112}
$$

$$
F_{st} = \left[-\frac{4}{9}\,L_s^2 + \left(\frac{40}{27} - \frac{4}{9}\,L_x\right)L_s + \frac{2}{9}\,\pi^2 - \frac{100}{81} + \frac{20}{27}\,L_x - \frac{2}{9}\,L_x^2\right]\frac{u^2}{st}. \tag{6.113}
$$

Some of these results overlap with the analytic expressions presented in Ref. [19] for the QED process $e^+e^-\rightarrow e^+e^-$. To obtain the QED limit from a QCD calculation corresponds to setting $C_A = 0$, $C_F = 1$, $T_R = 1$ as well as setting the cubic Casimir $C_3 = (N^2-1)(N^2-2)/N^2$ to 0. This means that we can directly compare $E_{st}(\propto C_F T_R\,N_F)$ and $F_{st}(\propto T_R^2\,N_F^2)$ but *not* C_{st} which receives contributions from both C_3 and C_F^2. We see that (6.112) and (6.113) agree with Eqs. (2.50) and (2.51) of [19] respectively.

The other coefficients, A_{st}, B_{st}, C_{st} and D_{st} are new results.

The process $q+q\to q+q$

The mixed t- and u-channel process, $q+q\to q+q$ is fixed by $\mathcal{B}^8(t,s,u)$. We find that the finite two-loop contribution is given by Eq. (6.107) with

$$\begin{aligned}
A_{ut} \;=\;& \Bigg[2\,\mathrm{Li}_4\left(\frac{x-1}{x}\right) - 2\,\mathrm{Li}_4(x) - 2\,\mathrm{Li}_4(y) + \left(2\,L_x + 2\,L_y + \frac{23}{3}\right)\mathrm{Li}_3(x) + \left(4\,L_y + \frac{59}{3}\right)\mathrm{Li}_3(y) \\
&+\left(-2\,L_x^2 + \left(-\frac{23}{3} + 2\,L_y\right)L_x + \frac{1}{3}\,\pi^2 + \frac{59}{3}\,L_y\right)\mathrm{Li}_2(x) + \left(2\,L_x\,L_y - 2\,L_y^2\right)\mathrm{Li}_2(y) \\
&-\frac{121}{9}\,L_s^2 + \left(\frac{11}{3}\,L_x^2 + \frac{592}{27} - \frac{22}{9}\,L_y - \frac{22}{9}\,L_x + \frac{11}{3}\,L_y^2\right)L_s - \frac{1}{6}\,L_x^4 + \left(-\frac{4}{3}\,L_y + \frac{14}{9}\right)L_x^3 \\
&+\left(-\frac{25}{12}\,L_y - \frac{31}{6} + \frac{7}{12}\,\pi^2 + \frac{7}{2}\,L_y^2\right)L_x^2 - \frac{1}{3}\,L_y^4 + \frac{113}{36}\,L_y^3 + \left(-\frac{8}{3} + \frac{7}{12}\,\pi^2\right)L_y^2 \\
&+\left(-\frac{2}{3}\,L_y^3 + \frac{77}{6}\,L_y^2 + \left(7 - \frac{17}{6}\,\pi^2\right)L_y + \frac{695}{216} + \frac{59}{36}\,\pi^2 - 8\,\zeta_3\right)L_x \\
&+\left(\frac{695}{216} - 8\,\zeta_3 - \frac{73}{18}\,\pi^2\right)L_y - \frac{23213}{1296} + \frac{17}{24}\,\pi^4 - \frac{485}{18}\,\zeta_3 + \frac{73}{18}\,\pi^2\Bigg]\frac{s^2}{ut} \\
&+\Bigg[4\,\mathrm{Li}_4\left(\frac{x-1}{x}\right) + \left(-2\,L_x + 2\,L_y - 12\right)\mathrm{Li}_3(x) + \left(2\,L_y + 12 - 2\,L_x\right)\mathrm{Li}_3(y) \\
&+\left(\left(2\,L_y + 12\right)L_x + \frac{2}{3}\,\pi^2 + 12\,L_y\right)\mathrm{Li}_2(x) + 2\,L_y\,L_x\,\mathrm{Li}_2(y) + \frac{1}{4}\,L_x^4 + \left(-L_y - \frac{19}{12}\right)L_x^3 \\
&+\left(-\frac{5}{2} + \frac{1}{6}\,\pi^2 + \frac{5}{2}\,L_y^2 + \frac{19}{4}\,L_y\right)L_x^2 + \left(\frac{29}{4}\,L_y^2 - \frac{1}{3}\,L_y\,\pi^2 + \frac{29}{12}\,\pi^2 + \frac{1}{3}\,L_y^3\right)L_x \\
&-\frac{1}{12}\,L_y^4 + \frac{19}{12}\,L_y^3 + \left(\frac{1}{6}\,\pi^2 + \frac{5}{2}\right)L_y^2 - \frac{53}{12}\,L_y\,\pi^2 - \frac{1}{60}\,\pi^4\Bigg]\frac{s}{u} + \Big[3\,L_x^2\Big]\frac{t^2}{u^2} + \Big[3\,L_y^2\Big]\frac{u^2}{t^2} \\
&+32\,\mathrm{Li}_4(x) + 32\,\mathrm{Li}_4(y) + \left(-18\,L_x - 10\,L_y - 2\right)\mathrm{Li}_3(x) + \left(-2 - 10\,L_x - 18\,L_y\right)\mathrm{Li}_3(y) \\
&+\left(2\,L_x^2 + \left(2 - 10\,L_y\right)L_x - 2\,L_y\right)\mathrm{Li}_2(x) + \left(-10\,L_x\,L_y + 2\,L_y^2\right)\mathrm{Li}_2(y) \\
&+\frac{5}{12}\,L_x^4 + \left(-L_y - \frac{7}{12}\right)L_x^3 + \left(2 - \frac{27}{2}\,L_y^2 + \frac{5}{4}\,L_y - \frac{4}{3}\,\pi^2\right)L_x^2 \\
&+\left(-L_y^3 - \frac{3}{4}\,L_y^2 + \left(-10 + 6\,\pi^2\right)L_y - \frac{1}{4}\,\pi^2\right)L_x + \frac{5}{12}\,L_y^4 - \frac{7}{12}\,L_y^3 + \left(2 - \frac{4}{3}\,\pi^2\right)L_y^2 \\
&+\frac{1}{12}\,L_y\,\pi^2 - \frac{391}{180}\,\pi^4 + 5\,\pi^2,
\end{aligned} \tag{6.114}$$

$$
\begin{aligned}
B_{ut} \; = \; & \Bigg[3\,\mathrm{Li}_4\left(\frac{x-1}{x}\right) + 8\,\mathrm{Li}_4(x) + 8\,\mathrm{Li}_4(y) + \left(-12\,L_x + 6\right)\mathrm{Li}_3(x) + \left(6 - 8\,L_y - 4\,L_x\right)\mathrm{Li}_3(y) \\
& + \left(\frac{13}{2}\,L_x^2 + \left(-6 - L_y\right)L_x + 6\,L_y + \frac{1}{2}\,\pi^2\right)\mathrm{Li}_2(x) + \frac{11}{2}\,L_y^2\,\mathrm{Li}_2(y) \\
& + \left(-\frac{11}{6}\,L_x^2 + \left(11\,L_y + \frac{22}{3}\right)L_x - \frac{11}{6}\,L_y^2 + \frac{176}{3} + \frac{44}{3}\,L_y - \frac{11}{2}\,\pi^2\right)L_s + \frac{1}{6}\,L_x^4 \\
& + \left(-\frac{7}{9} + \frac{2}{3}\,L_y\right)L_x^3 + \left(-3\,L_y + 4\,\pi^2 - \frac{19}{36} - \frac{1}{4}\,L_y^2\right)L_x^2 + \frac{1}{12}\,L_y^4 \\
& + \left(L_y^3 + \frac{13}{6}\,L_y^2 + \left(-\frac{39}{2} - \frac{1}{3}\,\pi^2\right)L_y + \frac{181}{9} + \frac{53}{6}\,\pi^2\right)L_x - \frac{1}{2}\,L_y^3 \\
& + \left(\frac{545}{36} + 4\,\pi^2\right)L_y^2 + \left(\frac{53}{9} + \frac{76}{9}\,\pi^2\right)L_y - \frac{161}{120}\,\pi^4 - \frac{30659}{324} + \frac{473}{18}\,\zeta_3 + \frac{113}{4}\,\pi^2\Bigg]\frac{s^2}{ut} \\
& + \Bigg[6\,\mathrm{Li}_4\left(\frac{x-1}{x}\right) + \left(4\,L_y - 4\,L_x\right)\mathrm{Li}_3(x) + \left(4\,L_y - 4\,L_x\right)\mathrm{Li}_3(y) \\
& + \left(L_x^2 + \pi^2 + 2\,L_x\,L_y\right)\mathrm{Li}_2(x) + \left(-L_y^2 + 4\,L_x\,L_y\right)\mathrm{Li}_2(y) + \left(\frac{22}{3}\,L_y - \frac{22}{3}\,L_x\right)L_s \\
& + \frac{5}{24}\,L_x^4 + \left(-\frac{5}{18} - \frac{5}{6}\,L_y\right)L_x^3 + \left(-\frac{47}{3} + \frac{5}{6}\,L_y + \frac{1}{4}\,\pi^2 + \frac{15}{4}\,L_y^2\right)L_x^2 \\
& + \left(\frac{128}{9} - \frac{1}{6}\,L_y^3 - \frac{11}{18}\,\pi^2 - \frac{1}{2}\,L_y\,\pi^2 - \frac{5}{6}\,L_y^2\right)L_x + \frac{1}{24}\,L_y^4 + \frac{5}{18}\,L_y^3 + \left(\frac{47}{3} + \frac{1}{4}\,\pi^2\right)L_y^2 \\
& + \left(-\frac{128}{9} + \frac{11}{18}\,\pi^2\right)L_y - \frac{1}{40}\,\pi^4\Bigg]\frac{s}{u} + \Bigg[4\,L_x^2\Bigg]\frac{t^2}{u^2} + \Bigg[4\,L_y^2\Bigg]\frac{u^2}{t^2} \\
& -16\,\mathrm{Li}_4(x) - 16\,\mathrm{Li}_4(y) + \left(12\,L_x - 4\,L_y - 2\right)\mathrm{Li}_3(x) + \left(-4\,L_x - 2 + 12\,L_y\right)\mathrm{Li}_3(y) \\
& + \left(-4\,L_x^2 + \left(2 - 4\,L_y\right)L_x - 2\,L_y\right)\mathrm{Li}_2(x) + \left(-4\,L_y^2 - 4\,L_x\,L_y\right)\mathrm{Li}_2(y) \\
& + \left(\frac{11}{3}\,L_y^2 + \frac{11}{3}\,L_x^2 + \frac{11}{3}\,\pi^2 - \frac{22}{3}\,L_x\,L_y\right)L_s - \frac{1}{24}\,L_x^4 + \left(-\frac{7}{6}\,L_y + 2\right)L_x^3 \\
& + \left(\frac{5}{12}\,\pi^2 - \frac{163}{9} - \frac{17}{4}\,L_y^2 - \frac{4}{3}\,L_y\right)L_x^2 + \left(-\frac{7}{6}\,L_y^3 - \frac{10}{3}\,L_y^2 + \left(\frac{1}{2}\,\pi^2 + \frac{254}{9}\right)L_y + \frac{7}{3}\,\pi^2\right)L_x \\
& -\frac{1}{24}\,L_y^4 + 2\,L_y^3 + \left(\frac{5}{12}\,\pi^2 - \frac{163}{9}\right)L_y^2 + \frac{8}{3}\,L_y\,\pi^2 + \frac{421}{360}\,\pi^4 - \frac{127}{9}\,\pi^2,
\end{aligned}
\tag{6.115}
$$

$$
\begin{aligned}
C_{ut} \;=\; & \Bigg[5\,\mathrm{Li}_4\left(\frac{x-1}{x}\right) + 2\,\mathrm{Li}_4(x) + 2\,\mathrm{Li}_4(y) + \left(2\,L_y - 6\,L_x - 1\right)\mathrm{Li}_3(x) + \left(-4\,L_x - 1\right)\mathrm{Li}_3(y) \\
& + \left(\frac{5}{2}\,L_x^2 + \left(1 + L_y\right)L_x - L_y + \frac{5}{6}\,\pi^2\right)\mathrm{Li}_2(x) + \left(2\,L_x\,L_y + \frac{3}{2}\,L_y^2\right)\mathrm{Li}_2(y) \\
& + \frac{1}{6}\,L_x^4 + \frac{5}{12}\,L_x^3 + \left(\frac{7}{4}\,\pi^2 - \frac{1}{2}\,L_y + \frac{5}{4} + \frac{5}{4}\,L_y^2\right)L_x^2 - \frac{1}{12}\,L_y^4 + \frac{3}{2}\,L_y^3 \\
& + \left(L_y^3 - \frac{19}{4}\,L_y^2 + \left(-\frac{5}{6}\,\pi^2 - \frac{31}{2}\right)L_y + \frac{41}{12}\,\pi^2 + 6\,\zeta_3 - \frac{45}{8}\right)L_x + \left(\frac{7}{4}\,\pi^2 + \frac{15}{4}\right)L_y^2 \\
& + \left(-\frac{141}{8} + 6\,\zeta_3 + \frac{13}{3}\,\pi^2\right)L_y - \frac{511}{16} + 20\,\zeta_3 + \frac{109}{12}\,\pi^2 - \frac{49}{90}\,\pi^4\Bigg]\frac{s^2}{ut} \\
& + \Bigg[10\,\mathrm{Li}_4\left(\frac{x-1}{x}\right) + \left(-6\,L_x + 6\,L_y\right)\mathrm{Li}_3(x) + \left(-6\,L_x + 6\,L_y\right)\mathrm{Li}_3(y) \\
& + \left(L_x^2 + 4\,L_x\,L_y + \frac{5}{3}\,\pi^2\right)\mathrm{Li}_2(x) + \left(6\,L_x\,L_y - L_y^2\right)\mathrm{Li}_2(y) + \frac{11}{24}\,L_x^4 + \left(-\frac{11}{6}\,L_y - \frac{13}{12}\right)L_x^3 \\
& + \left(\frac{25}{4}\,L_y^2 + \frac{13}{4}\,L_y + \frac{5}{12}\,\pi^2 - \frac{5}{2}\right)L_x^2 + \left(-\frac{3}{4}\,\pi^2 + 12 + \frac{1}{6}\,L_y^3 - \frac{13}{4}\,L_y^2 - \frac{5}{6}\,L_y\,\pi^2\right)L_x \\
& - \frac{1}{24}\,L_y^4 + \frac{13}{12}\,L_y^3 + \left(\frac{5}{2} + \frac{5}{12}\,\pi^2\right)L_y^2 + \left(-12 + \frac{3}{4}\,\pi^2\right)L_y - \frac{1}{24}\,\pi^4\Bigg]\frac{s}{u} + \Bigg[L_x^2\Bigg]\frac{t^2}{u^2} \\
& + \Bigg[L_y^2\Bigg]\frac{u^2}{t^2} - 8\,\mathrm{Li}_4(x) - 8\,\mathrm{Li}_4(y) + \left(6\,L_x - 2\,L_y - 4\right)\mathrm{Li}_3(x) + \left(-4 - 2\,L_x + 6\,L_y\right)\mathrm{Li}_3(y) \\
& + \left(-2\,L_x^2 + \left(4 - 2\,L_y\right)L_x - 4\,L_y\right)\mathrm{Li}_2(x) + \left(-2\,L_x\,L_y - 2\,L_y^2\right)\mathrm{Li}_2(y) \\
& + \frac{5}{24}\,L_x^4 + \left(-\frac{3}{2}\,L_y - \frac{5}{12}\right)L_x^3 + \left(-9 - \frac{3}{4}\,L_y^2 + \frac{7}{4}\,L_y + \frac{5}{12}\,\pi^2\right)L_x^2 \\
& + \left(-\frac{3}{2}\,L_y^3 - \frac{9}{4}\,L_y^2 + \left(16 - \frac{1}{6}\,\pi^2\right)L_y + \frac{1}{4}\,\pi^2\right)L_x + \frac{5}{24}\,L_y^4 - \frac{5}{12}\,L_y^3 + \left(-9 + \frac{5}{12}\,\pi^2\right)L_y^2 \\
& + \frac{11}{12}\,L_y\,\pi^2 + \frac{203}{360}\,\pi^4 - 8\,\pi^2,
\end{aligned}
\tag{6.116}
$$

$$
\begin{aligned}
D_{ut} \;=\; & \Bigg[-\frac{2}{3}\,\mathrm{Li}_3(x) - \frac{2}{3}\,\mathrm{Li}_3(y) + \left(-\frac{2}{3}\,L_y + \frac{2}{3}\,L_x\right)\mathrm{Li}_2(x) + \frac{44}{9}\,L_s^2 \\
& + \left(\frac{26}{9}\,L_x - \frac{2}{3}\,L_x^2 + \frac{26}{9}\,L_y - \frac{389}{27} - \frac{2}{3}\,L_y^2\right)L_s - \frac{5}{9}\,L_x^3 + \left(\frac{37}{18} + \frac{1}{3}\,L_y\right)L_x^2 \\
& + \left(-\frac{7}{18}\,\pi^2 - \frac{1}{3}\,L_y^2 - \frac{40}{9}\right)L_x - \frac{5}{9}\,L_y^3 + \frac{37}{18}\,L_y^2 + \left(-\frac{40}{9} - \frac{5}{18}\,\pi^2\right)L_y \\
& + \frac{49}{9}\,\zeta_3 - \frac{25}{18}\,\pi^2 + \frac{455}{27}\Bigg]\frac{s^2}{ut},
\end{aligned}
\tag{6.117}
$$

$$
\begin{aligned}
E_{ut} \;=\; & \Bigg[-2\,\mathrm{Li}_3(x) - 2\,\mathrm{Li}_3(y) + \left(-2\,L_y + 2\,L_x \right) \mathrm{Li}_2(x) + \frac{1}{9}\,L_x^3 - \frac{19}{18}\,L_x^2 \\
& + \left(\frac{1}{3}\,L_x^2 + \left(-2\,L_y - \frac{4}{3} \right) L_x - \frac{29}{3} + \frac{1}{3}\,L_y^2 + \pi^2 - \frac{8}{3}\,L_y \right) L_s \\
& + \left(-\frac{5}{3}\,L_y^2 + 2\,L_y + \frac{2}{3}\,\pi^2 - \frac{43}{9} \right) L_x - \frac{31}{18}\,L_y^2 + \left(\frac{8}{9}\,\pi^2 - \frac{11}{9} \right) L_y \\
& + \frac{1370}{81} - \frac{5}{2}\,\pi^2 + \frac{47}{9}\,\zeta_3 \Bigg] \frac{s^2}{ut} \\
& + \Bigg[\left(\frac{4}{3}\,L_x - \frac{4}{3}\,L_y \right) L_s + \frac{1}{9}\,L_x^3 + \left(-\frac{1}{3}\,L_y + \frac{2}{3} \right) L_x^2 + \left(\frac{1}{3}\,L_y^2 + \frac{1}{9}\,\pi^2 - \frac{32}{9} \right) L_x \\
& - \frac{1}{9}\,L_y^3 - \frac{2}{3}\,L_y^2 + \left(-\frac{1}{9}\,\pi^2 + \frac{32}{9} \right) L_y \Bigg] \frac{s}{u} \\
& + \left(-\frac{2}{3}\,L_y^2 - \frac{2}{3}\,L_x^2 - \frac{2}{3}\,\pi^2 + \frac{4}{3}\,L_x\,L_y \right) L_s - \frac{1}{3}\,L_x^3 + \left(\frac{1}{3}\,L_y + \frac{16}{9} \right) L_x^2 \\
& + \left(-\frac{32}{9}\,L_y + \frac{1}{3}\,L_y^2 - \frac{1}{3}\,\pi^2 \right) L_x + \frac{16}{9}\,L_y^2 - \frac{1}{3}\,L_y^3 + \frac{16}{9}\,\pi^2 - \frac{1}{3}\,L_y\,\pi^2,
\end{aligned} \tag{6.118}
$$

$$
F_{ut} \;=\; \left[-\frac{4}{9}\,L_s^2 + \left(-\frac{4}{9}\,L_y + \frac{40}{27} - \frac{4}{9}\,L_x \right) L_s + \frac{20}{27}\,L_x - \frac{2}{9}\,L_x^2 + \frac{20}{27}\,L_y - \frac{2}{9}\,L_y^2 - \frac{100}{81} \right] \frac{s^2}{ut}. \tag{6.119}
$$

As in Section 6.6.2, we can compare some of these results with the analytic expressions presented in Ref. [19] for the QED process $e^+e^-\to e^+e^-$, and we see that (6.118) and (6.119) agree with Eqs. (2.55) and (2.56) of [19] respectively.

The other coefficients, A_{ut}, B_{ut}, C_{ut} and D_{ut} represent new results.

6.7 Summary

In this chapter we presented the $\mathcal{O}(\alpha_s^4)$ QCD corrections to the $2\to 2$ scattering processes $q\bar{q}\to q\prime\bar{q}\prime$, $qq\to q\bar{q}$ and the associated crossed processes in the high energy limit, where the quark masses can be ignored. We computed renormalised analytic expressions for the interference of the tree-level diagrams with the two-loop ones and for the self-interference of one-loop graphs in the $\overline{\mathrm{MS}}$ scheme. Throughout we employed conventional dimensional regularisation.

The renormalised matrix elements are infrared divergent and contain poles down to $\mathcal{O}(1/\epsilon^4)$. The singularity structure of one- and two-loop diagrams has been thoroughly studied by Catani [17] who provided a procedure for predicting the infrared behaviour of renormalised amplitudes. The anticipated pole structure agrees exactly with that obtained by direct Feynman diagram evaluation. In fact Catani's method does not determine the $1/\epsilon$ poles exactly, but expects that the remaining unpredicted $1/\epsilon$ poles are non-logarithmic and proportional to constants (colour factors, π^2 and ζ_3). We find that this is indeed the case, and the constant $H^{(2)}$ is given in Eq. 6.58. This provides a very strong check on the reliability of our results. Similarly, the infrared divergent structure of the squared one-loop diagrams we found by direct evaluation agrees with the expected pole structure.

The results presented here, together with those computed for quark-gluon and gluon-gluon scattering [1, 5] complete the set of matrix-elements required for the next-to-next-to-leading order predictions for jet cross sections in hadron-hadron collisions. On their own, they are insufficient to make physical predictions and much work remains to be done. First, a systematic procedure for analytically canceling the infrared divergences between the tree-level $2\rightarrow4$, the one-loop $2\rightarrow3$ and the $2\rightarrow2$ processes needs to be established for semi-inclusive jet cross sections. Second, there are additional problems due to initial state radiation. Third, a numerical implementation of the various contributions must be developed, enabling the construction of numerical programs to provide next-to-next-to-leading order QCD estimates of jet production in hadron collisions.

Chapter 7

Conclusions

The purpose of this thesis has been the calculation of matrix elements for massless $2 \to 2$ QCD scattering processes. This is a very important step in the construction of numerical programs for the cross-section of hadron-hadron jet production at NNLO. It is expected that knowledge of the cross-section at this order will increase the precision of the theoretical predictions and will match better the anticipated experimental accuracy at the Tevatron and LHC.

The matrix-elements involve Feynman diagrams which are divergent in $D = 4$ dimensions. In Chapter 1 we described the Conventional Dimensional Regularisation (CDR) method which serves to quantify the divergences by shifting the number of dimensions to $D = 4 - 2\epsilon$, where ϵ may be considered as a small non-integer number. The Feynman integrals manifest their singular behavior as poles in $\epsilon = 0$.

Singularities arise from two different limits. The first is related to the ultra-violet behavior of the integrals where the loop momenta become infinite. The singularities of this type can be consistently absorbed at each order in perturbation series, by a multiplicative renormalisation of the fields and parameters of the QCD Lagrangian. Renormalisation is not a uniquely defined procedure, and fixed order perturbation theory results depend on the prescription used for the subtraction of the divergences. We have chosen to renormalise with the $\overline{\text{MS}}$ scheme.

The second type of divergences is associated with the existence of massless particles in the theory. The denominators of the gluon and light-quark propagators in loop integrals often vanish for some loop-momentum configurations, leading to the generation of (infrared) singularities. In Chapter 2 we saw that the IR divergences cancel for appropriately defined physical quantities, where we sum over all degenerate external states. Based on that, Catani worked out a process-independent algorithm to predict the singular behavior of two-loop renormalised amplitudes. We made an extensive use of his formalism in order to verify our results for the quark scattering NNLO virtual corrections.

The calculation of one and two loop Feynman integrals is a very challenging task. In Chapter 3 we detailed a general algorithm, based on the Schwinger parametrisation, which relates tensor multi-loop integrals to scalar integrals of the same topology with extra powers of propagators and in higher dimension. Then we concentrated on the evaluation of scalar one and two-loop integrals through their representations in Feynman parameters providing analytic expressions for several of them in terms of Γ functions.

In order to obtain expressions for more difficult integrals with a richer structure in terms of hypergeometric functions, we employed a Mellin-Barnes (MB) decomposition of the sums raised to a power in the Feynman representation. After an explicit integration of the Feynman parameters we were able to derive representations of one-loop Feynman integrals in a quite general way. For multi-loop integrals we used the insertion method using one-loop MB representations as building blocks to construct the MB representation of the total graph.

The MB representations were used in two different ways. Closing the contours of integration either to the left or to the right and summing up all residue contributions, we obtain representations in terms of hypergeometric series. Quite often hypergeometric functions have integral representations which can be expanded in ϵ. However, this is not always possible and we extract the singularities directly from the MB representation. First, we isolate the poles in ϵ by adding the contribution of the residues which cross the contour of integration when we perform an analytic continuation of ϵ to zero. The remaining integrals are well defined at $\epsilon = 0$ and may be expanded in a Taylor series. Finally, we evaluate the finite integrals by summing up all residues enclosed in the contour of integration, yielding harmonic sums which can be identified in terms of logarithms and generalized polylogarithms.

In Chapter 4 we examined the method of integration in Negative Dimensions (NDIM) which is based on the property of Feynman integrals to be analytic functions in D. From the Schwinger representation of the scalar integrals, we obtain a template solution and a system of constraints. Inserting the constraints into the template solution we derive hypergeometric representations of the integral in the various kinematic regions. The method is very powerful for one-loop calculations or for the evaluation of two-loop integrals with a bubble subgraph. However, limited progress has been achieved for general two-loop integrals where the method is disfavored in comparison with the MB integral representation technique.

Due to the large number of Feynman scalar and tensor integrals involved in two-loop matrix elements calculations, it is crucial to develop computer programs which reduce the number of the independent (master) integrals which are ultimately needed. In Chapter 5 we used Integration By Parts (IBP) and Lorentz Invariance (LI) identities to find relations between the general Feynman integrals appearing in one and two-loop massless $2 \rightarrow 2$ scattering matrix elements and the master integrals. We also constructed differential equations relating many of the master integrals with each other completing the computation of the analytic expansions in ϵ of all master integrals relevant to the physical processes we examined.

Our approach for the building of the reduction algorithm was to find a symbolic solution of the IBP and LI identities decreasing the extra powers of the propagators and the dimension of the integrals produced from the tensor decomposition method of Chapter 3. However, this approach becomes cumbersome for complex topologies (for example the crossed-box) and it cannot be generalized for integrals with more mass scales and loops. A different approach is to generate all identities involving extra powers of propagators and dimensions (or equivalently irreducible numerators) and solve their system of equations by means of a computer program. This method has been used by Tarasov [31], Gehrmann and Remiddi [25], and Laporta [32, 33]. Their method is in principle suitable for any multi-loop integral calculation. The only limitation is due to computer resources (CPU time and memory) and it has been proven a very serious obstacle for a completely automatic solution of the IBP and LI recursive relations for practical calculations. However, there is hope that these problems will be resolved by means of increasing computing power or programming on platforms specialized to the needs of multi-loop calculations.

The prospect of an automated numerical or analytic calculation of the master integrals is also strong. Binoth and Heinrich [20] have suggested an algorithm for the isolation of the poles from Feynman representations and the numerical evaluation of the finite integrals. Unfortunately, their results are limited to the kinematic regions below all branch cuts where the Feynman representation has a real value. In addition, Gehrmann and Remiddi have proposed a largely automated method for the analytic solution of the differential equations satisfied by the master integrals [28, 29, 26, 27], in terms of generalized harmonic polylogarithms, order by order in ϵ. Recently, Tarasov [30] and Laporta [32, 33] have proposed the evaluation of master integrals through difference equations produced from IBP identities. Their approach is also promising and it can be directed to both numerical or analytic evaluations. The differential or difference equations methods can be applied given the existence of an IBP algorithm for the reduction of multi-loop topologies to master integrals. Mellin-Barnes representations are independent of such an algorithm and a numerical or analytic expansion in ϵ through MB integrals can be further established as a very important tool for the calculation of master integrals and verification of the IBP algorithms. Further development of the above techniques is expected to revolutionize multi-loop integral evaluations and facilitate high precision calculations.

In Chapter 6 we computed the virtual corrections for quark scattering at NNLO accuracy. Similar results were produced for the QCD processes of quark-gluon [1] and gluon-gluon [5], and the QED Bhabha scattering [19]. Given the recent progress on multi-loop calculations more matrix-elements at NNLO accuracy will be known soon. Yet the above results are insufficient to make physical predictions on their own and much work remains to be done. A major challenge is a systematic procedure for the analytic cancellation of infrared divergences between the tree level 2$\rightarrow$4, the one-loop 2$\rightarrow$3 and the 2$\rightarrow$2 processes. We should note recent progress in this direction with the determination of singular limits of tree-level matrix elements when two particles are unresolved [83, 84, 85, 86, 87] and the soft and collinear limits of one-loop amplitudes [88, 89, 90, 91, 92], together with the analytic cancellation of the infrared singularities in the somewhat simpler case of $e^+e^-\rightarrow photon + jet$ at next to leading order [93] A further complication is due to initial state radiation. Factorization of the collinear singularities from the incoming partons requires the evolution of the pdf's to be known to an accuracy matching the hard scattering matrix element. This entails knowledge of the three-loop splitting functions. We should here note the contribution of References [94, 95, 96, 97, 98, 99, 100, 101].

We hope that the problem of the numerical cancellation of infrared divergences will be soon addressed thereby enabling the construction of numerical programs to provide NNLO QCD estimates of jet production in hadron collision.

Appendix A

Hypergeometric definitions and identities

In Appendix A.1 we give the definitions of the hypergeometric functions as a series together with their regions of convergence. Integral representations for the ${}_2F_1$, F_1 and F_2 functions are given in Appendix A.2 while identities for reducing the F_1 and F_2 functions to simpler functions are given in Appendix A.4.

A.1 Series representations

The hypergeometric functions of one variable are sums of Pochhammer symbols over a single summation parameter m

$$
\begin{aligned}
{}_2F_1\left(\alpha, \beta, \gamma, x\right) &= \sum_{m=0}^{\infty} \frac{(\alpha, m)(\beta, m)}{(\gamma, m)} \frac{x^m}{m!} && \text{(A.1)} \\
{}_3F_2\left(\alpha, \beta, \beta', \gamma, \gamma', x\right) &= \sum_{m=0}^{\infty} \frac{(\alpha, m)(\beta, m)(\beta', m)}{(\gamma, m)(\gamma', m)} \frac{x^m}{m!}, && \text{(A.2)}
\end{aligned}
$$

which are convergent when $|x| < 1$.

The hypergeometric functions of two variables can be written as sums over the integers m and n: F_i, $i = 1, \ldots, 4$ are the Appell functions, H_2 a Horn function and

S_1 and S_2 generalised Kampé de Fériet functions:

$$F_1(\alpha,\beta,\beta',\gamma,x,y) = \sum_{m,n=0}^{\infty} \frac{(\alpha,m+n)(\beta,m)(\beta',n)}{(\gamma,m+n)} \frac{x^m}{m!} \frac{y^n}{n!} \tag{A.3}$$

$$F_2(\alpha,\beta,\beta',\gamma,\gamma',x,y) = \sum_{m,n=0}^{\infty} \frac{(\alpha,m+n)(\beta,m)(\beta',n)}{(\gamma,m)(\gamma',n)} \frac{x^m}{m!} \frac{y^n}{n!} \tag{A.4}$$

$$F_3(\alpha,\alpha',\beta,\beta',\gamma,x,y) = \sum_{m,n=0}^{\infty} \frac{(\alpha,m)(\alpha',n)(\beta,m)(\beta',n)}{(\gamma,m+n)} \frac{x^m}{m!} \frac{y^n}{n!} \tag{A.5}$$

$$F_4(\alpha,\beta,\gamma,\gamma',x,y) = \sum_{m,n=0}^{\infty} \frac{(\alpha,m+n)(\beta,m+n)}{(\gamma,m)(\gamma',n)} \frac{x^m}{m!} \frac{y^n}{n!} \tag{A.6}$$

$$H_2(\alpha,\beta,\gamma,\gamma',\delta,x,y) = \sum_{m,n=0}^{\infty} \frac{(\alpha,m-n)(\beta,m)(\gamma,n)(\gamma',n)}{(\delta,m)} \frac{x^m}{m!} \frac{y^n}{n!} \tag{A.7}$$

$$S_1(\alpha,\alpha',\beta,\gamma,\delta,x,y) = \sum_{m,n=0}^{\infty} \frac{(\alpha,m+n)(\alpha',m+n)(\beta,m)}{(\gamma,m+n)(\delta,m)} \frac{x^m}{m!} \frac{y^n}{n!} \tag{A.8}$$

$$S_2(\alpha,\alpha',\beta,\beta',\gamma,x,y) = \sum_{m,n=0}^{\infty} \frac{(\alpha,m-n)(\alpha',m-n)(\beta,n)(\beta',n)}{(\gamma,m-n)} \frac{x^m}{m!} \frac{y^n}{n!}. \tag{A.9}$$

These series converge according to the criteria collected in Table A.1. The do-

Function	Convergence criteria
F_1, F_3	$\lvert x\rvert < 1,\ \lvert y\rvert < 1$
F_2, S_1	$\lvert x\rvert + \lvert y\rvert < 1$
F_4	$\sqrt{\lvert x\rvert} + \sqrt{\lvert y\rvert} < 1$
H_2, S_2	$-\lvert x\rvert + 1/\lvert y\rvert > 1, \lvert x\rvert < 1, \lvert y\rvert < 1$

Table A.1: Convergence regions for some hypergeometric functions of two variables.

main of convergence of the Appell and Horn functions are well known. That one for S_1 and S_2 may be worked out using Horns general theory of convergence [102].

A.2 Integral representations

Euler integral representations of ${}_2F_1$, F_1 and F_2 are well known [103, 102, 104, 105] and we list the relevant formulae here.

$$
{}_2F_1\left(\alpha,\beta,\gamma,x\right) = \frac{\Gamma\left(\gamma\right)}{\Gamma\left(\beta\right)\Gamma\left(\gamma-\beta\right)} \times \int_0^1 du\, u^{\beta-1}(1-u)^{\gamma-\beta-1}(1-ux)^{-\alpha}
$$
$$
\mathrm{Re}(\beta)>0, \quad \mathrm{Re}(\gamma-\beta)>0. \tag{A.10}
$$

$$
F_1(\alpha,\beta,\beta',\gamma,x,y) = \frac{\Gamma\left(\gamma\right)}{\Gamma\left(\alpha\right)\Gamma\left(\gamma-\alpha\right)} \int_0^1 du\, u^{\alpha-1}(1-u)^{\gamma-\alpha-1}(1-ux)^{-\beta}(1-uy)^{-\beta'}
$$
$$
\mathrm{Re}(\alpha)>0, \quad \mathrm{Re}(\gamma-\alpha)>0. \tag{A.11}
$$

$$
F_2\left(\alpha,\beta,\beta',\gamma,\gamma',x,y\right) = \frac{\Gamma\left(\gamma\right)\Gamma\left(\gamma'\right)}{\Gamma\left(\beta\right)\Gamma\left(\beta'\right)\Gamma\left(\gamma-\beta\right)\Gamma\left(\gamma'-\beta'\right)}
$$
$$
\times \int_0^1 du \int_0^1 dv\, u^{\beta-1}v^{\beta'-1}(1-u)^{\gamma-\beta-1}(1-v)^{\gamma'-\beta'-1}(1-ux-vy)^{-\alpha}
$$
$$
\mathrm{Re}(\beta)>0, \quad \mathrm{Re}(\beta')>0, \quad \mathrm{Re}(\gamma-\beta)>0, \quad \mathrm{Re}(\gamma'-\beta')>0. \tag{A.12}
$$

A.3 Example of explicit evaluation of an integral representation

In working out the integral representation for hypergeometric functions in $D=4-2\epsilon$ dimensions, we have often to deal with the ϵ expansion of integrals of the form

$$
I(x) = \int_0^1 du\, d(u)\, f(u), \tag{A.13}
$$
$$
d(u) = u^{-1+\alpha\epsilon}(1-u)^{-1+\beta\epsilon} \tag{A.14}
$$

where α and β are real numbers and $f(u)$ is a smooth function in the domain $0 \le u \le 1$: in particular, it is finite at the boundary points.

The procedure to deal with this kind of integrals is quite standard. The integral has a pole in ϵ when the integration variable u approaches either of the end points. We concentrate first on the point $u=0$, and we rewrite the integral in such a way to expose the pole in ϵ

$$
I(x) = \int_0^1 du\, d(u)\, f(0) + \int_0^1 du\, d(u) \Big[f(u)-f(0)\Big] = I_{[1]} + I_{[2]}. \tag{A.15}
$$

The integral $I_{[1]}$ can be easily done

$$I_{[1]} = f(0)\frac{\Gamma(\alpha\,\epsilon)\,\Gamma(\beta\,\epsilon)}{\Gamma((\alpha+\beta)\,\epsilon)} = \frac{f(0)}{\epsilon}\frac{\alpha+\beta}{\alpha\beta}\frac{\Gamma(1+\alpha\,\epsilon)\,\Gamma(1+\beta\,\epsilon)}{\Gamma(1+(\alpha+\beta)\,\epsilon)}, \tag{A.16}$$

and the integrand of $I_{[2]}$ is now finite in the limit $u \to 0$. In fact, we can make a Taylor expansion

$$f(u) - f(0) = u f'(0) + \frac{u^2}{2!} f''(0) + \ldots \equiv u\, g(u), \tag{A.17}$$

and write $I_{[2]}$ as

$$I_{[2]} = \int_0^1 du\, d(u)\, u\, g(u) = \int_0^1 du\, u^{\alpha\epsilon}(1-u)^{-1+\beta\epsilon} g(u). \tag{A.18}$$

We repeat now the same steps done for Eq. (A.15) with respect to the point $u = 1$, to obtain

$$I_{[2]} = \int_0^1 du\, u^{\alpha\epsilon}(1-u)^{-1+\beta\epsilon}\, g(1) + \int_0^1 du\, u^{\alpha\epsilon}(1-u)^{-1+\beta\epsilon}\Big[g(u) - g(1)\Big] = I_{[3]} + I_{[4]}. \tag{A.19}$$

The integral $I_{[3]}$ gives

$$I_{[3]} = g(1)\,\frac{\Gamma(1+\alpha\,\epsilon)\,\Gamma(\beta\,\epsilon)}{\Gamma(1+(\alpha+\beta)\,\epsilon)} = \frac{f(1)-f(0)}{\beta\,\epsilon}\,\frac{\Gamma(1+\alpha\,\epsilon)\,\Gamma(1+\beta\,\epsilon)}{\Gamma(1+(\alpha+\beta)\,\epsilon)}, \tag{A.20}$$

while $I_{[4]}$ is finite at $u \to 1$

$$I_{[4]} = \int_0^1 du\, u^{\alpha\epsilon}(1-u)^{\beta\epsilon}\, h(u), \qquad g(u) - g(1) \equiv (1-u)\, h(u), \tag{A.21}$$

and can be solved with an ϵ expansion of the integrand. Adding all the contributions together we have

$$I(x) = \frac{1}{\alpha\,\beta\,\epsilon}\,[\beta\, f(0) + \alpha\, f(1)]\,\frac{\Gamma(1+\alpha\,\epsilon)\,\Gamma(1+\beta\,\epsilon)}{\Gamma(1+(\alpha+\beta)\,\epsilon)} + \int_0^1 du\, u^{\alpha\epsilon}(1-u)^{\beta\epsilon}\, h(u), \tag{A.22}$$

where

$$h(u) = \frac{1}{u(1-u)}\Big(f(u) - (1-u)\, f(0) - u\, f(1)\Big). \tag{A.23}$$

In the case where we have two integration variables, the procedure outlined above can be re-iterated in a straightforward manner. To illustrate the procedure, we evaluate explicitly the following F_2 functions to $\mathcal{O}(\epsilon^2)$.

The integral representation for F_2 (see Eq. (A.12)) is given by

$$F_2(1, 1, \epsilon, \epsilon+1, 1-\epsilon, x, y) = \frac{\epsilon^2\,\Gamma(1-\epsilon)}{\Gamma(1+\epsilon)\,\Gamma(1-2\epsilon)}\; I(x, y), \tag{A.24}$$

where

$$I(x,y) = \int_0^1 du\, dv\, d(u,v)\, f(u,v), \tag{A.25}$$

and

$$\begin{aligned} d(u,v) &= v^{-1+\epsilon}(1-u)^{-1+\epsilon}(1-v)^{-2\epsilon} \\ f(u,v) &= (1-ux-vy)^{-1}, \end{aligned}$$

and $I(x,y)$ must be computed to $\mathcal{O}(\epsilon^0)$. In order to expose the poles (see Eq. (A.15)), we add and subtract the value of the finite function $f(u,v)$, computed at the boundary points, in the following way:

$$\begin{aligned} I(x,y) &= \int_0^1 du\, dv\, d(u,v) \Big\{ \Big[f(1,0)\Big] + \Big[f(u,0) - f(1,0)\Big] + \Big[f(1,v) - f(1,0)\Big] \\ &\qquad + \Big[f(u,v) - f(u,0) - f(1,v) + f(1,0)\Big]\Big\} \\ &= I_{[1]} + I_{[2]} + I_{[3]} + I_{[4]}. \end{aligned} \tag{A.26}$$

We are now in a position to evaluate the single contributions in the square brackets. In fact

$$\begin{aligned} I_{[1]} &= (1-x)^{-1} \int_0^1 du\, (1-u)^{-1+\epsilon} \int_0^1 dv\, v^{-1+\epsilon}\, (1-v)^{-2\epsilon} = (1-x)^{-1} \frac{\Gamma(1+\epsilon)\,\Gamma(1-2\epsilon)}{\epsilon^2\,\Gamma(1-\epsilon)} \\ I_{[2]} &= \frac{-x}{1-x} \frac{\Gamma(1+\epsilon)\,\Gamma(1-2\epsilon)}{\epsilon\,\Gamma(1-\epsilon)} \int_0^1 du\, \frac{(1-u)^\epsilon}{(1-ux)} \\ I_{[3]} &= \frac{(1-x)^{-1}}{\epsilon} \int_0^1 dv\, \frac{v^\epsilon\,(1-v)^{-2\epsilon}}{1-x-vy} \\ I_{[4]} &= \frac{xy}{1-x} \int_0^1 du\, dv\, (1-u)^\epsilon\, v^\epsilon\, (1-v)^{-2\epsilon} \frac{(vy+ux+x-2)}{(1-ux)(1-x-vy)(1-vy-ux)}. \end{aligned} \tag{A.27}$$

The remaining integrals are finite in the limit $\epsilon \to 0$, so that we can make a Taylor expansion to $\mathcal{O}(\epsilon)$ for the integrands of $I_{[2]}$ and $I_{[3]}$, and we can put directly $\epsilon = 0$ in $I_{[4]}$. Recalling the definition of the dilogarithm function

$$\mathrm{Li}_2(x) = -\int_0^x dz\, \frac{\log(1-z)}{z} \qquad x \le 1\,, \tag{A.28}$$

it is straightforward to carry on the last integrations and express the result in terms of Li_2 functions.

A.4 Identities amongst the hypergeometric functions

The F_1 and F_2 functions have the following reduction formulae which leave a single remaining Euler integral at most [103, 102, 104, 105]:

$$F_1\left(\alpha,\beta,\beta',\beta+\beta',x,y\right) = (1-y)^{-\alpha}{}_2F_1\left(\alpha,\beta,\beta+\beta',\frac{x-y}{1-y}\right) \tag{A.29}$$

$$F_2\left(\alpha,\beta,\beta',\gamma,\alpha,x,y\right) = (1-y)^{-\beta'}F_1\left(\beta,\alpha-\beta',\beta',\gamma,x,\frac{x}{1-y}\right) \tag{A.30}$$

$$F_2\left(\alpha,\beta,\beta',\alpha,\gamma',x,y\right) = (1-x)^{-\beta}F_1\left(\beta',\beta,\alpha-\beta,\gamma',\frac{y}{1-x},y\right) \tag{A.31}$$

$$F_2\left(\alpha,\beta,\beta',\beta,\gamma',x,y\right) = (1-x)^{-\alpha}{}_2F_1\left(\alpha,\beta',\gamma',\frac{y}{1-x}\right) \tag{A.32}$$

$$F_2\left(\alpha,\beta,\beta',\alpha,\alpha,x,y\right) = (1-x)^{-\beta}(1-y)^{-\beta'}{}_2F_1\left(\beta,\beta',\alpha,\frac{xy}{(1-x)(1-y)}\right) \tag{A.33}$$

$$F_2\left(\alpha,\beta,\beta',\alpha,\beta',x,y\right) = (1-y)^{\beta-\alpha}(1-x-y)^{-\beta} \tag{A.34}$$

$$F_2\left(\alpha,\beta,\beta',\beta,\beta',x,y\right) = (1-x-y)^{-\alpha}. \tag{A.35}$$

A.5 Analytic continuation formulae

Here we give only those analytic continuation properties that relate the argument and inverse argument. Gauss' hypergeometric function has the following analytic continuation properties (see for example [103])

$$\begin{aligned}{}_2F_1\left(\alpha,\beta,\gamma,z\right) &= (-z)^{-\alpha}\frac{\Gamma\left(\gamma\right)\Gamma\left(\beta-\alpha\right)}{\Gamma\left(\beta\right)\Gamma\left(\gamma-\alpha\right)}\,{}_2F_1\left(\alpha,1+\alpha-\gamma,1+\alpha-\beta,\frac{1}{z}\right)\\ &+(-z)^{-\beta}\frac{\Gamma\left(\gamma\right)\Gamma\left(\alpha-\beta\right)}{\Gamma\left(\alpha\right)\Gamma\left(\gamma-\beta\right)}\,{}_2F_1\left(\beta,1+\beta-\gamma,1+\beta-\alpha,\frac{1}{z}\right).\\ &|\arg(-z)|<\pi,\end{aligned} \tag{A.36}$$

$$\begin{aligned}{}_2F_1\left(\alpha,\beta,\gamma,z\right) &= z^{-\alpha}\frac{\Gamma\left(\gamma\right)\Gamma\left(\gamma-\alpha-\beta\right)}{\Gamma\left(\gamma-\alpha\right)\Gamma\left(\gamma-\beta\right)}\,{}_2F_1\left(\alpha,1+\alpha-\gamma,1+\alpha+\beta-\gamma,1-\frac{1}{z}\right)\\ &+z^{\alpha-\gamma}\left(1-z\right)^{\gamma-\alpha-\beta}\frac{\Gamma\left(\gamma\right)\Gamma\left(\alpha+\beta-\gamma\right)}{\Gamma\left(\alpha\right)\Gamma\left(\beta\right)}\,{}_2F_1\left(\gamma-\alpha,1-\alpha,1+\gamma-\alpha-\beta,1-\frac{1}{z}\right)\\ &|\arg(z)|<\pi,\ \ |\arg(1-z)|<\pi.\end{aligned} \tag{A.37}$$

There are many possible analytic continuations; however, we list only those that are relevant to link the groups of solutions for the one-loop box discussed in Sec. 4.1.2, that is the connections between the Appell and Horn functions.

$$
\begin{aligned}
F_4(\alpha,\beta,\gamma,\gamma',x,y) = &\frac{\Gamma(\gamma')\Gamma(\beta-\alpha)}{\Gamma(\gamma'-\alpha)\Gamma(\beta)}(-y)^{-\alpha}F_4\left(\alpha,\alpha+1-\gamma',\gamma,\alpha+1-\beta,\frac{x}{y},\frac{1}{y}\right)\\
&+\frac{\Gamma(\gamma')\Gamma(\alpha-\beta)}{\Gamma(\gamma'-\beta)\Gamma(\alpha)}(-y)^{-\beta}F_4\left(\beta,\beta+1-\gamma',\gamma,\beta+1-\alpha,\frac{x}{y},\frac{1}{y}\right)
\end{aligned}
\tag{A.38}
$$

$$
\begin{aligned}
F_3(\alpha,\alpha',\beta,\beta',\gamma,x,y) = &\frac{\Gamma(\beta-\alpha)\Gamma(\gamma)}{\Gamma(\gamma-\alpha)\Gamma(\beta)}(-x)^{-\alpha}H_2\left(\alpha+1-\gamma,\alpha,\alpha',\beta',\alpha+1-\beta,\frac{1}{x},-y\right)\\
&+\frac{\Gamma(\alpha-\beta)\Gamma(\gamma)}{\Gamma(\gamma-\beta)\Gamma(\alpha)}(-x)^{-\beta}H_2\left(\beta+1-\gamma,\beta,\alpha',\beta',\beta+1-\alpha,\frac{1}{x},-y\right)
\end{aligned}
\tag{A.39}
$$

$$
\begin{aligned}
H_2(\alpha,\beta,\gamma,\gamma',\delta,x,y) = &\frac{\Gamma(\gamma'-\gamma)\Gamma(1-\alpha)}{\Gamma(1-\alpha-\gamma)\Gamma(\gamma')}(y)^{-\gamma}F_2\left(\alpha+\gamma,\beta,\gamma,\delta,\gamma+1-\gamma',x,-\frac{1}{y}\right)\\
&+\frac{\Gamma(\gamma-\gamma')\Gamma(1-\alpha)}{\Gamma(1-\alpha-\gamma')\Gamma(\gamma)}(y)^{-\gamma'}F_2\left(\alpha+\gamma',\beta,\gamma',\delta,\gamma'+1-\gamma,x,-\frac{1}{y}\right)
\end{aligned}
\tag{A.40}
$$

$$
\begin{aligned}
F_2(\alpha,\beta,\beta',\gamma,\gamma',x,y) = &\frac{\Gamma(\beta-\alpha)\Gamma(\gamma)}{\Gamma(\gamma-\alpha)\Gamma(\beta)}(-x)^{-\alpha}S_1\left(\alpha,\alpha+1-\gamma,\beta',\alpha+1-\beta,\gamma',-\frac{y}{x},\frac{1}{x}\right)\\
&+\frac{\Gamma(\alpha-\beta)\Gamma(\gamma)}{\Gamma(\gamma-\beta)\Gamma(\alpha)}(-x)^{-\beta}H_2\left(\alpha-\beta,\beta',\beta,\beta+1-\gamma,\gamma',y,-\frac{1}{x}\right)
\end{aligned}
\tag{A.41}
$$

$$
\begin{aligned}
H_2(\alpha,\beta,\gamma,\gamma',\delta,x,y) = &\frac{\Gamma(\beta-\alpha)\Gamma(\delta)}{\Gamma(\delta-\alpha)\Gamma(\beta)}(-x)^{-\alpha}S_2\left(\alpha,\alpha+1-\delta,\gamma',\gamma,\alpha+1-\beta,\frac{1}{x},-xy\right)\\
&+\frac{\Gamma(\alpha-\beta)\Gamma(\delta)}{\Gamma(\delta-\beta)\Gamma(\alpha)}(-x)^{-\beta}F_3\left(\beta,\gamma',\beta+1-\delta,\gamma,\beta+1-\alpha,\frac{1}{x},-y\right)
\end{aligned}
\tag{A.42}
$$

$$
\begin{aligned}
S_1(\alpha,\alpha',\beta,\gamma,\delta,x,y) = &\frac{\Gamma(\alpha'-\alpha)\Gamma(\gamma)}{\Gamma(\gamma-\alpha)\Gamma(\alpha')}(-y)^{-\alpha}F_2\left(\alpha,\beta,\alpha+1-\gamma,\delta,\alpha+1-\alpha',-\frac{x}{y},\frac{1}{y}\right)\\
&+\frac{\Gamma(\alpha-\alpha')\Gamma(\gamma)}{\Gamma(\gamma-\alpha')\Gamma(\alpha)}(-y)^{-\alpha'}F_2\left(\alpha',\beta,\alpha'+1-\gamma,\delta,\alpha'+1-\alpha,-\frac{x}{y},\frac{1}{y}\right)
\end{aligned}
\tag{A.43}
$$

$$
\begin{aligned}
S_2(\alpha,\alpha',\beta,\beta',\gamma,x,y) = &\frac{\Gamma(\alpha'-\alpha)\Gamma(\gamma)}{\Gamma(\gamma-\alpha)\Gamma(\alpha')}(-x)^{-\alpha}H_2\left(\alpha,\alpha+1-\gamma,\beta',\beta,\alpha+1-\alpha',\frac{1}{x},-xy\right)\\
&+\frac{\Gamma(\alpha-\alpha')\Gamma(\gamma)}{\Gamma(\gamma-\alpha')\Gamma(\alpha)}(-x)^{-\alpha'}H_2\left(\alpha',\alpha'+1-\gamma,\beta',\beta,\alpha'+1-\alpha,\frac{1}{x},-xy\right)
\end{aligned}
\tag{A.44}
$$

Appendix B

Polylogarithms

The purpose of this appendix is to define the generalised polylogarithms that occur in the expansion in ϵ of the pentabox scalar and tensor loop integrals and to give useful identities amongst the polylogarithms. In Appendix B.1 we give the definitions of the polylogarithm functions $\mathrm{S}_{n,p}(x)$. These functions are real when $x \leq 1$ but they develop an imaginary part for $x > 1$. Analytic continuation formulae are given in Appendix B.2. Finally, useful identities between polylogarithms are listed in Appendix B.3.

B.1 Definition

The generalised polylogarithms of Nielsen are defined by

$$\mathrm{S}_{n,p}(x) = \frac{(-1)^{n+p-1}}{(n-1)!\,p!} \int_0^1 dt\, \frac{\log^{n-1}(t) \log^p(1-xt)}{t}, \qquad n,p \geq 1, \quad x \leq 1. \tag{B.1}$$

For $p = 1$ we find the usual polylogarithms

$$\mathrm{S}_{n-1,1}(x) \equiv \mathrm{Li}_n(x). \tag{B.2}$$

The $S_{n,p}$'s with argument x, $1-x$ and $1/x$ can be related to each other via [82]

$$\begin{aligned}
\mathrm{S}_{n,p}(1-x) &= \sum_{s=0}^{n-1} \frac{\log^s(1-x)}{s!} \left[\mathrm{S}_{n-s,p}(1) - \sum_{r=0}^{p-1} \frac{(-1)^r}{r!} \log^r(x)\, \mathrm{S}_{p-r,n-s}(x) \right] \\
&+ \frac{(-1)^p}{n!\,p!} \log^n(1-x) \log^p(x), \qquad \text{(B.3)} \\
\mathrm{S}_{n,p}\left(\frac{1}{x}\right) &= (-1)^n \sum_{s=0}^{p-1} (-1)^s \sum_{r=0}^{s} \frac{(-1)^r}{r!} \log^r(-x) \frac{(n+s-r-1)!}{(s-r)!(n-1)!}\, \mathrm{S}_{n+s-r,p-s}(x) \\
&+ \sum_{r=0}^{n-1} \frac{(-1)^{r+p}}{r!} \log^r(-x)\, C_{n-r,p} + \frac{(-1)^n}{(n+p)!} \log^{n+p}(-x), \qquad \text{(B.4)}
\end{aligned}$$

with

$$\begin{aligned}
C_{n,p} &= (-1)^{n+1} \sum_{r=1}^{p-1} (-1)^{p-r} \frac{(n+r-1)!}{r!(n-1)!} \mathrm{S}_{n+r,p-r}(-1) \\
&+ (-1)^p \left(1-(-1)^n\right)\, \mathrm{S}_{n,p}(-1)\,. \qquad \text{(B.5)}
\end{aligned}$$

We also need the definition of the Riemann Zeta functions

$$\zeta_n = \sum_{s=1}^{\infty} \frac{1}{s^n}, \qquad \text{(B.6)}$$

and in particular

$$\zeta_2 = \frac{\pi^2}{6}, \qquad \zeta_3 = 1.20206\ldots \qquad \zeta_4 = \frac{\pi^4}{90}. \qquad \text{(B.7)}$$

B.2 Analytic continuation formulae

For $x > 1$, the following analytic continuations should be used

$$\mathrm{Li}_2\,(x+i0) = -\,\mathrm{Li}_2\left(\frac{1}{x}\right) - \frac{1}{2}\log^2(x) + \frac{\pi^2}{3} + i\pi\log(x) \tag{B.8}$$

$$\mathrm{Li}_3\,(x+i0) = \mathrm{Li}_3\left(\frac{1}{x}\right) - \frac{1}{6}\log^3(x) + \frac{\pi^2}{3}\log(x) + \frac{i\pi}{2}\log^2(x) \tag{B.9}$$

$$\mathrm{Li}_4\,(x+i0) = -\,\mathrm{Li}_4\left(\frac{1}{x}\right) - \frac{1}{24}\log^4(x) + \frac{\pi^2}{6}\log^2(x) + \frac{\pi^4}{45} + \frac{i\pi}{6}\log^3(x) \tag{B.10}$$

$$\begin{aligned}\mathrm{S}_{1,2}\,(x+i0) = {} & -\mathrm{S}_{1,2}\left(\frac{1}{x}\right) + \mathrm{Li}_3\left(\frac{1}{x}\right) + \log(x)\,\mathrm{Li}_2\left(\frac{1}{x}\right) + \frac{1}{6}\log^3(x) - \frac{\pi^2}{2}\log(x) + \zeta_3 \\ & + i\pi\left[\frac{\pi^2}{6} - \mathrm{Li}_2\left(\frac{1}{x}\right) - \frac{1}{2}\log^2(x)\right]\end{aligned} \tag{B.11}$$

$$\begin{aligned}\mathrm{S}_{1,3}\,(x+i0) = {} & -\mathrm{S}_{1,3}\left(\frac{1}{x}\right) + \mathrm{S}_{2,2}\left(\frac{1}{x}\right) + \log(x)\mathrm{S}_{1,2}\left(\frac{1}{x}\right) - \mathrm{Li}_4\left(\frac{1}{x}\right) - \log(x)\,\mathrm{Li}_3\left(\frac{1}{x}\right) \\ & - \frac{1}{2}\log^2(x)\,\mathrm{Li}_2\left(\frac{1}{x}\right) + \frac{\pi^2}{2}\mathrm{Li}_2\left(\frac{1}{x}\right) - \frac{1}{24}\log^4(x) + \frac{\pi^2}{4}\log^2(x) - \frac{19\pi^4}{360} \\ & + i\pi\left[\mathrm{Li}_3\left(\frac{1}{x}\right) - \mathrm{S}_{1,2}\left(\frac{1}{x}\right) + \log(x)\,\mathrm{Li}_2\left(\frac{1}{x}\right) + \frac{1}{6}\log^3(x) - \frac{\pi^2}{6}\log(x)\right]\end{aligned} \tag{B.12}$$

$$\begin{aligned}\mathrm{S}_{2,2}\,(x+i0) = {} & \mathrm{S}_{2,2}\left(\frac{1}{x}\right) - 2\,\mathrm{Li}_4\left(\frac{1}{x}\right) - \log(x)\,\mathrm{Li}_3\left(\frac{1}{x}\right) + \frac{1}{24}\log^4(x) - \frac{\pi^2}{4}\log^2(x) \\ & + \zeta_3\log(x) + \frac{\pi^4}{45} + i\pi\left[\mathrm{Li}_3\left(\frac{1}{x}\right) - \frac{1}{6}\log^3(x) + \frac{\pi^2}{6}\log(x) - \zeta_3\right].\end{aligned} \tag{B.13}$$

B.3 Useful identities

We often need the following transformations

$$\mathrm{Li}_2\left(\frac{x}{x-1}\right) = -\,\mathrm{Li}_2(x) - \frac{1}{2}\log^2(1-x)\,, \tag{B.14}$$

$$\mathrm{Li}_3\left(\frac{x}{x-1}\right) = -\,\mathrm{Li}_3(x) + \mathrm{S}_{1,2}(x) + \log(1-x)\,\mathrm{Li}_2(x) + \frac{1}{6}\log^3(1-x)\,, \tag{B.15}$$

$$\begin{aligned}\mathrm{Li}_4\left(\frac{x}{x-1}\right) &= -\,\mathrm{Li}_4(x) + \mathrm{S}_{2,2}(x) - \mathrm{S}_{1,3}(x) + \log(1-x)\,\mathrm{Li}_3(x) - \log(1-x)\,\mathrm{S}_{1,2}(x)\\ &\quad -\frac{1}{2}\log^2(1-x)\,\mathrm{Li}_2(x) - \frac{1}{24}\log^4(1-x)\,,\end{aligned} \tag{B.16}$$

$$\mathrm{S}_{1,2}\left(\frac{x}{x-1}\right) = \mathrm{S}_{1,2}(x) - \frac{1}{6}\log^3(1-x)\,, \tag{B.17}$$

$$\mathrm{S}_{1,3}\left(\frac{x}{x-1}\right) = -\,\mathrm{S}_{1,3}(x) - \frac{1}{24}\log^4(1-x)\,, \tag{B.18}$$

$$\mathrm{S}_{2,2}\left(\frac{x}{x-1}\right) = \mathrm{S}_{2,2}(x) - 2\,\mathrm{S}_{1,3}(x) - \log(1-x)\,\mathrm{S}_{1,2}(x) + \frac{1}{24}\log^4(1-x)\,. \tag{B.19}$$

Bibliography

[1] C. Anastasiou, E. W. N. Glover, C. Oleari, and M. E. Tejeda-Yeomans, (2001), hep-ph/0101304.

[2] C. Anastasiou, E. W. N. Glover, C. Oleari, and M. E. Tejeda-Yeomans, (2000), hep-ph/0012007.

[3] C. Anastasiou, E. W. N. Glover, C. Oleari, and M. E. Tejeda-Yeomans, (2000), hep-ph/0011094.

[4] C. Anastasiou, E. W. N. Glover, C. Oleari, and M. E. Tejeda-Yeomans, (2000), hep-ph/0010212.

[5] E. W. N. Glover, C. Oleari, and M. E. Tejeda-Yeomans, (2001), hep-ph/0102201.

[6] M. E. Peskin and D. V. Schroeder, *An Introduction to Quantum Field Theory*, Reading, USA: Addison-Wesley (1995) 842 p.

[7] G. Sterman, *An Introduction to Quantum Field Theory*, Cambridge, UK: Univ. Pr. (1993) 572 p.

[8] L. H. Ryder, *Quantum Field Theory*, Cambridge, UK: Univ. Pr. (1985) 487p.

[9] R. K. Ellis, W. J. Stirling, and B. R. Webber, *QCD and Collider Physics*, Cambridge, UK: Univ. Pr. (1996) 435 p. (Cambridge Monographs on Particle Physics, Nuclear Physics and Cosmology: 8).

[10] T. Muta, *Foundations of Quantum Chromodynamics: An Introduction to Perturbative Methods in Gauge Theories*, Singapore, Singapore: World Scientific (1987) 409 P. (World Scientific Lecture Notes In Physics, 5).

[11] Y. L. Dokshitzer, V. A. Khoze, A. H. Mueller, and S. I. Troian, *Basics of Perturbative QCD*, Gif-sur-Yvette, France: Ed. Frontieres (1991) 274 p.

[12] E. . A. H. Mueller, *Perturbative Quantum Chromodynamics*, Singapore, Singapore: World Scientific (1989) 614 P. (Advanced Series On Directions In High Energy Physics, 5).

[13] C. G. Bollini and J. J. Giambiagi, Nuovo Cim. **B12**, 20 (1972).

[14] J. F. Ashmore, Lett. Nuovo Cim. **4**, 289 (1972).

[15] G. 't Hooft and M. Veltman, Nucl. Phys. **B44**, 189 (1972).

[16] D. I. O. R. J. Eden, P. V. Landshoff and J. C. Polkinghorne, *The Analytic S-Matrix*, Cambridge University Press, 1966.

[17] S. Catani, Phys. Lett. **B427**, 161 (1998), hep-ph/9802439.

[18] S. Catani and M. H. Seymour, Acta Phys. Polon. **B28**, 863 (1997), hep-ph/9612236.

[19] Z. Bern, L. Dixon, and A. Ghinculov, Phys. Rev. **D63**, 053007 (2001), hep-ph/0010075.

[20] T. Binoth and G. Heinrich, Nucl. Phys. **B585**, 741 (2000), hep-ph/0004013.

[21] V. A. Smirnov, Phys. Lett. **B460**, 397 (1999), hep-ph/9905323.

[22] J. B. Tausk, Phys. Lett. **B469**, 225 (1999), hep-ph/9909506.

[23] V. A. Smirnov, Phys. Lett. **B491**, 130 (2000), hep-ph/0007032.

[24] V. A. Smirnov, Phys. Lett. **B500**, 330 (2001), hep-ph/0011056.

[25] T. Gehrmann and E. Remiddi, Nucl. Phys. **B580**, 485 (2000), hep-ph/9912329.

[26] T. Gehrmann and E. Remiddi, Nucl. Phys. Proc. Suppl. **89**, 251 (2000), hep-ph/0005232.

[27] T. Gehrmann and E. Remiddi, (2000), hep-ph/0008287.

[28] T. Gehrmann and E. Remiddi, (2001), hep-ph/0101124.

[29] T. Gehrmann and E. Remiddi, (2001), hep-ph/0101147.

[30] O. V. Tarasov, Nucl. Phys. Proc. Suppl. **89**, 237 (2000), hep-ph/0102271.

[31] O. V. Tarasov, Acta Phys. Pol. **B29**, 2655 (1998), hep-ph/9812250.

[32] S. Laporta, Int. J. Mod. Phys. **A15**, 5087 (2000), hep-ph/0102033.

[33] S. Laporta, (2000), hep-ph/0102032.

[34] O. V. Tarasov, Phys. Rev. **D54**, 6479 (1996), hep-th/9606018.

[35] R. J. Gonsalves, Phys. Rev. **D28**, 1542 (1983).

[36] G. Kramer and B. Lampe, J. Math. Phys. **28**, 945 (1987).

[37] J. A. M. Vermaseren, Int. J. Mod. Phys. **A14**, 2037 (1999), hep-ph/9806280.

[38] J. Fleischer, A. V. Kotikov, and O. L. Veretin, Nucl. Phys. **B547**, 343 (1999), hep-ph/9808242.

[39] O. M. Ogreid and P. Osland, J. Comput. Appl. Math. **98**, 245 (1998), hep-th/9801168.

[40] O. M. Ogreid and P. Osland, (1999), hep-th/9904206.

[41] O. M. Ogreid and P. Osland, (2000), math-ph/0010026.

[42] F. A. Berends, M. Buza, M. Bohm, and R. Scharf, Z. Phys. **C63**, 227 (1994).

[43] S. Bauberger, F. A. Berends, M. Bohm, and M. Buza, Nucl. Phys. **B434**, 383 (1995), hep-ph/9409388.

[44] I. G. Halliday and R. M. Ricotta, Phys. Lett. **B193**, 241 (1987).

[45] G. V. Dunne and I. G. Halliday, Nucl. Phys. **B308**, 589 (1988).

[46] A. T. Suzuki and A. G. M. Schmidt, (1997), hep-th/9707187.

[47] A. T. Suzuki and A. G. M. Schmidt, JHEP **09**, 002 (1997), hep-th/9709024.

[48] A. T. Suzuki and A. G. M. Schmidt, Eur. Phys. J. **C5**, 175 (1998), hep-th/9709144.

[49] A. T. Suzuki and A. G. M. Schmidt, (1997), hep-th/9709167.

[50] A. T. Suzuki, A. G. M. Schmidt, and R. Bentin, Nucl. Phys. **B537**, 549 (1999), hep-th/9807158.

[51] A. T. Suzuki and A. G. M. Schmidt, Eur. Phys. J. **C10**, 357 (1999), hep-th/9903076.

[52] A. T. Suzuki and A. G. M. Schmidt, Can. J. Phys. **78**, 769 (2000), hep-th/9904195.

[53] A. T. Suzuki and A. G. M. Schmidt, J. Phys. A **A33**, 3713 (2000), hep-th/0005082.

[54] A. T. Suzuki and A. G. M. Schmidt, (2000), hep-th/0009075.

[55] D. J. Broadhurst, Phys. Lett. **B197**, 179 (1987).

[56] F. V. Tkachov, Phys. Lett. **B100**, 65 (1981).

[57] K. G. Chetyrkin and F. V. Tkachov, Nucl. Phys. **B192**, 159 (1981).

[58] V. A. Smirnov and O. L. Veretin, Nucl. Phys. **B566**, 469 (2000), hep-ph/9907385.

[59] P. A. Baikov and V. A. Smirnov, Phys. Lett. **B477**, 367 (2000), hep-ph/0001192.

[60] E. W. N. Glover and M. E. Tejeda-Yeomans, Nucl. Phys. Proc. Suppl. **89**, 196 (2000), hep-ph/0010031.

[61] CDF, F. Abe *et al.*, Phys. Rev. Lett. **77**, 438 (1996), hep-ex/9601008.

[62] D0, B. Abbott *et al.*, Phys. Rev. Lett. **82**, 2451 (1999), hep-ex/9807018.

[63] Z. Bern, L. Dixon, and D. A. Kosower, Phys. Rev. Lett. **70**, 2677 (1993), hep-ph/9302280.

[64] Z. Bern, L. Dixon, and D. A. Kosower, Nucl. Phys. **B437**, 259 (1995), hep-ph/9409393.

[65] Z. Kunszt, A. Signer, and Z. Trocsanyi, Phys. Lett. **B336**, 529 (1994), hep-ph/9405386.

[66] J. F. Gunion and J. Kalinowski, Phys. Rev. **D34**, 2119 (1986).

[67] S. J. Parke and T. R. Taylor, Nucl. Phys. **B269**, 410 (1986).

[68] F. A. Berends and W. Giele, Nucl. Phys. **B294**, 700 (1987).

[69] M. Mangano, S. Parke, and Z. Xu, Nucl. Phys. **B298**, 653 (1988).

[70] Z. Kunszt, Nucl. Phys. **B271**, 333 (1986).

[71] S. J. Parke and T. R. Taylor, Phys. Rev. **D35**, 313 (1987).

[72] J. F. Gunion and Z. Kunszt, Phys. Lett. **B159**, 167 (1985).

[73] J. F. Gunion and Z. Kunszt, Phys. Lett. **B176**, 163 (1986).

[74] Z. Bern, L. Dixon, and D. A. Kosower, JHEP **01**, 027 (2000), hep-ph/0001001.

[75] R. K. Ellis and J. C. Sexton, Nucl. Phys. **B269**, 445 (1986).

[76] Z. Kunszt, A. Signer, and Z. Trocsanyi, Nucl. Phys. **B411**, 397 (1994), hep-ph/9305239.

[77] C. Anastasiou, E. W. N. Glover, and C. Oleari, Nucl. Phys. **B565**, 445 (2000), hep-ph/9907523.

[78] C. Anastasiou, T. Gehrmann, C. Oleari, E. Remiddi, and J. B. Tausk, Nucl. Phys. **B580**, 577 (2000), hep-ph/0003261.

[79] C. Anastasiou, J. B. Tausk, and M. E. Tejeda-Yeomans, Nucl. Phys. Proc. Suppl. **89**, 262 (2000), hep-ph/0005328.

[80] C. Anastasiou, E. W. N. Glover, and C. Oleari, Nucl. Phys. **B575**, 416 (2000), hep-ph/9912251.

[81] P. Nogueira, J. Comput. Phys. **105**, 279 (1993).

[82] K. Kolbig, J. Mignaco, and E. Remiddi, B.I.T **10**, 38 (1970).

[83] J. M. Campbell and E. W. N. Glover, Nucl. Phys. **B527**, 264 (1998), hep-ph/9710255.

[84] S. Catani and M. Grazzini, Nucl. Phys. **B570**, 287 (2000), hep-ph/9908523.

[85] S. Catani and M. Grazzini, Phys. Lett. **B446**, 143 (1999), hep-ph/9810389.

[86] V. D. Duca, A. Frizzo, and F. Maltoni, Nucl. Phys. **B568**, 211 (2000), hep-ph/9909464.

[87] F. A. Berends and W. T. Giele, Nucl. Phys. **B313**, 595 (1989).

[88] Z. Bern, V. D. Duca, W. B. Kilgore, and C. R. Schmidt, Phys. Rev. **D60**, 116001 (1999), hep-ph/9903516.

[89] Z. Bern, V. D. Duca, and C. R. Schmidt, Phys. Lett. **B445**, 168 (1998), hep-ph/9810409.

[90] S. Catani and M. Grazzini, Nucl. Phys. **B591**, 435 (2000), hep-ph/0007142.

[91] D. A. Kosower, Nucl. Phys. **B552**, 319 (1999), hep-ph/9901201.

[92] D. A. Kosower and P. Uwer, Nucl. Phys. **B563**, 477 (1999), hep-ph/9903515.

[93] A. G.-D. Ridder and E. W. N. Glover, Nucl. Phys. **B517**, 269 (1998), hep-ph/9707224.

[94] S. A. Larin, P. Nogueira, T. van Ritbergen, and J. A. M. Vermaseren, Nucl. Phys. **B492**, 338 (1997), hep-ph/9605317.

[95] S. A. Larin, T. van Ritbergen, and J. A. M. Vermaseren, Nucl. Phys. **B427**, 41 (1994).

[96] A. Retey and J. A. M. Vermaseren, (2000), hep-ph/0007294.

[97] J. A. Gracey, Phys. Lett. **B322**, 141 (1994), hep-ph/9401214.

[98] W. L. van Neerven and A. Vogt, Nucl. Phys. **B568**, 263 (2000), hep-ph/9907472.

[99] W. L. van Neerven and A. Vogt, Nucl. Phys. **B588**, 345 (2000), hep-ph/0006154.

[100] W. L. van Neerven and A. Vogt, Phys. Lett. **B490**, 111 (2000), hep-ph/0007362.

[101] A. D. Martin, R. G. Roberts, W. J. Stirling, and R. S. Thorne, Eur. Phys. J. **C18**, 117 (2000), hep-ph/0007099.

[102] H. Exton, *Multiple Hypergeomtric Functions and Applications*, Ellis Horwood, 1976.

[103] F. O. A. Erdélyi, W. Magnus and F. Tricomi.

[104] P. Appell and J. K. de Fériet, *Fonctions Hypergéométriques et Hypersphériques, Polynomes D'Hermite,* Gauthiers-Villars, Paris 1926.

[105] W. Bailey, *Generalised Hypergeometric Series*, Cambridge University Press, 1966.